ANALGESIC AND ANTI-INFLAMMATORY CONSTITUENTS OF *ANNICKIA POLYCARPA* STEM AND ROOT BARKS AND *CLAUSENA ANISATA* ROOT

A THESIS SUBMITTED IN PARTIAL FULFILMENT OF THE REQUIREMENTS FOR THE DEGREE OF

DOCTOR OF PHILOSOPHY

IN THE

DEPARTMENT OF PHARMACOGNOSY
FACULTY OF PHARMACY AND PHARMACEUTICAL SCIENCES
COLLEGE OF HEALTH SCIENCES

BY

EMMANUEL KOFI KUMATIA

KWAME NKRUMAH UNIVERSITY OF SCIENCE AND TECHNOLOGY (KNUST)

KUMASI-GHANA

AUGUST, 2016

DECLARATION

I declare that this thesis is the product of my own research work. It does not contain any manuscript that was earlier accepted for the award of any other degree in any University nor any published work of anybody except where cited and due acknowledgments made in the text.

…….. ……

Emmanuel Kofi Kumatia Date

…… ……

Prof. (Mrs.) Rita Akosua Dickson Date

(Supervisor)

……..... ……

Prof. Kofi Annan Date

(Supervisor)

……..... ……

Prof. Abraham Yeboah Mensah Date

(Head of Department of Pharmacognosy)

DEDICATIONS

This work is especially dedicated to my mother, Madam Veronica Akoto, my wife, Mrs. Anne Boakyewaa Anokye-Kumatia and my children, Evzen Fifii Kumatia and Eliora Nana Akua Kumatia.

ABSTRACT

Clausena anisata and *Annickia polycarpa* are medicinal plants used to treat various painful and inflammatory disorders among other ailments in traditional medicine. The aim of this study was to investigate the analgesic/antinociceptive and anti-inflammatory activities of the ethanol extracts of *C. anisata* root (CRE), *A. polycarpa* stem (ASE) and root barks (AR) in order to provide scientific justification for their use as anti-inflammatory and analgesic agents. Analgesic activity was evaluated using the hot plate and the acetic acid induced writhing assays. The mechanism of antinociception was evaluated by employing pharmacological antagonism assays at the opioid and cholinergic receptors in the hot plate and the writhing assays. Anti-inflammatory activity was also evaluated by carrageenan induced edema in rats' paw assay. The compounds were isolated using bioassay-guided fractionation and their structures identified by spectroscopic methods. CRE at 1000 mg/kg *p.o.* produce significant ($p < 0.001$) analgesic activity of 72.15 and 48.05 % in the hot plate and writhing assays respectively and significant ($p < 0.01$) anti-inflammatory activity of 27.53 %. ASE also produced significant ($p < 0.001$) analgesic activity of 82.54 and 44.03 % in the hot plate and writhing assays respectively and significant anti-inflammatory activity of 69.64 %. Furthermore, the results also showed that the petroleum ether (pet ether) fraction (PEF) of *C. anisata* root extract and the chloroform fraction (AC) of *A. polycarpa* stem bark extract were the most active fractions among the petroleum ether, chloroform and aqueous fractions of these extracts. A total of seven (7) compounds were isolated. Four (4) coumarins, namely, anisocoumarin B, osthol, imperatorin and xanthotoxol in addition to a carbazole alkaloid, heptaphyline were isolated from PEF. Two (2) protoberberine alkaloids namely jatrorrhizine and palmatine were also isolated from AC. Palmatine was further isolated from the chloroform fraction of *A. polycarpa* root bark. The seven isolated compounds were tested for analgesic activity in the writhing test. Six of them at 6 mg/kg *p.o.*, produced significant analgesic activity of 38.13 to 47.28 %. One of the isolates (xantothoxol) was inactive. Analgesic activity of diclofenac in the writhing test was 32.92 % at 6 mg/kg *p.o*. Four of the isolates were also tested for analgesic activity in the hot plate assay. These isolates at 9 mg/kg p.o. produced immence analgesic effect of 30.13 to 93.87 %. The analgesic effect of tramadol 9 mg/kg p.o. was 27.13 % in the hot plate test. Furthermore, naloxone antagonized the analgesic

effect of CRE, ASE, anisocoumarin B, xanthotoxol and palmatine in the hot plate test. This indicates that *C. anisata* root and *A. polycarpa* stem bark, anisocoumarin B, xanthotoxol and palmatine produce analgesia by acting on the central opioidergic nociceptors. Moreover, the isolates administered at 9 mg/kg p.o. produced significant anti-inflammatory activity of 33.39 % to 66.50 %. The anti-inflammatory activity of indomethacin was 58.15 % at 9 mg/kg *p.o.* The anti-inflammatory and analgesic activities and the mechanism of antinociceptive action of *C. anisata* root, *A. polycarpa*, anisocoumarin B and heptaphyline are being reported for the first time in this study. In addition, the analgesic activities of jatrorrhizine and the mechanism of antinociception of palmatine are also being reported for the first time by this study to the best of my knowledge. Lastly, LD_{50} of the crude ethanol extracts were found to be above 5000 mg/kg *p.o.* indicating that they were safe for short term usage. These findings provide scientific justification for the use of *C. anisata* root and *A. polycarpa* stem bark as anti-inflammatory and analgesic agent in traditional medicine.

ACKNOWLEDGEMENTS

I am thankful to God for what He has done for me throughout the period of this study.
I am very grateful to my supervisors Prof. (Mrs.) Rita Akosua Dickson and Prof. Kofi Annan who have advised, supported and encouraged me during all the years that I spent pursuing this degree. I am highly indebted to Prof. Dominic Adotei Edoh, the Chief Executive Director of the World Health Organization (W.H.O) collaborative Centre for Plant Medicine Research (CPMR) at Mampong - Akwapim, Ghana. I am also immensely grateful to Dr. Alfred Apomah Appiah, the Deputy Chief Executive Director of CPMR for his assistance. Words cannot express my in-depth gratitude to Dr. Nguyen Hung Tung of the Pharmacognosy Department of Nagasaki International University (NIU), Japan and Dr. Solomon Habtemariam of University of Greenwich, United Kingdom, for running the NMR spectra of the compounds and helping with the structure elucidations.

Special mention is also made of Mr. Charles Kweku Adomako, the Administrative Secretary of the Centre for Plant Medicine Research (CPMR) for his support. I am forever grateful to all the Board members of CPMR for granting me study leave to pursue the PHD degree. I would like to express my appreciation to all Senior Members of the Pharmacognosy Department, especially Prof. Abraham Yeboah Mensah and Dr. Isaac Kingsley Aponsah for their support.

I cannot end the list without mentioning the technical assistance given to me by the staff of the Animal House Unit of the Centre for Plant Medicine Research (C.P.M.R) especially Messrs. Samuel Collins Addo, Francis Ansah and Theophilus Ansah Kyene.

Finally, I am thankful to all persons who in diverse ways assisted me in one way or the other during the course of this work.

TABLE OF CONTENT

DECLARATION ..... **ii**
DEDICATIONS ..... **iii**
ABSTRACT ..... **iv**
ACKNOWLEDGEMENTS ..... **vi**
TABLE OF CONTENT ..... **vii**
LIST OF TABLES ..... **xi**
LIST OF FIGURES ..... **xiii**
LIST OF APPENDICES ..... **xv**
LIST OF ABREVIATIONS AND SYMBOLS ..... **xvii**

CHAPTER ONE **1**
INTRODUCTION **1**
1.1 GENERAL INTRODUCTION 1
1.1.1 Natural products and their derivatives as drugs 1
1.2 JUSTIFICATION AND IMPORTANCE OF THE STUDY 26
1.3 AIMS AND OBJECTIVES 26
1.3.1 Aims 26
1.3.2 Specific Objectives 26

CHAPTER TWO **28**
LITERATURE REVIEW **28**
2.1 BOTANICAL AND MORPHOLOGICAL FEATURES OF THE PLANTS 28
2.1.1 *Clausena anisata* (Wild) Hook f. ex. Benth 28
2.1.2 *Annickia polycarpa*, Stten and Mass 29
2.2 ETHNOPHARMACOLOGICAL USES OF THE PLANTS 30
2.2.1 Ethnopharmacological uses of *C.anisata* 30
2.2.2 Non medicinal uses of *C. anisata* 31
2.2.3 Ethnopharmacological uses of *A. polycarpa* 31

2.2.4 Non medicinal uses of *A. polycarpa* 31
2.3 THE CHEMISTRY AND BIOLOGICAL ACTIVITIES OF *C. ANISATA* 32
2.3.1 Biological activities of the crude extracts of *C. anisata* 32
2.3.2 Compounds isolated from *C. anisata* and their biological activities 32
2.4 THE CHEMISTRY AND BIOLOGICAL ACTIVITIES OF *A. POLYCARPA* 45
2.4.1 Biological activities of the crude extracts of *A. polycarpa* 45
2.4.2 Compounds isolated from *A. polycarpa* and their biological activities 46
2.4.2.1 Protoberberine alkaloids 46
2.5 NOCICEPTION AND PAIN 55
2.5.1 Nociception 55
2.5.2 Pain 55
2.5.3 Mechanism of antinociceptive action 57
2.5.4 Current analgesic drugs and problems associated with them 58
2.5.5 Experimental models of pain in animals 58
2.5.6 Experimental models used in determination of antinociceptive mechanisms 60
2.6 THE ROLE OF INFLAMMATION IN HUMAN DISEASES 61
2.6.1 Current anti-inflammatory drugs and challenges associated with them 63
2.6.2 In vivo anti-inflammatory assays using animal models 63

CHAPTER THREE 65
MATERIALS AND METHODS 65
3.1 Collection and authentication of plant materials 65
3.2. MATERIALS AND METHODS **65**
3.2.1 Extraction and partitioning 65
3.2.2 CHROMATOGRAPHY AND DETECTING REAGENTS 66
3.2.2.1 Column chromatography over normal phase silica gel 66
3.2.2.2 Thin layer chromatography (TLC) 67
3.2.2.3 10 % Sulphuric acid reagent 67
3.2.2.4 Iodine vapour 67
3.2.2.5 Dragendorff's spray reagent 68
3.2.3 SPECTROSCOPIC TECHNIQUES 68

3.2.3.1. Nuclear magnetic resonance (NMR) spectroscopy 68
3.2.3.2 Fourier transform-infra red (FTIR) spectrometry 68
3.2.3.3 Gas chromatography connected with mass spectrometry (GC-MS) 68
3.2.4. PHARMACOLOGICAL STUDIES 69
3.2.4.1. Drugs and other chemicals 69
3.2.4.2 Animals 69
3.2.4.3 Acute toxicity assay 69
3.2.4.4 Antinociceptive or analgesic activity assays 70
3.2.4.4.3 Evaluation of antinociceptive mechanism 71
3.2.4.5 Anti-inflammatory activity assay 72
3.3 STATISTICAL ANALYSIS 72
3.4 PHYTOCHEMICAL INVESTIGATIONS 73
3.4.1 Phytochemical screening of the extracts 73
3.4.2 TLC analysis of the ethanol extracts and fractions of *C. anisata* and *A. polycarpa* 73
3.4.3 Isolation of compounds from petroleum ether fraction of *C. anisata* root 73
3.4.4 Isolation of compounds from chloroform fraction of *A. polycarpa* stem bark 75
3.4.5 Isolation of compound(s) from the chloroform fraction (RP) of *A. polycarpa* root bark 78

CHAPTER FOUR 80
RESULTS 80
4.1 PHYTOCHEMICAL SCREENING 80
4.2 TLC PROFILES 81
4.2.1 TLC profiles of extracts and their fractions 81
4.2.2 Retention factor (R_f) values and solubility profiles of the isolated compounds 82
4.3 STRUCTURE ELUCIDATION OF ISOLATED COMPOUNDS 84
4.3.1 Compounds isolated from *C. anisata* root 84
4.3.2 Compounds isolated from *A. polycarpa* stem bark 104
4.3.2 Characterization of compound from the root bark of *A. polycarpa* 112
4.4 ACUTE TOXICITY 115
4.5 ANALGESIC ACTIVITIES 115
4.5.1 Hot plate assay 115

4.5.2 Acetic acid-induced writhing assay 125
4.6 MECHANISM OF ANTINOCICEPTIVE ACTION 133
4.6.1 *C. anisata* root and *A. polycarpa* stem bark..... 133
4.6.2 Isolated compounds 135

CHAPTER FIVE 153
DISCUSSIONS, CONCLUSIONS AND RECOMMENDATIONS 153
5.1 DISCUSSIONS..... 153
5.1.1 Phytochemical screening tests 153
5.1.2 TLC profiles of the plants extracts..... 153
5.1.3 Acute toxicity assay 153
5.1.4 Antinociceptive effects 154
5.1.4.2 Acetic acid-induced writhing pain stimulation 155
5.1.5 Mechanism of antinociceptive action 159
5.1.6 Anti-inflammatory effects..... 161
5.2 CONCLUSIONS..... 168
5.3 RECOMMENDATIONS..... 169

REFERENCES..... 170
APPENDICES..... 195

LIST OF TABLES

Table 1.1: Structure, name, plant source and use(s) of some drugs obtained from plants..... 3
Table 1.2: Some compounds derived from plants used as leads to synthesize other useful drugs 8
Table 1.3: Structure and other uses of some compounds obtained from plants..... 15
Table 1.4: Structure, name and uses of some drugs obtained from marine organisms..... 17
Table 1.5: Structure, name and uses of some drugs isolated from microorganism 20
Table 3.1: Percentage (%) yield 66
Table 4.1: Results of the phytochemical screening tests of the crude ethanol extracts 80
Table 4.2: R_f values of isolated compounds on normal phase TLC plate..... 83
Table 4.3: ^{1}H and ^{13}C NMR chemical shifts (ppm) of C1D and anisocoumarin B 86
Table 4.4: ^{13}C NMR chemical shifts of C1D, clausenalansimin B and 6-hydroxy-7-methoxycoumarin 87
Table 4.5: ^{13}C NMR data of the prenyloxy substituent of C1D and phellopterin..... 88
Table 4.6: Wave numbers (υ/cm^{-1}) of absorption bands obtained in the I.R spectrum of C1D... 88
Table 4.7: ^{1}H and ^{13}C NMR chemical shifts (ppm) of P2A and xanthotoxol..... 91
Table 4.8: Wave numbers (υ) of absorption bands obtained in the I.R spectrum of P2A 92
Table 4.9: ^{1}H and ^{13}C NMR chemical shifts (ppm) of C1F and osthol 94
Table 4.10: Wave numbers (υ/cm^{-1}) of absorptions obtained in the I.R spectrum of C1F 95
Table 4.11: ^{1}H and ^{13}C NMR chemical shifts (ppm) of C1G and imperatorin..... 98
Table 4.12: Wave numbers (υ/cm^{-1}) of absorptions obtained in the I.R spectrum of C1G 99
Table 4.13: ^{1}H and ^{13}C NMR chemical shifts (ppm) of CI-1, heptaphyline and 7-methoxyheptaphyline..... 102
Table 4.14: Wave numbers (υ/cm^{-1}) of absorptions obtained in the I.R spectrum of C1-I..... 103
Table 4.15: ^{1}H and ^{13}C NMR chemical shifts (ppm) of A6C and palmatine chloride..... 106
Table 4.16: Wave numbers (υ/cm^{-1}) of absorptions obtained in the I.R spectrum of A6C 107
Table 4.17: ^{1}H and ^{13}C NMR chemical shifts (ppm) of A8C and Jatrorrhizine chloride 110
Table 4.18: Wave numbers (υ/cm^{-1}) of absorptions obtained in the I.R spectrum of A8C 111
Table 4.19: ^{1}H NMR chemical shifts (ppm) of A9C and palmatine..... 114
Table 4.20: Analgesic activity of the ethanol extract of *C. anisata* root and its fractions on thermally induced pain..... 121

Table 4.21: Analgesic activity of the ethanol extract of *A. polycarpa* stem bark and its fractions on thermally induced pain..... 121
Table 4.22: Analgesic activity (%) of some of the isolated compounds and tramadol on thermally induced pain in C57BL/6 mice..... 125
Table 4.23: Analgesic activity of the ethanol extract of *C. anisata* root and its fractions in acetic acid-induced writhing test..... 129
Table 4.24: Analgesic activity of *A. polycarpa* stem bark ethanol extract and its fractions in acetic acid-induced writhing test 129
Table 4.25: Analgesic activity of *A. polycarpa* root bark ethanol extract 130
in acetic acid-induced writhing test 130
Table 4. 26: Analgesic activity of the isolated compounds in the acetic acid-induced writhing assay..... 132
Table 4.27: Effect of naloxone and atropine on analgesic activity of the extracts and some of the isolates in the hot plate and acetic acid-induced writhing assays respectively..... 139
Table 4.28: Anti-inflammatory activity of the ethanol extract of *C. anisata* root and its fractions 146
Table 4.29: Anti-inflammatory activity of the ethanol extract of *A. polycarpa* stem bark and its fractions..... 146
Table 4.30: Anti-inflammatory activity of compounds isolated from *C. anisata*..... 152
Table 4.31: Anti-inflammatory activity of compounds isolated from *A. polycarpa*..... 152

LIST OF FIGURES

Figure 2.1: Whole plant and roots of *C. anisata*..... 28
Figure 2.2: Wholeplant and slashed stem of *A. polycarpa* 29
Figure 2.3: Structures of carbazole and a quinolone alkaloid(s) isolated from *C. anisata*..... 36
Figure 2.4: Structures of phytosteroids and amide derivatives from *C. anisata* 37
Figure 2.5: Structures of coumarins isolated from *C. anisata* 43
Figure 2.6: Structures of limonoids isolated from *C. anisata*..... 44
Figure 2.7: Structures of protoberberine alkaloids isolated from *A. polycarpa* 48
Figure 2.8: Structures of aporphine alkaloids from *A. polycarpa* 50
Figure 2.9: Structures of oxoaporphine alkaloids isolated from *A. polycarpa* 52
Figure 2.10: Structures of benzyltetrahydroisoquinoline, isoquinoline and cinchona alkaloids from *A. polycarpa* 54
Figure 3.1: Scheme for isolation and purification of compounds from pet ether fraction of *C. anisata* root 75
Figure 3.2: Scheme for isolation and purification of compounds from chloroform fraction of *A. polycarpa* stem bark..... 77
Figure 3.3: Scheme for isolation and purification of compounds from the chloroform fraction of *A. polycarpa* root bark 79
Figure 4.1: Comparative TLC chromatograms of the ethanol extracts of the leaf, stem and root of *C. anisata* (A) and *A. polycarpa* (B) developed in pet ether/ethyl acetate 4:1..... 81
Figure 4.2: TLC chromatograms of ethanol extracts of *C. anisata* root (C) and *A. polycarpa* stem bark (D) and their respective fractions 82
Figure 4.3: Analgesic effect of the ethanol extracts of *C. anisata* root (CRE), *A. polycarpa* stem bark (ASE); 120
Figure 4.4: Antinociceptive effects of the isolated compounds; anisocoumarin B, xanthotoxol palmatine, jatrorrhizine or tramadol……..……123
Figure 4.5: Antinociceptive effect of the ethanol extract of the root of *C. anisata* and *A. polycarpa* stem and root bark and their fractions on acetic acid induced writhing pain in mice.....127

Figure 4.6: Antinociceptive effect of the isolates: anisocoumarin B [92], xanthotoxol [80], osthol [86], imperatorin [79], heptaphylline, palmatine [107], jatrorrhizine [108] or diclofenac……..…...130

Figure 4.7: Effect of naloxone (2 mg/kg i.p) on the ethanol extracts of *C. anisata* (CRE) or *A. polycarpa* bark (ASE) (at 10 mg/kg p.o) thermal mediated antinociception on time course curve and Overall analgesic activity…...……...133

Figure 4.8: Effect of atropine (5 mg/kg i.p.) on antinociceptive action of the ethanol extract of *C. anisata* root and *A. polycarpa* stem bark...…….……134

Figure 4.9: Effect of naloxone (2 mg/kg i.p.) on analgesic effect of anisocoumarin B, xanthotoxol or palmatine on thermal mediated antinociception……...…….……..135

Figure 4.10: Effects of atropine (5 mg/kg i.p.) on analgesic effects of the anisocoumarin B, palmatine and jatrorrhizine in the mouse writhing test……137

Figure 4.11: Anti-inflammatory effect of the ethanol extracts of *C. anisata* root (CRE), *A. polycarpa* stem bark (ASE); pet ether (PEF), chloroform (CF) and aqueous (EMF) fractions……144

Figure 4.12: Anti-inflammatory effect of the isolated compounds: anisocoumarin B, xanthotoxol, osthol, imperatorin and heptaphyline from *C. anisata* root and palmatine, jatrorrhizine from *A. polycarpa* and the reference drug, indomethacin……..……..150

LIST OF APPENDICES

Appendix 1: ^{1}H NMR spectrum of C1D (Anisocoumarin B) in chloroform-d……..195
Appendix 2: ^{13}C NMR spectrum of C1D (Anisocoumarin B) in chloroform-d...……..196
Appendix 3: GC-MS spectrum of C1D (Anisocoumarin B) in chloroform ……..197
Appendix 4: I.R spectrum of C1D (Anisocoumarin B) in potassium bromide.……..…...198
Appendix 5: ^{1}H NMR spectrum of P2A (Xanthotoxol) in methanol-d……...…….…….199
Appendix 6: ^{13}C NMR spectrum of P2A (Xanthotoxol) in chloroform-d ……..…...200
Appendix 7: GC-MS spectrum of P2A (Xanthotoxol) in methanol …….....201
Appendix 8: I.R spectrum of P2A (Xanthotoxol) in potassium bromide …….……..…….……..202
Appendix 9: ^{1}H NMR spectrum of C1F (Osthol) in chloroform-d……..……....…..203
Appendix 10: ^{13}C NMR spectrum of C1F (Osthol) in chloroform-d ……...…….204
Appendix 11: G.C-MS spectrum of C1F (Osthol) in chloroform…….,……...205
Appendix 12: I.R spectrum of C1F (Osthol) ..……...206
Appendix 13: ^{1}H NMR spectrum of C1G (Imperatorin) in chloroform-d ……...…….....207
Appendix 14: ^{13}C NMR spectrum of C1G (Imperatorin) in chloroform-d ……....208
Appendix 15: GC-MS spectrum of C1G (Imperatorin) in chloroform……...209
Appendix 16: I.R spectrum of C1G (Imperatorin)…….210
Appendix 17: ^{1}H NMR spectrum of C1-I (Heptaphyline) in chloroform-d ……..……...….211
Appendix 18: ^{13}C NMR spectrum of C1-I (Heptaphyline) in chloroform-d ……..…...…...212
Appendix 19: GC-MS spectrum of C1-I (Heptaphyline) in chloroform ……..……213
Appendix 20: I.R spectrum of C1-I (Heptaphyline)…….…….…….....214
Appendix 21: ^{1}H NMR spectrum of A6C (Palmatine) in methanol-d …….…….....215
Appendix 22: ^{13}C NMR spectrum of A6C (Palmatine) methanol-d …….……216
Appendix 23: GC-MS spectrum of A6C (Palmatine) in methanol…….…….....217
Appendix 24: I.R spectrum of A6C (Palmatine) in potassium bromide……..…...218
Appendix 25: ^{1}H NMR spectrum of A8C (Jatrorrhizine) in methanol-d ……..219
Appendix 26: ^{13}C NMR spectrum of A8C (Jatrorrhizine) in methanol-d ……..…...…220
Appendix 27: GC-MS spectrum of A8C (Jatrorrhizine) in methanol….……..….221
Appendix 28: I.R spectrum of A8C (Jatrorrhizine) in potassium bromide ….…….. ...222

Appendix 29: ^{1}H NMR spectrum of A9C (Palmatine) in methanol-d …….…….....223
Appendix 30: ^{13}C NMR spectrum of A9C (Palmatine) in methanol-d …….…..…….....224

LIST OF ABREVIATIONS AND SYMBOLS

AA	Arachidonic Acid
AC	Chloroform fraction of ethanol extract of stem bark of *A. polycarpa*
Ach	Acetylcholine
AER	Aqueous fraction of ethanol extract of the stem bark of *A. polycarpa*
EMF	Aqueous fraction of ethanol root extract of *C. anisata*
AIDS	Acquired Immune Deficiency Syndrome
AI	Antifeedant Indices
a.m. u	atomic mass unit
AO	Acridine Orange
AOM	Azoxymethane
AP	Pet ether fraction of ethanol extract of the stem bark of *A. polycarpa*
AR	Ethanol extract of *A. polycarpa* root
ASE	Ethanol extract of the stem bark of *A. polycarpa*
cAMP	cyclic Adenosine Monophosphate
CC	Column Chromatography
CGRP	Calcitonin Gene Related Peptide
cm	Centimeter
COPD	Chronic Obstructive Pulmonary Disease
CS	Correlation Spectroscopy
COX-1	Cycloxygenase-1
COX-2	Cycloxygenase-2
CPMR	Centre for Plant Medicine Research
CRE	Ethanol root extract of *C. anisata*
CF	Chloroform fraction of ethanol root extract of *C. anisata*
C. I	Confidence Interval
d	Doublet
EC_{50}	Effective Concentration
ED_{50}	Effective Dose
EI	Electron Impact

FRAP	Ferric Reducing Antioxidant Power
FTIR	Fourier transform-infra red spectrometry
g	Gram
GABA	Gamma - Aminobutyric Acid
GAPDH	Glyceraldehyde-3-Phosphate Dehydrogenase
GC-MS	Gas chromatography coupled with Mass Spectrometry
GST	Glutathione S-transferase
h	Hour
Hz	*Hertz*
HHDL	Human High Density Lipoprotein
IC_{50}	Concentration that produce 50 % inhibition
i.p.	intraperitoneal
i.t.	Intrathecal
i.v.	intravenous injection
J	Nuclear spin-spin coupling constant
kg	Kilogram
κ-opioid	kappa-opioid receptor system
L	Liter
LDH	Lactate dehydrogenase
LD_{50}	Lethal Dose
LGTase	Limonoid Glucosyl Transferase
LTB_4	Leukotrienes B4
m	Meter
MBC	Minimal Bactericidal Concentration
MDA	Malonaldelhyde
mg	Milligram
mL	Milliliter
mol	Mole
MOR	*mu*-opioid receptors
MMP	Mitochondrial Membrane Potential
NCDs	Non-Communicable Diseases

NMR	Nuclear Magnetic Resonance spectrometry
NO	Nitric Oxide
NSAIDs	Nonsteroidal Anti-Inflammatory Drugs
PAF	Platelet-Activation Factor
PEF	Pet ether fraction of ethanol root extract of *C. anisata*
p.o.	per oral/per os
PGs	Prostaglandins
PTF 1B	Protein Tyrosine Phosphatase 1B
PTZ	Petylenetetrazole
R_f	Retention factor
ROS	Reactive Oxygen Species
s	Seconds
s	Singlet
STZ	Streptozotocin
t	Triplet
TBARS	Thiobarbituric Acid Reactive Products
TD_{50}	Mean Toxic Dose
TLC	Thin Layer Chromatography
TMS	Tetramethylsilane
UV	Ultraviolet spectrometry
µM	Micromole
µL	Microliter
WHO	World Health Organization
VSCCs	Voltage-Sensitive Calcium Channels
°C	Degree Celsius
%PTI	Percentage Pain Threshold Inhibition
%OPTI	Overall Percentage Pain Threshold Inhibition
%AE	Percentage Analgesic Effect
δ	Chemical shift (in ppm from TMS)

CHAPTER ONE

INTRODUCTION

1.1 GENERAL INTRODUCTION

The application of natural products including compounds that are derived from natural sources such as plants, animals or micro-organisms for medicinal purposes predates documented human history most likely by millennia of years (Hong-Fang*et al.*, 2009). This study seeks to investigate the anti-inflammatory, analgesic or antinociceptive properties and the mechanism(s) of antinociceptive effects of the root of *Clausena anisata* **(**Wild.) Hook f.ex. Benth, (Rutaceae) and stem and root barks of *Annickia polycarpa*, Stten and Mass (Annonaceae) also known as *Enantia polycarpa* Engl. and Diels. These two medicinal plants are employed in the treatment of various ailments including pain, inflammation and malaria in Ghanaian traditional medicine.

1.1.1 Natural products and their derivatives as drugs

Natural products are products that are derived from natural sources (Sarker *et al.*, 2006a) including plants. Plants are utilized in four major ways as sources of therapeutic principles. These are (i): the use of the whole plant or some of its morphological part(s) as a herbal medication (Fabricant and Farnsworth, 2001) e.g ginger, lemon, onion and lemon glass (ii): isolation of biologically active compounds from plants for direct use as drugs (Fabricant and Farnsworth, 2001). (iii): molecules from plants are used as prototypes or leads for semi-synthesis of new drugs with higher activity or lower toxicity; (iv): compounds from natural products are also used as pharmacological devices to search for other bioactive agents (Fabricant and Farnsworth, 2001).

Secondary metabolites are small molecules with molecular weight less than 2000 a.m.u which are produced by an organism but are not basically required for the organism's existence (Sarker *et al.*, 2006a). They consist of flavonoids, alkaloids, coumarins, glycosides, lignans, steroids or terpenoids isolated from plants, animals or microorganisms (Samuelsson, 1999).

It has been estimated that almost 60 % of present drugs were directly or indirectly derived from natural sources (Newman, 2008). Moreover, a total of 122 compounds isolated from plants are used as drugs (Fabricant and Farnsworth, 2001). The current uses of 80 % of these compounds

correlates with the ethnobotanical uses of the parent plants (Fabricant and Farnsworth, 2001). Isolation and structural elucidation of many bioactive compounds from natural sources allows chemists to synthesize them rather than repeatedly isolating them from these sources thereby decreasing the cost of drug production remarkably (Hong-Fang *et al.*, 2009). The early 1990s witnessed a shift from using natural products as tools for drug discovery to focus on combinatorial chemistry and high-throughput screening to generate and identify new drug candidates (Hong-Fang *et al.*, 2009). Yet, this strategy did not yield the anticipated outcomes in terms of novel drug candidates (Hong-Fang *et al.*, 2009). This was evident in the fact that only seventeen (17) new drugs were approved in 2007, as compared to fifty-three (53) in 1996 (Hughes, 2008). Besides, given the standard period of drug discovery and development which is twelve to fourteen (12-14) years, the majority of the latter were initially identified in the 1980s (Patwardhan *et al.*, 2008; Hughes, 2008). This is turning the attention of researchers back to the use of natural products for drug discovery. A number of potential drug candidates such as curcumin, huperzine A, capsaicin, celastrol and triptolide have been discovered from this latest spotlight on natural products (Corson and Crews, 2007; Ji and Zhang, 2008). Curcumin, huperzine A, capsaicin, celastrol and triptolide were isolated from the plants *Curcuma long Lin, Huperzia serrata, Capsicum annuum and Tripterygium wilfordi* respectively (Ringman *et al.*, 2012; Wang *et al.*, 2006; Caterina *et al.*, 1997; Liu *et al.*, 2015; Wang *et al.*, 2011).

Structures of some drugs obtained directly from plants are shown in Table 1.1. Morphine **[1]** is a major analgesic drug used to treat severe and chronic pain. For instance, pain due to cancer and surgery. Morphine was the first drug isolated from a plant source, *Papaver somniferum* (opium puppy), (Hamilton and Baskett, 2000). The opium puppy has been used for centuries to relieve pain, diarrhea, sleeplessness and to induce euphoria (Rang and Dale, 1987). Reserpine **[2]**, an alkaloid isolated from the root of *Rauwolfia serpentina* and other *Rauwolfia* species, is a drug employed in the clinical treatment of hypertension and some psychiatric disorders such as schizophrenia (Slotkin, 1974; Hoch, 1957). Digoxin **[4]** and Digitoxin **[5]** are cardiac glycosides isolated from *Digitalis* spp. and are used to treat congestive heart failure and cardiac arrhythmias due to atrial fibrillation (Lopez-Lazaro *et al.*, 2005). Vinblastine **[5]** and vincristine **[6]** are vinca alkaloids isolated from the herb, *Catharanthus roseus* (Johnson *et al.*, 1963). Vinblastine **[6]** is a potent drug employed against Hodgkin's disease, lymphomas, chorioepithelioma and certain

cancers of the breast and the bronchus (Johnson *et al.*, 1963). Vincristine **[7]** is also used to hematologically reverse completely acute lymphocytic and myelocytic leukemia in children and to also treat some other kinds of tumors (Johnson *et al.*, 1963). Paclitaxel, marketed under the trade name, Taxol **[3]**, a complex diterpene isolated from the Pacific yew tree *Taxus brevifolia* is a very potent anticancer drug (Sarker *et al.*, 2006b) used to treat ovarian cancer and some other malignant growths (Li and Vederas, 2009).

Table 1.1: Structure, name, plant source and use(s) of some drugs obtained from plants

Name of drug and its structure	**Plant source**	**Clinical use(s)**
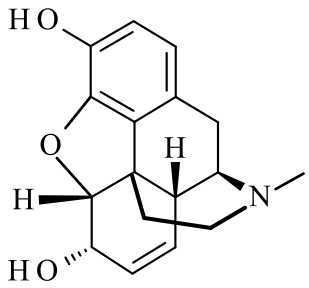 Morphine **[1]**	*Papaver somniferum*	Opioid analgesic drug
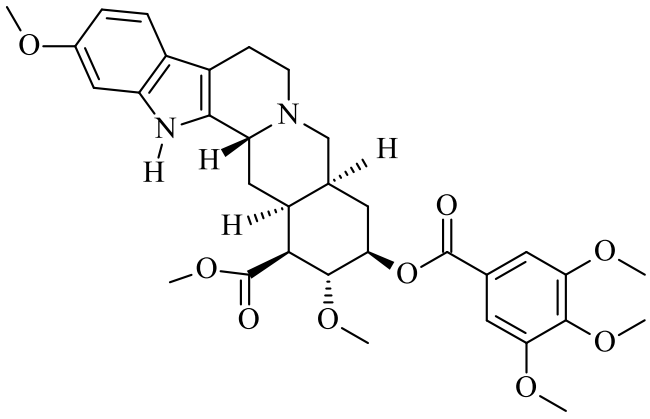 Reserpine **[2]**	*Rauwolfia serpentina* and other *Rauwolfia* species	Anti-hypertensive drug

Name of drug and its structure	Plant source	Clinical uses
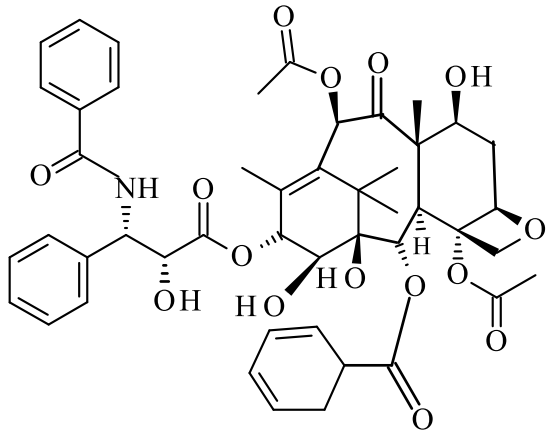 Taxol **[3]**	*Taxus brevifolia* .	Anti-cancer drug
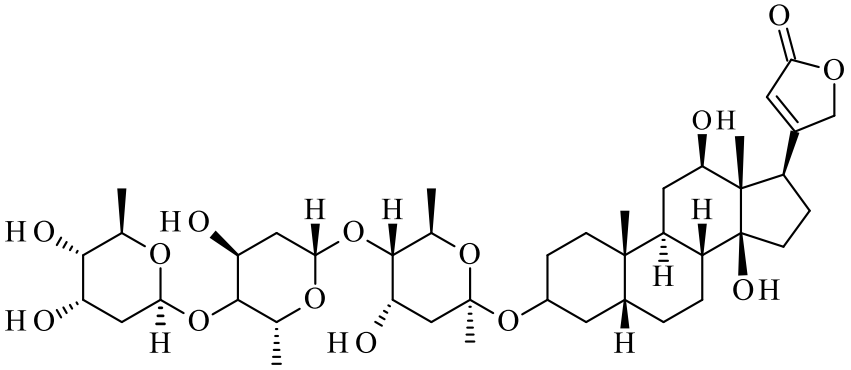 Digoxin **[4]**	*Digitalis spp.*	Drug used to treat congestive heart failure and cardiac arrhythmias
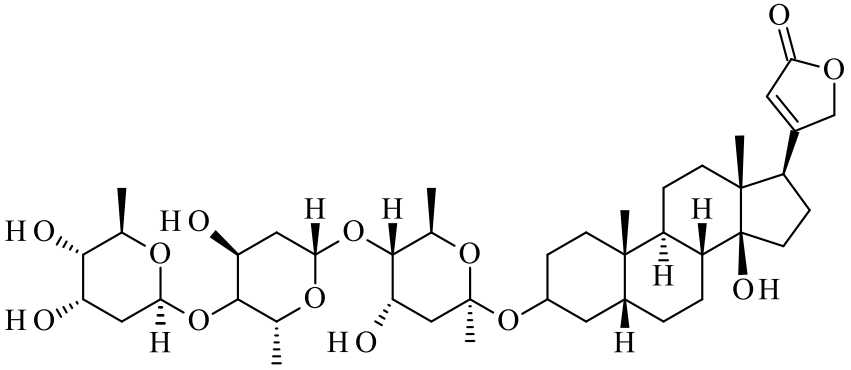 Digitoxin **[5]**		Congestive heart failure and cardiac arrhythmias drug

Name of drug and its structure	Plant source	Clinical use(s)
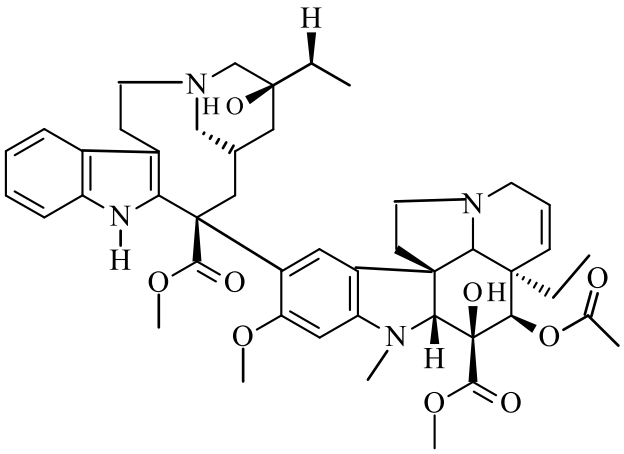 Vinblastine **[6]**	*Catharanthus roseus*	Drug use to treat Hodgkin's disease and cancers
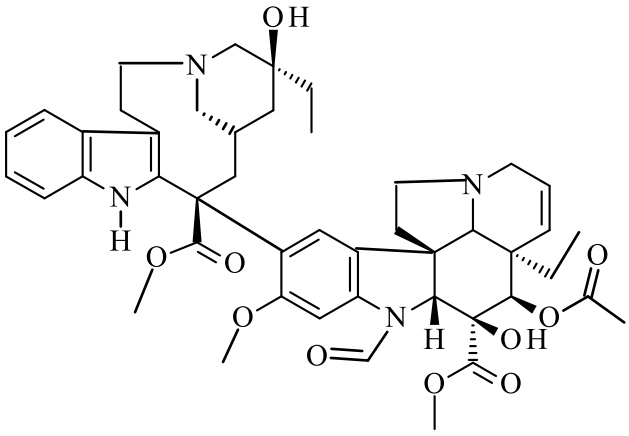 Vincristine **[7]**		Acute lymphocytic and myelocytic leukemia and anticancer drug

Table 1.2 shows structures of some drugs that were synthesized using some plant derived molecules as lead compounds. Artemisinin **[8]** is a sesquiterpenoid isolated from the plant *Artemesia annua*, an herb used in Chinese traditional medicine for more than two millennia as malaria remedy; artemisinin is an effective malaria remedy against multi–drug resistant *Plasmodium* spp; the semi-synthetic analogue of artemisinin called artemether **[9]** is also a potent anti-malaria drug (Li and Vederas, 2009; Klayman *et al.*, 1984). Quinine **[10]** and its derivative,

amodiaquine **[11]** are other valuable drugs used to treat severe malaria caused by *Plasmodium falciparum* (Rosenthal, 2003). Quinine was isolated from the bark of *Cinchona succirubra* and other *Cinchona* spp. (Rates, 2001). Based on the structure of salicin **[12]**, one of the foremost nonsteroidal anti-inflammatory drugs (NSIADs), aspirin **[13]** also known as acetylsalicylic acid was developed. Salicin was obtained from the bark of the willow tree (*Salix alba*) and other *Salix* species. The barks of these plants have been used to treat fevers and inflammatory disorders for more than one and half centuries (Schmid *et al.*, 2001; Vane and Botting, 1987).

The antihyperglycemic principle, galegine **[14]** is the parent molecule of the antidiabetic drug, metformin **[15]** and other biguanidine class of antidiabetic medicines. Galegine was isolated from *Galega officinalis*; a plant use to manage diabetes in traditional medicine (Sneader, 1985). Based on the structure of papaverine **[16]**, the antihypertensive drug, verapamil **[17]**, was developed; papaverine itself is a very valuable smooth muscle relaxant drug (Sneader, 1985). A semi-synthetic form of camptothecin **[18]** obtained from the plant *Camptotheca acuminata* (Kinghorn, 1994), is the anticancer drug, topotecan **[19]** which has been licensed for the treatment of recurring ovarian cancers (Gordon *et al.*, 2001).

Other drugs synthesized based on the structures of plant derived lead molecules were sodium chromoglycate **[21]** and amiodarone **[22]** which are analogues of khellin **[20]** (Sneader, 1985). Naloxone **[23]** and apomorphine **[24]** which are used to treat symptoms of opioid addictions and Parkinson's disease respectively were also derived based on the structure of morphine (Deleu *et al.*, 2004; Rang and Dale, 1987). Chemical simplification of the molecular structure of morphine resulted in the synthesis of the benzomorphan or benzazocine group of opiate analgesic drugs such as levorphanol **[25]**, pentazocin **[26]** and cyclazocin **[27]** which generate mixed agonist-antagonist action at the opioid receptors (Rang and Dale, 1987; Archer *et al.*, 1996).
Atropine **[28]** is the parent compound of tiotropium **[29]**. Tiotropium bromide is an essential drug which effectively inhibits muscarinic receptors irreversibly and is used to treat chronic obstructive pulmonary diseases (COPD) such as chronic bronchitis and emphysema (Komis and Samuel, 2005). Atropine is a tropane alkaloid noted for its antagonism of the muscarinic receptors. It was isolated from the plant *Atropa belladonna* and some plants from the Solanaceae family. Atropine is a major drug listed among the essential medicines by the World Health

Organization (W.H.O.) (WHO, 2005). Atropine is useful in treating bradycardia, gastrointestinal disorders and as premedication for anesthesia (Rang and Dale, 1987). In ophthalmology, atropine is used for the treatment of refractive and accommodative amblyopia (Georgievski *et al.*, 2008). It is also used to suppress further development of myopia in children (Fang *et al.*, 2013).

Other molecules such as mescaline **[30]** and yohimbine **[31]** (Table 1.3) isolated from plant sources are employed as tools (Fabricant and Farnsworth, 2001) to study the pharmacological mechanisms of action of other chemical substances or as drugs. Atropine **[28]** is also employed as a pharmacological tool to search for chemical substances that elicit their pharmacological effects by acting through the muscarinic cholinergic receptor systems.

Table 1.2: Some compounds derived from plants used as leads to synthesize other useful drugs

Lead compound's name and structure	**Drug's name and structure**	**Plant source of lead compound**	**Clinical use(s) of drug**
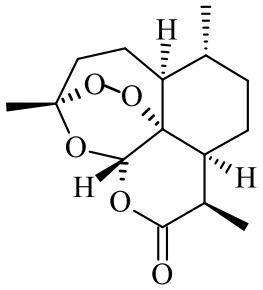 Artemisinin **[8]**	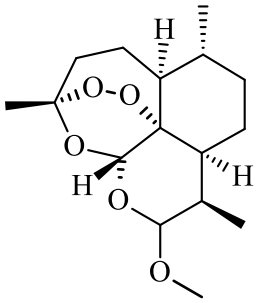 Artemether **[9]**	*Artemisia annua* (Asteraceae)	Antimalaria drug especially for malaria due to chloroquine resistance *Plasmodium falciparum*
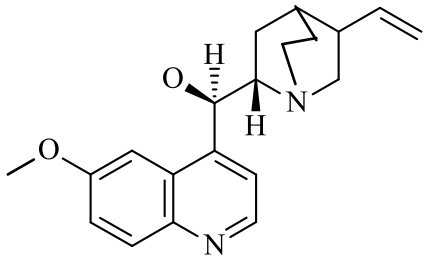 Quinine **[10]**	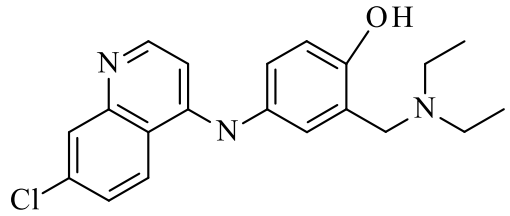 Amodiaquine **[11]**	*Cinchona succirubra* and other *Cinchona* spp. (Rubiaceae)	Antimalaria drug, especially for severe chloroquine resistance malaria

Lead compound'sname and structure	**Drug's name and structure**	**Plant source of lead**	**Clinical use(s) of drug**
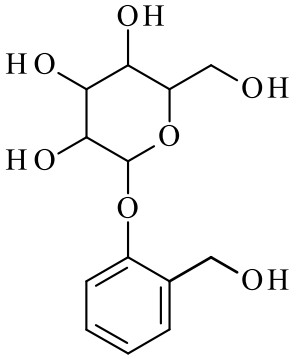 Salicin **[12]**	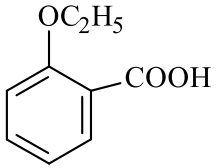 Aspirin **[13]**	*Salix alba*, *Salix purpurea* and *Salix fragilis* (Salicaceae)	Treatment of mild to moderate pain, inflammation and pyrexia
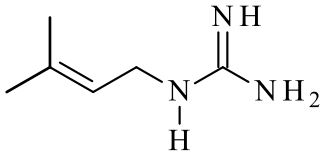 Galegine **[14]**	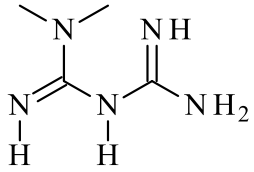 Metformin **[15]**	*Galega officinalis* (Fabaceae)	Antidiabetic agent

Lead compound's name and structure	**Drug's name and structure**	**Plant source of lead compound**	**Clinical use(s) of drug**
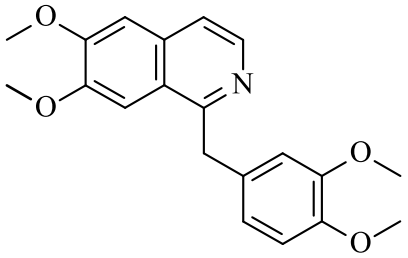 Papaverine **[16]**	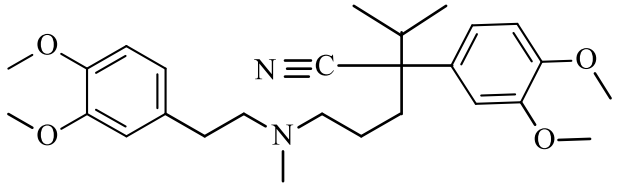 Verapamil **[17]**	*Papaver somniferum* (Papaveraceae)	Treatment of hypertension
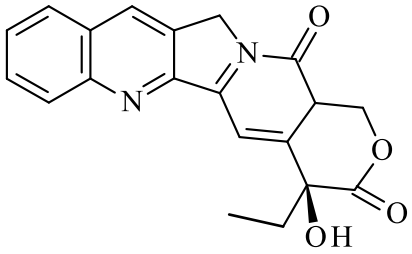 Camptothecin **[18]**	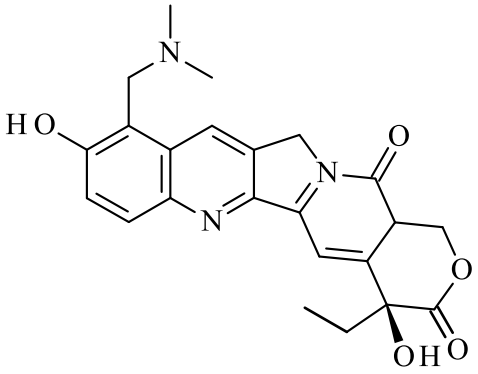 Topotecan [**19**]	*Camptotheca acuminata* (Nyssaceae)	Use to treat recurrent ovarian cancers

Lead compounds name and structure	**Drug's name and structure**	**Plant source of lead compound**	**Clinical use(s)**
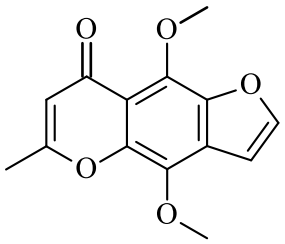 Khellin **[20]**	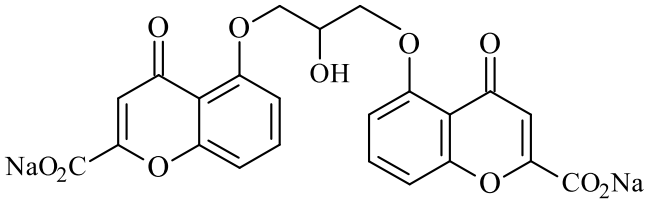 Sodium chromoglycate **[21]**	*Ammi visnaga* (Umbelliferae)	Treatment for asthma and symptomatic relief of breathing difficulties
	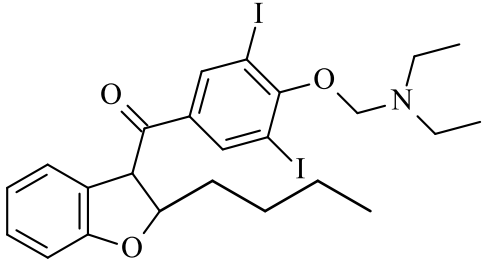 Amiodarone **[22]**		Antiarrhythmic drug

<table>
<tr><th>Lead compound’s name and structure</th><th>Drug’s name and structure</th><th>Plant source of lead compound</th><th>Clinical use(s) of drug</th></tr>
<tr><td rowspan="2"> 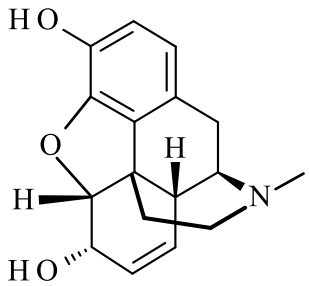
Morphine [1]</td><td> 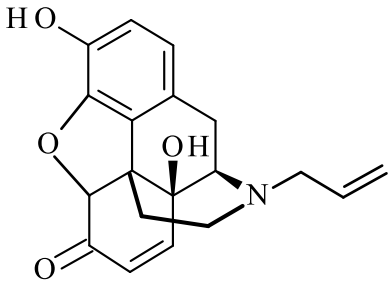
Naloxone [23]</td><td rowspan="2">Papaver somniferum
(Papaveraceae)</td><td>Treatment of symptoms such as respiratory depression, comma and other sings of opioid addiction, e.g. cocaine addiction. It is also used as a tool to search for opioid analgesics</td></tr>
<tr><td> 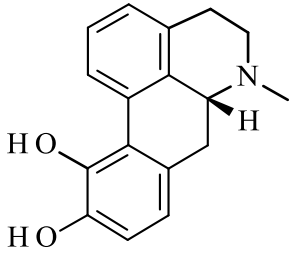
Apomorphine [24]</td><td>Treatment of Parkinson’s disease</td></tr>
</table>

Lead compound's name and structure	**Drug's name and structure**	**Plant source of lead compound**	**Clinical use(s) of drug**
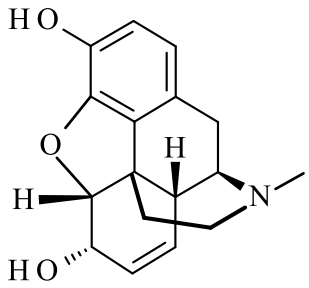 Morphine **[1]**	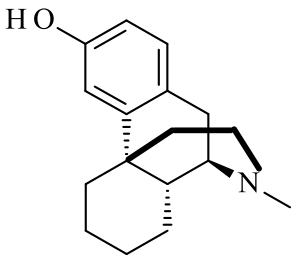 Levorphanol **[25]**	*Papaver somniferum* (Papaveraceae)	Treatment of severe pain and *neuropathic pain that is irresponsive to other opioid drugs
	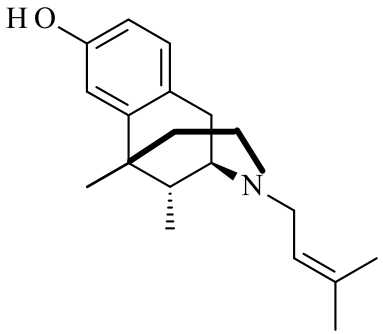 (*R*)-Pentazocin **[26]**		Opioid analgesic drug; Also co-injected with naloxone to effect withdrawal in narcotic addicts

*(Prommer, 2007)

Lead compound's name and structure	**Drug's name and structure**	**Plant source of lead compound**	**Clinical use(s) of drug**
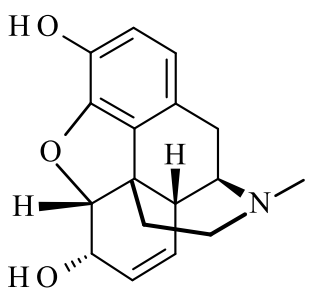 Morphine **[1]**	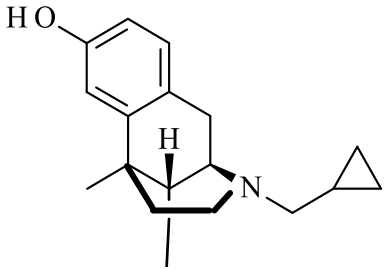 Cyclazocin **[27]**	*Papaver somniferum* (Papaveraceae)	Use in small doses as an analgesic drug and in large doses as treatment for opiate addiction
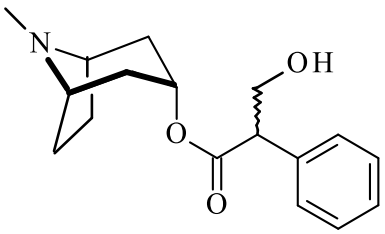 Atropine **[28]**	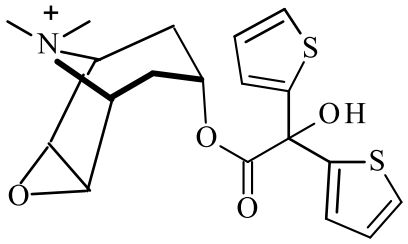 Tiotropium **[29]**	*Atropa belladonna* (Solanaceae)	Treatment of chronic obstructive pulmonary disease (COPD) including bronchitis and emphysema

Table 1.3: Structure and other uses of some compounds obtained from plants

Name of drug and its structure	Plant source	Uses
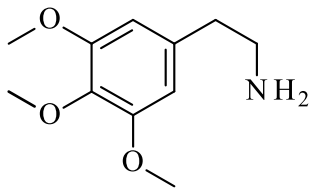 Mescaline **[30]**	*Lophophora williamsii* (Cactaceae)	Use as a psychodelic drug especially for recreational purposes
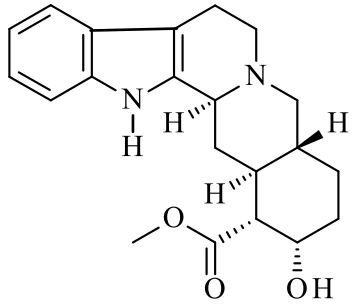 Yohimbine **[31]**	*Pausinystalia yohimbe* (Rubiaceae)	Treatment of symptoms relating to erectile dysfunction. Also used as a pharmacological tool tosearch for α_2-adrenoceptors

Some natural products including secondary metabolites obtained from other sources apart from plant origins have also been successfully developed into drugs that are clinically used in the treatment of various human ailments. Extensive scientific investigations of marine organisms for drug candidates have yielded neurotoxic and cytotoxic molecules (Li and Vederas, 2009) some of which have successfully been developed into drugs (Table 1.4). The cytotoxic drug trabectedin (Yondelis) **[32]**, a product of *Ecteinascidia turbinata,* anocean squirt found in the tropics, is used to treat advanced spongy-tissue cancers (Dalisay *et al.*, 2008).

Ziconotide **[33]** is a new non-opioid analgesic drug which is a synthetic form of ω-conotoxin MVIIA (ω-MVIIA). ω-conotoxin MVIIA (ω-MVIIA) is a peptide toxin isolated from the venom of the carnivorous sea cone snail (*Conus magnus*) (McGivern, 2007; Li and Vederas, 2009).

Ziconotide **[33]** has distinctive mechanism of action which involves effective and selective inhibiton of N-type neuronal voltage-sensitive calcium channels (VSCCs) which direct neuro transmission at many synapses along the neuronal circuit (McGivern, 2007). Ziconotide **[33]** was approved just a decade ago for the treatment of severe chronic pain due to spinal cord injury, cancers and neuropathic pain in patients only by intrathecal (i.t) administration and it was found to produce more potent analgesia than morphine and does not produce addiction or tolerance over prolong use (McGivern, 2007; Li and Vederas, 2009).

Spongothymidine **[34]** and spongouridine **[35]** which were isolated from the Caribbean sea sponge (Newman and Cragg, 2004) provided prototypes in the synthesis of the anti-HIV drug zidovudine (Azidothymidine) **[36]** (Fischl *et al.*, 1990). Moreover, Spongothymidine and spongouridine are believed to be the parent compounds of all nucleoside drugs (Suckling, 1991).

Microorganisms have also been providing mankind with some extraordinary medicines such as antiparasitic drugs (e.g. ivermectin B1a **[37]** and B1b **[38]**), lipid management agents (e.g., lovastatin **[39]** and mevastatin **[40]**), immunosuppressants for organ transplants (e.g. rapamycin **[41]**), anticancer drugs (e.g. doxorubicin **[42]**) antibiotic agents (e.g. penicillin G **[43]**, tetracyclines represented by chlortetracycline **[44]**, erythromycin **[45]** and streptomycin **[46]**) and antidiabetic agents (e.g. acarbose **[47]**), (Harvey, 2000; Li and Vederas, 2009; Laube, 2013; Zhang *et al.*, 2013; Lomovskaya *et al.*, 1999) (Table 1.5).

Some chemical substances found in the human body (e.g., adrenaline, histamine, levodopa, histamine, hydrocortisone, estrogen, progesterone and testosterone) are also employed as drugs in treating ailments linked to their physiological activities (Sneader, 2005).

Table 1.4: Structure, name and uses of some drugs obtained from marine organisms

Name of drug and its structure	Marine source	Clinical use(s)
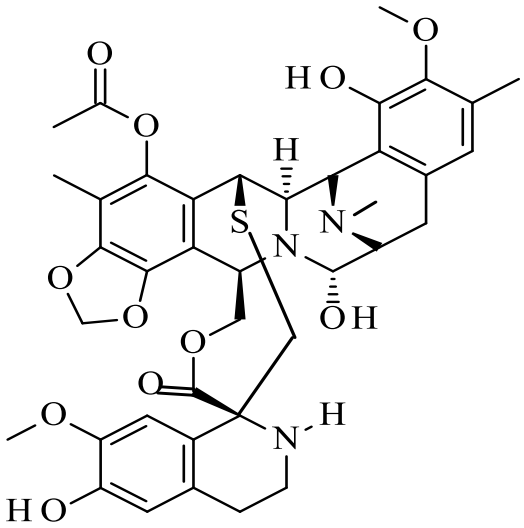 Trabectedin (Yondelis) **[32]**	*Ecteinascidia turbinata*	Treatment of progressive spongy-tissue cancer

Name of drug and its structure	Marine organism	Clinical uses
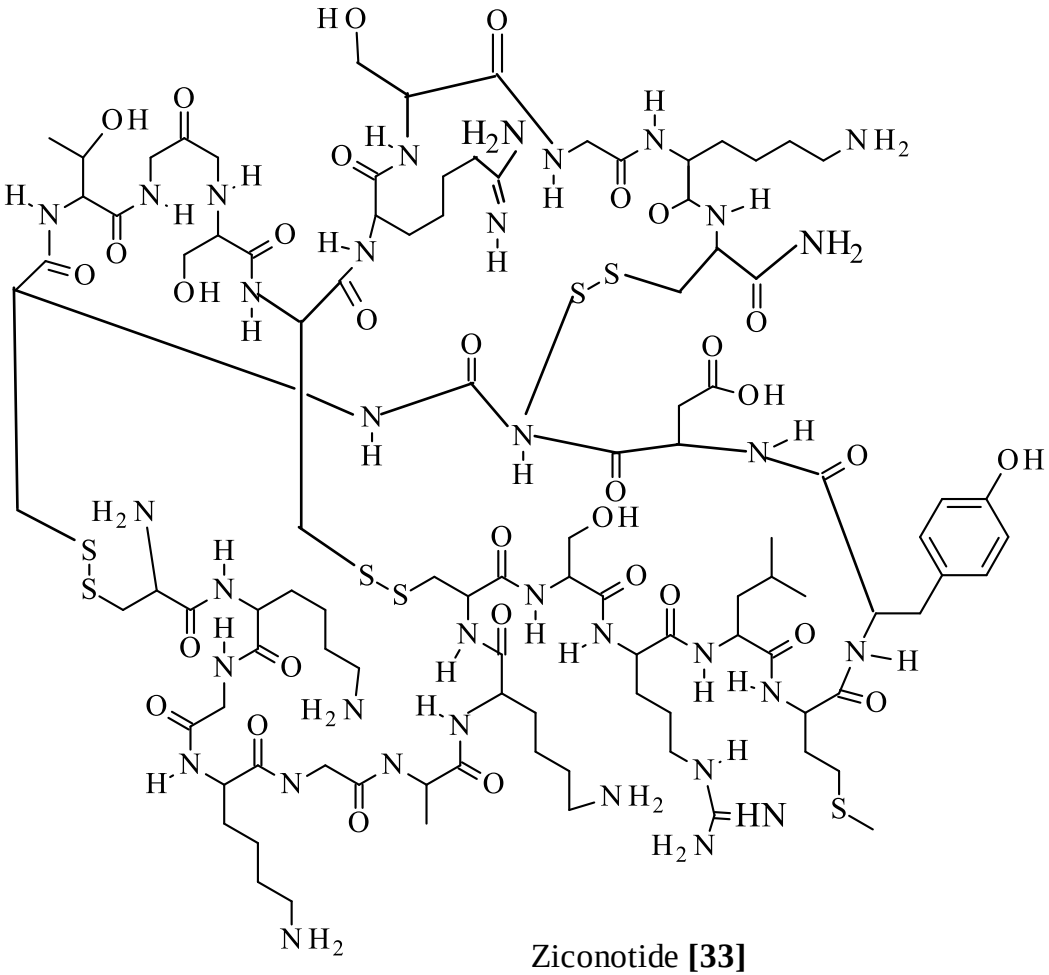 Ziconotide **[33]**	*Conus magnus* (Conidae)	Treatment of severe chronic pain emanating from neuropathic or spinal cord injury or cancers and other chronic diseases

Lead compounds	Drug's name and structure	Marine organism	Clinical uses of the drug
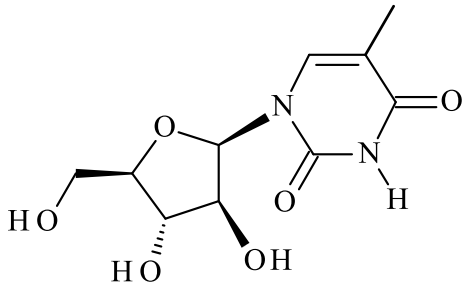 Spongothymidine **[34]**	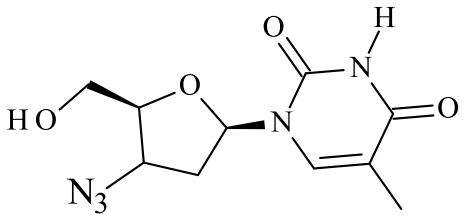 Azidothymidine (AZT) **[36]**	*Tectitethya crypta* (Tethyidae)	Use for treatment of HIV and other viral infections
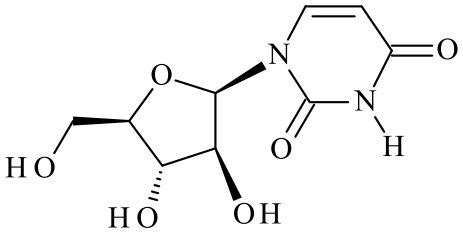 Spongouridine **[35]**			

Table 1.5: Structure, name and uses of some drugs isolated from microorganism

Name of drug and its structure	Source microorganism	Clinical use(s)
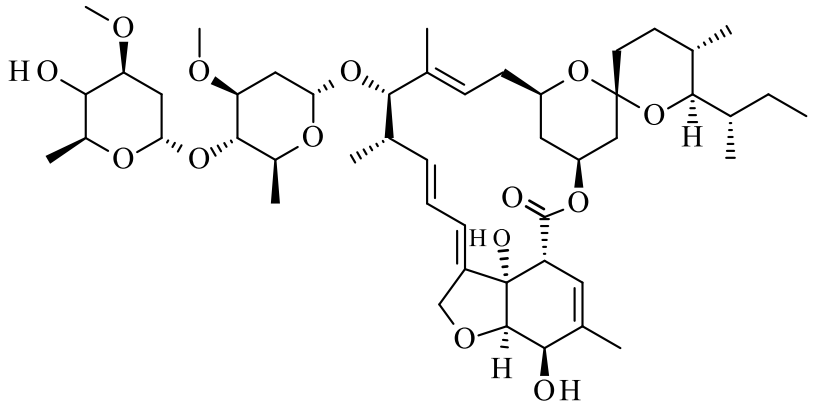 Ivermectin B1a **[37]**	*Streptomyces avermitilis* (Streptomycetaceae)	Broad range antiparasitic drugs employed against arthropods and helminthes
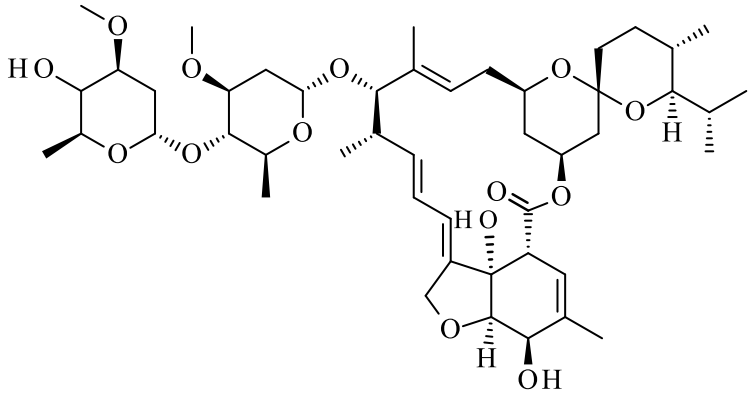 Ivermectin B1b **[38]**		

Name of drug and its structure	Source microorganism	Clinical use(s)
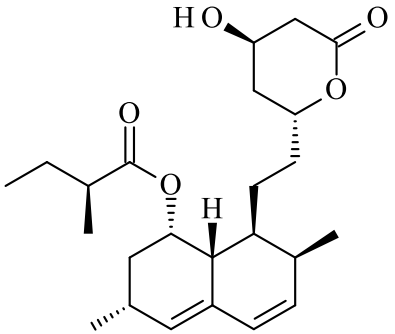 Lovastatin **[39]**	*Pleurotus astreatus* (Pleurotaceae)	Hypercholesterolemia drug use in treatment of high cholesterol level
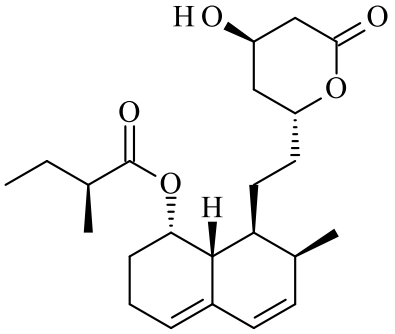 Mevastatin **[40]**	*Penicillium citrinum* (Trichocomaceae)	

Name of drug and its structure	Source microorganism	Clinical use(s)
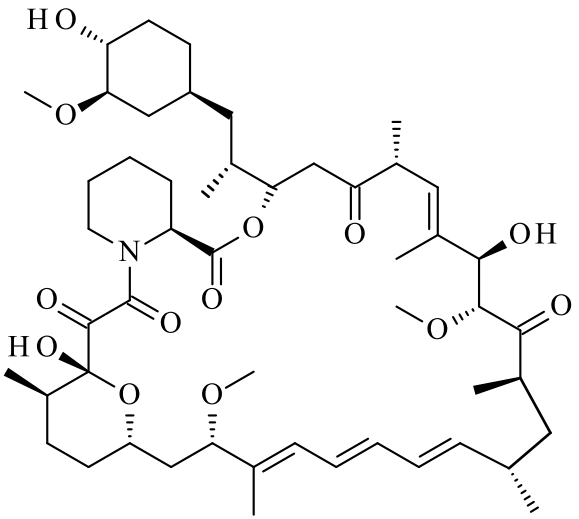 Rapamycin **[41]**	*Streptomyces hygroscopicus* (Streptomycetaceae)	Used as an immunosuppressant in organ transplant in other to prevent rejection
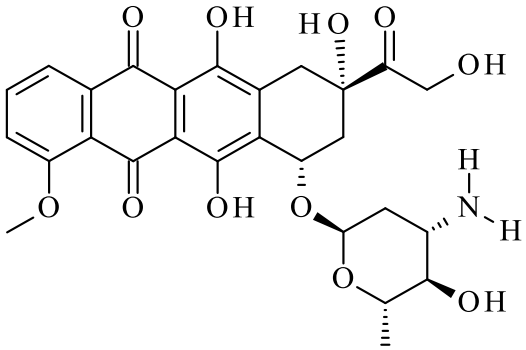 Doxorubicin **[42]**	*Streptomyces peucetius* (Streptomycetaceae)	Cytotoxic drug use to treat ovarian, breast and lung cancers

Name of drug and its structure	Source microorganism	Clinical use(s)
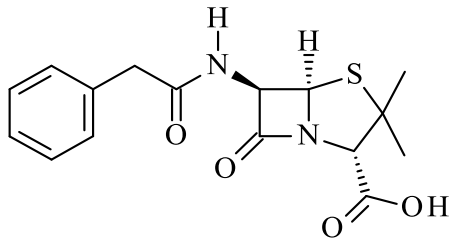 Penicillin G **[43]**	*Penicillium chrysogenum* (Trichocomaceae)	Antibiotic drug. Used especially against infections caused by gram-positive bacteria
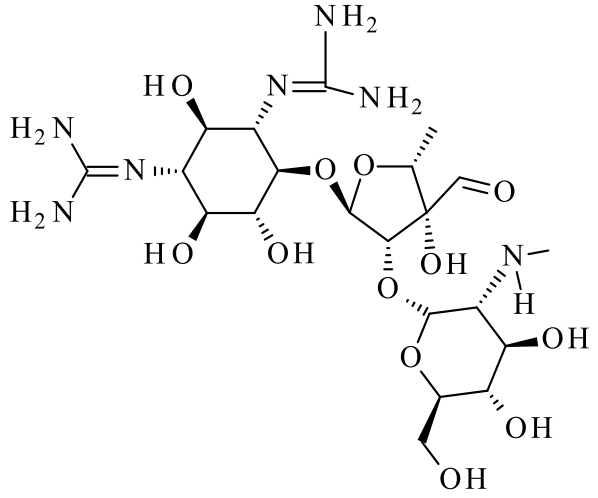 Streptomycin **[44]**	*Streptomyces griseus* (Streptomycetaceae)	Employed in the treatment of bacterial infections and tuberculosis

Name of drug and its structure	Source microorganism	Clinical use(s)
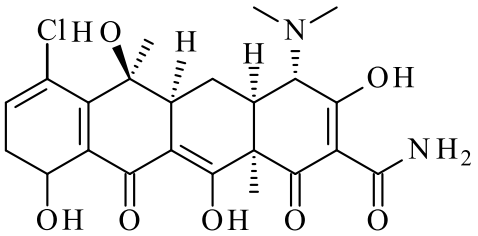 Chlortetracycline **[45]**	*Streptomyces aureofaciens* (Streptomycetaceae)	Broad spectrum antibiotic drug
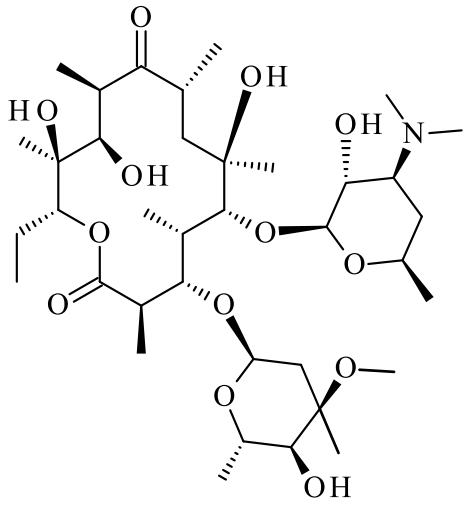 Erythromycin A **[46]**	*Saccharopolyspora erythraea* (Streptomycetaceae)	Antibiotic drug

Name of drug and its structure	Source microorganism	Clinical uses
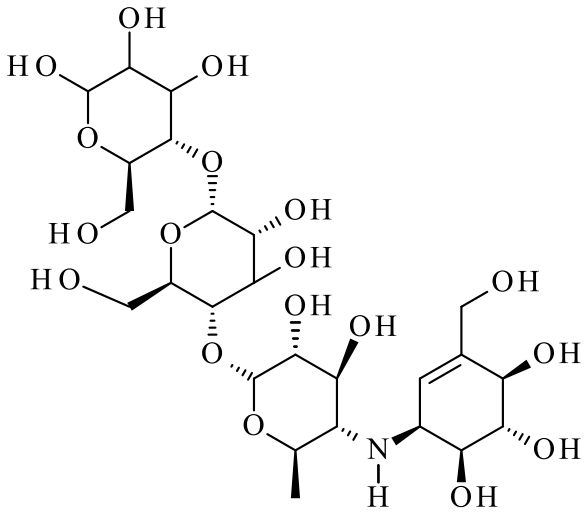 Acarbose **[47]**	*Streptomyces luteogriseus* (Streptomycetaceae)	Employed in the treatment of type 2 diabetes

1.2 JUSTIFICATION AND IMPORTANCE OF THE STUDY

Considering the adverse effects and other problems associated with current anti-inflammatory and analgesic drugs, the search for alternative anti-inflammatory and pain killing agents with more potency has become necessary, especially from folkloric medicinal plants which have provided the human race with many known vital drugs. Besides, the literature survey indicated that the anti-inflammatory and analgesic activities in addition to the mechanism of antinociceptive action of *C. anisata* root and *A. polycarpa* stem and root barks have not been investigated. The chemical compounds responsible for these pharmacological actions of these plants have also not been investigated despite their use in traditional medicine to treat various inflammatory and painful conditions. This research work is therefore necessary and important so as to provide scientific basis for the use of these plants as anti-inflammatory and analgesic agents in traditional medicine and in addition, investigate the chemical compounds in the plants that are responsible for these pharmacological effects.

1.3 AIMS AND OBJECTIVES

1.3.1 Aims

This research therefore seeks to investigate the anti-inflammatory and analgesic properties of *C. anisata* root and *A. polycarpa* stem and root barks with the major goal of isolating the active constituents responsible for their observed activities. The study is also focused on determining the mechanism of antinociceptive action of the crude extracts and isolates so as to classify them as opioids or cholinergic agonists.

1.3.2 Specific Objectives

The following specific objectives were laid down to help achieve the above aims.

- To investigate the analgesic and anti-inflammatory activities of the ethanol extracts of *C. anisata* root and *A. polycarpa* stem and root bark.
- To fractionate the crude ethanol extracts and evaluate the anti-inflammatory and analgesic activities.

- To isolate and characterize the anti-inflammatory and analgesic constituents from the active fraction(s) of *C. anisata* root and *A. polycarpa* stem and root barks.
- To evaluate the anti-inflammatory and analgesic activities of the isolated compounds where possible.
- To study the mechanisms of antinociception of the extracts of *C. anisata* root and *A. polycarpa* stem bark and their active isolates where possible.

CHAPTER TWO

LITERATURE REVIEW

2.1 BOTANICAL AND MORPHOLOGICAL FEATURES OF THE PLANTS

2.1.1 *Clausena anisata* (Wild) Hook f. ex. Benth

Clausena anisata (Wild) Hook f. ex. Benth (Figure 2.1) is a medicinal plant in the Rutaceae family of flowering plants which grows up to 10 m high and thrives in and on the boundaries of evergreen forest (Mshana *et al.*, 2000). Its leaves are made of 10 to 17 opposite or alternate leaflets which are pinnately compound with a terminal one (Mshana *et al.*, 2000). The leaves are compactly spotted with glands and turn out strong scent similar to aniseed when pressed. Its branched inflorescences start off with an axillary spray which bears small, white and attractive flowers with yellow to orange stamens (Mshana *et al.*, 2000). The plant is indigenous to Africa, mostly in West and North Africa (Ayensu, 1978; Burkill, 1966). It is called "Horse wood" by the natives of Mozambique (Burkill, 1966). It is commonly known as Clausena or spirit plant; Synonyms of *C. anisata* include *Amyris anisata* (Wild), *Clausena inequalis* (DC) Benth, *Clausena pobeguini* and Var *abyssinica* Engl. Its stem bark is grey or mottled in color. *C. anisata* bears drupe-like yellowish green fruits which become blue-black on ripening (Hutchings *et al.*, 1996; Ghana Herbal Pharmacopoeia, 1992).

Figure 2.1:Whole plant and roots of *C. anisata*

2.1.2 *Annickia polycarpa,* Stten and Mass

Annickia polycarpa, Stten and Mass (Hawthorne and Gyakari, 2006) also known as *Enantia polycarpa* Engl. and Diels (Irvine, 1961) is a member of the Annonaceae family of flowering plants. The description of *A. polycarpa* is given below according to Irvine (Irvine, 1961). It is a tree that grows up to 18.30 m high and 0.91 m wide with thin unbuttressed trunk, and hard greenish grey bark which show a bright yellow color and dazzling yellow wood when slashed. The wood however, slowly turns brown. The leaves are 20.30 - 30.50 cm long and 8.90 cm wide, ovate to elliptic – oblong or oblong-lanceolate in shape without indentation with an obtuse base. Simple and stellate hairs are located on their lower surface. The leaves also possess 8 - 10 pairs of lateral nerves. The tree bears flowers with diminutive external silky hairs from May – June with 30 or extra free hairless carpels. The stalks of the carpels are 2.54 - 3.80 cm long. The flowers are solitary, 1 to 2 in number situated on thickened pedicels up to 2.54 cm long. The greenish petals of the flowers are thick and up to 1.90 - 2.54 cm long. The black elliptical fruits which are 1.24 - 2.54 cm long are connected to their base by 5.08 cm long stalks.

Figure 2.2: Wholeplant and slashed stem of *A. polycarpa*

2.2 ETHNOPHARMACOLOGICAL USES OF THE PLANTS

2.2.1 Ethnopharmacological uses of *C.anisata*

The leaves are used to prepare tea which is employed as blood cleanser and as a remedy against halitosis due to hepatic disorders; leave decoctions are also drunk or inhaled to cure mental illness (Pujol, 1990). The leaves of *C. anisata* are used in the management of hypertension in South Africa (Okunade, 1987). Moreover, dermatitis and intestinal helminthiasis are also treated with the leaves. The leaves' essential oil is also employed as parasiticide (Mshana *et al.*, 2000). The leaves' decoction is taken as a stomachic and a laxative post-partum in addition it being used to treat several gastrointestinal disorders (Adesina and Adewunmi, 1985; Ayensu, 1978).

A root preparation of *C. anisata* is given as an enema or bathing lotion to treat inconsequential health conditions and to mitigate early signs of pyrexia or to avert the incidence of pyrexia in children. Furthermore, decoction of *C. anisata* root is taken at half a wine glass twice a day to remedy cardiovascular disorders and halitosis (Pujol, 1990). Asthmatic conditions are also treated with the roots (Mshana *et al.*, 2000). A decoction made from the roots is drunk by children to manage convulsions and taken by expectant mothers as a tonic (Ngadjui *et al.*, 1989a). The roots also find use in the treatment of rheumatism and abdominal pain in children (Adesina and Adewunmi, 1985; Ayensu, 1978).

The leaves and roots are also used to treat dysentery fever, toothache and arthritis (Adesina and Adewunmi, 1985; Ayensu, 1978; Mshana *et al.*, 2000). A mouth wash made from the boiled roots and leaves is used to alleviate toothache and to treat oral infections (Adesina and Adewunmi, 1985; Ayensu, 1978). The roots and stem barks are used against herpes zoster (Mshana *et al.*, 2000).

The leaf, root and stem of *C. anisata* have been reported as effectual remedy against flatworm infestations, like taeniasis and schistosomiasis (Hutchings *et al.*, 1996).

It has also been reported that *C. anisata* is used in the treatment of oral candidiasis and fungal skin diseases by Tanzanian traditional healers (Hamza *et al.*, 2006). The use of *C. anisata* to treat

epilepsy and convulsions by traditional healers in Temeke district of Daressalam (Tanzania) has also been reported (Moshi *et al.*, 2005). The plant has also been reported as a remedy for broad array of other ailments such as insanity, dementia, infertility, impotence, leprosy, syphilis, gonorrhea, gingivitis, headaches, respiratory and cardiovascular disorders, constipation and gastroenteritis (Hutchings *et al.*, 1996).

'Agbo' is a concoction made of *C. anisata*, *Azadirachtha indica* and *Afraegle paniculata* which is used as an antimalaria preparation in Nigeria (Uwaifo, 1984).

2.2.2 Non medicinal uses of *C. anisata*

C. anisata is broadly used as insect-repellent (Ayensu, 1978). The fresh leaves are burnt to repel mosquitoes in Philippines and various parts of Africa (Uwaifo, 1984). The plant is also employed as tool handles, firewood and building poles (Hutchings *et al.*, 1996). Chewing sticks made from *C. anisata* are used as tooth brushes in several areas of Africa (Hutchings *et al.*, 1996).

2.2.3 Ethnopharmacological uses of *A. polycarpa*

The bark is used in Côte d'Ivoire traditional medicine to treat malaria (Atindehou *et al.*, 2004). The juice of the bark or its (bark) decoction is used in treating eye infections, leprous wounds and injuries (Bouquet and Debray, 1974; Irvine, 1961). The bark extracts are used in Nigeria as antimalaria and antibacterial remedies (Ajali, 2000). The bark of wild *A. polycarpa* is used to prepare a drink that is taken by Anyi-Ndenye women in Eastern Côte d'Ivoire during the first trimester of pregnancy for maintenance (Malan and Neuba, 2011).

In Ghana, *A. polycarpa* is employed in the treatment of malaria fever, fever and stomach ulcer (Govindasamy *et al.*, 2007). *A. polycarpa* also found uses in traditional medicine as antipyretic and ulcer therapy in diverse West African countries (Bep, 1986). Furthermore, *A. polycarpa* is widely used in keeping dental hygiene as chewing stick in Cote d'Ivoire (Cunningham, 1993).

2.2.4 Non medicinal uses of *A. polycarpa*

The wood is widely employed in constructing furniture, for example beds, and building houses due to its malleability and lightness (Irvine, 1961). The wood is also used in making canoes, paddles and xylophones (Irvine, 1961). The Guere people in the southeast Ivory Coast also make

use of *A. polycarpa* as part of ingredients in making a hunting arrow poison (Neuwinger, 1998; Irvine, 1961).

2.3 THE CHEMISTRY AND BIOLOGICAL ACTIVITIES OF *C. ANISATA*

2.3.1 Biological activities of the crude extracts of *C. anisata*

Okokon and co-workers (Okokon *et al.*, 2012) investigated the anti-inflammatory and antipyretic activities of the ethanolic leaves extract of *C. anisata* and found out that the extract administered intraperitoneally (i.p) at 39–117 mg/kg, dose dependently reduced inflammation and pyrexia in different experimental animal models. The mean lethal dose (LD_{50}) of the ethanolic leaves extract was 393.7 ± 25.64 mg/kg (Okokon *et al.*, 2012). The methanolic roots extract of *C. anisata* was shown to demonstrate significant dose-dependent hypoglycemic activity in fasted streptozotocin treated and fasted normal diabetic rats at a dose of 100-800 mg/kg (p.o). (Ojewole, 2002). A comparative study on the anti-epileptic activity of the root, stem and leaf of *C. anisata* revealed that the ethanol extract of the root bark possessed anti-epileptic activity with 33.33 % anti-convulsant effect (Kenechukwu *et al*., 2012).

2.3.2 Compounds isolated from *C. anisata* and their biological activities

Several phytochemical studies have been previously carried out on all morphological parts of *C. anisata* which led to isolation of many secondary metabolites which were mainly carbazole alkaloids, coumarins, limonoids and few phytosteroids and amine derivatives.

2.3.2.1 Carbazole alkaloids

Phytochemical investigations of the stem and root of *C. anisata* led to isolation of the carbazole alkaloids; atanisatin **[49]** and clausanitin **[50]** respectively (Okorie, 1975). Isolation of mupamine **[51]** from C. *anisata* was also reported (Mester and Reisch, 1977). Furthermore, clausenine **[52]** and clausenol **[53]** were isolated from the alcoholic extract of the dried stem bark of *C. anisata* (Chakraborty *et al.*, 1995).

Antibiotic activities of the carbazole alkaloids, clausenine **[52]** and clausenol **[53]** were investigated against Gram-positive and Gram-negative bacteria in addition to fungi; clausenol **[53]** was found to be extremely active than clausenine **[52**] and its (clausenol) inhibition against some bacteria was comparable to that observed for streptomycin (Chakraborty *et al.*, 1995).

Three new lactonic carbazole alkaloids called clausamine A **[54]**, clausamine B **[55]** and clausamine C **[56]** were further isolated from the branches of *C. anisata* in their racemic forms (Ito *et al.*, 1998). These new alkaloids contained a 1-oxygenated carbazole structure with an annulated six-member lactone ring in the 3,4-position and were the first examples of carbazole alkaloids with a lactone moiety isolated from natural source (Ito *et al.*, 1998).

Chromatography of the acetone extract of the dry branches of *C. anisata* also yielded four new carbazole alkaloids, namely; clausamine D **[57]**, clausamine E **[58]**, clausamine F **[59]** and clausamine G **[60]** in addition to clausine E **[61]**, clausine F **[62]**, methyl carbazole, 3-carboxylate **[63]**, *O*-demethylmurrayanine **[64]** and ekebergine **[65]** which were known (Ito *et al.*, 2000). The new carbazoles, clausamine D **[57]**, clausamine E [**58**], clausamine F **[59]** and clausamine G [**60**] were classified as 1-oxygenated 3-carbomethoxy carbazole alkaloids possessing a prenyl or related substituent group at C-4 of the carbazole nucleus. Additionally, clausamine G **[60]** have a hydroperoxy group in its structure and was the first peroxygenated carbazole alkaloid isolated from natural source (Ito *et al.*, 2000). All these alkaloids demonstrated antitumor - promoting activity against Epstein-Barr virus early antigen activation induced by 12-*O*-tetradecanoylphorbol-13-acetate in Raji cells assay (Ito *et al.*, 2000). Furthermore, clausamine E **[58]** exhibited cytotoxic action against human leukemia cell line HL-60 (Ito *et al.*, 2009). Clausine E **[61]** and clausine F [**62]** were shown to inhibit rabbit platelet aggregation and induced vasocontraction (Wu *et al.*, 1996; Wu and Huang, 1992). Two gamma lactone carbazole alkaloids named furanoclausamine A **[66]** and furanoclausamine B **[67]** isolated from the stem of *C. anisata* have also been reported (Ito *et al.*, 2009).

The isolation of the novel quinolone alkaloid, 1-methyl-3, 4-dimethoxy-2-quinolone **[68]** together with the carbazole alkaloids:3-methylcarbazole **[69]**, heptaphyline **[70]**, girinimbine **[71]** and 3-formyl-1-hydroxycarbazole **[72]** from the collective stem bark and root extracts of *C.*

anisata have been described (Ngadjui *et al.*, 1989d). Finally, the recent isolation of murrayamine A **[73]** from the methanol extract of the stem bark of *C. anisata* is also worth noting (Songue *et al.*, 2012).

The compound, 3-methylcarbazole **[69]** is the core intermediate involved in the biogenesis of carbazole alkaloids in higher plants; the isolation of 3-methylcarbazole **[69]** and many of its C-3 oxidized substituted analogs from plants shows that its methyl group is oxidatively removed in the formation of the carbazole alkaloids in the biogenetic reaction (Chakraborty and Roy, 1991; Bhattacharyya and Chakraborty, 1987).

Heptaphyline **[70]** exhibited anti-plasmodia activity against *Plasmodium falciparum* with an IC_{50} value of 5.5-10.7 µg/mol (Yenjai *et al.*, 2000). Girinimbine **[71]** was shown to possess anticancer activity by induction of apoptosis on lung cancer cells *in vitro* with IC_{50} of 19.01 μM which was mediated via both intrinsic and extrinsic pathways reliant on caspase mediation (Syam *et al.*, 2013). Murrayamine A was shown to produce rabbit platelet aggregation inhibition with an IC_{50} of 2 µg/mL (Wu *et al.*, 1998).

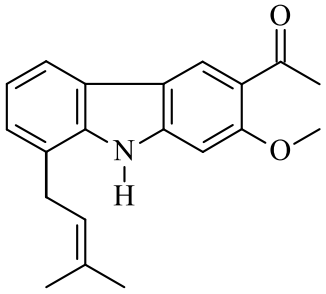

Atanisatin **[49]**

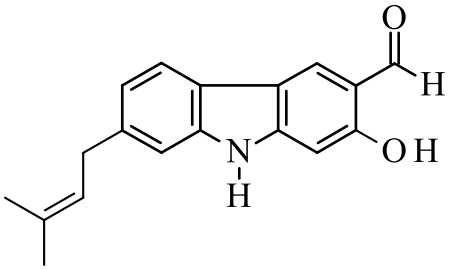

Clausanitin **[50]**

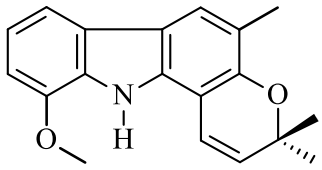

Mupamine **[51]**

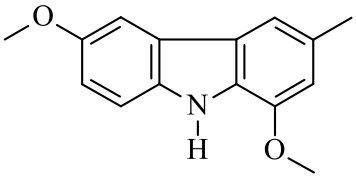

Clausenine **[52]**

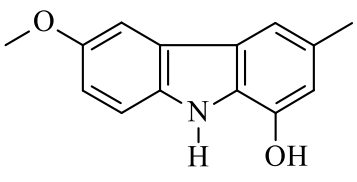

Clausenol **[53]**

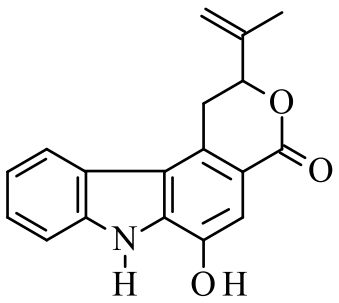

Clausamine A **[54]**

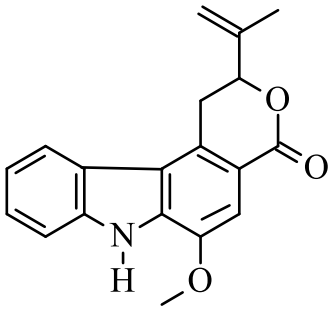

Clausamine B **[55]**

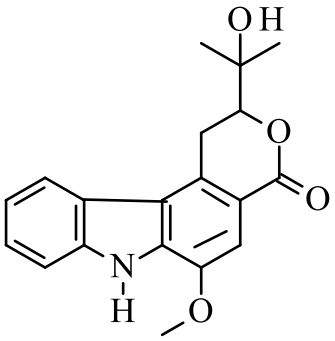

Clausamine C **[56]**

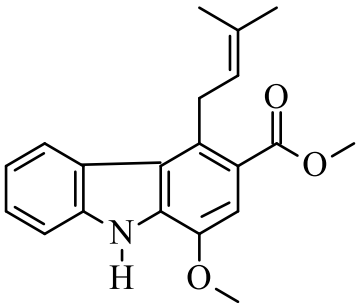

Clausamine D **[57]**

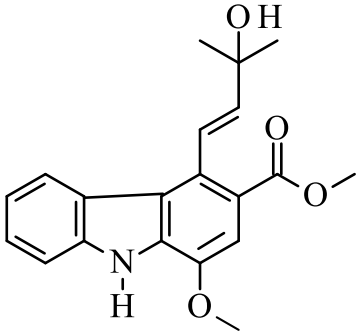

Clausamine E **[58]**

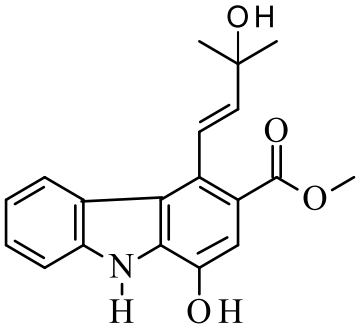

Clausamine F **[59]**

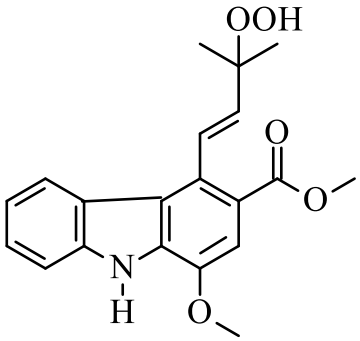

Clausamine G **[60]**

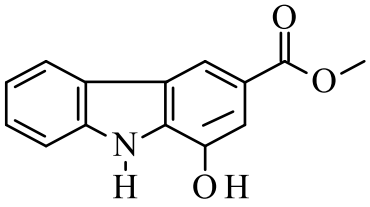

Clausine E **[61]**

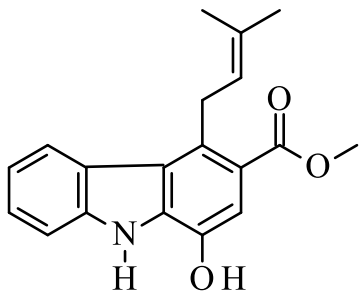

Clausine F **[62]**

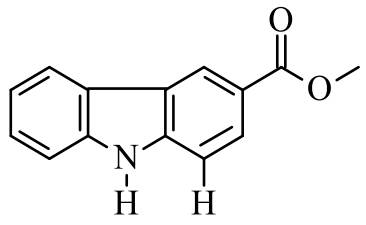

Methyl carbazole-3-carboxylate **[63]**

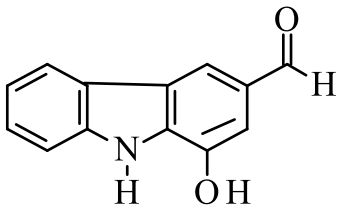

O-demethylmurrayanine **[64]**

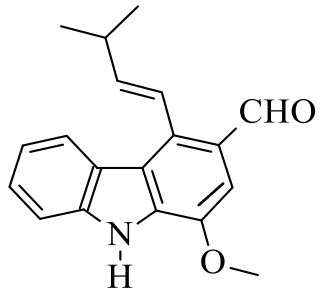

Ekebergine **[65]**

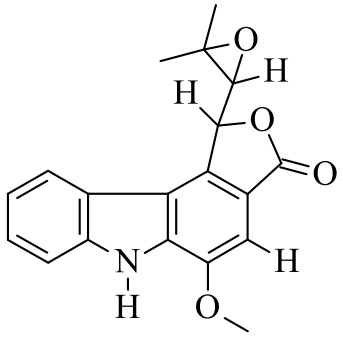

Furanoclausamine A **[66]**

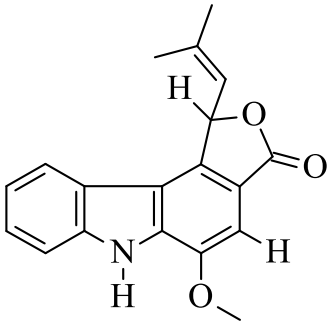

Furanoclausamine B **[67]**

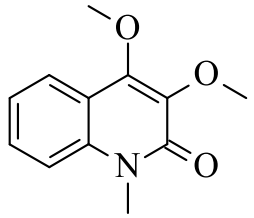

1-methyl-3,4-dimethoxy-2-quinolone **[68]**

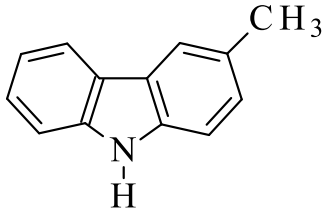

3-methylcarbazole **[69]**

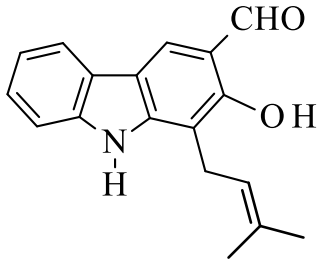

Heptaphyline **[70]**

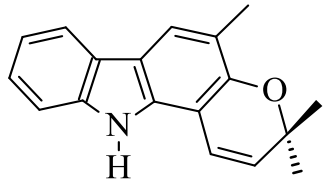

Girinimbine **[71]**

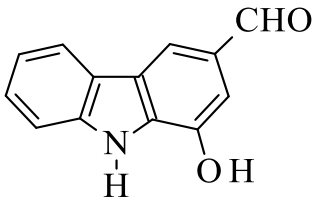

3-formyl-1-hydroxycarbazole **[72]**

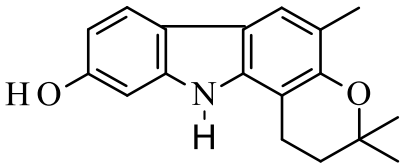

Murrayamine A **[73]**

Figure 2.3: Structures of carbazole and a quinolone alkaloid(s) isolated from *C. anisata*

2.3.2.2 Peptide derivatives and phytosterols

Some other compounds previously isolated from *C. anisata* include amide derivatives such as N-benzoylphenylalaninyl-N-benzoylphenylalaninate **[74]**, aurantiamide acetate **[75]**, lansamide-I **[76]** (Lakshmi *et al.*, 1984) in addition to a mixture of two phytosterols namely;sitosterol **[77]** and stigmastorol **[78]** (Songue *et al.*, 2012) (Figure 2.4).

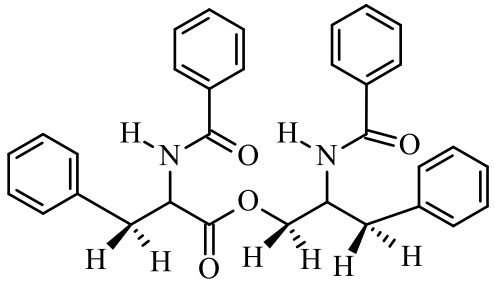

N-benzoylphenylalaninyl-N-benzoylphenylalaninate **[74]**

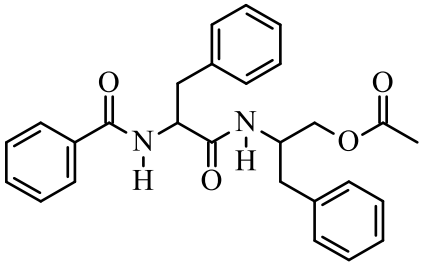

Aurantiamide acetate **[75]**

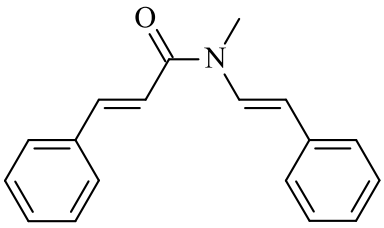

Lansamide -I **[78]**

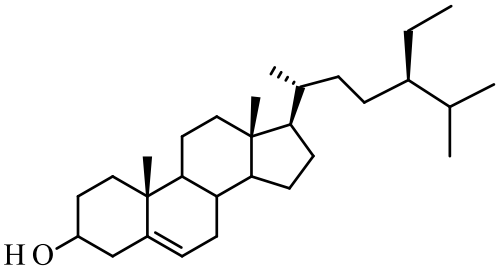

Sitosterol **[76]**

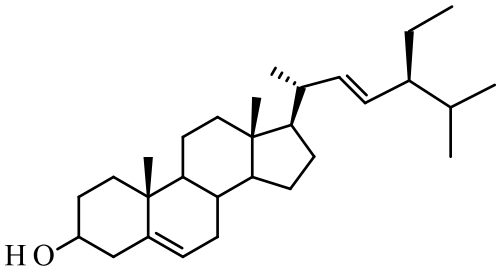

Stigmasterol **[77]**

Figure 2.4: Structures of phytosteroids and amide derivatives from *C. anisata*

Aurantiamide acetate showed effective antioxidant and antibacterial activity (Tamokou *et al.*, 2012). Additionally, aurantiamide acetate was found to inhibit cysteine proteinases, especially, cathepsin L (3.4.22.15) and B (3.4.22.1) with IC_{50} values of 12 and 49 µM, respectively, and

further suppressed hind paw edema when administered at 10 mg/kg body weight subcutaneously (s.c.) in adjuvant induced-arthritic model in rat (Isshiki *et al.*, 2001). Aurantiamide acetate and *N*-benzoylphenylalaninyl-*N*-benzoylphenylalaninate inhibited AChE with IC_{50} of 111.34 μM and 137.6 μM in Ellman's assay, respectively, which compares to that of the standard drug, physostigmine (IC_{50} = 141.51 μM) (Alves *et al.*, 2013).

2.3.2.3 Coumarins

Lakshmi and coworkers isolated two furanocoumarins; imperatorin **[79]** and xanthotoxol **[80]** in addition to three new furanocoumarin lactone analogues namely, 2', 3'-epoxyanisolactone **[81]**, indicolactone **[82]** and anisolactone **[83]** during their phytochemical investigation of *C. anisata* (Lakshmi *et al.*, 1984). In addition, other furanocoumarins such as chalepin **[84]** and oxypeucedanin **[85]** (Emerole *et al.*, 1981) and a prenylated coumarin, osthol **[86]** were isolated from the root of *C. anisata* (Olufemi *et al.*, 2009). Chromatographic investigation of the collective stem bark and root extracts of *C. anisata* also yielded coumarins such as: xanthoxyletine **[87]**, swietnocoumarin I **[88]**, gravelliferonemethylether **[89]**, heliettin **[90]**, anisocoumarin A **[91]**, anisocoumarin B **[92]**, anisocoumarin C **[93]** and anisocoumarin D **[94]** (Ngadjui *et al.*, 1989a). Furthermore, the leaves of *C. anisata* also yielded prenylated coumarins such as capnolactone **[95]**, anisocoumarin E **[96]**, anisocoumarin F **[97]**, anisocoumarin G **[98]**, anisocoumarin H **[99]**, and triphasiol **[100]** upon chromatography (Ngadjui *et al.*, 1989c). The structures of these coumarins from *C. anisata* are shown in Figure 2.5.

Imperatorin demonstrated anti-inflammatory action in lipopolysaccharide-stimulated mouse macrophage (RAW264.7) *in vitro* and in carrageenan-induced mouse paw edematogenic test; in addition, imperatorin also inhibited protein expression of inducible nitric oxide (NO) synthase and cyclooxygenase-2 in lipopolysaccharide-stimulated RAW264.7 (Huang *et al.*, 2012).

The furanocoumarin, xanthotoxol is known to demonstrate various biological activities. Xanthotoxol showed anti-inflammatory effects in both acute and chronic inflammation models in rats and mice and also lowered the prostaglandin E content in the inflammatory tissue exudate from rat hind paw induced by means of carrageenan (Qishen *et al.*, 1998). Furthermore, xanthotoxol showed efficient remedy for arrhythmia induced by aconitine in rats, raised the

threshold of ventricular fibrillation induced in rabbits using electrical stimulation and inhibited action potential amplitude of isolated sciatic nerves in toads. These results proved that xanthotoxol possessed antiarrhythmic activity (Qishen *et al.,* 1996). Dose-dependent sedative effect was also observed for xanthotoxol in mice, rats, hamsters, cats and dogs; xanthotoxol further abolished predatory mouse/rat killing actions in cats and dogs when given at 5-20 mg/kg intraperitoneally (i.p.) and 3-100 mg/kg orally (p.o.) respectively, caused a dose-dependent decline in locomotor action, blocked amphetamine-induced hyper mobility in hamsters and mice, increased the electrical threshold in foot-shock-induced aggressive activity and antagonized conditioned and unconditioned reaction in rats (Sethi *et al.*, 1992). The LD_{50} of xanthotoxol in mice was 47.0 mg/kg (i.v.) (Qishen *et al.*, 1996) and 468 mg/kg (i.p) (Sethi *et al.*, 1992) respectively. Moreover, no dysfunction in reproductive effects or endocrine activities were observed in rats treated with xanthotoxol at 10-80 mg/kg p.o in a chronic toxicity studies for six months with the F1 generations of rats from these parents showing no sign of teratogenicity (Sethi *et al.*, 1992). The furanocoumarin, xanthotoxol also demonstrated effective antioxidant capacity in both lipid peroxidation and hemolysis tests (Ng *et al.*, 2000). In addition, antitussive, antiasthmatic and expectorant activities of xanthotoxol were reported (Xiao *et al.*, 2006). Xanthotoxol stopped brain injury induced by focal cerebral ischemia-reperfusion, an effect thought to be mediated by its anti-inflammatory properties (He *et al.*, 2009).

Imperatorin and xanthotoxol along with some other coumarins isolated from *Clausena lansium* twigs demonstrated weak cytotoxic effects against oral cavity cancer (KB), breast cancer (MCF7) and small cell lung cancer (NCI-H187) human melanoma cell lines with respective IC_{50} values of 26.97, 11.92 and 40.41 µg/mL for imperatorin and 9.60, 37.62 and 28.58 µg/mL for xanthotoxol (Wisanu *et al.*, 2010).

By employing the procedure of bioactivity guided-isolation, 2',3'-epoxyanisolactone and anisolactone were isolated from the root of *Feroniella lucida* and were shown to demonstrate antioxidant activity by protecting rat's brain homogenate against lipid peroxidation with IC_{50} of 56 and 58 µM respectively (Phuwapraisirisan *et al.*, 2006).

Chalepin showed the highest inhibition of the glycolytic enzyme glycossomal glyceraldehyde-3-phosphate dehydrogenase (GAPDH) in *Trypanosoma cruzi* (the causative agent of Chagas'

disease) with IC_{50} of 64 μM among 13 different compounds hence making chalepin a possible drug candidate against Chagas' disease (Vieira *et al.*, 2001).

Imperatorin and oxypeucedanin were reported to have antimutagenic effects (Wall *et al.*, 1988; Cai *et al.*, 1997), induced uterus contraction, raised blood pressure (Chi and Kim, 1970) and exhibited anticancer activity (Oh *et al.*, 2002). Oxypeucedanin has also been employed as a drug in treating headache, perspiration, and edema (Chi and Kim, 1970). Moreover, oxypeucedanin has been reported to stop the growth of human prostate carcinoma DU145 cell by G2-M cell cycle arrest, and cause apoptotic cell death (Kang *et al.*, 2009). When oxypeucedanin was assayed for its phytotoxic, antibacterial, antifungal, antioxidant and cytotoxic activities using various biological models, it was found to possess high degree of phytotoxicity and cytotoxicity with IC_{50} of 314 μg/mL in the cytotoxic test but inactive in the rest of the assays (Razavi *et al.*, 2010). Oxypeucedanin showed significant antifeedant activity against the larvae of *Spodoptera littoralis* with antifeedant index (AI) of 41.92 ± 18.747; in that same experiment, imperatorin showed phagostimulant effect (Ballesta-Acosta *et al*., 2008).

Imperatorin and osthol exhibited anticonvulsant activity in mice with ED_{50} values ranging from 167 to 290mg/kg and 253 to 639 mg/kg respectively and when they were further assayed for their neurotoxicity in the chimney test, imperatorin gave mean toxic dose (TD_{50}) of 329 - 443 mg/kg and that of osthol was 253 – 639 mg/kg (Baek *et al.*, 2000; Luszczki *et al*., 2009).

Osthol inhibited the movement and invasion of breast cancer cells by wound healing and transwell tests, stopped matrix metalloproteinase-s promoter and enzyme action in luciferase and zymography tests (Yang *et al.*,2010). Additionally, osthol was reported to show broad spectrum of antifungal action against major plant pathogens like *Rhizoctonia solani*, *Phytophtora capsici*, *Botrytis cinerea, Sclerotinia sclerotiorum,* and *Fusarium graminearum* (Wang *et al.*,2009*).*

The major link between osthol presence and antifeedant activity of the root and leaf extracts of *C. anisata* were studied and osthol content was reported to be responsible for 99% of the difference in antifeedant effect of the root as compared to the leaf indicating osthol as the

possible active antifeedant principle of *C. anisata* root against *Helicoverpa armigera* (Olufemi *et al.*, 2009).

The hypoglycemic action of osthol was shown when it was administered at 50 mg/kg and it effectively maintained and/or decreased the blood glucose level in db/db diabetic mice after 3 weeks of treatment at about 210 mg/dL whiles that of the control group was increased to 400 mg/dL from baseline glucose level of 200 mg/dL in both groups of animals (Liang *et al.*, 2012).

Earlier investigations by Tsassi *et al.*, 2010, established that xanthoxyletin possesses antibacterial, fungicidal and algicidal activities. Furthermore, xanthoxyletin demonstrated cytotoxic action by inducing S-phase arrest and apoptosis in human gastric adenocarcinoma SGC-7901 cells (Azhar *et al.*, 2011).

Heliettin showed larvicidal activity against *Aedes aegypti* and *Anopheles stephensi* mosquitoes with IC_{50} value of 67.5 µg/mL (Ravi *et al.*, 2012).

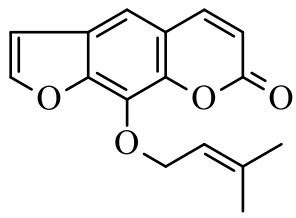

Imperatorin **[79]**

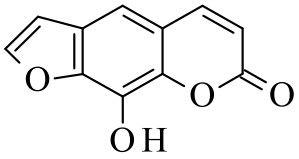

Xanthotoxol **[80]**

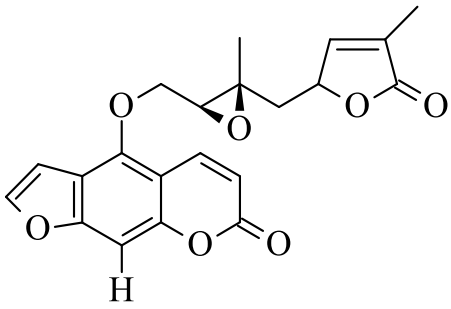

2',3'-epoxyanisolactone **[81]**

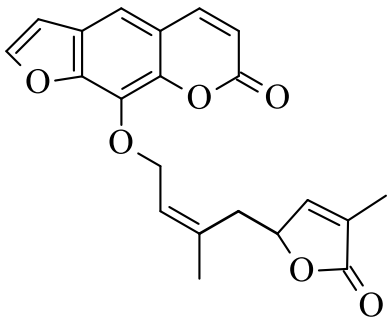

Indicolactone **[82]**

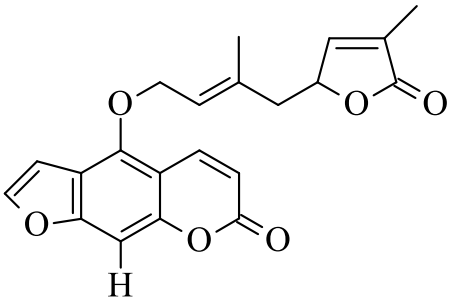

Anisolactone **[83]**

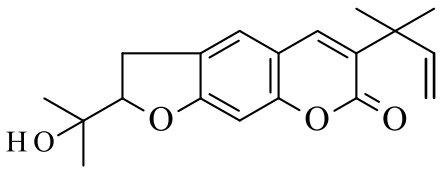

Chalepin **[84]**

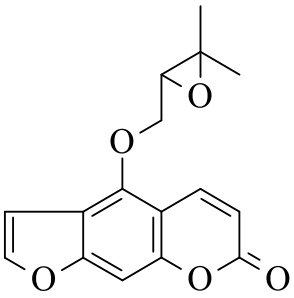

Oxypeucidanin **[85]**

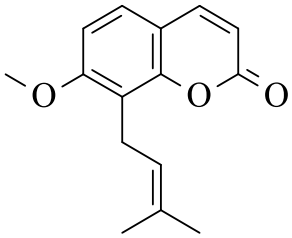

Osthol **[86]**

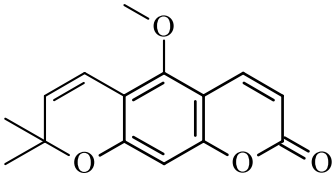

Xanthoxyletin **[87]**

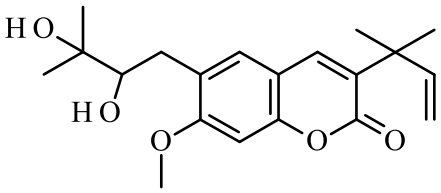

Swietnocoumarin I **[88]**

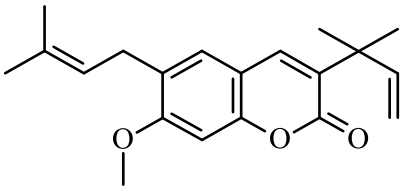

Gravelliferone methyl ether **[89]**

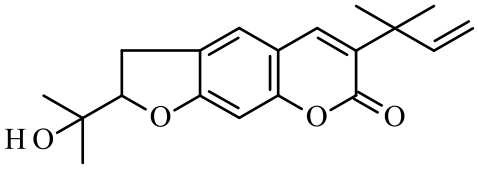

Heliettin **[90]**

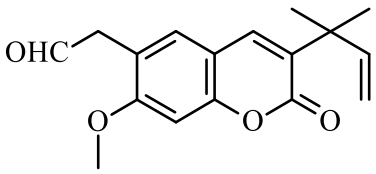

Anisocoumarin A **[91]**

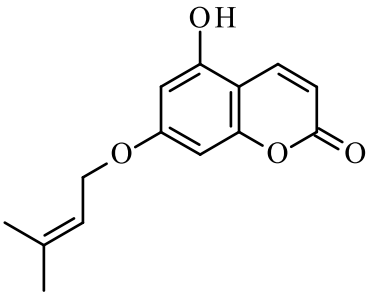

Anisocoumarin B **[92]**

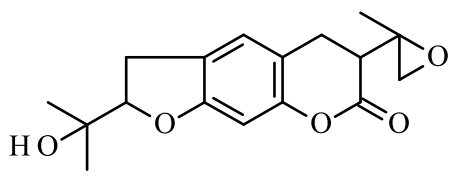

Anisocoumarin C **[93]**

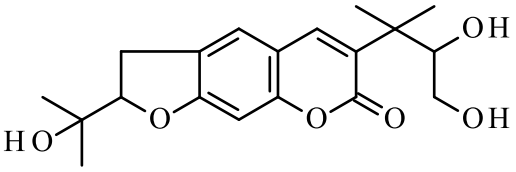

Anisocoumarin D **[94]**

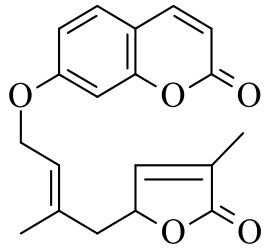

Capnolactone **[95]**

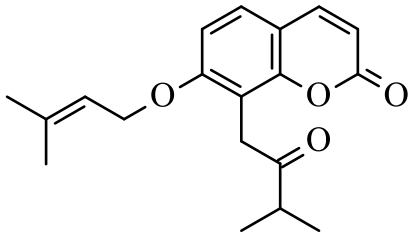

Anisocoumarin E **[96]**

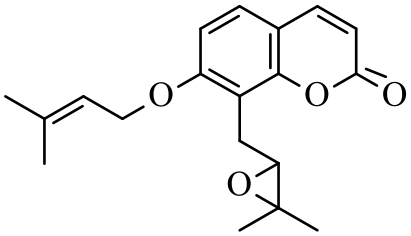

Anisocoumarin F **[97]**

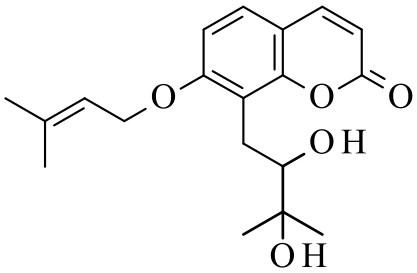

Anisocoumarin G **[98]**

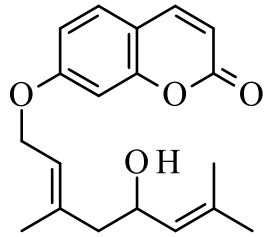

Anisocoumarin H **[99]**

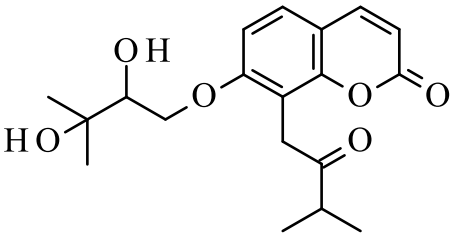

Triphasiol **[100]**

Figure 2.5: Structures of coumarins isolated from *C. anisata*

2.3.2.4 Limonoids

The limonoids, clausenolide **[101]**, clausenarin **[102]**, zapoterin **[103]**, clausenolide -1 -ethyl ether **[104]** and limonin **[105]** (Figure 2.6) were isolated from the chloroform and pet ether extracts of the collective root and stem of *C. anisata* (Ngadjui *et al.*, 1989b).

Clausenolide -1-ethyl ether showed anti-HIV property in 1A2 cell line in syncytium assay (Sunthitikawinsakul *et al.*, 2003).

Limonin given orally at 30 or 100 mg/kg body weight showed significant antinociceptive and anti-inflammatory activities in various animal models (Matsuda *et al.*, 1998). Limonin also demonstrated anti-HIV activity by inhibiting HIV-1 protease and production of HIV-1 p-24 antigen in infected monocytes and macrophages (Battinelli *et al.*, 2003). Moreover, naturally occurring limonin showed significant ($p < 0.01$) antifeedant activity against the insect pest, *Spodoptera frugiperda* (Ruberto *et al.*, 2002).

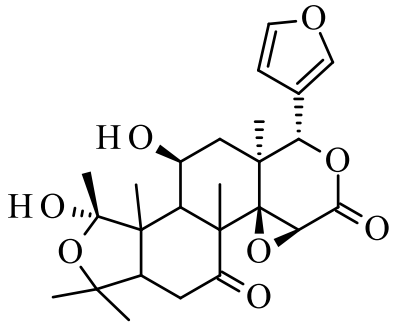

Clausenolide **[101]**

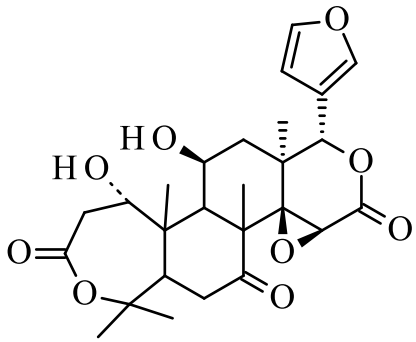

Clausenarin **[102]**

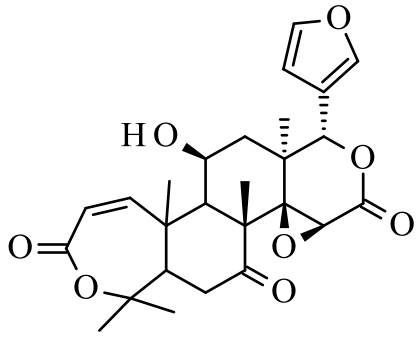

Zapoterin **[103]**

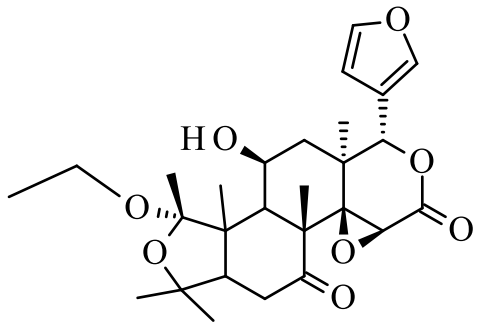

Clausenolide -1-ethyl ether **[104]**

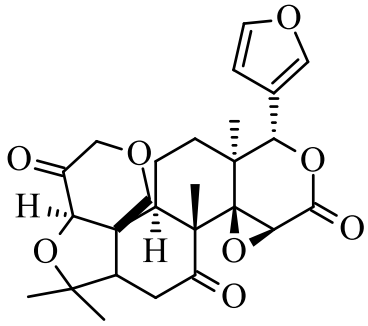

Limonin **[105]**

Figure 2.6: Structures of limonoids isolated from *C. anisata*

In a study conducted on *Evodia officinalis* fruits extract to classify its constituent that showed preincubation-time dependent inhibitory effects on cytochrome P450 3A4 (CYP3A4) in human liver microsomal erythromycin N-demethylation activity assay, limonin was isolated as one of the components which induced remarkable reduction in residual CYP3A4 activity with an IC_{50} values of 23.5 and 1.8 µM respectively (Iwata *et al.*, 2005). Limonin was reported to exhibit various biological activities such as potentiating glutathione S-transferase (GST) in different organs of mice (Lam *et al.*, 1989), anticancer activity in rodents by inhibition of forestomach, buccal punch, lung skin carcinogens (Lam *et al.*, 1994) and suppressed colon tumor formation in azoxymethane (AOM)-induced tumorigenesis assay in male rats by significantly reducing the proliferation of aberrant crypt foci (AFC) (Tanaka *et al.*, 2000).

2.4 THE CHEMISTRY AND BIOLOGICAL ACTIVITIES OF *A. POLYCARPA*

2.4.1 Biological activities of the crude extracts of *A. polycarpa*

Bolou *et al.*,2011 reported that the aqueous and 70% ethanolic extract of the bark of *A. polycarpa* showed antibacterial activity against *Salmonella typhimurium*, *Samonella typhi* and *Pseudomonas aeruginosa*. The aqueous extract was most active against *Samonella typhi* with MIC and MBC of 10 ± 2.5 µg/mL and 10 mg/mL respectively (Bolou *et al.*, 2011). The antibacterial activity of the petroleum ether, chloroform, acetone, ethanol and methanol stem bark extracts of *A. polycarpa* were determined against five microorganisms using the agar diffusion assay (Ajali, 2000). The acetone and ethanol extract showed activity against only *Bacillus subtilis* with IC_{50} values of 5.4 and 4.8 ug/mL respectively (Ajali, 2000). The methanol extract was most active against *Bacillus subtilis* with IC_{50} value of 3.0 ug/mL; the chloroform and the petroleum ether extracts were inactive (Ajali, 2000). The 90% ethanolic stem bark extract of *A. polycarpa* showed a high *in vitro* activity against *Trypanosoma brucei rhodesiense* with IC_{50} value of 0.5 ug/mL and cytotoxicity against L-6 rat skeletal myoblast cells (IC_{50} = 318.2 ug/mL) and selectivity index of 616 (Atindehou *et al.*, 2004). In this same investigation, the 90% ethanolic extract was found to be active against chloroquine and pyrimethamine resistant K1 strain of *Plasmodium falciparum* with IC_{50} of 0.126 ug/mL (Atindehou *et al.*, 2004).

2.4.2 Compounds isolated from *A. polycarpa* and their biological activities

All previously isolated compounds from this plant were alkaloids. They include protoberberine, aporphine, oxoaporphine, isoquinoline, benzyltetrahydroisoquinoline and some cinchona alkaloids.

2.4.2.1 Protoberberine alkaloids

Five quaternary protoberberine alkaloids namely; columbamine **[106]**, palmatine **[107]**, jatrorrhizine **[108]**, oxypalmatine **[109**] and pseudopalmatine [**110]** (Figure 2.7) have been isolated from this plant by various investigators (Jossang *et al.*, 1977; Buzas *et al.*, 1959).

Meimei and co-workers showed that columbamine **[106]** could be a potential remedy for osteosarcoma by demonstrating the effectiveness of columbamine **[106]** to suppress the propagation and neovascularization of metastatic osteosarcoma U2OS cells *in vitro* with IC_{50} of 21.31 ± 0.38 μM (Meimei *et al.*, 2012). Columbamine **[106]** and palmatine **[107]** were found to significantly suppress xylene-induced ear inflammation and acetic acid induced pain in mice and in-vitro production of nitric oxide and nuclear factor-kB activation in RAW264.7 macrophage cells in response to lipopolysaccharide or tumor necrosis factor stimulation (Liu *et al.*, 2010).

In a separate study, columbamine **[106]** and palmatine **[107]** demonstrated anti-inflammatory, anti-nociceptive and antipyretic activities in serotonin-induced hind paw edema, acetic acid-induced increase in vascular permeability, p-benzoquinone-induced writhing and FCA-induced increased rectal temperature tests (Küpelia *et al.*, 2002).

Columbamine **[106]**, jatrorrhizine **[108]** and the aporphinoid, magnoflorine **[114]**, which were isolated from *Mahonia aquifolium*, a plant used to treat psoriasis, were found to exhibit antioxidant activity in lipoxygenase and lipid hydroperoxide assays (Mišík *et al.*, 1995). Columbamine **[106]** and jatrorrhizine **[108]** showed potent antifungal action against the spores of plant pathogenic fungi such as *Alternaria cajani*, *Helminthosporium* spp. *Fusariumudum Bipolaris* spp. and *Curvularia* spp.(Singha *et al.*, 2010). Columbamine **[106]**, palmatine **[107]**, jatrorrhizine **[108]** and the oxoaporphine alkaloid lysicamine **[120]** all demonstrated anti-malaria, anti-trypanosomiasis and anti-leishmaniasis activities (Malebo *et al.*, 2013).

Palmatine **[107]** inhibited monoamine oxidase enzyme with IC_{50} of 90.6 µM, attenuated apoptosis of hepatocytes and relieved liver injury by controlling cytokine reaction (Lee *et al.*, 1999; Lee *et al.*, 2010b). Palmatine **[107]** protected the hearts of rat against myocardial ischemia-reperfusion (I/R) damage due to its antioxidant and anti-inflammatory properties (Kim *et al.*, 2009). Hsieh and a team of researchers (Hsieh *et al.*, 1993) established that palmatine **[107]** increased the hypomotility effect by alpha-methyl-p-tyrosine, reserpine and 5-hydroxytryptophan but decreased the hypermotility generated by L-dopa plus benserazide and p-chlorophenylalanine. They also found out that palmatine **[107]** significantly lowered the level of dopamine and homovanillic acid in the cortex and the concentration of serotonin in the brain stem. It however increased the concentration of 5-hydroxytryptophan in the cortex and 5-hydroxyindole acetic acid in the brain stem. It was concluded that the sedative properties of palmatine **[107]** may be due to its ability to reduce the concentration of catecholamine in the cortex and serotonin in brain stem and to elevate the amount of 5-hydroxytryptophan, in the cortex of the brain (Hsieh *et al.*, 1993).

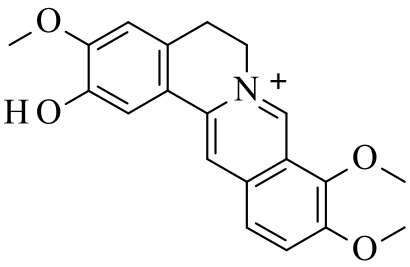

Columbamine **[106]**

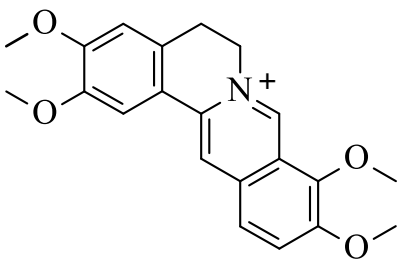

Palmatine **[107]**

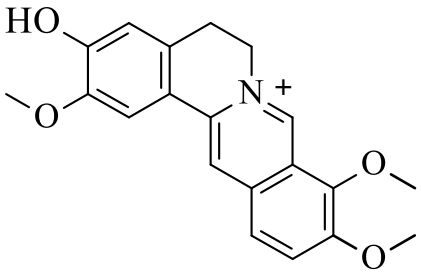

Jatrorrhizine **[108]**

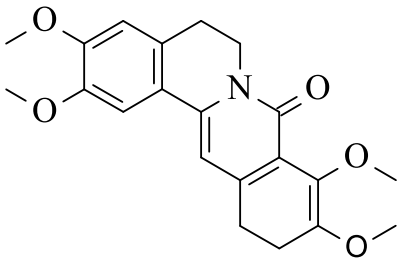

Oxypalmatine **[109]**

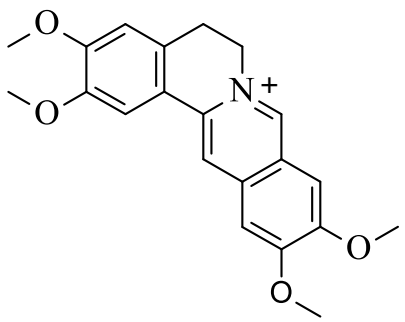

Pseudopalmatine **[110]**

Figure 2.7: Structures of protoberberine alkaloids isolated from *A. polycarpa*

Vasodilatory action of palmatine **[107]** was also reported as being mediated by its ability to lower intracellular free calcium ion levels as well as affecting intracellular free calcium ion level sensitivity of the contractile apparatus in isolated rat arterial strips (Ying-Lin *et al.*, 1999). Palmatine **[107]** showed anti-resorptive activity by exerting an inhibitory action on osteoclast segregation and function (Lee *et al.*, 2010a). The inhibitory effects of palmatine **[107]** and jatrorrhizine **[108]** were studied against different types of dermatophytes and two *Candida* species of human origin in agar plate dilution assay, jatrorrhizine **[108]** was the most effective against all the organisms tested with MIC ranging from 62.5 to 125 µg/ml whereas palmatine **[107]** exhibited weak activity with MIC values between MIC 500 to ≥ 1000 µg/ml (Volleková *et al.*, 2003). Palmatine **[107]** and jatrorrhizine **[108]** were also assayed against Gram-positive and Gram-negative bacteria and fungi and the results showed that palmatine demonstrated more activity against the organisms than jatrorrhizine (Yang *et al.*, 2007).

Fu *et al.*, 2005 showed that jatrorrhizine **[108]** demonstrated hypoglycemic (anti-diabetic) activity by considerably lowering blood glucose levels in both normal mice and alloxan-induced diabetic mice which could be ascribed to augmentation of aerobic glycolysis in the mice and in addition created rabbit platelet aggregation. A different study conducted later also revealed that columbamine **[106]** and jatrorrhizine **[108]** possessed anti-diabetic activity when tested in Protein Tyrosine Phosphatase 1B (PTP 1B), a negative insulin regulator assay, as well as antimicrobial activity against *Staphylococcus aureus, Escherichia coli, Staphylococcus epidermidis, Klebsiella pneumoniae* and *Bacillus subtilis* (Ali *et al.*, 2013). Jatrorrhizine **[108]**

also exhibited anti-inflammatory activity (Arens *et al.*, 1985). Jatrorrhizine **[108]** administered at 0.1, 0.3 and 1 mg/kg counteract postoperative ileus-induced deferred gastric emptying and intestinal transfer in rats mediated by the cholinergic system (BeiBei *et al.*, 2012). Jatrorrhizine **[108]** demonstrated competitive blocking effects on both α_1- and α_2-adrenoceptors, which could be responsible for its hypotensive and anti-arrhythmic activities (Han *et al.*, 1989). Moreover, jatrorrhizine **[108]** also demonstrated neuroprotective and antioxidant activities (Luoa *et al.*, 2011). Jatrorrhizine was also reported to elevate the amplitude of impulsive contractions of isolated rat ileum longitudinal muscles in concentration-response manner with EC_{50} value of $30.0 \pm 8.4\,\mu$M (Yuana *et al* 2011). Jatrorrhizine had been reported to demonstrate anti-mutagenetic activity against acridine orange (AO)-induced chloroplast mutagenesis of *Euglena gracilis* as eukaryotic assay type in a concentration-response manner (Cernakova *et al.*, 2002).

2.4.2.2 Aporphine alkaloids

Jossang and his team of investigators reported the isolation of the aporphine alkaloids; anonaine **[111]**, isoboldine **[112]**, isopiline **[113]**, magnoflorine **[114]**, N-methyllaurotetanine **[115]**, nornuciferine **[116]** and minisperine **[117]** from the leaves and stems of *A. polycarpa* during their evaluation of the alkaloid content of this plant (Jossang *et al.*, 1977).

Anonaine **[111]** was assayed for antiparasitic action against some micro-organisms and arthropods of agricultural importance and was found to demonstrate antifungal activity (Bettarinia *et al.*, 1993). Antibacterial and fungicidal activity of anonaine **[111]** and isoboldine **[112]** were also reported (Paulo Mde *et al.*, 1992). Furthermore, anonaine **[111]**, isopiline **[113]**, liriodenine **[119]** and lysicamine **[120]** were among 14 benzylisoquinoline alkaloids tested against a battery of Gram-positive and Gram-negative bacteria. It was concluded that these alkaloids showed less effective inhibitory effect against the Gram-positive bacteria and the fungus, *Candida albicans* ATCC26555 with MIC of 3-12 mg/L but were inactive against the Gram-negative bacteria (Villar *et al.*, 1987).

The anti-malaria activity of anonaine **[111]** had been established by some research groups. Anonaine **[111]** was shown to demonstrate antiplasmodial activity against both chloroquine sensitive D10 strain and chloroquine resistant D12 strain of *Plasmodium falciparum* with IC_{50} values of 25.9 ± 0.2 and 19.6 ± 1.1 μM respectively (Graziose *et al.*, 2011). In a different study

using *in vitro* radiometric assay, anonaine inhibited the growth of *Plasmodium falciparum* with IC_{50} of 7 ± 2 μM (Levrier *et al.*, 2013).

Anonaine **[111]** showed dose-dependent inhibition of cell proliferation, cell immigration and DNA-destructive action on human lung cancer H1299 cells line (Bing-Hung *et al.*, 2011). Anonaine **[111]** was also reported to show selective inhibition of dopamine absorption (Almudena *et al.*, 1995).

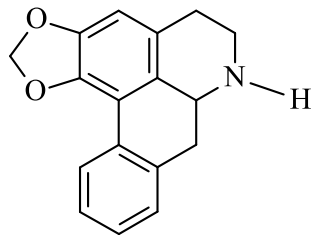

Anonaine **[111]**

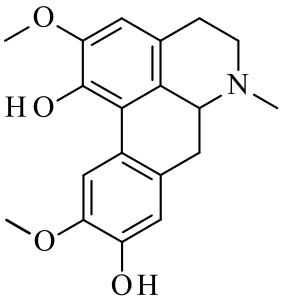

Isoboldine **[112]**

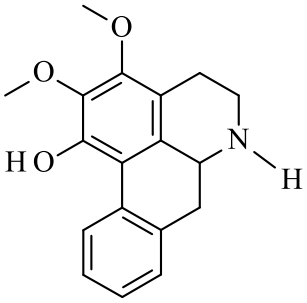

Isopiline **[113]**

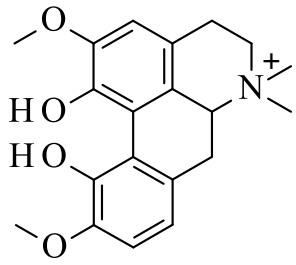

Magnoflorine **[114]**

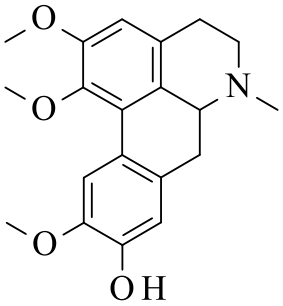

N- methyllaurotetanine **[115]**

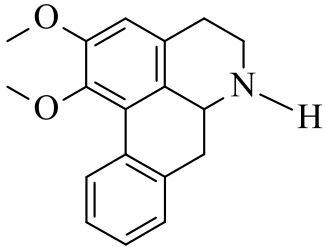

Nornuciferine **[116]**

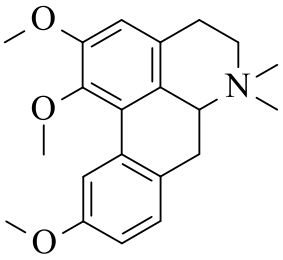

Minisperine **[117]**

Figure 2.8: Structures of aporphine alkaloids from *A. polycarpa*

The CD45 protein tyrosine phosphatase inhibitory activity of anonaine **[111]** and nornuciferine **[116]** were also published (Miskia *et al.*, 1995). The antioxidant activity of anonaine **[111]** was evaluated in three different assay models of microsomal lipid peroxidation precipitated by Fe^{2+}/ascorbate, CCl_4/NADPH or Fe^{3+}ADP/NADPH and was found to demonstrate dose-response antioxidant activity in all the three test models with more potency in CCl_4/NADPH and Fe^{3+}ADP/NADPH assays (Ubeda *et al.*, 1993). Anonaine **[111]** has Ca^{2+} channel blocking ability via voltage-operated channel and α_1-adrenoceptor blocking effect in isolated rat thoracic aorta which accounted for its vaso relaxant activity (Chulia *et al.*, 1995).

Anonaine **[111]** and lysicamine **[120]** at 100 μM were reported to possess anticancer activity in the MTT assay against human skin cancer cell line A375 with IC_{50} values of 97.16 and 58.12 μM respectively. In addition, these two compounds exhibited antioxidant activity in ferric reducing antioxidant power (FRAP) test model, with reducing power of 0.1 each at 100 μM which was same as that of the standard reagent, 3-*tert*-butyl-4-hydroxyanisole (BHA) (Ya-Fei *et al.*, 2014).

Some pharmacological studies conducted on magnoflorine **[114]** revealed that it possessed anti-hypertensive activity by lowering blood pressure significantly for about 1 - 2 hours in anesthetized cats when administered at 2 mg/kg (i.v.) and in rats and Gold blatt hypertensive dog when given intraperitoneally (i.p.) or intravenously (i.v.) mainly mediated by its ganglionic blockade ability (Jia-Quan *et al.*, 1964). Magnoflorine **[114]** also produced an inhibition of the N-cholinergic reactive pathway and its LD_{50} value was 0.02 g/kg (i.v.) in mice (Jia-Quan *et al.*, 1964). Magnoflorine **[114]** lower arterial blood pressure in rabbits and caused hypothermia in mice as well as induced contractions in isolated pregnant rat uterus and stimulated the isolated guinea pig ileum (El Tahir, 1991). Experiments also imply that magnoflorine **[114]** exerts action on muscarinic and serotonergic systems either by direct or indirect activation of these systems (El Tahir, 1991).

Another study also reported that magnoflorine **[114]** had antifeedant activity against *Spodoptera frugiperda* larvae (Tringali *et al.*, 2001). In some other study, magnoflorine **[114]** was reported to exhibit antioxidant activity against Cu^{2+}- induced lipid peroxidation of human high density lipoprotein (HDL) by extending the lag time from 62 to 123 min at the concentration of 3.0 mM and inhibiting the creation of thiobarbituric acid reactive products (TBARS) dose-dependently with IC_{50} of 2.3 ± 0.2 and 6.2 ± 0.5 mM (Hung *et al.*, 2007).

N-methyllaurotetanine **[115]** and liriodenine **[119]** were reported as potent inhibitors of arachidonic acid (AA)-induced platelet aggregation agents (Keh-Shaw *et al.*, 1996). Tzong-Cherng and his team of researchers also investigated the antihyperglycemic activity of some aporphines alkaloids and their derivatives including N-methyllaurotetanine **[115]** in normal Wistar, streptozotocin (STZ)-induced diabetic and nicotinamide-STZ induced diabetic rats and found out that N-methyllaurotetanine **[115]** administered intravenously (i.v.) demonstrated anti-diabetic activity by dose-dependently lowering blood glucose levels in both species of animal subjects (Tzong-Cherng *et al.*, 2006).

2.4.2.3 Oxoaporphine alkaloids

Moreover, three oxoaporphinoids namely atherospermidine **[118]**, liriodenine **[119]** and lysicamine **[120]** (Figure 2.9) have been isolated in addition to the aporphine alkaloids in that same investigation by Jossang and his co-workers (Jossang *et al.*, 1977).

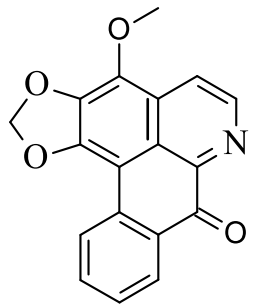

Atherospermidine **[118]**

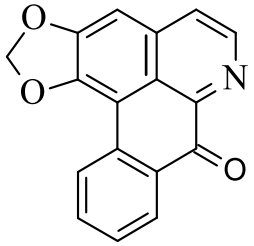

Liriodenine **[119]**

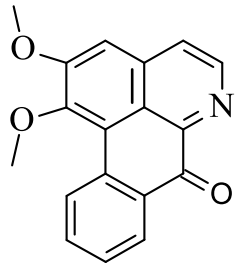

Lysicamine **[120]**

Figure 2.9: Structures of oxoaporphine alkaloids isolated from *A. polycarpa*

The aporphinoids, anonaine **[111]** and nornuciferine **[116]** in addition to the oxoaporphines liriodenine **[119]** and lysicamine **[120]** were shown to demonstrate anthelmintic activity towards the common human intestinal worm, *Hymenolepis nana* (Rong-Jyh *et al.*, 2014), which produce symptoms of headache, anorexia, diarrhea, abdominal pain and weakness (Chitchang *et al.*, 1985). Another report stated that nornuciferine **[116]** showed significant leishmanicidal effect against *Leishmania mexicana* with IC_{50} of 14 ± 1.0 μM (Montenegro *et al.*, 2003).

Atherospermidine **[118]** was shown to display smooth muscle relaxant activity on rat uterine contractions effected by potassium chloride (KCl) or periodic contractions caused by oxytocin in a calcium-dependent medium as well as relax oxytocin or vanadate-induced contractions in a calcium-free system (Cortes *et al.*, 1990).

2.4.2.4 Benzyltetrahydroisoquinoline, isoquinoline and cinchona alkaloids

Finally, isolation of a novel benzyltetrahydroisoquinoline alkaloid, polycarpine **[122]** and the known benzylisoquinoline, corydaldine **[121]** from *A. polycarpa* were also reported (Jossang *et al.*, 1977) in addition to the famous cinchona alkaloids; quinidine **[123]** and dihydroquinidine **[124]** (Buzas *et al.*, 1959).

Quinidine **[123]** is clinically used as an antiarrhythmic (Dikshit *et al.*, 1995) and antimalarial drug (Philipsa *et al.*, 1985). Some other biological activities of quinidine **[123]** have also been reported in both animal and human subjects. Quinidine **[124]** stopped ischemia-induced rise in liberation of antioxidant enzymes malonaldelhyde (MDA) and lactate dehydrogenase (LDH) in cats heart (Dikshit *et al.*, 1995). Quinidine **[123]** was reported to demonstrate hypoglycemic activity by significantly ($p < 0.05$) reducing blood plasma glucose levels in human subjects suffering from malaria (Phillips *et al.*, 1986).

Dihydroquinidine **[124]** also showed significant antiarrhythmic effect in 75 % of patients suffering from chronic stable high frequency premature ventricular beats by lowering the premature ventricular beats by more than 70 % per hour (Chimienti *et al.*, 1984).

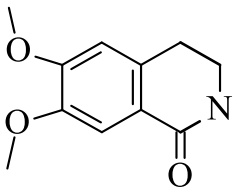

Corydaldine **[121]**

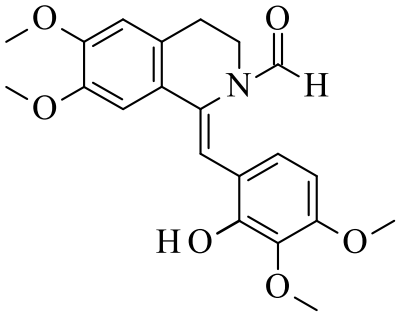

Polycarpine **[122]**

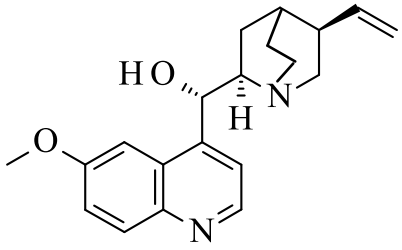

Quinidine **[123]**

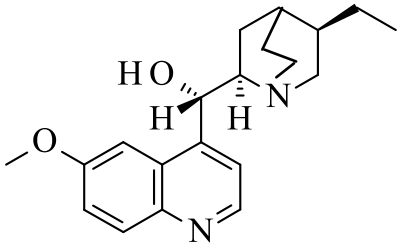

Dihydroquinidine **[124]**

Figure 2.10: Structures of benzyltetrahydroisoquinoline, isoquinoline and cinchona alkaloids from *A. polycarpa*

The cinchona alkaloids quinidine **[123]**, dihydroquinidine **[124]**, quinine and dihydroquinine were reportedly studied regarding their α_1- and α_2-adrenoceptor-induced vasoconstriction antagonistic actions in pithed normotensive rats; quinidine **[123]** and dihydroquinidine **[124]** were found to be the most efficient α_1-adrenoceptor blockers than quinine and dihydroquinine. However, all the four alkaloids exhibited weak α_2-adrenoceptor blocking activity (De Zoeten *et al.*, 1982).

2.5 NOCICEPTION AND PAIN

2.5.1 Nociception

Nociception is the detection of toxic stimuli and the ensuing transmission of encoded information in a form of electrical stimuli to the brain (Kidd and Urban, 2001). The capacity of an organism to sense harmful stimuli in its immediate environment enable the organism to call to play various protective reflexes in order to escape from or get rid of the stimuli hence avoiding fatality. Nociception involves four major processes namely; transduction, conduction, transmission and detection of the stimuli by the brain (Kidd and Urban, 2001). Transduction involves detection of noxious stimuli by primary afferent neurons of the body. The resulting effect flows from the peripheral nerve endings to the spinal cord, this is called Conduction (Kidd and Urban, 2001). The process is completed by transmission which is the synaptic transport of the effect to neurons within definite lamina of the dorsal horn (Kidd and Urban, 2001). Sensory perception as pain resulting from the toxic stimuli is then propelled to the supraspinal regions among which are the brainstem and the thalamus (Kidd and Urban, 2001). Some individuals are unable to sense obnoxious stimuli (Basbaum *et al.*, 2009). These persons are therefore, unable to engage the appropriate protective reactions against deadly stimuli (Basbaum *et al.*, 2009). On the other hand, changes in the pain pathway leads to hypersensitivity, such that pain outlives its usefulness as short term warning signal but instead becomes chronic and devastating (Basbaum *et al.*, 2009).

2.5.2 Pain

The perceptual aspect that result in reaction to nociception is termed pain (Kidd and Urban, 2001). Pain is defined by the International Association for the Study of Pain (IASP) as ‘an unpleasant sensory and emotional experience that is associated with actual or potential tissue damage’. It can be classified according to a variety of characteristics including; duration (acute or chronic) or intensity (mild, moderate or severe) (McGivern, 2007). Pain is felt by means of a complex neural system that has two structurally defined and functionally communicating systems which manage pain perception and pain modulation (Almeida *et al.*, 2004; Apkarian *et al.*, 2005).

2.5.2.1 Acute pain

Acute pain is mostly temporary and warns the body about ongoing tissue injury so that the appropriate defensive actions could be taken to stop further damage. It also lessens when the stimulus is removed and healing takes place (McGivern, 2007).

In usual acute pain sensation, processes of the pain perception system are activated first and then the pain modulation system may put in an inhibitory or augmentative contribution to change the intensity and the length of the pain sensitivity (McGivern, 2007). Peripheral nerve terminals of high-threshold mechanosensitive and polymodal nociceptive neurons are agitated by harmful stimuli in pain perception (McGivern, 2007). This releases and propel sodium channel-dependent action potentials along myelinated (Aδ fiber) or unmyelinated (C fiber) axons (McGivern, 2007). The Aδ and C fibers protrude largely into the superficial laminae of the dorsal horn within the spinal cord where they link with the secondary sensory neurons through synaptic transmissions (Light and Perl, 1979 ; Light and Perl, 1979; Light *et al.*, 1979). Calcium inflow through pre-synaptic voltage-gated calcium channels causes the discharge of pronociceptive neurotransmitters and neuromodulators like substance P, calcitonin gene related peptide (CGRP), and glutamate, after the action potentials reach the inner terminals of the primary afferent neurons (Bennett, 2000; Dickenson *et al.*, 1997; Levine *et al.*, 1993).

2.5.2.2 Chronic pain

Chronic pain, on the other hand, constitutes an unusual long-term experience and remains in the absence of any evident body injury and is of no beneficial effect to the body. Chronic pain indicates sickness such as tissue inflammation or injury to peripheral or central neurons (McGivern, 2007).

In chronic pain states, forced alterations in the nervous system may arise, probably resulting in hyperactivity in the pain perception pathway and/or unevenness in the inhibitory and/or augmentative constituents of the pain modulation system; peripheral and central maladaptive processes may equally play a role in the creation of sensory deficits (McGivern, 2007; Katz and Rothenberg, 2005).

More than one-third of the world's population suffers from chronic or prolonged pain with the American public alone spending in the region of US$100 billion each year on health care, litigations and compensations owing to pain (Loeser *et al.*, 2001). Pain is associated with nearly all human diseases. Acute pain is implicated in common conditions such as inflammation, injuries, malaria, headaches, stress and fatigue. Chronic pain is connected with such conditions as migraine, herpes zoster, back injury, arthritis, diabetic neuropathy, temporomandibular joint syndrome, cancers (Stucky *et al.*, 2001) and AIDS. Chronic untreated pain could become self-perpetuating, since pain has immune suppressive effects that leave subjects prone to consequent diseases; nonetheless existing pain remedies are either inadequate for certain kinds of pain or induced undesirable side effects (Stucky *et al.*, 2001). Hence the need to search for alternative agents in pain therapy.

2.5.3 Mechanism of antinociceptive action

Knowing the type of receptor that a drug binds to helps us to determine the disease conditions the drug can be used to treat and the kind of antagonist that could be employed to reverse its effects in cases of over-dose and/or poisoning. The process by which drugs interact with these receptor system(s), enzymes, hormones or any other chemical substance to generate their effects on the body is known as that drug's mechanism of action. Many types of neurotransmitters such as endogenous opioid peptides, gamma-aminobutyric acid (GABA), cholinergic and dopamine transmitters are involved in the synaptic transmission of nociceptive stimuli in the central nervous system. Analgesic drugs exert their antinociceptive actions by specifically binding to these neurotransmitter(s). This inhibits the transfer of nociceptive stimuli to the spinal cord and the brain. Activation of the heterogeneous μ, δ, and κ endogenous opioid nociceptors with agonist in the central and peripheral nervous system produce analgesia, e.g. opioid such as morphine produce analgesia by acting on the μ-opioid nociceptors in the central nervous system (Chen and Robinson, 1990). Cholinergic agonist which stimulates the muscarinic or nicotinic nociceptor systems are also known to be potent analgesic agents e.g., cobratoxin -a long-chain α-neurotoxin and cobrotoxin - a short-chain postsynaptic α-neurotoxin isolated from cobra venoms which are employed in treating severe pain (Chen *et al.*, 2006; Chen and Robinson, 1990).

With regard to this study, determining the mechanism of action of the extracts and the isolated compounds can lead to their classification as nonsteroidal anti-inflammatory drugs (NSAIDs), opioids or cholinergic agonist.

2.5.4 Current analgesic drugs and problems associated with them

Mild to moderate acute pain is mostly treated with over-the-counter drugs, such as acetaminophen while stronger analgesics like opioids are used to treat severe acute pain (McGivern, 2007). Opioids, however, have the disadvantage of causing addiction and tolerance with protracted or frequent utilization (McGivern, 2007). Pain related to inflammation is treated with non-steroidal anti-inflammatory drugs (NSAIDs) (McGivern, 2007). NSAIDs are classified into two groups. They are the non-selective inhibitors of both COX-1 and COX-2 (the two isoforms of cyclo-oxygenase enzyme) and the inhibitors of only COX-2. The use of the non-selective inhibitors of both COX-1 and COX-2 are associated with the development of gastric ulcers, probably as a result of COX-1 inhibition whereas the COX-2 selective inhibitors also predispose patient to cardiovascular hazards (McGivern, 2007) such as stroke, hypertension, myocardial infarction and heart failure (Graham, 2006; Mukherjee *et al.*, 2001). Ziconotide [**33**] is the most potent analgesic drug currently available which is used to treat neuropathic pain and more severe types of pain (McGivern, 2007). However, the therapeutic index of intrathecal (i.t.) administered ziconotide tends to be low; it also inhibits motor activities at higher doses and may also induce hypotension if it crosses the blood-brain barrier into the general circulatory system (Bowersox, *et al.,* 1992; Wright *et al.,* 2000; Takahara, *et al.,* 2002). Moreover, ziconotide is difficult to use since it is only effective by intrathecal (i.t.) administration (Smith, *et al*., 2002).

2.5.5 Experimental models of pain in animals

Laboratory rodents are the most frequently used animals in pain studies although primates and other mammals are rarely used (Wang and Wang, 2003; Bars *et al.*, 2001). One key advantage of using animal models in studying fundamental physiological mechanisms of pain is that it could forecast analgesic potency resulting in scientific drug development (Mogil *et al.,* 2010). These tests are based on input-output or stimulus- response reactions in experimental animals and make use of adequate stimuli which are measurable, reproducible and noninvasive to evoke pain perception in acute models of nociceptive studies; these experimental studies are termed

behavioral studies since the responses elicited by the stimuli constitute the animal's normal conduct (Lineberry, 1981; Beecher, 1957; Bars *et al.*, 2001). The types of stimuli used to produce pain stimulation in acute models of antinociceptive studies include thermal, mechanical, electrical or chemical which elicits responses such as tail or paw withdrawal, lifting or biting of the limbs, vocalization, flight, evasion or body stretchings from the animals (Bars *et al.*, 2001).

2.5.5.1 The hot plate assay

The hot plate test is an example of a thermal model of nociceptive or pain assay. A rodent is placed on a metallic plate that is heated by a thermostat or a boiling liquid and restricted by an open-ended cylinder (Eddy and Leimbach, 1953; O'Callaghan and Holzman, 1975; Woolfe and MacDonald, 1944). The plate is heated to a constant temperature and it generates two brain controlled behavioral patterns in the animal specifically, paw biting and jumping that can be quantified in terms of the animal's response time. For analgesic agents, the paw biting response is produced only by opioids. Conversely, the less potent analgesics like acetylsalicylic acid and other NSIADs or acetaminophen, elicits the jumping behavior especially when the plate is maintained at 50°C or less (Ankier, 1974) or if the plate is heated gradually and in a linear manner, e.g., commencing at 43 to 52 °C at 2.5 °C per min (Hunskaar *et al.*, 1985).

2.5.5.2 The writhing assay

It is a very sensitive method that is able to detect major analgesic in addition to very weak ones that could otherwise not have been detected by other experimental procedures (Bars *et al.*, 2001). It is a chemical pain model which involves injection of an algogenic agent into the intraperitoneal cavity of a mouse or rat to elicit pain typified by contraction of the abdomen, stretching of the whole body especially the hind limbs, twisting of dorsal-abdominal muscles, and a decrease in motor action and motor incoordination (Bars *et al.*, 2001). A variety of chemical agents such as phenylbenzoquinone (Siegmund *et al.*, 1957); radio-opaque elements (Van der Wende and Margolin, 1956); acetylcholine and dilute hydrochloric or acetic acid (Eckhardt *et al.*, 1958; Koster *et al.*, 1959; Niemegeers *et al.*, 1975); are employed to induce the writhing movements depending on the duration and the expected effect. This test is also called the abdominal contortion test, the abdominal constriction response or the stretching test (Bars *et al.*, 2001). Truly, the writhing assay is also able to detect other pharmacologically active

substances like adrenergic blockers, antihistamines and muscle relaxants which lack analgesic effect; however, all analgesics inhibit abdominal spasms. Hence this method is a useful starting point in the development of analgesic drugs (Pearl *et al.*, 1968; Loux *et al.*, 1978; Hendershot and Forsaith, 1959).

2.5.6 Experimental models used in determination of antinociceptive mechanisms

Receptors involved in activation of the pharmacological effects of drugs could be studied by employing *in vivo* pharmacological antagonist obstruction method in experimental animals or *in vitro* cell line binding assays (Wen *et al.*, 2011; Shi *et al.*, 2011; Chen *et al.*, 2006) especially for differentiating subtype receptors in heterogeneous systems. The former is easier and less expensive than the later. The pharmacological antagonist obstruction method in experimental animals' procedure involves co-administration of a specific receptor antagonist and the drug separated by some time interval in one group of animal and another group that receives the drug without the antagonist. The effect of the drug is then investigated. The two groups are then compared to see if the action of the drug has been blocked by the antagonist in the first group. For instance, if the nonselective opioid receptor antagonist, naloxone or nonselective cholinergic antagonist, atropine blocked the analgesic effect of a drug in the group it was co-administered with the drug compared with the group treated with only the drug, it means that the endogenous opioid receptors or the cholinergic receptors are involved in mediating the pharmacological response of that drug (Wen *et al.*, 2011; Chen *et al.*, 2006).

2.6 THE ROLE OF INFLAMMATION IN HUMAN DISEASES

Inflammation is the body's instant response to damage to its tissues and cells (Weiss, 2008). Inflammation may occur as a result of infection by bacteria, fungi, viruses and protozoa (which cause damage by producing poisons that obliterate host cells); painful incisive injury; direct trauma; thermal injury; chemical injury; immunologically modulated injury (which may be humoral or cellular) and failure of blood flow to a tissue or an organ - a condition known as ischemia (Robbins and Cortran, 2004). The release of inflammatory mediators such as histamine, prostaglandins (PGs), leukotrienes (LTB_4), nitric oxide (NO), platelet-activation factor (PAF), bradykinin, serotonin, lipoxins, cytokines and growth factors from the cells and proteins of the complement, kinins and coagulation systems from the plasma (Sarulkah *et al.*, 2008) are initiated by agents of inflammation leading to the inflammation reaction (Gerhard Vogel *et al.*, 2002). Inflammation involves three separate phases modulated by specific mechanisms (Gerhard Vogel *et al.*, 2002). Phase one is acute and short lived, involves vasodilatation and augmented capillary permeability of the affected area (Gerhard Vogel *etal.*, 2002). This is followed by a sub-acute phase which involved localized invasion of leukocytes and phagocytes (Gerhard Vogel *etal.*, 2002). The last stage is a chronic, proliferative and repair phase encompassing tissue disintegration, fibrosis, blood vessels and granulation tissues formation (Swingle, 1974; Gerhard Vogel *et al.*, 2002). The first century Roman author, Celsius listed the four symptoms of inflammation as rubor (redness), tumor (swelling/edema), calor (heat) and dolor (pain) which have become known as the four cardinal signs of inflammation (Vane and Botting, 1987). In clinical settings these symptoms could otherwise be described as erythema, edema, pyrexia and pain (Gerhard Vogel *et al.*, 2002).

Inflammation is one of the most vital self defense mechanisms of the body with the chief aim of eliminating the noxious substance or limiting its damaging effects by reducing its spread (Mitul *et al.*, 2012) and hence protecting the body. However, if it is not controlled, it can lead to harmful consequences. Inflammation could be acute or chronic. Acute inflammation involves the body reaction at the onset and is of short period, resolves rapidly and is regularly followed with healing of the affected part. In chronic inflammation, both tissue degeneration and inflammation take place simultaneously for protracted duration without healing (Harsh, 2005).

Failed resolution of acute inflammation can lead to chronic inflammatory responses and ultimate loss of function of the affected tissue (Yacoubian and Serhan, 2007). Chronic inflammatory reactions are implicated in the pathogenesis of countless non-communicable diseases such as periodontal disease, cardiovascular disease, chronic kidney disease and Alzheimer's disease (Serhan and Savill, 2005; Himmelfarb *et al.*, 2002). Chronic immune modulated inflammation is also known to govern the pathogenesis of diseases such as obesity, diabetes, fatty liver, atherosclerosis and rheumatoid arthritis (Hotamisligil, 2004; Vane, 1982; Yacoubian and Serhan, 2007).

The chronic inflammatory processes of wound healing are also comparable to those involved in cancer (Dvorak, 1986). Several type of the frequent cancers are preceded by years of chronic inflammation (Moss and Blaser, 2005). Examples are cancers of the lung, in which cigarette smoking generally results in inflammation; adenocarcinoma of the esophagus, which is most often preceded by years of inflammation due to gastroesophageal reflux; colon cancers are also occasionally associated with chronic inflammatory bowel illness (Moss and Blaser, 2005). Furthermore, inflammation is also known to be involved in the etiology of most prevalent mental conditions such as panic disorders (Hoge *et al.*, 2009), post-traumatic stress disorders (Gill *et al.*, 2009; Spitzer *et al.*, 2010) and generalized anxiety disorders (Bankier *et al.*, 2008).

Chronic inflammatory disease accounts for high burden of suffering and economic expenditure worldwide (Bloom *et al.*, 2011). Treatment and loss of work force due to chronic diseases can therefore create a huge indentation in a country's productive ability (Bloom *et al.*, 2011). Widespread chronic disease could undoubtedly obstruct the recent improvements in economic advancement made in both developed and developing countries (Bloom *et al.*, 2011). Moreover, inflammatory diseases as well as various forms of rheumatic ailments account for the major causes of morbidity in man (Shah *et al.*, 2006).

2.6.1 Current anti-inflammatory drugs and challenges associated with them

Various drugs are currently used in inflammation therapy and they could be classified into three groups. The non-steroidal anti-inflammatory drugs (NSAIDs), such as aspirin or diclofenac sodium and other aspirin-like drugs are employed in treating inflammatory conditions and pain associated with inflammation; but they produce gastrointestinal ulcers (McGivern, 2007). The second group of anti-inflammatory drugs is corticosteroids. Overdose or prolong use of this class of anti-inflammatory agents could lead to an increase in some of their biological action in the body such as diabetes, euphoria, mental disturbances, Cushing syndrome and osteoporosis in addition to mineralocorticoid involving sodium and water retention, potassium lost and high blood pressure (Ekuadzi, 2013). Protracted use of corticosteroids could result in adrenal atrophy with extended courses resulting in increased susceptibility to infection and severity of infections and abrupt withdrawal could cause hypotension, renal insufficiency or even death (Schimmer and Parker, 2001). The biologics, which are the third class of drugs employed to treat inflammatory conditions, suppress the body's immune system so as to lessen inflammation (Singh *et al.,* 2011). The suppression of the body's immune system weakens its ability to fight infections. Therefore, the use of biologics makes the body susceptible to key infections such as opportunistic and bacterial infections in addition to tuberculosis reactivation (Singh *et al.*, 2011). Moreover, biologics are expensive and could also cause cardiac problems (Lim *et al.,* 2006; Strand *et al.*, 2007).

2.6.2 In vivo anti-inflammatory assays using animal models

A number of acute and chronic experimental designs have been developed which are employed to evaluate the anti-inflammatory effects of substances and/or drugs in laboratory animals during the pre-clinical stage of the drug development process. The acute models of inflammation rely on the measurements of the clinical signs of the acute phase and the sub-acute phase deals with the measurement of inhibitory effects at the vascular level of the inflammatory reaction whereas in chronic models, the inhibitory effect on granulomatous tissue formation is measured.

2.6.2.1 Acute inflammation models in experimental animals

In the acute models, inflammation is induced at selected parts of an experimental animal's body by injecting irritant agents such as formalin, zymozan, monosodium urate crystals and Freud's adjuvant (Singh *et al.*, 2000; Higgs, 1989). Deactivated bacteria like *E. coli*, vaso-active agents e.g., platelet-activation factor (PAF) or histamine and arachidonic acid (AA) in acetone, chemotactic factors e.g., leukotrienes (LTB_4) (Issekutz and Issekutz, 1989), and phlogestic agents such as carrageenan, brewer's yeast, dextran, egg albumin, kaolin, aerosil, croton oil and cotton wool could also be employed (Mitul P. *et al.*, 2012).

Carrageenan induced paw edema in experimental laboratory rats (Winter *et al.*, 1962) is a valuable technique used to access orally potent anti-inflammatory substances/drugs (Di Rosa *et al.*, 1971). Hence it has been employed in this study to evaluate the anti-inflammatory activity of the selected plants extracts, various fractions of the extracts and their isolated constituents.

CHAPTER THREE

MATERIALS AND METHODS

3.1 Collection and authentication of plant materials

C. anisata root and *A. Polycarpa* stem and root barks were collected from Ayikumah (Eastern Region) and Bobiri (Ashanti Region) in March and Nov 2012 respectively. *C. anisata* was authenticated by Mr. H. R. Blaggoge, a botanist at the Plant Development Department of Centre for Plant Medicine Research (C.P.M.R.), and *A. polycarpa* by Mr. Ntim Gyakari, a retired botanist. Voucher specimen numbers CPM0312, CPM0412 and CPM0512 were assigned to *C. anisata* root, *A. polycarpa* root bark and *A. polycarpa* stem bark respectively and samples deposited at the herbarium of C.P.M.R. *C. anisata* root was selected based on its use in traditional medicine in treating pain and inflammatory conditions.

3.2. MATERIALS AND METHODS

3.2.1 Extraction and partitioning

The plant materials were chopped, air dried for 34 days and pulverized. The pulverized stem bark of *A. polycarpa* (4.5 kg) was extracted with ethanol (30 L) at room temperature for 4 days. It was decanted, filtered and dried with a rotary evaporator. The mark was re-extracted with the recovered ethanol (26 L x 3) filtered and dried with rotary evaporator. The entire solids were combined to obtain a total of 312.30 g of a yellowish brown solid. The solid (208.2 g) was suspended in 80 % ethanol-water (2.4 L) and divided into 3 equal portions of 0.8 L each. Each portion was extracted with petroleum ether (0.8 L x 4). The petroleum ether fractions obtained were combined and dried in a rotary evaporator at 40 ^{o}C. The ethanol was thereafter evaporated from the petroleum ether insoluble fractions using the rotary evaporator. The mixtures obtained were diluted with extra distilled water and extracted with chloroform (0.8 L x 4), combined and dried in a rotary evaporator at 45 ^{o}C to obtain brownish yellow syrup chloroform fraction. The aqueous fractions left were freeze dried. A total of 18.44 g of petroleum ether (AP), 87.37 g of chloroform and 102.38 g of aqueous (AER) fractions were obtained. The pulverized root bark of

A. polycarpa (1.5 kg) was treated in a similar manner to obtain dark green solid ethanol extract coded ARE (98.60 g), dark brown semi-solid petroleum ether fraction coded RP (22.3 g), brownish green solid chloroform fractions code RC (55.6 g) and yellow solid aqueous fraction (20.7 g) labelled RA.

C. anisata root 5.0 kg was also taken through a similar process to obtain 147.0 g of dark brown gummy crude ethanol extract (CRE), 16.80 g of brown syrup pet ether fraction (PEF), 35.60 g of dark gummy chloroform fraction (CF) and 47.60 g of dark-brown aqueous fraction (EMF). The yields are shown in Table 3.1.

Table 3.1: Percentage (%) yield

	Yield of extract (%w/w)		
	***C. anisata* root**	***A. polycarpa* stem bark**	***A. polycarpa* root bark**
Ethanol extract	2.94	6.94	6.57
Pet ether fraction	16.80	8.86	22.62
Chloroform fraction	35.60	41.96	56.39
Aqueous fraction	47.60	49.17	20.99

3.2.2 CHROMATOGRAPHY AND DETECTING REAGENTS

3.2.2.1 Column chromatography over normal phase silica gel

Open column chromatography over normal phase silica gel was used to fractionate the most fraction of *C. anisata* root (petroleum ether fraction) and *A. polycarpa* stem bark (chloroform fraction). Moreover, the chloroform fraction of *A. polycarpa* root bark was also fractionated. The column was loaded with a measured quantity of silica (Merck 60 - 170 mesh size) using wet

packing. The fractions were introduced onto the column bed by the dry method. Fractions were eluted from the column under gravity and aliquots collected in sample bottles.

3.2.2.2 Thin layer chromatography (TLC)

TLC was employed in analyzing the crude extracts and their various fractions. TLC was also used to analyze fractions collected from the column in other to find those that were similar and thereby combine them. The purity of the compounds was also assessed using TLC. TLC plates used were made of silica gel F_{254} precoated with aluminum plates and were of 0.25 mm thickness procured from Merk, Germany. The plates were developed in glass chromatographic tanks which were saturated with 5 mL each of the right solvent systems.

The developed plates were first visualized in a U.V lamp chamber (Transillminator/Handy UV lamp AS ONE SLUV-8, 254/365 nm) at 254 and 365 nm respectively. The compounds appeared as various colorful spots under 365 nm on a dark background and as dark brown spot or invisible on yellowish green background at 254 nm.

3.2.2.3 10 % Sulphuric acid reagent

This was prepared by adding 10 mL of concentrated stock solution of sulphuric acid to 90 mL of distilled water in a 250 mL beaker in the fume chamber. The resultant solution was stirred, allowed to cool and then kept by covering. The dry TLC plate was totally submerged in this solution and quickly removed using a pair of forceps. The plates were then dried using a hand dryer before heating them at 120 – 130 ^{o}C (on IKA® C-MAG HP4 hot plate for about 2 - 6 min) for the spots detections.

3.2.2.4 Iodine vapour

A glass tank was saturated with iodine vapour by introducing a small quantity of iodine crystals onto its base and covering them with a piece of white sheet of paper. The plates were positioned on this sheet to develop. Compounds were detected as yellow to dark brown spots on a pale yellow background. Iodine is used as a universal detection reagent.

3.2.2.5 Dragendorff's spray reagent

It is used to detect alkaloids and other nitrogen containing compounds. In this study, it was used in the phytochemical screening and on the isolated compounds to find out if they were alkaloids. The reagent was prepared by mixing equal portions of 1.7 g of bismuth nitrate in 100 mL water/ ethanoic acid in the ratio of 4:1 and 100 mL water were mixed with 100 mL ethanoic acid together with 20 mL ethanoic acid and 100 mL water. Alkaloids are observed as orange spots upon application of Dragendorff's spray reagent.

3.2.3 SPECTROSCOPIC TECHNIQUES

3.2.3.1. Nuclear magnetic resonance (NMR) spectroscopy

^{1}H and ^{13}C NMR experiments were performed on each isolated compound using JOEL ECX 400 NMR spectrometer (JOEL, Tokyo, Japan) to obtain the spectra.

3.2.3.2 Fourier transform-infra red (FTIR) spectrometry

The infrared spectrum of the compounds was measured in the solid state with Interspectrum's Interspec 200-X FTIR spectrometer operated at humidity and temperature below 28 % and 28 ^{o}C respectively connected to a monitor.

3.2.3.3 Gas chromatography connected with mass spectrometry (GC-MS)

The molecular weights of the isolated compounds were determined using GC-MS. Four of the samples (P2A, A2C, A6C and A8C) were dissolved in methanol. The others were dissolved in chloroform. The system used composed of Varian CP-3800 GC-MS coupled with a CP-8400 auto sampler and analytical column of 30 m +10 m EZ Guard x 0.25 mm internal diameter fused silica capillary coated with VF-5 ms (0.25 μm film) from Varian Inc. Helium gas flowing at a constant rate of 1.0 mL/min was employed as the carrier. The samples were injected at 270 °C splitless mode with an oven temperature of 50 °C/min $^{25\ °C/min}$ 180 °C $^{5\ °C/min}$ 300 °C/min. Ions were produced using electron impact (EI) ionization process and were trapped at 200 ^{o}C from transfer and manifold temperatures of 260 and 80 ^{o}C respectively. Each segment starts in 3 min and ends in 30 min.

3.2.4. PHARMACOLOGICAL STUDIES

Anti-inflammatory activity was studied using carrageenan-induced oedema in rat's paw assay (Winter *et al.*, 1962). Anti-nociceptive or analgesic activity was evaluated using Eddy's hot plate test (Eddy and Leimbach, 1953) to study central analgesic activity and acetic acid-induced writhing assay in studying peripheral and central analgesic activity (Koster *et al.*, 1959) of the extracts, their various fractions and isolates. Antinociceptive mechanisms were studied by the procedure of pharmacological antagonism using nonselective opioid and cholinergic antagonists, naloxone and atropine (Chen *et al*., 2006).

3.2.4.1. Drugs and other chemicals

Carrageenan, naloxone hydrochloride dihydrate, atropine sulphate and acetic acid were procured from Sigma Chemical Co. (St. Louis, USA). Indomethacin was procured from Cayman Chemical Company (Ann Arbor, USA). Diclofenac sodium chloride was purchased from Bliss GVS, (India), tramadol hydrochloride was purchased from Bristol Laboratories Ltd and Tween 80 was from VWR International, PROLABO (CE). Sodium chloride (Analytical grade) was from Timstar Laboratory Suppliers Ltd., Herald Drive Way, Cheshire. Normal saline (0.9 %) from Intravenous Infusions (Koforidua, Ghana) was also used.

3.2.4.2 Animals

Animals used in the research were bred at Animal House Unit of CPMR except C57BL/6 mice which were procured from Nuguchi Memorial Institute of Medical Research (NMIMR), Legon-Accra, and used or allowed to breed before being used. The animals were fed on palette feed purchased from Agricare limited located in Kumasi, Ghana; and were allowed free access to sterile water and feed *ad libitum* and were housed in aluminum cages under standard temperature and pressure. Animals were cared for and handled according to the guidelines and procedures by Foundation for Biomedical Research on the use of animals in research (F.B.R., 1987).

3.2.4.3 Acute toxicity assay

The safety or toxicity associated with the short term use of the ethanol extracts of *C. anisata* root (CRE), *A. polycarpa* root bark (ARE) and *A. polycarpa* stem bark (ASE) were studied in two groups (n = 6) each of male Sprague-Dawley rats and male Swiss albino mice. The test was

conducted using established protocol (OECD, 20011). Briefly, CRE, ARE or ASE at 2 500 and 5 000 mg/kg p.o. in 2 % tween 80 solution was administered at 10 mL/kg to each animal. The animals were observed for signs of toxicity such as pilo-erection, motor impairment, sedation, salivation, hyper excitability and death within 24 hours and for extra 16 days.

3.2.4.4 Antinociceptive or analgesic activity assays

3.2.4.4.1 Hot plate assay

The mouse hot plate test used to evaluate the antinociceptive action of CRE was performed as previously reported (Eddy and Leimbach, 1953). C57/BL6 mice (28) of either sex were divided into 7 groups (n = 4). The mice were separately placed on an electric hot plate (UGO Basile hot/cold plate 35 100) maintained at 55 ± 0.5 °C and the time taken to lick, lift, shake or stamp any of the hind limbs or jump constitute latency time, recorded as antinociceptive response. Baseline latencies (T_o) were obtained as means of two determinations prior to any treatment (Chen *et al*., 2006). Only mice with baseline latency of 3.5 – 10 s were used. CRE was administered at 10, 100, and 1000 mg/kg p.o. (Group 1-3): tramadol at 3, 9 and15 mg/kg p.o. (Group 4 – 6): 2% tween 80 aqueous solution was used as vehicle control (Group 7). Latency of each mouse was measured at an hour (T_t) interval for 5 h post each treatment. The antinociceptive responses were expressed as percentage pain threshold inhibition (% PTI, Yong *et al*., 2012) calculated as:

$$\%PTI = ((T_t - T_o)/T_o) \times 100$$

Over all Pain Threshold Inhibition (OPTI, %) was calculated as the sum of mean % PTI over the experimental period. (% OPTI) is the overall analgesic effect of the drug or vehicle control treatment on each group of mice. ASE, AP, AC, AER, PEF, CF, EMF and isolates were also taken through a similar process. The isolates were given at two doses of 3 or 9 mg/kg p.o respectively.

3.2.4.4.2 Acetic acid-induced writhing assay

Analgesic effect of the ethanol extract of *C. anisata* (CRE) was evaluated in the acetic acid induced-writhing model as described (Koster *et al.*, 1959). Swiss albino mice (35) were divided

into 7 groups (n = 5). CRE was administered at 10, 100, 1000 mg/kg p.o. (Group 1–4), diclofenac sodium at 2, 10, 50 mg/kg p.o. (Group 4-6): aqueous tween 80, 2 %, served as vehicle control (Group 7). Each mouse was injected with aqueous acetic acid (1 %v/v) at 1 mL/100 g (i.p) 45 min post treatment and isolated into separate plastic cages. The number of writhing movements and stomach contortions produced by each mouse was counted for 20 min after induction. The inhibition of writhing movements in the treated group(s) compared with the control group was taken as the percentage analgesic effect (% AE) which was calculated using the formula:

$$\%AE = ((MRc - MRt)/MRc) \times 100$$

Where: MRc = mean writhing count of the control. MR_t = mean writhing count of CRE/drug treated group. The crude ethanol extract of *A. polycarpa* (ASE), AP, AC, AER, PEF, CF, EMF and the isolates were also taken through a similar process. The isolates were administered at two doses of 2 or 6 mg/kg p.o respectively.

3.2.4.4.3 Evaluation of antinociceptive mechanism

The involvement of the opioid or muscarinic cholinergic receptors in modulating the antinociceptive action of the extracts and the isolated compounds were also studied.

In order to find out whether the crude extracts and the isolated compounds produce the antinociceptive actions through the central endogenous opioid peptide receptor systems, the effect of the non-selective opioid antagonist, naloxone on the antinociceptive activities of the extracts and isolates was studied in the mouse hot plate test using 3 groups (n=4) of C57BL/6 mice. ASE or CRE were given at 10 mg/kg p.o. followed by naloxone 2 mg/kg (i.p) (in distilled water) at 10 mL/100 g was administered 45 min post CRE or ASE (Group 1). CRE or ASE (10 mg/kg p.o) alone (Group 2) and 2 % aqueous tween 80 as vehicle control (Group 3). Latencies were determined as in Section 3.2.4.4.1 above. The isolated compounds were also taken through the same procedure. The involvement of muscarinic cholinergic acetylcholine receptors in the antinociceptive actions of these extracts and their isolated compounds were also studied using the antagonist atropine in the writhing test. Swiss albino in 3 groups (n = 4) were used. Administration was done as follows: CRE at 10 mg/kg p.o. preceding atropine 5 mg/kg (i.p.) (in

water) 30 min (Group 1), CRE at 10 mg/kg p.o (Group 2) and control (Group 3). The test was performed as described above in Section 3.2.4.4.2. This same procedure was applied to ASE and the isolates to evaluate their mechanisms of anti-nociception.

3.2.4.5 Anti-inflammatory activity assay

3.2.4.5.1 Carrageenan-induced paw edema

The anti-inflammatory activity of CRE was studied in rats using the carrageenan induced paw oedema model (Winter *et al.*, 1962). Sprague–Dawley rats (35) of either sex was divided into 7 groups (n=5). CRE was administered at 10, 100 and 1 000 mg/kg p.o. (Group 1-3); indomethacin at 9, 15, 30 mg/kg p.o. (Group 4-6) as the reference drug and 2 % aqueous tween 80 p.o.as vehicle control (Group 7). Inflammation was induced by injection of 0.1 mL of 1 % w/v carrageenan in 0.9 % normal saline into the sub plantar area of right hind paw of rats 1 hour post each treatment. Paw volumes were measured by volume displacement using Plethysmometer (UGO Basile 7140) before (Vo) and at an hour interval (Vt) from 1-5 h after carrageenan injection. The anti-inflammatory activity was calculated as percentage inhibition of the oedema using the formular:

$$\% \text{ inhibition of inflamation} = ((Vt\text{-}Vo)_{tmec} - (Vt\text{-}Vo)_{tmet}) / (Vt\text{-}Vo)_{tmec}) \times 100$$

Where $(Vt\text{-}Vo)_{tmet}$ = total mean oedema of drug treated group. $(Vt\text{-}Vo)_{tmec}$ = total mean edema of control group. The anti-inflammatory effects of the isolated compounds were studied at two doses of 3 or 9 mg/kg p.o. using this same method. ASE, AP, AC, AER, PEF, CF, EMF and the isolates were also taken through a similar process.

3.3 STATISTICAL ANALYSIS

All statistical analysis was performed using Graph Pad Prism Version 5.03 with the level of significant set at 95 % confidence interval of difference. Total mean edema and the Overall Analgesic effect calculated as the Overall Percentage Pain Threshold Inhibition (%OPTI) were computed using column statistics under XY analysis in Graph Pad Prism software to obtain the

summation of the edema or %PTI for each treatment group over the experimental period in the anti-inflammatory and the hot plate assays respectively.

3.4 PHYTOCHEMICAL INVESTIGATIONS

3.4.1 Phytochemical screening of the extracts

The crude ethanol extracts of *C. anisata* root and *A. polycarpa* stem and root barks were screened for the presence or absence of some classes of secondary metabolites as described (Farnsworth and Dobberstein, 1977).

3.4.2 TLC analysis of the ethanol extracts and fractions of *C. anisata* and *A. polycarpa*

Comparative TLC chromatograms of the ethanol extracts of the leaf, stem and root of *C. anisata* and *A. polycarpa* were obtained respectively. The petroleum ether (PEF) and chloroform fractions (CF) of the ethanol extract of *C. anisata* root (CRE) and *A. polycarpa* stem bark were also developed in petroleum ether/ethyl acetate 5:1 or petroleum ether/chloroform 5:1.

3.4.3 Isolation of compounds from petroleum ether fraction of *C. anisata* root

The pharmacological assays showed that the pet ether fraction of *C. anisata* root was the most active. It was therefore selected for chromatography.

The dried petroleum ether fraction (PEF), 16.8 g of *C. anisata* root was subjected to column chromatography over normal phase silica gel (400 g). Elution was started with 100 % petroleum ether. This was followed by gradient system of petroleum ether/ethyl acetate. When 100 % ethyl acetate was achieved, ethanol was introduced at 10 % incremental basis until 100 % ethanol was achieved. Aliquots of fractions from the column were collected and grouped by similarity in TLC profiles and concentrated to about 100 mL each. A total of 7 main fractions (P1-P7) were obtained.

Fraction P1 eluted with petroleum ether/ethyl acetate (95:5) precipitated colorless crystals. The crystals were filtered and washed with petroleum ether/chloroform (6:1) and recrystallized with petroleum ether/ethyl acetate (70:30) to obtain **C1D** (40.5 mg). Fraction P4 eluted with pet ether/ethyl acetate (60:40) precipitated a colorless crystal which was subjected to repeated

recrystallization with petroleum ether/chloroform (4:1) to obtain **C1F** (20.5 mg). Fraction P5 eluted with petroleum ether/ethyl acetate (30:70) precipitated white crystals. The mother liquor was decanted off. And the crystals recrystallized with petroleum ether/ethyl acetate (5:1) to obtain **C1G** (30.3 mg).

Fraction P2 precipitated yellow crystals. The TLC chromatogram of this crystal developed in petroleum ether/chloroform 2:3 produced 4 spots with anisaldehyde spray reagent. The crystals were further chromatographed over 40 g of silica. Elution was done with petroleum ether/chloroform solvent system. Three sub-fractions (P3A - P3C) were obtained. P3B eluted with petroleum ether/chloroform (90:10) gave **CI-1** (10 mg) as bright yellow crystals.

Fraction P4 was subjected to further fractionation with gradient elution with petroleum ether/chloroform/ethyl acetate. The fractions were collected in about 30 mL aliquot. A total of 87 fractions were obtained and grouped into four sub-fractions (PA - PD). **P2A** (35.0 mg) was obtained from fraction PC eluted with pet ether/chloroform/ethyl acetate (40:40:20) as brown precipitate. The isolation procedures are summarized below in Figure 3.1.

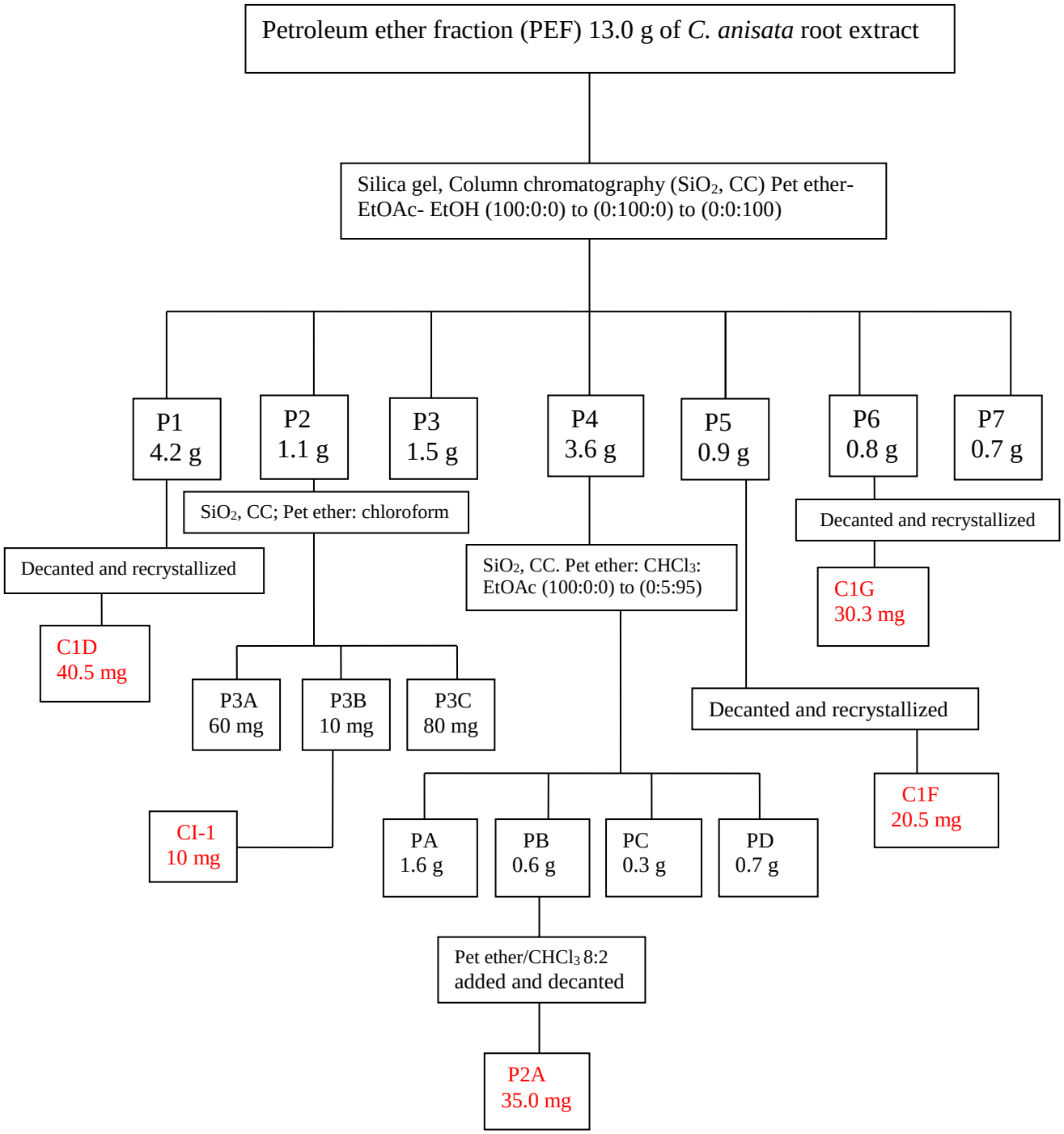

EtOAc = Ethyl acetate; $CHCl_3$ = chloroform; EtOH = ethanol; SiO_2 = Silica gel; CC = Column chromatography

Figure 3.1: Scheme for isolation and purification of compounds from petroleum ether fraction of *C. anisata* root

3.4.4 Isolation of compounds from chloroform fraction of *A. polycarpa* stem bark

The results of the pharmacological assays of the various fractions on the stem bark of *A. polycarpa* extract showed that the chloroform fraction was the most active. It was therefore selected for fractionation so as to isolate the active constituents.

The dried chloroform fraction of *A. polycarpa* stem bark, AC (34.0 g), was subjected to column chromatography over normal phase silica gel (500 g) (Merck; 60 - 120 mesh size). Elution was carried out with gradient mixture of petroleum ether/ethyl acetate until 100 % ethyl acetate was achieved. It was followed by gradual introduction of ethanol (at increasing rate of 10 %) to the ethyl acetate until 100 % ethanol was achieved. A total of 250 fractions (about 200 mL per fraction) were collected from the column. The fractions were grouped by their TLC profile to obtain a total of nine groups (A1 - A9). Each was concentrated to about 150 mL.

Fraction **A6** eluted with ethyl acetate/ethanol (30:70) precipitated dark black solid after seven days. The brown mother liquor was decanted off the solid and allowed to dry. This led to the formation of dark amorphous solid. The solid obtained was thoroughly washed with a mixture of acetone with few drops of methanol to obtained **A8C** (15 mg) as bright orange amorphous solid.

Fraction A8 eluted with ethyl acetate/ethanol (10:90) precipitated yellow to orange solid which was collected by decanting off the mother liquor. The yellow to orange solid was washed several times with excess acetone containing 10 % methanol and the yellow liquid decanted off. The yellow liquid was allowed to dry. TLC on the solid revealed two distinct spots. The solid was subjected to repeated sonication and recrystallization using acetone/methanol until it produced a single spot on the TLC plate. The solid was coded **A6C** (100 mg).

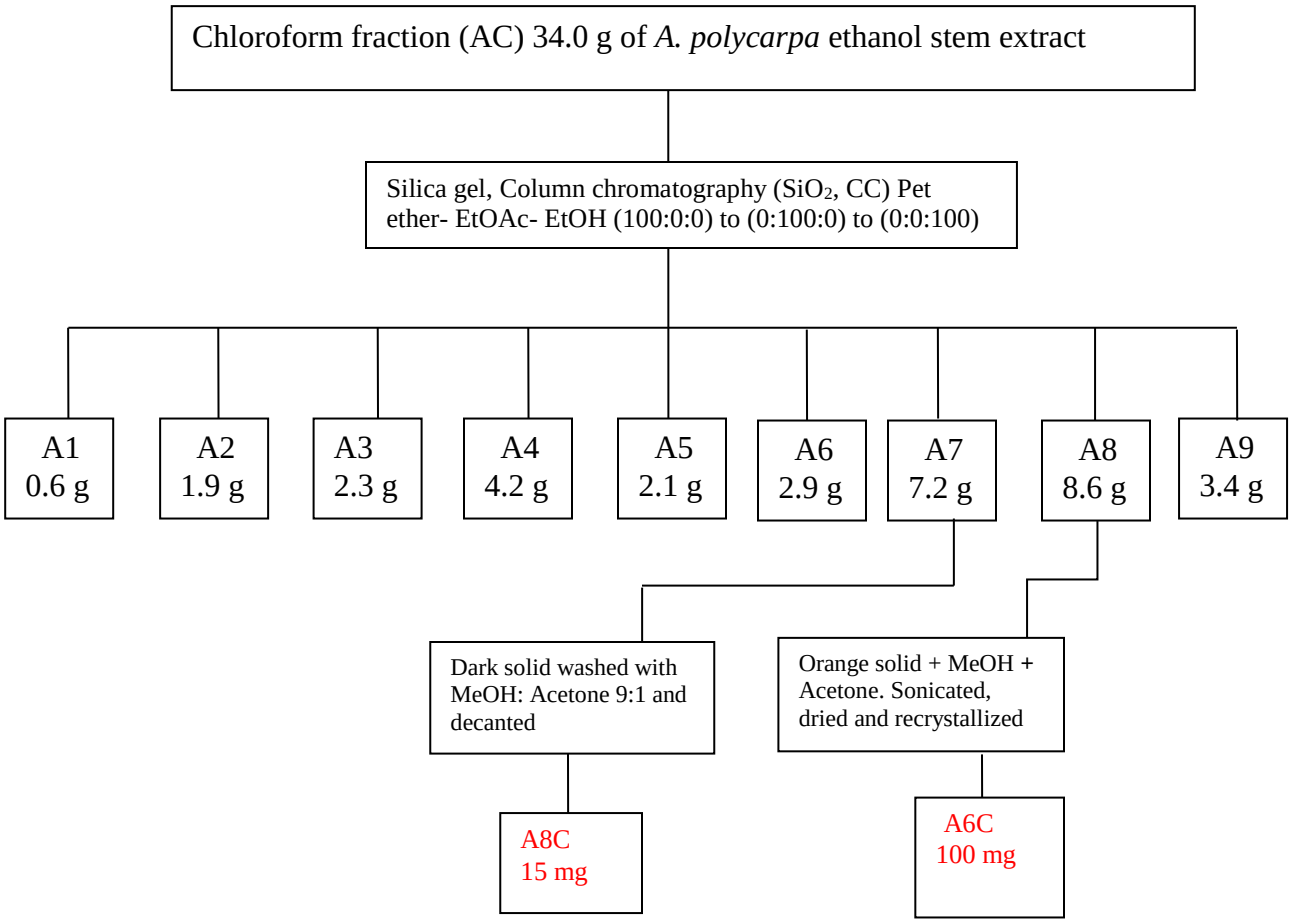

Figure 3.2: Scheme for isolation and purification of compounds from chloroform fraction of *A. polycarpa* stem bark

3.4.5 Isolation of compound(s) from the chloroform fraction (RP) of *A. polycarpa* root bark

The chloroform fraction (RC) was adsorbed onto silica gel and dried. A glass column was packed with a slurry of silica gel (500 g). The sample was introduced onto the column. Elution was started with petroleum ether followed by addition of ethyl acetate at incremental rate of 10 %. When 100% ethyl acetate was achieved, ethanol was introduced at 10 % incremental basis until 100 % ethanol was achieved. Aliquots of 150 mL fractions from the column were collected and grouped by similarity in TLC profiles and concentrated to about 100 mL each. A total of 9 main fractions (D1 – D9) were obtained.

Fraction D8 (1.6 g) was subjected to further chromatography over 150 g of silica gel. The column was eluted with chloroform/ethanol (100:0 - 70:30). A total of 50 fractions collected in 30 mL aliquots were obtained which were grouped into 5 (D8a – D8e). **A9C** was obtained as red powder from D8d eluted with chloroform/ethanol (70:30).

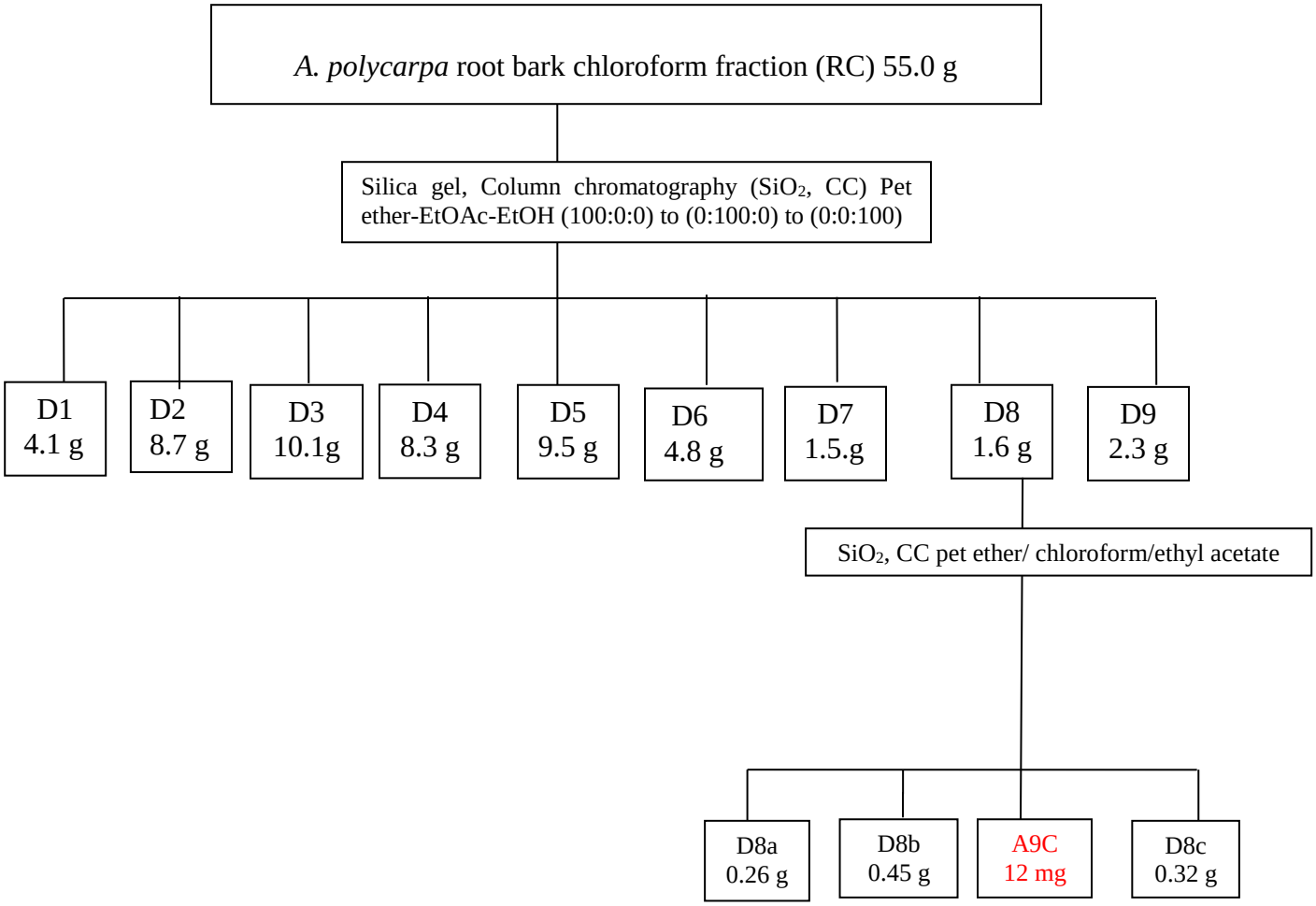

Figure 3.3: Scheme for isolation and purification of compounds from the chloroform fraction of *A. polycarpa* root bark

CHAPTER FOUR

RESULTS

4.1 PHYTOCHEMICAL SCREENING

Table 4.1 below shows the results obtained for the phytochemical screening of the extracts.

Table 4.1: Results of the phytochemical screening tests of the crude ethanol extracts

Secondary metabolite	***C. anisata* root**	***A. polycarpa* stem bark**	***A. polycarpa* root bark**
Alkaloids	+	+	+
Coumarins	+	-	-
Terpenoids	+	+	-
Saponins	-	+	-
Free reducing sugars	+	+	+
Flavonoids	-	-	-
Phytosteroids	-	-	-
Anthracenosides	-	-	-
Polyuronoids	-	-	+

+ = present; - = absent

4.2 TLC PROFILES

4.2.1 TLC profiles of extracts and their fractions

Figure 4.1 shows the comparative TLC chromatograms of ethanol extracts of the leaf, stem and root of *C. anisata* and *A. polycarpa* respectively. TLC chromatograms of the extracts and their various fractions are also shown in Figure 4.2. The petroleum ether (PEF) and chloroform (CF) fractions of the extract of *C. anisata* root developed in petroleum ether/ethyl acetate 5:1 produced 7 and 6 distinctive spots respectively and poor resolution of 2 spots each in petroleum ether/chloroform 5:1. Ethanol extract of *A. polycarpa* stem bark and its fractions were also developed in petroleum ether/ethyl acetate 5:1. AP and AC gave 8 and 6 spots each. But in petroleum ether/chloroform 5:1 no resolutions were observed.

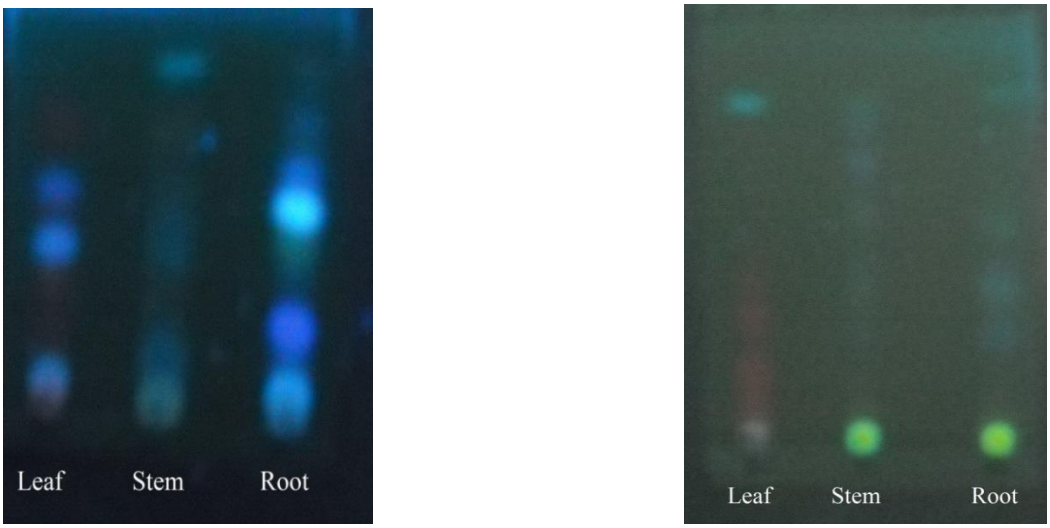

A **B**

Figure 4.1: Comparative TLC chromatograms of the ethanol extracts of the leaf, stem and root of *C. anisata* (A) and *A. polycarpa* (B) developed in pet ether/ethyl acetate 4:1 under UV 365 nm

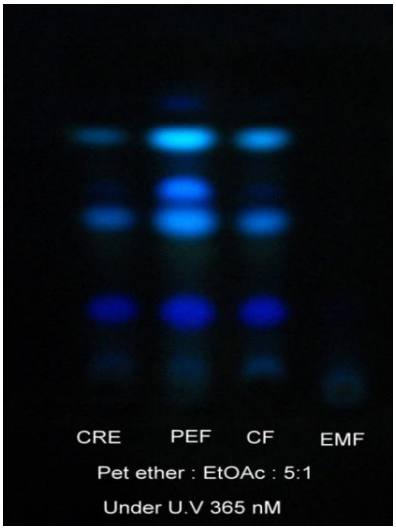

C **D**

Figure 4.2: TLC chromatograms of ethanol extracts of *C. anisata* root (C) and *A. polycarpa* stem bark (D) and their respective fractions

4.2.2 Retardation factor (R_f) values and solubility profiles of the isolated compounds

C1D, C1F, C1G and C1-I from *C. anisata* root were soluble in chloroform and ethyl acetate. In addition, P2A which was also isolated from *C. anisata* root was soluble in methanol.

The three compounds from *A. polycarpa* i.e A6C and A8C and A9C were soluble in methanol, ethanol and water. The R_f values of the isolated compounds are shown in the Table below (Tables 4.2).

Table 4.2: R_f values of isolated compounds on normal phase TLC plate

Compound code	Solvent system	Ratio	R_f
C1D	Petroleum ether/ethyl acetate	5:1	0.57
	Petroleum ether/ethyl acetate	4: 1	0.58
C1F	Petroleum ether/ethyl acetate	3:1	0.70
	Petroleum ether/chloroform	1:2	0.50
C1G	n-hexane/ethyl acetate	4:1	0.36
	Petroleum ether/chloroform	1:1	0.66
C1-1	Petroleum ether/ethyl acetate	6:1	0.56
	Petroleum ether/chloroform	2:1	0.54
P2A	Petroleum ether/ethyl acetate	2:1	0.47
	Chloroform/ethyl acetate	20:7	0.60
A6C	Methanol: ethanoic acid	30:1	0.72
	Methanol: ethanoic acid	40:1	0.38
A8C	Methanol: ethanoic acid	30:1	0.76
	Methanol: ethanoic acid	50:1	0.65
A9C	Methanol: ethanoic acid	30:1	0.72
	Methanol: ethanoic acid	40:1	0.38

4.3 STRUCTURE ELUCIDATION OF ISOLATED COMPOUNDS

4.3.1 Compounds isolated from *C. anisata* root

4.3.1.1 Characterization of C1D

Coumarins are known to show fluorescence under UV light (Selim and Ouf, 2012). C1D produce yellow fluorescence under UV lamp at 365 nm, indicating that it may have a coumarin nucleus.

^{1}H NMR spectrum of C1D taken in deuterated chloroform ($CDCl_3$) (Table 4.3; Appendix 1) displayed four aromatic proton doublets (δ_H 6.37, 6.81, 7.69 and 7.76 ppm). Two of the proton doublets which resonated at 6.37 ppm (J = 9.76 Hz) and 7.76 ppm (J = 9.24 Hz) indicates the presence of ^{3}J *ortho* coupling olefinic protons H-3 and H-4 of an α, β-unsaturated lactone of the coumarin skeleton. The other two aromatic proton which resonated at δ 6.81 (J = 2.4 Hz) and 7.69 ppm (J = 2 Hz) were also indicative of a ^{4}J *meta*-coupling protons which were assigned to H-6 and H-8 respectively (Ngadjui *et al.*, 1989a). This showed that the isolated compound was substituted at two positions on the aryl ring of the coumarin nucleus since the other two aryl coumarinic protons were absent in its spectrum. Furthermore, the two ^{4}J *meta*-coupling proton doublets in the structure also indicate that the compound possessed a 5, 7- disubstituted coumarin skeleton. The presence of a hydroxyl moiety in the compound was confirmed by a proton which resonated as a singlet at δ7.36 ppm (1H, *s*, 5-OH) (Ngadjui *et al.*, 1989a). The ^{1}H NMR spectrum revealed a second substituent group in the structure of C1D to be 3,3- dimethylallyloxy or prenyloxy moiety. This was shown by the presence of two vinylic methyl proton singlets which appeared at δ 1.56 ppm (H-4') and δ 1.73 ppm (H-5'); an olefinic proton as a triplet at 5.65 ppm (J = 7.62 Hz) attached to a two-proton doublet system at 5.0 ppm (Ngadjui *et al.*, 1989a). These data from the ^{1}H NMR of C1D are consistent with those reported for 5-hydroxy-7-(3,3-dimethylallyloxy) coumarin also known as anisocoumarin B (Ngadjui *et al.*, 1989a). Anisocoumarin B **[92]** was isolated from *C. anisata* collected from Cameroun as a novel coumarin (Ngadjui *et al.*, 1989a). Hence C1D was characterized as anisocoumarin B.

The ^{13}C NMR of C1D, taken in deuterated chloroform, $CDCl_3$ (Table 4.5; Appendix 2) showed resonance for 13 carbon atoms instead of 14 due to the overlap of signals from C-4 and C-3' carbons. Nine of these carbon atoms accounted for the coumarin skeleton with the remaining five

accounting for the prenyloxy side chain. Out of the nine carbons of the coumarin nucleus, five were tertiary aromatic carbons and the other four being sp^2 hybridized aromatic methine carbons with signals at δ_C 114.7, 139.8, 125.9 and 113.2 ppm which were assigned to C-3, C-4, C-6 and C-8 respectively. Among the tertiary aromatic carbons, one appeared at far downfield of δ_C 160.6 ppm; indicative of the presence of a carbonyl carbon (C=O) of a coumarin at C-2, confirming that C1D is a coumarin; and another one at δ_C 146.6 ppm assignable to C-5 (the carbon bonded to the hydroxyl group); the remaining three tertiary carbons were C-4a, C-7 and C-8 which showed signals at δ_C 116.5, 144.4 and 113.2 ppm. The presence of the 3,3-dimethylallyloxy group in the molecule of C1D was confirmed by: one sp^3 hybridized aliphatic carbon atom which resonated at δ_C 70.2 ppm (signal shifted downward) indicating that this carbon, assignable to C-1', was bonded to an oxygen atom; one sp^2 hybridized olefinic aliphatic methine carbon with signal at δ_C 119.8 ppm which was assigned to C-2'; one sp^2 hybridized olefinic carbon atom which also resonated further downfield at δ_C 139.8 assigned to C-3' which was bonded to two sp^3 hybridized methyl carbons at δ_C 25.8 and 18.1 ppm, assigned to C-4' and C-5' respectively. The ^{13}C chemical shift was assigned by comparing the analytical results of the ^{13}C NMR spectrum measurement of C1D with compounds of similar structures shown below (Table 4.4).

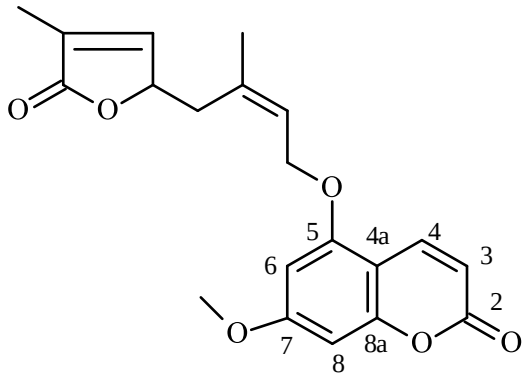

Clausenalansimin B **[125]**

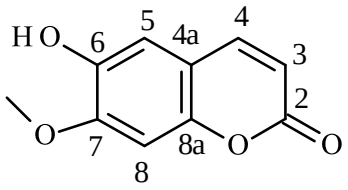

6-hydroxy-7-methoxycoumarin **[126]**

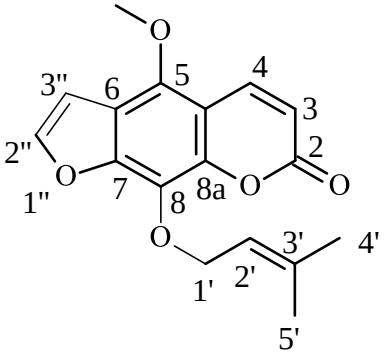

Phellopterin **[127]**

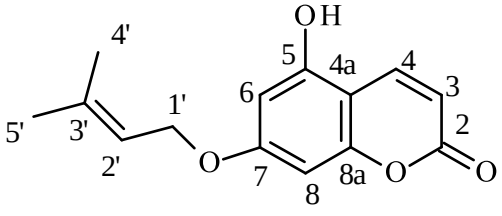

CID (Anisocoumarin B **[92]**)

Table 4.3: ^{1}H and ^{13}C NMR chemical shifts (ppm) of C1D and anisocoumarin B

C1D (in $CDCl_3$, 400 MHz)				Anisocoumarin B* (90 MHz)	
Proton /Carbon number	Chemical shift (ppm) ^{1}H NMR	*J* (Hz)	Chemical shift (ppm) ^{13}C NMR	Chemical shift (ppm) ^{1}H NMR	*J* (Hz)
2	-	-	160.6	-	-
3	6.37, *d*	9.76	114.7	6.35, *d*	10
4	7.76, *d*	9.24	139.8	7.75, *d*	10
4a	-	-	116.5	-	-
5	-	-	146.6	-	-
6	7.69, *d*	2.00	125.9	7.70, *d*	2
7	-	-	144.4	-	-
8	6.81, *d*	2.4	106.7	6.82, *d*	2
8a	-	-	113.2	-	-
5-OH	7.36, *s*	-	-	7.35, *br s*	-
1’	5.00, *d*	7.32	70.2	5.00, *d*	8
2’	5.61, *t*	7.62[a]	119.8	5.65, *t*	8
3’	-	-	139.8	-	-
4’ (Me)	1.56, *s*	-	25.8	1.72, *br s*	-
5’ (Me)	1.73, *s*	-	18.1	1.76, *br s*	-

* (Ngadjui *et al.*, 1989a)

[a] The expanded ^{1}H NMR showed triplet with middle peak at 5.6127 ppm, the third peak to the left was calculated (aided by measuring with a ruler) to be 1.5 x 0.0127 + 5.6127 ppm = 5.63175 ppm. This resulted in calculated *J* value of 7.62 Hz.

The coumarin nucleus of anisocoumarin B was compared with clausenalansimin B **[125]** and 6-hydroxy-7-methoxycoumarin **[126]** (Table 4.4); and the prenyloxy side-chain with phellopterin **[127]** (Table 4.5) (Maneerat *et al.*, 2010; Nakatani *et al.*, 1991; Selim and Ouf, 2012).

Table 4.4: ^{13}C NMR chemical shifts of C1D, clausenalansimin B and 6-hydroxy-7-methoxycoumarin

	^{13}C NMR Chemical shift (ppm) ($CDCl_3$)		
	C1D	Clausenalansimin B* (in $CDCl_3$, 150 MHz)	6-hydroxy-7-methoxycoumarin*
2	160.6	162.1	161.8
3	114.7	110.3	117.05
4	139.8	139.2	147.8
4a	116.5	103.8	113.4
5	146.6	156.1	143.6
6	125.9	96.4	146.2
7	144.4	161.0	104.0
8	106.7	96.9	149.7
8a	113.2	156.6	111.3

*(Maneerat *et al.*, 2010; Selim and Ouf, 2012).

Table 4.5: ^{13}C NMR data of the prenyloxy substituent of C1D and phellopterin

	1’	2’	3’	4’	5’
Phellopterin* ($CDCl_3$)	70.4	119.9	139.3	25.8	18.1
C1D ($CDCl_3$)	70.2	119.8	139.8	25.8	18.1

*(Nakatani *et al.*, 1991).

The GC-MS spectrum of C1D (Appendix 3) showed fragmentation with molecular ion [M^+] peak at m/z 246.2476 which gave the molecular formula of $C_{14}H_9O_4$. This molecular mormular is in agreement with the structure of anisocoumarin B ((Ngadjui *et al.*, 1989a). The base mass peak with m/z at 245.2112 of relative abundance of 100 % represents the $[M-H]^-$ ion.

Table 4.6 and Appendix 4 show the I.R spectrum of C1D. The absorption bands at υ_{max} 3420 and 1717 cm^{-1} confirmed the presence of a hydroxyl (OH) moiety and an α, β-unsaturated lactone of a coumarin carbonyl in the structure of C1D (Ngadjui *etal.*, 1989a). In addition, the absorption bands located at υ_{max} 3110, 2980, 1624 and 1296 cm^{-1} also confirmed the presence of an aryl ring, methyl group, aromatic ring and C-O group respectively.

Table 4.6: Wave numbers (υ/cm^{-1}) of absorption bands obtained in the I.R spectrum of C1D

C1D, (KBr), υ_{max} (cm^{-1})					
3420	3325	3110	2980	1717	1624
1585	1468	1401	1298	1214	1145
1081	1026	987	876	836	794

4.3.1.2 Characterization of P2A

Coumarins are known to show fluorescence under UV light (Selim and Ouf, 2012). P2A exhibited fluorescence under UV lamp at 365 nm; thus suggesting that it may be a coumarin compound.

The ^{1}H NMR spectrum (Table 4.7; Appendix 5) of P2A (taken in deuterated methanol) revealed five aromatic protons. Two were *ortho*-coupled aromatic proton doublets resonating at δ 6.33 (1H, *d, J* = 9.28 Hz) and 7.98 ppm (1H, *d, J* = 9.76 Hz) which are indicative of the H-3 and H-4 protons of α, β-unsaturated lactone of the pyrone ring of coumarin nucleus respectively. Additional, two of the five protons were *meta*-coupled proton doublets resonating in the aromatic region of the ^{1}H NMR spectrum at δ 7.82 (1H, *d, J* = 2 Hz) and 6.89 ppm (1H, *d, J* = 2.4 Hz) indicates the presence of H - 2' and H - 3' protons of a furan ring (*J* = 2 - 2.5 Hz) attached to the coumarin nucleus; the fifth proton resonated as an aromatic singlet at δ 7.33 ppm (Steck and Bailey, 1969). These spectra features are characteristics of a mono-substituted linear furanocoumarin (Steck and Bailey, 1969). Hence P2A is a mono-substituted furanocoumarin molecule. Since only one aryl proton singlet was found in the aromatic region at δ 7.33 ppm of the ^{1}H NMR spectrum instead of two for positions C-5 and C-8, it means that this aromatic proton singlet could either be bonded to C-5 or C-8 carbon and the hydroxyl moiety substituted to the other carbon. The substitution pattern in linear furanocoumarins is identified by the chemical shift (δ) values of the H-4 proton in the ^{1}H NMR spectrum. When the δ value of the H-4 is greater than 8 ppm then the linear furanocoumarin is substituted at C-5 (Steck and Bailey, 1969). It follows to reason that when the δ value of H-4 is less than 8 ppm then the substitution is at C-8. The H-4 proton of P2A showed resonance at δ 7.98 ppm (δ < 8 ppm) in the ^{1}H NMR spectrum, indicating that P2A is substituted at the C-8 carbon of the furanocoumarin skeleton (Razdan *et al.*, 1982). Hence the hydroxyl group in the structure of P2A is substituted on C-8 and the aryl proton singlet located at δ 7.33 ppm in the aromatic region of the ^{1}H NMR spectrum assigned to H-5 proton.

The ^{13}C NMR spectrum of P2A (Table 4.7; Appendix 6) showed ten instead of eleven carbon atoms with signals in the aromatic region; all of which accounted for the furanocoumarin

skeleton of the isolated compound. This may be due to an overlap of C-7 and C-4 signals as a result of low sensitivity of the spectrometer since these positions are similar.

Further analysis of the ^{13}C NMR of P2A revealed that six out of the eleven carbons were tertiary aromatic carbon atoms and the remaining five were sp^2 hybridized aromatic methene carbons. The first tertiary aryl carbon that showed more downfield shift at δ_C 163.0 was indicative of the ketone functional group (C=O) of a coumarin located at C-2. The remaining five tertiary carbons (C4a, C-6, C-7, C-8 and C-8a) resonated at δ_C 117.8, 127.3, 146.9, 131.7 and 141.0 ppm respectively. The chemical shifts of C-7, C-8a or C-8 were located more downfield because of their attachment to a more electronegative oxygen atom in a heterocyclic furan or pyran ring systems or a hydroxyl substituent group as compared to C-4a and C-6 which were bonded to a total of three electropositive sp^2 hybridized carbon atoms each. The signals at δ_C 114.6, 147.2, 111.2, 107.9 and 148.4 ppm were allocated to C-3, C-4, C-5, C-3' and C-2' respectively, being the five sp^2 hybridized aromatic methene carbon atoms. The C-2 signal was shifted more downfield as a result of its attachment to the oxygen atom and an olefinic bond in the aromatic furan ring. These results indicate that P2A is a furanocoumarin with a hydroxyl moiety bonded to the C-8 position. P2A was therefore characterized as xanthotoxol **[80]** (Nakatani *et al.*, 1991). Xanthotoxol **[80**] was also obtained from *C. anisata* (Lakshmi *et al.*, 1984).

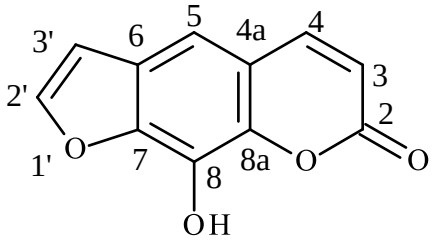

P2A (Xanthotoxol **[80]**)

Table 4.7: ^{1}H and ^{13}C NMR chemical shifts (ppm) of P2A and xanthotoxol

	P2A (in CD_3OD, 500 MHz)			Xanthotoxol * (in $CDCl_3$)		
Proton /Carbon number	Chemical shift (ppm) ^{1}H NMR	*J* (Hz)	Chemical shift (ppm) ^{13}C NMR	Chemical shift (ppm) ^{1}H NMR	*J* (Hz)	Chemical shift (ppm) ^{13}C NMR
2	-	-	163.0	-	-	160.0
3	6.33, *d*	9.28	114.6	6.37, *d*	9.50	114.6
4	7.98, *d*	9.76	147.2	7.80, *d*	9.50	145.3
4a	-	-	117.8	-	-	116.2
5	7.33, *s*	-	111.2	7.28, *s*	-	110.9
6	-	-	127.3	-	-	125.2
7	-	-	146.9	-	-	145.2
8	-	-	131.7	-	-	130.8
8a	-	-	141.0	-	-	140.6
2’	7.82, *d*	2.00	148.4	7.72, *d*	2.20	147.2
3’	6.89, *d*	2.44	107.9	6.82, *d*	2.20	107.1

* (Nakatani *et al.*, 1991)

The GC-MS of P2A (Appendix 7) displayed a molecular peak [M^+] ion at m/z = 202.0332 which is in agreement with the formular $C_{11}H_6O_4$. The [M^++ H] peak was also observed at m/z = 203.0785.

The infrared (IR) spectrum of P2A is shown in Table 4.8 and Appendix 8. The infrared (IR) spectrum of this compound revealed absorption bands at υ_{max} 3415 cm^{-1} characteristic of a hydroxyl (-OH) group. The other band located at υ_{max} 1703 cm^{-1} is also indicative of α, β-unsaturated lactone of a coumarin nucleus. Those at υ_{max} 3112, 1290, 1640 and 865 cm^{-1} respectively, signifies the presence of C=C stretching of benzene ring, C-O stretching, C=C stretching of aromatic rings and furan ring respectively in the molecular structure of this compound.

The I.R data confirmed that P2A is a furanocoumarin which possess a hydroxyl group as indicated by the ^{1}H and ^{13}C NMR data.

Table 4.8: Wave numbers (υ) of absorption bands obtained in the I.R spectrum of P2A

P2A, (KBr), υ_{max} (cm^{-1})					
3415	3292	3112	1703	1640	1593
1499	1421	1346	1290	1223	1183
1149	1127	1421	1346	1290	1223
1184	1150	1128	1095	1026	991
865	821	763	690	662	-

4.3.1.3 Characterization of C1F

C1F exhibited four aromatic proton doublets in the ^{1}H NMR (Table 4.9 and Appendix 9) spectrum. Two of these protons which were ^{3}J *ortho*-coupled, resonated at δ 6.25 ppm (1H, *d*, *J* = 9.45 Hz, H-3) and δ 7.63 ppm (1H, *d*, *J* = 9.45 Hz, H-4), indicating the H-3 and H-4 olefinic proton doublets of a coumarin nucleus. The other two proton doublets were also ^{3}J *ortho*-coupled aryl protons which resonated at δ 7.30 ppm (1H, *J* = 8.55 Hz, H-5) and 6.85 ppm (1 H, *J* = 8.55 Hz, H-6) which are assigned to H-5 and H-6 respectively. Furthermore, the ^{1}H NMR spectrum of

C1F showed resonance for a hetero-methyl proton singlet at δ 3.94 ppm indicating a methoxy group attached to C-7 carbon atom. Additionally, the ^{1}H NMR spectrum of the isolate indicates two aliphatic methyl protons which showed resonance at δ 1.68 ppm (3H, *s*, H-5') and δ 1.86 ppm (3H, *s*, H-4'); an aliphatic olefinic proton doublet at δ 3.55 (2H, *d*, *J* = 7.3 Hz, H-1') which is vicinally-coupled to a triplet proton system at δ 5.24 ppm (1H, *t*, *J* = 6.95 Hz, H-2'). This spectrum characteristic indicates the presence of a prenyl chain substited at C-8 position.

The ^{13}C NMR spectrum (Table 4.9 and Appendix 10) showed resonance for a total of 14 carbons instead of 15 which may be due to an overlap of C-3 and C-4a carbon signals. Nine of which accounted for the coumarin nucleus. Five for the prenyl chain substitute and the one which resonated at δ_C 56.1 confirmed the presence of the methoxy substitute (-OCH_3) bonded to C-7. Out of the nine carbon atoms of the coumarin nucleus, five were tertiary aromatic carbons; one of which resonated far downfield at δ_C 161.4 ppm, indicating the presence of a ketone functional group (C=O) of a coumarin at C-2, confirming that C1F is a coumarin. The remaining four which resonated at δ_C 113.0, 118.0, 152.9 and 160.2 ppm were assigned to C-4a, C-8, C-8a and C-7 respectively. The remaining four carbons of the coumarin nucleus are sp^2 hybridized aromatic methine carbons with signals at δ_C 107.3, 113.0, 121.1 and 143.7 ppm which were assigned to C-6, C-3, C-5 and C-4 respectively. The prenyl chain was confirmed by two aliphatic methyl carbons with signals at δ_C 17.9 and 25.8 ppm assigned to C-5' and C-4', an aliphatic sp3 hybridized carbon at δ_C 21.9 ppm (C-1'), an sp^2 aliphatic carbon at δ_C 121.1 ppm (C-2') bonded to a tertiary carbon at δ_C 132.6 ppm (C-3'). C1F was identified as osthol based on these spectra characteristics and comparing these data with data obtained from literature (Sajjadi, *et al.*, 2009). Osthol was also previously isolated from *C. anisata* (Olufemi *et al.*, 2009).

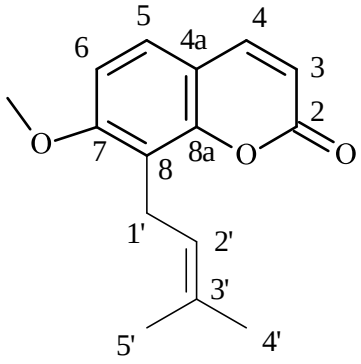

C1F (Osthol **[86]**)

Table 4.9: ^{1}H and ^{13}C NMR chemical shifts (ppm) of C1F and osthol

	C1F (in $CDCl_3$, 500 MHz)			Osthol * (in $CDCl_3$, 500 MHz)		
Proton /Carbon number	Chemical shift (ppm) ^{1}H NMR	*J* (Hz)	Chemical shift (ppm) ^{13}C NMR	Chemical shift (ppm) ^{1}H NMR	*J* (Hz)	Chemical shift (ppm) ^{13}C NMR
2	-	-	161.4	-	-	161.8
3	6.25, *d*	9.45	113.0	6.20, *d*	9.50	113.3
4	7.63, *d*	9.45	143.7	7.60, *d*	9.50	144.2
4a	-	-	113.0	-	-	113.4
5	7.30, *d*	8.55	121.1	7.30, *d*	8.00	126.7
6	6.85, *d*	8.55	107.3	6.80, *d*	8.00	107.8
7	-	-	160.2	-	-	160.6
8	-	-	118.0	-	-	118.3
8a	-	-	152.9	-	-	153.2
7-OMe	3.94, *s*	-	56.1	3.92, *s*	-	56.5
1’	3.55, *d*	7.30	21.9	3.55, *d*	7.30	22.3
2’	5.24, *t*	6.95	121.1	5.25, *t*	7.30	121.6
3’	-	-	132.6	-	-	133.0
4’(Me)	1.86, *s*	-	25.8	1.86, *s*	-	26.2
5’(Me)	1.68, *s*	-	17.9	1.69, *s*	-	18.3

*(Sajjadi, *et al.,* 2009).

The mass spectrum of C1F (Appendix 11) displayed molecular ion [M^+] peak of 244.8321 which corresponds to the molecular formula of $C_{15}H_{16}O_3$. This is in agreement with the molecular formular of osthol **[80]** (Sajjadi, *et al.,* 2009). Moreover, the M+H and M+2H peaks with m/z at 245.7171 and 246.5232 respectively were also observed in the mass spectrum of C1F.

Coumarins are reported to show fluorescence in UV light (Selim and Ouf, 2012). C1F exhibit blue fluorescence under UV lamp. This confirmed that it has the coumarin nucleus.

The I.R spectrum of C1F (Table 4.10 and Appendix 12) showed absorption band at υ_{max} 1715 cm^{-1} indicating the presence of an α, β-unsaturated lactone of a coumarin carbonyl in the structure of C1F. In addition, the absorption bands located at υ_{max} 2966, 1602, 1278 and 825 cm^{-1} indicates the presence of C-H of methyl group, aromatic ring, C-O and -C=C-H groups respectively.

Table 4.10: Wave numbers (υ/cm^{-1}) of absorptions obtained in the I.R spectrum of C1F

C1F, (KBr), υ_{max} (cm^{-1})					
2966	1715	1602	1564	1498	1432
1401	1382	1303	1278	1250	1182
1159	1121	1088	1031	987	914
862	825	803	782	761	712

4.3.1.4 Characterization of C1G

The ^1H NMR spectrum of C1G (Table 4.11; Appendix 13), taken in deuterated chloroform, exhibited five aromatic protons. Two of these protons were *ortho*-coupled proton doublets resonating at δ 6.36 (1H, *d, J* = 9.60 Hz) and 7.77 ppm (1H, *d, J* = 9.40 Hz) indicating H-3 and H-4 protons of α, β-unsaturated lactone of a coumarin respectively. Additional two of the five protons were *meta*-coupled proton doublets which resonated at δ 7.69 (1H, *d, J* = 2.05 Hz) and

6.82 ppm (1H, *d, J* = 2.05 Hz) indicates the presence of H-2'' and H-3'' protons of a furan ring (*J* = 2 - 2.5 Hz) attached to the coumarin nucleus; the fifth proton resonated as an aromatic singlet at δ 7.36 ppm (Steck and Bailey, 1969). These spectra features are characteristics of a mono-substituted linear furanocoumarin. Hence CIG is a mono-substituted furanocoumarin molecule, since only one aryl proton singlet was found in the aromatic region at δ 7.36 ppm of the ^{1}H NMR spectrum instead of two for positions C-5 and C-8. Furthermore, the ^{1}H NMR of C1G revealed the presence of two vinylic methyl proton singlets which resonated at δ 1.72 ppm (3H, *s*) and δ 1.74 (3H, *s*) indicating the H-4' and H-5', an olefinic proton triplet at 5.65 ppm (1H, *t, J* = 7.35 Hz) attached to a two proton doublet system at 5.0 ppm (2H, *d, J* = 7.10 Hz). This indicates the presence of of 3,3- dimethylallyloxy group (Ngadjui *et al.*, 1989a) in C1G.

The substitution pattern in linear furanocoumarins is identified by the chemical shift (δ) values of the H-4 proton in the ^{1}H NMR spectrum. When the δ value of the H-4 is greater than 8 ppm then the linear furanocoumarin is substituted at C-5 (Steck and Bailey, 1969). The δ of H-4 of C1G is 7.77 ppm (δ < 8 ppm). Hence the 3, 3- dimethylallyloxy group is substituted at C-8.

The ^{13}C NMR spectrum of C1G (Table 4.11; Appendix 14) produced resonance for a total of sixteen carbon atoms. Eleven of these carbons exhibited resonance signals in the aromatic region. These carbons accounted for the furanocoumarin skeleton of C1G. Further examination of the ^{13}C NMR spectrum showed that six out of the eleven carbons were tertiary aromatic carbons and the remaining five were sp^2 hybridized aromatic methine carbons. The first tertiary aryl carbon that showed more downfield shift at δ_C 160.5 ppm was indicative of the ketone functional group (C=O) of a coumarin located at C-2. The other five tertiary carbons with resonance at δ_C 116.5, 125.8, 131.6, 144.3 and 148.6 ppm were assigned to C4a, C-6, C-8, C-8a and C-7 respectively. The chemical shifts of C-8, C-8a and C-7 were located more downfield because of their attachment to a more electronegative oxygen atom in a heterocyclic furan or pyran ring systems or an oxy substituent group as compared to C-4a and C-6 which are each bonded to a total of three electropositive sp^2 hybridized carbon atoms. The signals at δ_C 106.7, 113.6, 114.6, 143.8 and 146.6 ppm were assigned to C-3'', C-5, C-3, C-4 and C-2'' respectively, being the five sp^2 hybridized aromatic methine carbon atoms. The C-2'' gave a more downfield

resonance signal due to its attachment to the oxygen atom and an olefinic bond in the aromatic furan ring.

Moreover, resonance signals for five additional carbons were also observed in the ^{13}C NMR spectrum of C1G. These include one sp^3 hybridized aliphatic carbon atom which resonated at δ_C 70.1 (signal shifted downward indicating that this carbon, assignable to C-1', was bonded to an oxygen atom); one sp^2 hybridized olefinic aliphatic methine carbon with signal at δ_C 119.7 which was assigned to C-2'; one sp^2 hybridized tertiary carbon atom which also appeared further downfield at δ_C 139.7 (assigned to C-3') due to its attachment to two sp^3 hybridized methyl carbons at δ_C 25.8 and 18.1 ppm corresponding to C-4' and C-5' respectively. These spectral features confirmed the presence of the 3, 3-dimethylallyloxy group in the structure of C1G. These results are consistent with those obtained for imperatorin **[79]** (Table 4.19) (Muller *et al.*, 2004). C1G was therefore characterized as imperatorin. Imperatorin was also isolated from *C. anisata* previously (Lakshmi *et al.*, 1984).

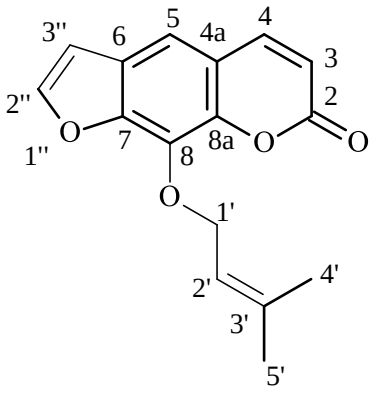

C1G (Imperatorin **[79]**)

Table 4.11: ^{1}H and ^{13}C NMR chemical shifts (ppm) of C1G and imperatorin

	C1G (in $CDCl_3$ at 500 MHz)			Imperatorin * (taken in $CDCl_3$ at 300 MHz)		
Proton /Carbon number	Chemical shift (ppm) ^{1}H NMR	*J* (Hz)	Chemical shift (ppm) ^{13}C NMR	Chemical shift (ppm) ^{1}H NMR	*J* (Hz)	Chemical shift (ppm) ^{13}C NMR
2	-	-	160.5	-	-	160.6
3	6.36, *d*	9.60	114.6	6.36, *d*	9.50	113.0
4	7.77, *d*	9.40	143.8	7.75, *d*	9.50	144.0
4a	-	-	116.5	-	-	116.4
5	7.36, *s*	-	113.6	7.35, *s*	-	114.8
6	-	-	125.8	-	-	126.0
7	-	-	148.6	-	-	148.6
8	-	-	131.6	-	-	132.0
8a	-	-	144.3	-	-	143.8
2''	7.69, *d*	2.05	146.6	7.68, *d*	2.40	146.6
3''	6.82, *d*	2.05	106.7	6.82, *d*	2.40	106.7
1'	5.00, *d*	7.10	70.1	4.95, *d*	7.00	69.9
2'	5.61, *t*	7.35	119.7	5.61, *t*	7.00	119.6
3'	-	-	139.7	-	-	139.7
4'(Me)	1.72, *s*	-	25.8	1.68, *s*	-	25.9
5'(Me)	1.74, *s*	-	18.1	1.73, *s*	-	18.2

*(Muller *et al.*, 2004).

The GC-MS spectrum of C1G (Appendix 15) gave m/z at 271.0191 and 272.2362 which indicates $[M+ H]^+$ and $[M+ 2H]^{2+}$ respectively, calculated for the formula of $C_{16}H_{14}O_4$.

The infrared (IR) spectrum of C1G (Table 4.12 and Appendix 16) displayed absorption band at υ_{max} 1719 cm^{-1} which also indicates α, β-unsaturated lactone of a coumarin nucleus. Those at υ_{max} 3133, 3109, 1297, 1625 and 875 cm^{-1} respectively, signifies C-H stretching of a methyl group, C=C stretching of benzene ring, C-O stretching, C=C stretching of aromatic rings and furan ring in the molecular structure of this compound. These findings suggest that C1G has a furanocoumarin skeleton.

Table 4.12: Wave numbers (υ/cm^{-1}) of absorptions obtained in the I.R spectrum of C1G

C1G, υ_{max} (cm^{-1})					
3133	3109	2972	1719	1705	1625
1585	1542	1467	1437	1399	1381
1339	1325	1297	1213	1181	1146
1131	1092	1080	1027	986	933
906	875	836	812	794	782
765	745	684	660	622	581
564	531	502	489	462	-

4.3.1.5 Characterization of CI-1

The ^{1}H-NMR of C1-I (Table 12 and Appendix 17) showed resonance for a singlet proton at δ 11.68 ppm (1H, *s*, OH), indicative of hydroxyl (OH) group. The signal of the hydroxyl group shifting far downfield to δ 11.68 ppm indicates that it is adjacent to a very polar group resulting in inter hydrogen bonding. In this case, a formyl group, hence making this proton act as a carboxylic proton. Additionally, a formyl proton singlet which resonated at δ 9.94 ppm (1H, *s*, CHO) and an amine proton singlet at δ 8.19 ppm (1H, *brs*, NH) (Joshi *et al*., 1972) were also observed in the ^{1}H-NMR spectrum of CI-1. The presence of prenyl moiety in the molecular structure of C1-I was indicated in the ^{1}H-NMR by the resonance of two aliphatic methy protons at δ 1.51 ppm (H-4') and δ 1.80 ppm (H-5'); olefinic triplet proton at δ 5.35 ppm (H-2', *t, J* = 5.96 Hz) which is *ortho* coupled to a proton doublet system at δ 3.66 ppm (H-1', *d, J* = 6.9 Hz). The presence of four multiplets which resonates at δ 7.28 - 8.22 ppm, indicates the four protons of the C-ring of the carbazole nucleus, hence the C-ring was unsubstituted (Joshi *et al*., 1972). The H-4 proton resonated as a singlet out of a multiplet at 8.07 ppm as a deshielded proton indicating that the formyl group is attached to the carbon atom adjacent to the carbon bearing the H-4 proton (Joshi *et al*., 1967).

^{13}C-NMR spectrum of C1-I (Table 4.13 and Appendix 18) showed resonance for eighteen (18) carbons. Twelve (12) of these carbon atoms accounted for the carbazole skeleton, five for the prenyl side chain and one for the formyl group at (δ_C 195.4 ppm). The twelve carbon atoms which constitute the carbazole skeleton are sp^2 hybridized carbons. The first among them was the carbon with signal at δ_C 157.9 ppm which indicates an aromatic carbon atom with a hydroxyl substituent adjacent to a formyl carbon. That was assigned to the C-2 carbon atom of ring A. In addition, six of the carbon atoms also showed resonance at δ_C 109.1, 115.5, 117.4, 125.3, 140.1 and 145.1 ppm which were assigned to C-1, C-3, C-4a, C-4b, C-8a, and C-9a respectively. The remaining five carbons of the carbazole nucleus were sp^2 hybridized aromatic methine carbons which resonated at δ_C 125.9 ppm (C-4), 119.8 ppm (C-5), 123.7 ppm (C-6), 120.9 ppm (C-7) and 110.8 ppm (C-8). The prenyl substituent was confirmed by one sp^3 hybridized aliphatic carbon which resonated at δ_C 25.7 ppm (C-1'); one sp^2 hybridized olefinic aliphatic methine carbon at δ_C

121.3 ppm (C-2'); one sp^2 hybridized tertiary carbon at δ_C 134.2 (C-3') bonded to two sp^3 hybridized methyl carbons at δ_C 22.8 ppm (C-4') and 18.1 ppm (C-5').

These spectra data are in agreement with those obtained for heptaphyline, a carbazole alkaloid isolated from *Clausena heptaphylla* (Joshi *et al*., 1972). C1-I was therefore, identified as heptaphyline **[70**] which was also previously isolated from *C. anisata* (Ngadjui *et al*., 1988b).

The ^{13}C-NMR of heptaphyline was assigned by comparing the empirical ^{13}C-NMR data measured for heptaphyline and that of 7-methoxyhepthaphyline (Chaichantipyuth *et al*., 1988) which has a similar structure as hepthaphiline.

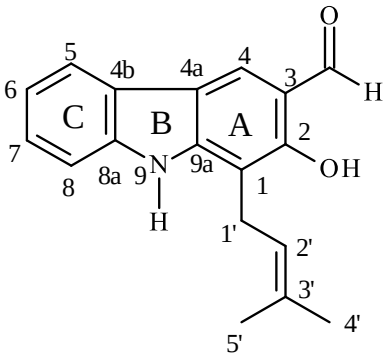

Heptaphyline **[70]**

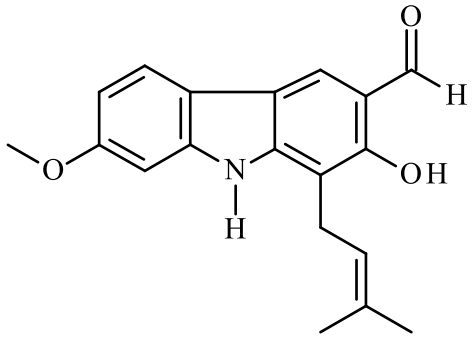

7-methoxyhepthaphyline **[128]**

Table 4.13: ^{1}H and ^{13}C NMR chemical shifts (ppm) of CI-1, heptaphyline and 7-methoxyheptaphyline

Proton/ Carbon No.	**C1-I (in $CDCl_3$ at 500 MHz)**			**Heptaphyline***		**7-methoxyheptaphy-line* (in DMSO-d_6 at 50 MHz)**
	Chemical shift (ppm) ^{1}H NMR	*J* (Hz)	Chemical shift (ppm) ^{13}CNMR	Chemical shift (ppm) ^{1}H NMR	*J* (Hz)	Chemical shift (ppm) ^{13}C NMR
CHO	9.94, *s*	-	195.4	9.9, s	-	196.0
2 (-OH)	11.68, *s*	-	157.9	11.7, *s*	-	156.3
NH	8.19, *s*		-	-	-	-
8a	-	-	140.1	8.25, s	-	142.3
9a	-		145.1	-	-	144.8
3	-	-	115.5	-	-	114.7
4	8.05, s	-	125.9	-	-	124.3
5	7.95, *d*	7.75	119.8	8.00, *d*	7.92	120.5
4b	-		125.3	-	-	116.3
6	7.41, *s*		123.7	-	-	108.5
7	7.43, *s*		120.9	-	-	158.5
8	7.99, *s*		110.8	-	-	95.6
4a	-		117.4	-	-	117.0
1	-		109.1	-	-	108.9
1’	3.66, *d*	6.90	25.7	3.65, *d*	7.0	25.4
2’	5.35, *t*	5.96	121.3	5.35, *t*	6.0	121.6
3’	-	-	134.2	-	-	131.7
4’(Me)	1.74, *s*	-	22.8	1.66, *s*	-	22.6
5’(Me)	1.80, *s*	-	18.13	1.82, *s*	-	17.9

*(Joshi *et al.,* 1972; Chaichantipyuth *et al*., 1988)

The GC-MS spectrum (Appendix 19) of C1-I displayed a base peak molecular ion [M^+] with m/z at 279.1000. This represent $C_{18}H_{17}NO_2$ (Joshi *et al*., 1972). The fragmentation also gave the $[M+H]^+$ peak at 280.1395.

The I.R spectrum of C1-I is shown in Table 4.14 and Appendix 20. The two prominent bands which absorbed at 1608 and 3290 cm^{-1} respectively, indicates a formyl substituent and a hydroxyl and/or N-H group which are typical of a 3-formyl-2-hydroxycarbazole skeleton (Reisch, *et al.*, 1994; Joshi*et al*., 1967).

Table 4.14: Wave numbers (υ/cm^{-1}) of absorptions obtained in the I.R spectrum of C1-I

C1-I, υ_{max} (cm^{-1})					
3290	3044	2959	2911	2853	1920
1755	1717	1643	1608	1584	4171
1448	1382	1329	1276	1252	1226
1195	1182	1147	1064	1024	1015
968	928	879	870	853	824
786	775	589	566	545	494
471	-	-	-	-	-

4.3.2 Compounds isolated from *A. polycarpa* stem bark

4.3.2.1 Characterization of A6C

A6C gave orange colored spot on the TLC plate when it was sprayed with Dragendorff's reagent, suggesting that it might be an alkaloid.

The ^{1}H NMR spectrum of compound A6C (Table 4.15; Appendix 21) revealed a pair of two vicinally-coupled aromatic proton doublets which resonated at δ 7.86 ppm (1H, *d, J* = 8.2 Hz, H-12) and 8.08 ppm (1H, *d, J* = 8.2 Hz, H-11) assignable to H-12 and H-11 respectively. Two pairs of *para*-substituted aromatic proton singlets with signals at δ 7.02 and 7.66 ppm were also observed in the ^{1}H NMR spectrum which corresponded to H-4 and H-1 of the protoberberine nucleus in A6C. In addition, two pairs of aliphatic methylene vicinally-coupled proton triplets which resonated at δ 3.30 ppm (2H, *t, J* = 8.80 Hz) designated to H-5 and δ 4.97 ppm to H-6 (2H, *t, J* = 6.36 Hz) shifting downfield due to the quaternary amine were observed in the 1H NMR spectrum of A6C (Yi - Chen *et al.*, 1998). Furthermore, two aromatic proton singlets which resonated at δ 8.82 ppm (1H, *s*) and 9.83 ppm (1H, *s*) in the ^{1}H NMR spectrum of A6C are typical characteristics of the H-13 and H-8 respectively of the berberine skeleton in the isolated compound (Yi - Chen *et al.*, 1998). The signals of H-8 and H-13 which resonated at downfield positions confirmed the presence of the desheilding quaternary nitrogen atom and four aromatic protons (two of which were *ortho*- coupled and the other two in broad singlet forms as described above) in the molecular structure of A6C (Sua *et al.*, 1993). The spectral features described above are characteristics of 2, 3, 9, 10-substituted quaternary protoberberine salt. Hence A6C possessed 2, 3, 9, 10-substituted quaternary protoberberinium salt structure.

Four signals for aromatic methoxy moieties were also observed at δ_H 3.93 (3H, *s*), 3.95 (3H, *s*), 4.09 ppm (3H, *s*) and 4.85 ppm (3H, *s*) in the ^{1}H NMR spectrum of the isolated compound; accounting for the four substituent groups at C-2, C-3, C-9 and C-10 positions respectively on the quanternary protoberberinium salt structure of A6C. The two pairs of *para*-substituted aromatic proton singlets which signals were observed in the ^{1}H NMR spectrum suggested that each proton was located at C-1 and C-4 positions of ring A respectively, hence the placement of one methoxy group at C-2 and a second one at C-3 positions on ring A of A6C. The assignment of the last two methoxy moieties on ring D at C-9 and C-10 positions have been established by

the pair of proton doublets with AB system and ortho coupling (J = 8.2 Hz as described above) between H-11 and H-12 in the ^{1}H NMR spectrum of A6C (Tanahashi *et al.*, 2000).

The ^{13}C NMR of A6C (Table 4.15; Appendix 22) showed resonance for 21 carbon atoms; out of which 17 accounted for the protoberberinium salt skeleton. Within these 17 carbon atoms, six appeared in the aromatic region of the ^{13}C NMR spectrum as sp^2 hybridized methine carbons corresponding to C-1 (δ_C 109.9 ppm), C-4 (δ_C 112.2 ppm), C-8 (δ_C 146.4 ppm), C-11 (δ_C 124.5 ppm), C-12 (δ_C 128.0 ppm) and C-13 (δ_C 120.5 ppm) respectively. This suggests that these aryl carbon atoms had only one hydrogen present on each of them. The signals of C-8, C-13 and C-13a which shifted downfield to δ_C 149.4, 120.5 and 139.8 ppm in the ^{13}C NMR spectrum of A6C respectively, were due to the desheilding effect of the quaternary nitrogen in ring C. The ^{13}C NMR spectrum of A6C also revealed five sp^2 hybridized aryl carbons which resonated at δ_C 135.3, 123.3, 130.1, 139.8 and 121.3 ppm which corresponded to C-4a, C-8a, C-12a, C-13a and C-13b in that order. Besides, two sp^3 hybridized methylene carbons appearing at δ_C 27.8 and 56.7 ppm assignable to C-5 and C-6 (which shifted to more downfield position due to its attachment to the quaternary nitrogen ion) respectively, also showed resonance in the ^{13}C NMR spectrum. The remaining four carbon atoms of A6C showed signals for aryl carbon bonded to oxymethyl moieties (δ_C 145-154 ppm) assignable to C-2, C-3, C-9 and C-10. These data confirmed that A6C is 2,3,9,10-tetra substituted quaternary protoberberine alkaloid. Lastly, the four carbon atoms which showed signals for aromatic methoxy groups in the ^{13}C NMR spectrum of A6C, at δ_C 57.6, 57.4, 62.5 and 57.0 ppm were respectively assigned to 2-OCH_3, 3-OCH_3, 9-OCH_3 and 10-OCH_3. A6C was hence identified as palmatine chloride **[107]**. These data also compared favorably with those obtained for palmatine chloride (Table 4.16) (Huasain *et al.*, 1989). Palmatine chloride **[107]** was previously isolated from *A. polycarpa* (Jössang *et al.*, 1977).

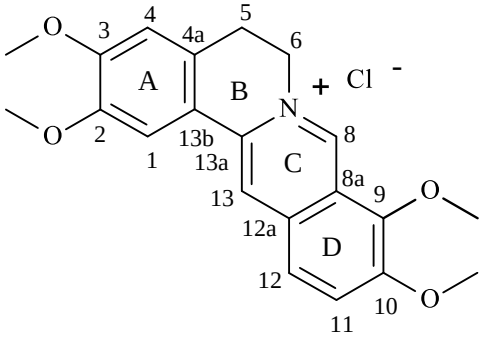

Palmatine chloride **[107]**

Table 4.15: ^{1}H and ^{13}C NMR chemical shifts (ppm) of A6C and palmatine chloride

Proton or Carbon number	A6C (in CD_3OD, 400 MHz)			Palmatine chloride*		
	Chemical shift (ppm) ^{1}H NMR	*J* (Hz)	Chemical shift (ppm) ^{13}C NMR	Chemical shift (ppm) ^{1}H NMR	*J* (Hz)	Chemical shift (ppm) ^{13}C NMR
1	7.65, *s*	-	109.9	7.66, *s*	-	108.7
2	-	-	150.9	-	-	149.6
3	-	-	151.9	-	-	150.6
4	7.04, *s*	-	112.2	7.02, *s*	-	111.2
4a	-	-	135.3	-	-	134.0
5	4.19, *t*	8.80	27.8	3.30, *t*	5.7	27.2
6	4.92, *t*	6.36	56.7	4.97, *t*	5.7	56.8
8	9.75, *s*	-	146.4	9.79, *s*	-	145.0
8a	-	-	123.3	-	-	119.1
9	-	-	153.8	-	-	152.4
10	-	-	145.7	-	-	144.5
11	8.10, *d*	9.28	124.5	8.08, *d*	8.2	123.6
12	8.01, *d*	8.76	128.0	7.86, *d*	8.2	126.8
12a	-	-	130.1	-	-	128.3
13	8.79, *s*	-	120.5	8.86, *s*	-	120.5
13a	-	-	139.8	-	-	138.3
13b	-	-	121.3	-	-	122.1
2-OMe	3.93, *s*	-	57.6	3.88, *s*	-	57.2
3-OMe	3.95, *s*	-	57.4	3.88, *s*	-	57.2
9-OMe	4.09, *s*	-	62.5	3.96, *s*	-	62.5
10-OMe	4.85, *s*	-	57.0	3.99, *s*	-	56.4

*(Huasain *et al*., 1989)

The GC-MS spectrum of A6C dissolved in methanol (Appendix 23) showed molecular ion peak at m/z 389 for $[M + 2]^+$ suggestive of the formula $C_{22}H_{21}NO_4Cl$. The increment in the m/z value of the molecular ion peak by 2 a.m.u, i.e. 389 observed for $C_{22}H_{21}NO_4Cl^+$ instead of 387 is due to the presence of ^{37}Cl isotope.

The infrared spectrum of A6C (Table 4.16; Appendix 24) revealed υ_{max} 3496 cm^{-1} for quanternary nitrogen ($C=N^+-H$) group. Five additional bands at υ_{max} 3072, 2979, 1634, 1384 and 1242 cm^{-1} corresponded to the presence of benzene ring stretching, C-H stretching of aliphatic methylene (CH_2) group, C=C stretching vibrations of aromatic rings, C-H stretching of methyl (CH_3) and C-O stretching groups in the molecular structure of A6C.

Table 4.16: Wave numbers (υ/cm^{-1}) of absorptions obtained in the I.R spectrum of A6C

A6C, (KBr) υ_{max} (cm^{-1})					
3496	3422	3318	3072	2979	1677
1635	1504	1500	1466	1425	1396
1384	1278	1242	1136	1112	1049
1015	967	898	806	733	689

4.3.2.2 Characterization of A8C

The spot of A8C turned orange on the TLC plate when it was sprayed with Dragendorff's reagent, indicating that it was an alkaloid.

The ^1H NMR spectrum of the compound A8C (Table 4.17; Appendix 25) taken at 400 MHz in deuterated methanol revealed a pair of two *ortho*-coupled aromatic proton doublets which resonated at δ 9.72 (1H, *d, J* = 8.2 Hz) and 8.75 ppm (1H, *d, J* = 8.2 Hz) and are indicative of the H-8 and H-13 of ring C of a quaternary protoberberium salt respectively. Two pairs of *para*-substituted aromatic proton singlets which showed resonance at δ 7.64 and δ 6.84 ppm (1H, s) in

the ^{1}H NMR spectrum are assignable to H-1 and H-4 of ring A of the protoberberine nucleus of the isolated compound, further showed that A8C is a quaternary protoberberine alkaloid. Moreover, two pairs of aliphatic methylene coupling proton triplets which resonated at δ 3.30 ppm (2H, *t, J* = 5.5 Hz) and δ 4.97 ppm (2H, *t, J* = 5.5 Hz) revealed the presence of H-5 and H-6 of the isoquinoline structure of the quaternary protoberberine alkaloid. The H-6 protons resonated downfield to H-5 protons due to the desheilding influence to the quanternary amine on the H-6 (Yi - Chen *et al.*, 1998). Furthermore, two aromatic protons which showed resonance as doublet at δ 8.08 ppm (1H, *d, J* = 7.88 Hz) and 8.00 ppm (1H, *d, J* = 7.36 Hz) with strong ortho coupling revealed H-11 and H-12 of the quaternary protoberberine nucleus of A8C. The above spectral features are all characteristic of 2, 3, 9, 10-substituted quaternary protoberberine alkaloid. Consequently, A8C possessed 2, 3, 9, 10-substituted quaternary protoberberinium skeleton.

Further analysis of the ^{1}H NMR spectrum of A8C revealed signals for singlet protons of three aromatic methoxyl moieties at δ 4.01(1H, s), 4.08 (1H, s) and 4.20 ppm (1H, s) which accounted for the three methyl groups attached to C-2, C-9 and C-10 positions on the quanternary protoberberine nucleus and hence leaving the substituent group bonded to C-3. The other small peaks appearing as singlets at δ 2.15, 4.06 and 4.218 ppm in the ^{1}H NMR spectrum of A8C could be peaks from impurities.

However, the I.R spectrum of A8C indicated the presence of a hydroxyl group. Therefore, this hydroxyl moiety could be bonded to C-3 position of the protoberberine skeleton of A8C.

The two pairs of *para* aromatic proton singlets observed in the ^{1}H NMR spectrum suggested that each of this proton could be located at C-1 and C-4 positions of ring A respectively. Hence one methoxy group was bonded to C-2 on ring A. Assignment of the last two methoxyl moieties of ring D to C-9 and C-10 positions have been established by the pair of proton doublets with AB spin system and ortho coupling (*J* = 8.2 Hz) between H-11 and H-12 in the ^{1}H NMR spectrum of A8C (Tanahashi *et al.*, 2000).

The ^{13}C NMR of A8C (Table 4.17; Appendix 26) showed resonance for 20 carbon atoms; out of which 17 accounted for the protoberberine skeleton and the other three for methoxy moieties. Within the 17 carbon atoms that accounted for the protoberberine framework, 12 appeared in the

aromatic region of the ^{13}C NMR spectrum accounting for the two aromatic rings A and D; 4 out of these 12 carbon atoms were sp^2 hybridized methine aryl carbons corresponding to C-1 (δ_C 110.0 ppm), C-4 (δ_C 115.9 ppm), C-11 (δ_C 123.2 ppm) and C-12 (δ_C 124.4 ppm) respectively. These suggest that the aryl carbon atoms had only one hydrogen atom. Another four of the 12 aryl carbons were also found to be bonded to heteroatoms linked to the rings by oxygen atom (δ_C = 145-152 ppm) or (δ_C 149.6, 151.8 and 145.6 ppm) accounting for the three carbon atoms of the methyl and one phenolic carbon (δ_C 146.2 ppm) at C-2, C-9, C-10 and C-3 positions respectively. The other four signals at δ_C 130.3, 119.4, 128.0 and 120.9 ppm corresponds to C-4a, C-8a, C-12a and C-13b respectively. The two methylene carbons at δ_C 27.7 and 56.9 ppm are assigned to C-5 and C-6, respectively. The signals at δ 146.2, 119.4 and 135.4 ppm in the ^{13}C NMR spectrum were also assigned to C-8, C-13 and C-13a respectively. The higher shifts in resonance observed for these carbon atoms and the C-6 methylene carbon were due to the presence of the quaternary nitrogen in ring C. These spectral characteristics confirmed that compound A8C is 2, 3, 9, 10-tetrasubstituted quaternary protoberberine alkaloid. Finally, the three signals for aromatic methoxy groups, in the ^{13}C NMR spectrum of A8C which appeared at δ 57.4, 62.5 and 57.6 ppm were respectively assigned to 2-OCH_3, 9-OCH_3 and 10-OCH_3. These data compared favorably with those obtained for jatrorrhizine chloride as shown in Table 4.17 below (Huasain *etal.,* 1989). Hence A8C was identified as jatrorrhizine chloride. Jatrorrhizine chloride had also been previously isolated from *A. polycarpa* (Jössang *et al.,* 1977).

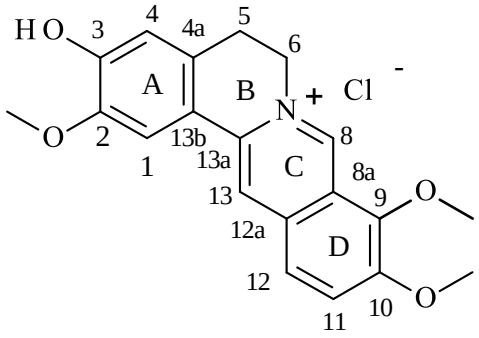

Jatrorrhizine chloride **[108]**

Table 4.17: ^{1}H and ^{13}C NMR chemical shifts (ppm) of A8C and Jatrorrhizine chloride

Proton or Carbon No.	A8C (in CD_3OD, 400 Hz)			Jatrorrhizine chloride*		
	Chemical shift (ppm) ^{1}H NMR	*J* (Hz)	Chemical shift (ppm) ^{13}C NMR	Chemical shift (ppm) ^{1}H NMR	*J* (Hz)	Chemical shift (ppm) ^{13}C NMR
1	7.63, *s*	-	110.0	7.58, *s*	-	110.9
2	-	-	149.6	-	-	149.4
3	-	-	146.2	-	-	146.5
4	6.84, *s*	-	115.9	6.98, *s*	-	116.3
4a	-	-	130.3	-	-	130.2
5	4.09, *t*	4.88	27.6	3.25, *t*	5.6	29.1
6	4.85, *t*	10.24	56.9	4.90, *t*	5.6	57.6
8	9.72, *s*	-	146.2	9.83, *s*	-	145.2
8a	-		119.4	-	-	119.2
9	-		151.8	-	-	151.5
10	-		145.6	-	-	145.2
11	8.08, *d*	7.36	123.2	8.01, *d*	8.0	122.9
12	8.00, *d*	7.88	124.4	7.90, *d*	8.0	125.7
12a	-	-	128.0	-	-	128.2
13	8.75, *s*	-	119.4	8.82, *s*	-	119.2
13a	-	-	135.4	-	-	134.9
13b	-	-	120.9	-	-	120.9
2-OMe	4.01, *s*	-	57.4	3.82, *s*	-	58.3
9-OMe	4.08, *s*	-	62.5	3.91, *s*	-	62.9
10-OMe	4.20, *s*	-	57.6	4.01, *s*	-	57.0

* (Huasain *et al.*, 1989)

The GC-MS spectrum of A8C taken in methanol (Appendix 27) revealed a fragmention at m/z of 396.6316. This molecular ion peak corresponds to the formula $C_{20}H_{20}NO_4Cl$ + Na. The fragment ion with relative abunbance of 100 % and m/z at 316.8225 indicates the removal of NaCl and H_2O from [$C_{20}H_{20}NO_4Cl$ + Na]. The m/z of 316.8225 which was obtained instead of 320 indicates that the chloride (Cl^-) and oxide (O^{2-}) removed from the parent compound (in the form of NaCl and H_2O) during the fragmentation were ^{37}Cl and ^{18}O isotopes respectively.

The infrared spectrum of A8C (Table 4.18 and Appendix 28) revealed absorption bands at υ_{max} 3428 and 3353 cm^{-1} for hydroxyl (OH) and quanternary nitrogen ($C=N^+$-H) moieties respectively. It has been reported that the value of the υ_{max} stretching vibration of the quanternary nitrogen-hydrogen bond in a compound is reduced greatly (by about 150 cm^{-1}) when hydrogen bonds are also in the structure of the molecule (Hesse *et al.*, 2008). Thus the decrease in $C=N^+$-H vibration in A8C as compared to A6C confirmed the presence of the hydroxyl group in A8C. The other bands located at υ_{max} 3067, 2941, 1364 and 1276 cm^{-1} represents C-H vibration of benzene ring, methylene (CH_2), methyl (CH_3) and C-O groups, respectively.

Table 4.18: Wave numbers (υ/cm^{-1}) of absorptions obtained in the I.R spectrum of A8C

A8C, (KBr) υ_{max} (cm^{-1})					
3428	3353	3204	3067	2941	2362
1632	1604	1534	1442	1364	1333
1276	1242	1142	1070	1024	974
908	878	813	736	689	652

4.3.2 Characterization of compound from the root bark of *A. polycarpa*

4.3.2.3 Characterization of A9C

A9C isolated from the root of *A. polycarpa* produced an orange spot when sprayed with Dragendoff's reagent. This indicates that it was an alkaloid.

The ^{1}H-NMR spectrum of A9C (Table 4.19; Appendix 29) revealed a pair of two vicinally-coupled aromatic proton doublets which resonated at δ 8.00 ppm (1H, *d, J* = 8.2 Hz) and 8.08 ppm (1H, *d, J* = 8.2 Hz,) assignable to H-12 and H-11 respectively. Two pairs of *para*-substituted aromatic proton singlets with signals at δ 7.02 and 7.66 ppm were also observed in the ^{1}H NMR spectrum which correspond to H-4 and H-1 of the protoberberine nucleus in A9C. Additionally, two pairs of aliphatic methylene vicinally-coupled proton triplets which resonated at δ 3.30 ppm (2H, *t, J* = 8.80 Hz) designated to H-5 and δ 4.97 ppm to H-6 (2H, *t, J* = 6.36 Hz) shifting downfield due to the quaternary amine were observed in the 1H NMR spectrum of A9C (Yi - Chen *et al.*, 1998). Moreover, the ^{1}H NMR spectrum of A9C showed two aromatic proton singlets which resonated at δ 8.78 (1H, *s*) and 9.74 ppm (1H, *s*) due to the desheilding influence of the quaternary nitrogen moiety. This indicates the H-13 and H-8 respectively of the protoberberine skeleton in the isolated compound (Yi - Chen *et al.*, 1998). The signals of H-8 and H-13 which resonated at downfield confirmed the presence of the desheilding quaternary nitrogen atom (Sua *et al.*, 1993) of A9C. All the above spectral features are characteristics of 2, 3, 9, 10-substituted quaternary protoberberine salt. Hence A9C possessed 2, 3, 9, 10-substituted quaternary protoberberine salt structure. The signal at δ_H 1.18 ppm is from an impurity in A9C.

Four signals for aromatic methoxy moieties were also observed at δ_H 3.93 (3H, *s*), 3.95 (3H, *s*), 4.09 (3H, *s*) and 4.85 ppm (3H, *s*) in the ^{1}H NMR spectrum of the isolated compound; accounting for the four substituent groups at C-2, C-3, C-9 and C-10 positions respectively on the protoberberine skeleton of A9C. The two pairs of *para*-substituted aromatic proton singlets which signals were observed in the ^{1}H NMR spectrum suggested that each proton was located at C-1 and C-4 positions of ring A respectively. Hence the placement of one methoxy group at C-2 and a second one at C-3 positions on ring A of compound A9C. The assignment of the last two methoxy moieties on ring D at C-9 and C-10 positions have been established by the pair of proton doublets with AB system and ortho coupling (*J* = 8.2 Hz) between H-11 and H-12 in the ^{1}H NMR spectrum of A9C (Tanahashi *et al.*, 2000).

The ^{13}C NMR of A9C (Table 4.19; Appendix 30) showed resonance for 21 carbon atoms; out of which 17 accounted for the protoberberine skeleton. Within these 17 carbon atoms, six appeared in the aromatic region of the ^{13}C NMR spectrum as sp^2 hybridized methine carbons corresponding to C-1 (δ_C 109.9), C-4 (δ_C 112.2), C-8 (δ_C 146.4), C-11 (δ_C 124.5), C-12 (δ_C 128.0) and C-13 (δ_C 120.5 ppm) respectively. This suggest that the aryl carbon atoms had only one hydrogen atom present on each of them. The signals of C-8, C-13 and C-13a which shifted downfield to δ_C 149.4, 120.5 and 139.8 ppm in the ^{13}C NMR spectrum of A9C, respectively due to the desheilding effect of the quaternary nitrogen in ring C. The ^{13}C NMR spectrum also revealed five sp^2 hybridized aryl carbons which resonated at δ_C 135.3, 123.3, 130.1, 139.8 and 121.3 ppm which correspond to C-4a, C-8a, C-12a, C-13a and C-13b respectively. Besides, two sp^3 hybridized methylene carbons appearing at δ_C 27.8 and 56.7 ppm assignable to C-5 and C-6 respectively were also observed in the ^{13}C NMR spectrum. The remaining four carbon atoms of the quaternary protoberberine alkaloid showed signals for aryl carbon bonded to oxymethyl moieties (δ_C 145-154 ppm) assignable to C-2, C-3, C-9 and C-10. These data confirmed that A9C is 2,3,9,10-tetra substituted quaternary protoberberine alkaloid. Lastly, the four carbon atoms which showed signals for aromatic methoxy groups in the ^{13}C NMR spectrum of A9C, at δ_C 57.6, 57.4, 62.5 and 57.0 ppm were respectively assigned to 2-OCH_3, 3-OCH_3, 9-OCH_3 and 10-OCH_3. A9C was therefore identified as palmatine chloride **[107]**. These data also compared favorably with those obtained for palmatine chloride from literature (Table 4.19) (Huasain *et al.*, 1989). Palmatine chloride **[107]** was previously isolated from *A. polycarpa* (Jössang *et al.*, 1977) and from the stem bark of *A. polycarpa* in this study as A6C (Section 4.3.2.1).

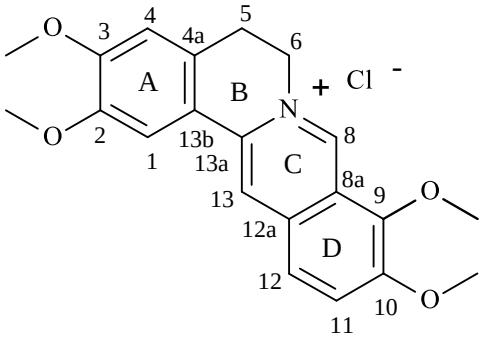

A9C (Palmatine chloride **[107]**)

Table 4.19: ^{1}H NMR chemical shifts (ppm) of A9C and palmatine

Proton or Carbon number	A9C (in CD_3OD, 400 MHz)			Palmatine chloride*		
	Chemical shift (ppm) ^{1}H NMR	Chemical shift (ppm) ^{13}C NMR	*J* (Hz)	Chemical shift (ppm) ^{1}H NMR	*J* (Hz)	Chemical shift (ppm) ^{13}C NMR
1	7.62, *s*	109.9	-	7.66, *s*	-	108.7
2	-	150.9	-	-	-	149.6
3	-	151.9	-	-	-	150.6
4	, *s*	112.2	-	7.02, *s*	-	111.2
4a	-	135.3	-	-	-	134.0
5	3.31, *t*	27.8	8.80	3.30, *t*	5.70	27.2
6	4.93, *t*	56.7	6.36	4.97, *t*	5.70	56.8
8	9.74, *s*	146.4	-	9.79, *s*	-	145.0
8a	-	123.3	-	-	-	119.1
9	-	153.8	-	-	-	152.4
10	-	145.7	-	-	-	144.5
11	8.08, *d*	124.5	9.28	8.08, *d*	8.2	123.6
12	8.00, *d*	128.0	8.76	7.86, *d*	8.2	126.8
12a	-	130.1	-	-	-	128.3
13	8.78, *s*	120.4	-	8.86, *s*	-	120.5
13a	-	139.8	-	-	-	138.3
13b	-	121.3	-	-	-	122.1
2-OMe	3.91, *s*	57.6	-	3.88, *s*	-	57.2
3-OMe	3.94, *s*	57.4	-	3.88, *s*	-	57.2
9-OMe	3.97, *s*	62.5	-	3.96, *s*	-	62.5
10-OMe	4.01, *s*	57.0	-	3.99, *s*	-	56.4

*(Huasain *et al*., 1989).

4.4 ACUTE TOXICITY

The ethanol extracts of the root of *C. anisata* (CRE), stem bark of *A. polycarpa* (ASE) and the root bark of *A. polycarpa* (AR) which were administered at 2 500 and 5 000 mg/kg p.o. showed no sign of toxicity or death during the observation period. This indicates that the mean lethal dose (LD_{50}) of CRE, ASE and AR were above 5 000 mg/kg p.o. and that CRE and ASE are safe for the short term use when taken orally even up to 5 000 mg/kg per day. These results also show that CRE, ASE and AR could be administered at any dose from 0 - 5 000 mg/kg p.o. to these experimental animals and the effects of the extracts accessed on the animal subjects without them dying during the course of the experiments. Thus three dose levels of 10, 100 and 1 000 mg/kg p.o. which were within the range (0 - 5 000 mg/kg p.o) were chosen for the extracts and all their fractions for all the investigations.

4.5 ANALGESIC ACTIVITIES

The analgesic activities of the ethanol extracts of *C. anisata* root and *A. polycarpa* stem bark and their respective petroleum ether, chloroform and aqueous fractions in addition to some of the isolated compounds were evaluated for their central analgesic activity in the hot plate test (Eddy and Leimbach, 1953) in C57BL/6 mice of either sex. The other compounds were not tested due to their paucity. Peripheral and/or central pain inhibitory activity of the extracts, fractions and isolates was again tested in the acetic acid - induced writhing assay (Koster *et al.*, 1959) in Swiss albino mice of both sex.

4.5.1 Hot plate assay

4.5.1.1 *C. anisata* root and *A. polycarpa* stem bark extracts

Ethanol extract of *C. anisata* root (CRE)

The ethanol extract of *C. anisata* root showed analgesic effect by significantly ($p < 0.05$ - 0.001) prolonging the latency of mice to respond to thermally induced pain in a dose-dependent manner compared to the vehicle treated control group. The analgesic effects of CRE became statistically significant at 1 h and attained its peak at 2 h (Figure 4.3 A and B). The highest analgesic response was exhibited by CRE at 1000 mg/kg p.o. with Overall Analgesic activity calculated

(OPTI) to be 72.15 %, and peak %PTI of 35.53 % Maximal % OPTI calculated for tramadol was 45.5 % at 15 mg/kg p.o. and peak %PTI of 17.93 % at 3 h (Figure 4.3; Table 4.20).

Ethanol extract of *A. polycarpa* stem bark (ASE)

The ethanol extract of *A. polycarpa* stem bark showed remarkable analgesic activity in increasing the reaction time of mice to respond to pain in the hot plate assay. The effect appeared to be inversely dose-dependent. The highest overall analgesic activity (%OPTI) was 82.54 % at 10 mg/kg p.o was significant ($p < 0.01$) (Figure 4.3 C and D; Table 4.21). ASE commenced significant analgesic activity at 1 h ($p < 0.05$) and peaked at 4 h ($p < 0.001$) at 10 mg/kg p.o

4.5.1.2 Fractions of *C. anisata* root extract

Petroleum ether fraction (PEF)

The petroleum ether fraction of the extract (PEF) also showed significant dose-dependent analgesic effect by elongating the latency of mice to react to thermally induced nociception. PEF commenced significant ($p < 0.001$) analgesic effect at 30 min which increased with time and peaked at 2 h after it was administered with peak mean %PTI of 38.50 % at 1 000 mg/kg p.o. (Figure 4.3 G). The highest overall analgesic effect of PEF was 96.23 % ($p < 0.001$) at 1 000 mg/kg p.o (Figure 4.3 H: Table 4.20).

Chloroform fraction (CF)

The chloroform fraction of the ethanol extract of *C. anisata* (CF) also showed a dose dependent increment in latency of mice to respond to pain in the hot plate test. Mice pretreated with CF at 1000 mg/kg p.o. showed the highest response which became significant ($p < 0.05$) at 1 h and peaked at 2 h ($p < 0.001$). The peak %PTI was 17.11 % and the overall analgesic effect was 38.41 % ($p < 0.01$) at 1 000 mg/kg p.o (Figure 4.3 I and J; Table 4.20).

Aqueous fraction (EMF)

The aqueous fraction of the ethanol extract of *C. anisata* (EMF) exhibited analgesic effect by increasing the latency of mice to respond to thermally induced pain. The most response was at 100 mg/kg p.o which commenced significant ($p < 0.05$) effect at 1 h and reach the peak at 3 h with overall analgesic effect of 35.41 % ($p < 0.01$) (Figure 4.3 K and L: Table 4.20).

4.5.1.3 Fractions of *A. polycarpa* stem bark extract

Petroleum ether fraction (PF)

Mice pretreated with the petroleum ether fraction (PF) of the ethanol extract of *A. polycarpa* stem bark (ASE) showed dose dependent analgesic activity in the hot plate test. The analgesic effect of ASE reached significant ($p < 0.001$) levels at 2 - 4 h period at 1 000 mg/kg p.o. The peak effect was observed at 3 h with mean %PTI of 29.43 % and highest overall analgesic effect ($p < 0.05$) was 73.04 % at 1 000 mg/kg p.o (Figure 4.3 M and N: Table 4.21).

Chloroform fraction (AC)

The chloroform fraction (AC) of the ethanol extract of *A. polycarpa* stem bark (ASE) exhibited significant analgesic activity in mice in the hot plate test by increasing the latency of mice to respond to thermally induced pain. The analgesic effect was significant ($p < 0.05$ - 0.001) from 1 to 4 h period. The maximum analgesic effect was observed at the 3rd h (peak % PTI of 39.61 at 1 000 mg/kg p.o). The most overall analgesic response was 95. 93 % at 100 mg/kg p.o. (Figure 4.3 O and P; Table 4.21).

The aqueous fraction of (ARE)

The aqueous fraction of (ARE) showed some significant ($p < 0.05$) analgesic effect on the time course curve. Yet, the overall analgesia was statistically insignificant ($p > 0.05$) (Figure 4.3 Q and R: Table 4.21).

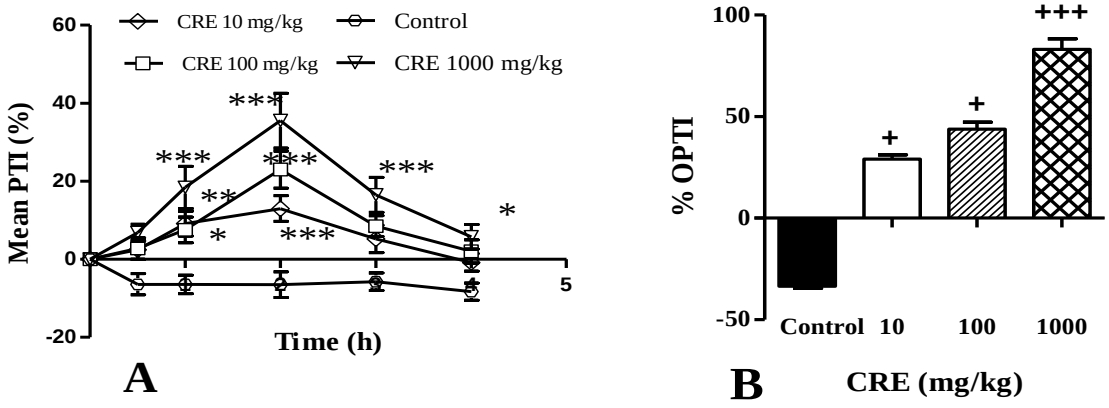

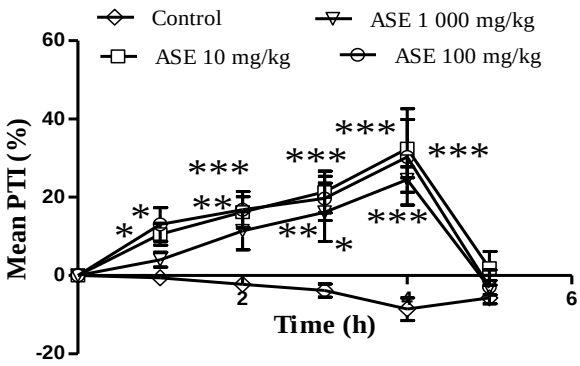
Control
ASE 1 000 mg/kg
ASE 10 mg/kg
ASE 100 mg/kg
Mean PTI (%)
Time (h)

C

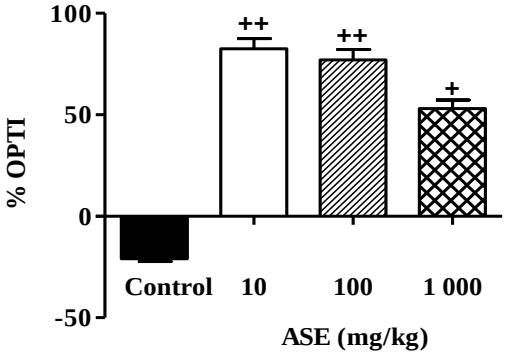
% OPTI
Control
10
100
1 000
ASE (mg/kg)

D

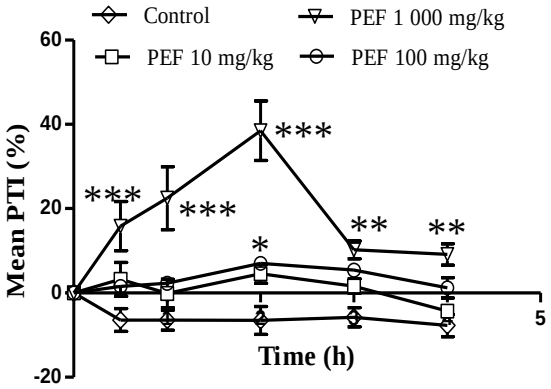
Control
PEF 1 000 mg/kg
PEF 10 mg/kg
PEF 100 mg/kg
Mean PTI (%)
Time (h)

E

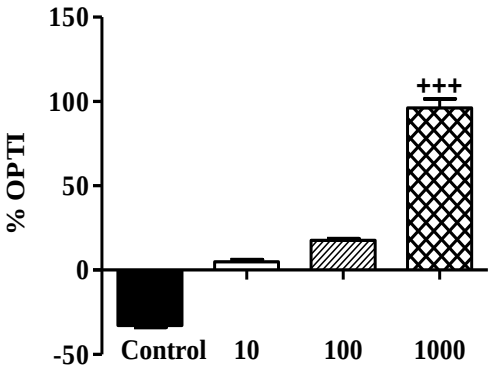
% OPTI
Control
10
100
1000
PEF (mg/kg)

F

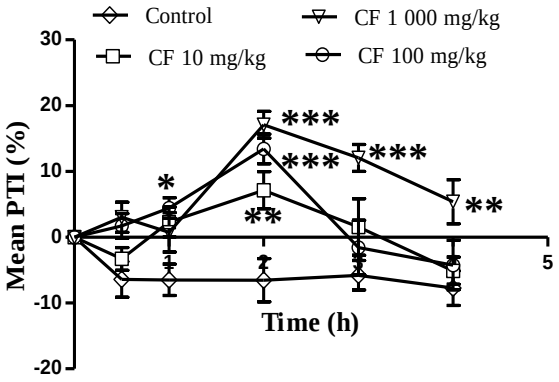
Control
CF 1 000 mg/kg
CF 10 mg/kg
CF 100 mg/kg
Mean PTI (%)
Time (h)

G

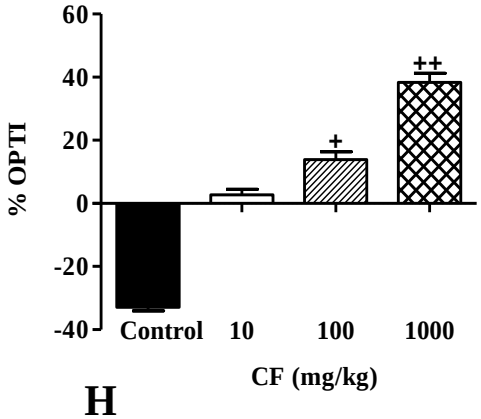
% OPTI
Control
10
100
1000
CF (mg/kg)

H

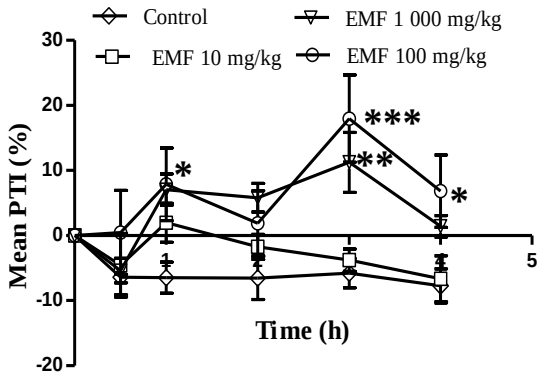
Control
EMF 1 000 mg/kg
EMF 10 mg/kg
EMF 100 mg/kg
Mean PTI (%)
Time (h)

I

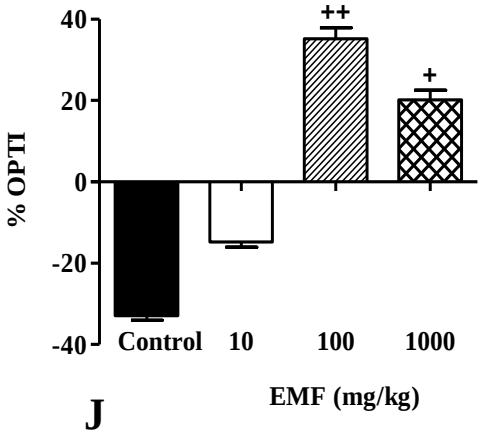
% OPTI
Control
10
100
1000
EMF (mg/kg)

J

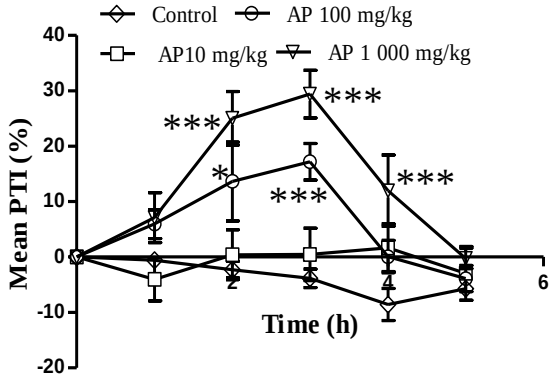
Control
AP 100 mg/kg
AP10 mg/kg
AP 1 000 mg/kg
Mean PTI (%)
Time (h)

K

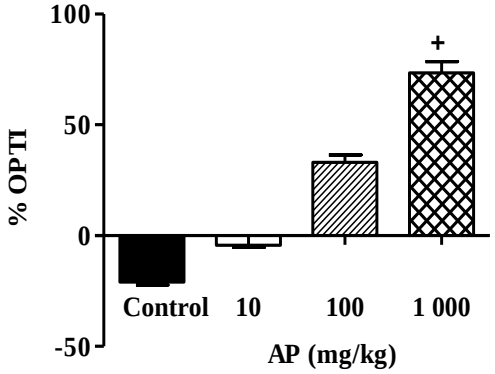
% OPTI
Control
10
100
1 000
AP (mg/kg)

L

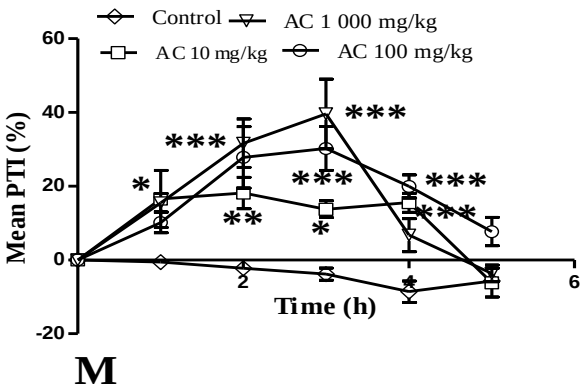
Control
AC 1 000 mg/kg
AC 10 mg/kg
AC 100 mg/kg
Mean PTI (%)
Time (h)

M

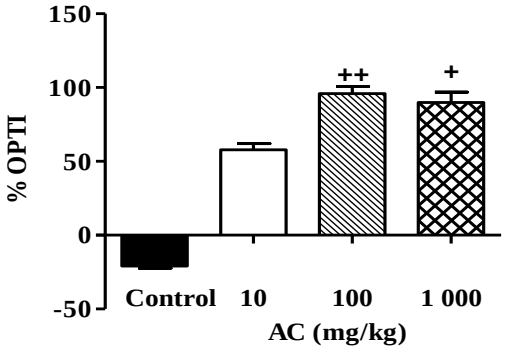
% OPTI
Control
10
100
1 000
AC (mg/kg)

N

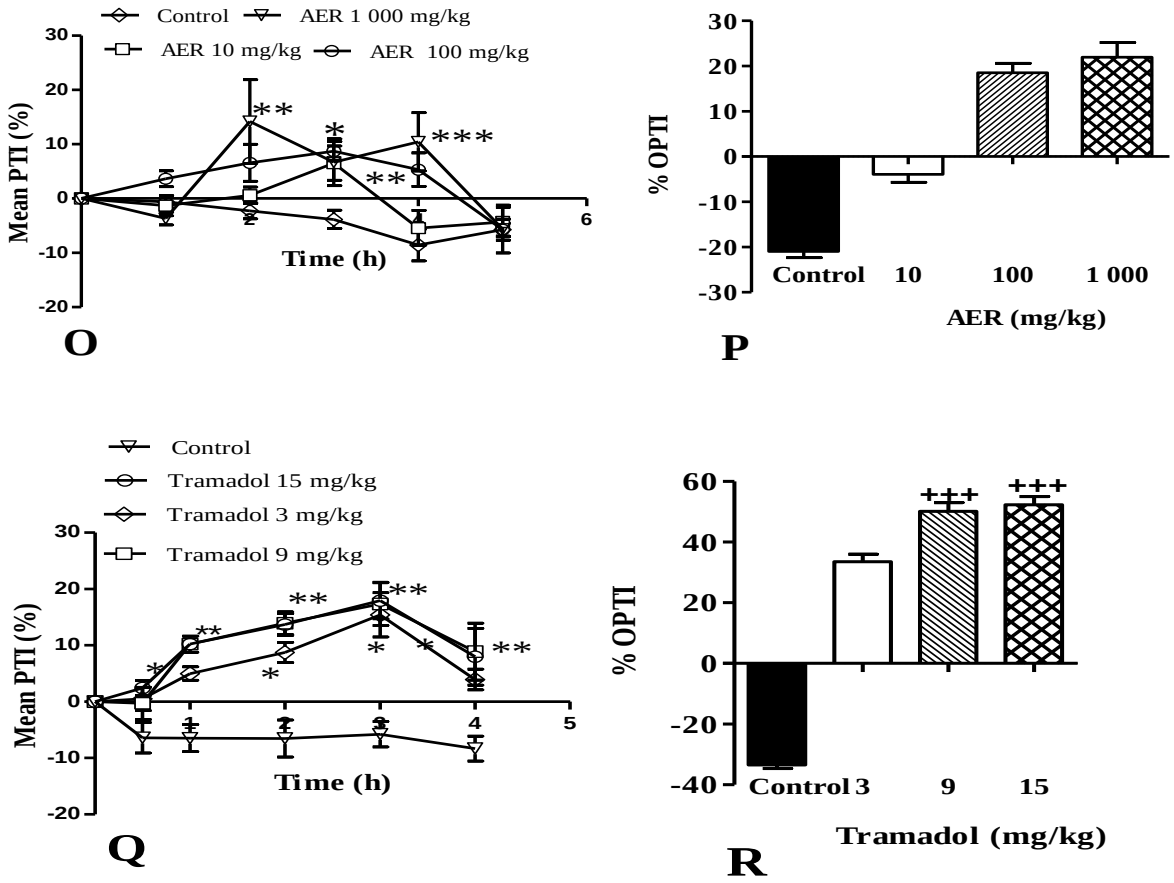

Figure 4.3: Analgesic effect of the ethanol extracts of *C. anisata* root (CRE), *A. polycarpa* stem bark (ASE); pet ether (PEF), chloroform (CF) and aqueous (EMF) fractions of the ethanol extracts of *C. anisata* root: pet ether (AP), chloroform (AC) or ethanolic fractions (AER) of ethanol stem extract of *A. polycarpa* at (10-1000 mg/kg p.o) and Tramadol (3-15 mg/kg p.o) respectively on time course curves (A, C, E,G, I, K, M, O, Q) and total mean analgesic response (B, D, F, H, J, L, N, P, R) respectively on thermally induced pain in mice. Values are expressed as means ± SEM (n= 5). *p < 0.05; **p < 0.01; ***p < 0.001 compared to vehicle treated control group (Two-way ANOVA followed by Bonferroni's *post hoc* test). $^{+}p < 0.05$; $^{++}p < 0.01$; $^{+++}p < 0.001$ compared to vehicle treated control group (One-way repeated measures ANOVA followed by Tukey's *post hoc* test).

Table 4.20:Analgesic activity of the ethanol extract of *C. anisata* root and its fractions on thermally induced pain

Extract/ Fraction	CRE	CRE	CRE	PEF	PEF	PEF	CF	CF	CF	EMF	EMF	EMF	Tram	Tram	Tram
Dose (mg/kg p.o)	10	100	1000	10	100	1000	10	100	1000	10	100	1000	3	9	15
Analgesic activity (%OPTI)	29.93	35.55	72.15	4.98	17.58	96.23	2.67	13.86	38.41	i/a	35.14	20.17	30. 10	43. 30	45.50

Table 4.21: Analgesic activity of the ethanol extract of *A. polycarpa* stem bark and its fractions on thermally induced pain

Extract/ Fraction	ASE	ASE	ASE	AP	AP	AP	AC	AC	AC	ARE	ARE	ARE	Tram	Tram	Tram
Dose (mg/kg p.o)	10	100	1000	10	100	1000	10	100	1000	10	100	1000	3	9	15
Analgesic activity (%OPTI)	82.54	77.07	53.07	-4.34	33.06	73.04	57.92	95.93	89.87	-3.94	18.51	21.96	30.10	43.30	45.50

Keys: CRE = Ethanol extract of *C. anisata* root; PEF = Petroleum ether fraction of CRE; CF = Chloroform fraction of CRE; EMF = Aqueous fraction of CRE; ASE = Ethanol extract of *A. polycarpa* stem bark; AP = Petroleum ether fraction of ASE; AC = Chloroform fraction of ASE; AER = Aqueous fraction of ASE; Tram = Tramadol; i/a = inactive.

4.5.1.4 Isolated compounds

The isolated compounds tested and the the reference drug, tramadol all demonstrated significant analgesic activity (Table 4.22). The results for the individual compounds are described below.

Anisocoumarin B (C1D)

The prenyloxy coumarin, anisocoumarin B from *C. anisata* root exhibited a remarkable ($p < 0.001 - 0.05$) prolongation in latency of mice to respond to thermally induced pain in the hot plate test from 2 - 5 h period in dose-dependent manner. The peak analgesia showed at 3 h with mean PTI of 24.26 % and overall analgesic effect of 50.34 % as the highest response at the dose of 9 mg/kg p.o. (Figure 4.4 A and B; Table 4. 22). The overall analgesic effect of tramadol was 27.13 % also at 9 mg/kg p.o. (Table 4. 22).

Xanthotoxol (P2A)

The furanocoumarin xanthotoxol also at 3 or 9 mg/kg p.o demonstrated significant ($p < 0.01$) increase in the latency of mice to act in response to heat-induced pain stimulation in the hot plate. The analgesic effect of xanthotoxol significantly ($p < 0.05 - 0.01$) showed up at 1 h to the peak at 4 h after administration (Figure 4.4 C). The peak analgesic activity was 9.12 %. The dose response relation was not clear since xanthotoxol at 3 or 9 mg/kg p.o showed similar overall analgesic effect of ($p < 0.01$) 25.94 and 25.34 % respectively (Figure 4.4 I and J; Table 4. 22).

Palmatine (A6C)

The quaternary protoberberine alkaloid palmatine at 3 or 9 mg/kg p.o exhibited dose-dependent elevation of the latency of mice to react to pain stimulation induced by heat. Analgesic activity of palmatine increased with time to significant ($p < 0.001$) levels from 3 - 4 h (Figure 4.4 E). The peak effect was observed at 4 h with mean %PTI of 29.30 % and the highest overall analgesia of 85.56 % ($p < 0.01$) at 9 mg/kg p.o (Figure 4.4 E; F and Table 4.22).

Jatrorrhizine (A8C)

The results obtained for jatrorrhizine in the hot plate assay shows that it has significant ($p < 0.05 - 0.001$) analgesic activity (Figure 4.4 G; H: Table 4.22). The analgesic effect of jatrorrhizine increased gradually with time and peak at 3 h. The effect was dose-dependent.

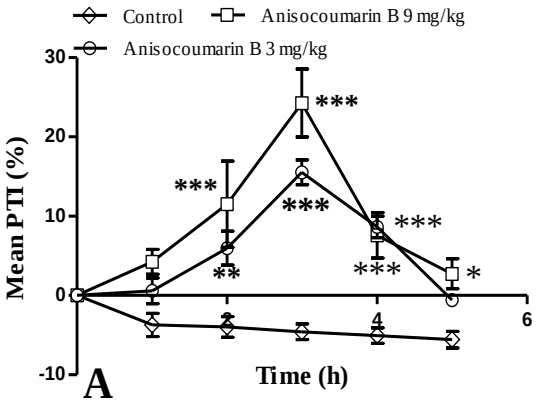
Control
Anisocoumarin B 9 mg/kg
Anisocoumarin B 3 mg/kg
Mean PTI (%)
Time (h)
A

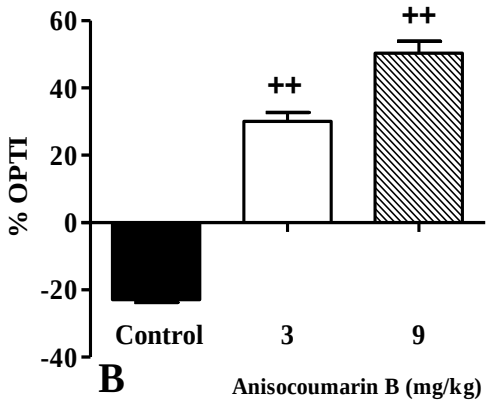
% OPTI
Control
3
9
Anisocoumarin B (mg/kg)
B

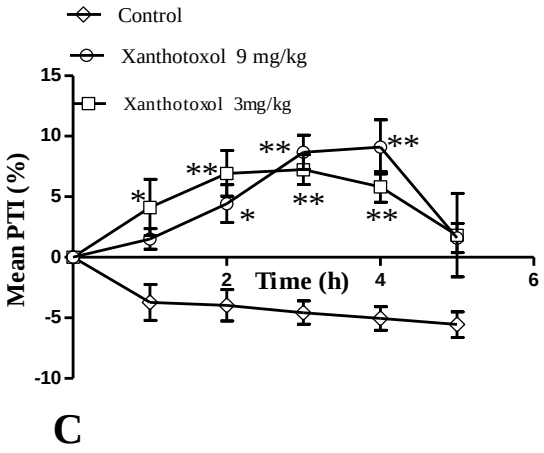
Control
Xanthotoxol 9 mg/kg
Xanthotoxol 3mg/kg
Mean PTI (%)
Time (h)
C

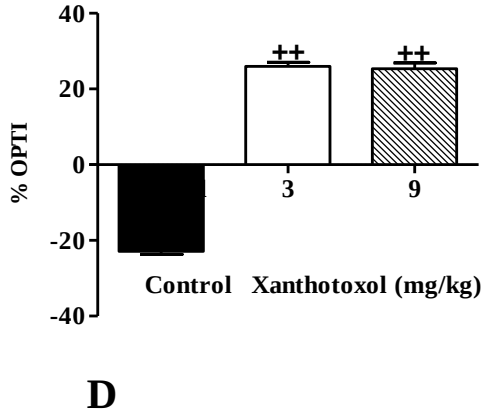
% OPTI
Control
Xanthotoxol (mg/kg)
D

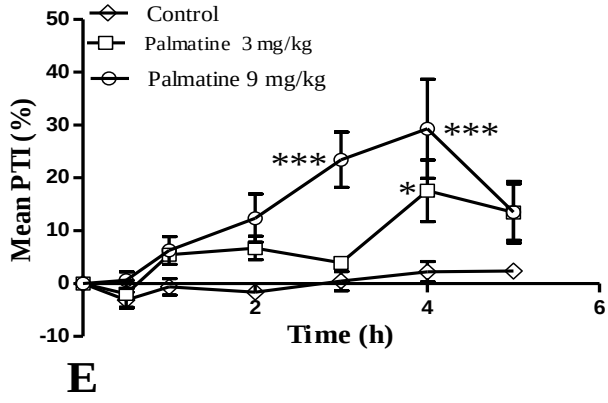
Control
Palmatine 3 mg/kg
Palmatine 9 mg/kg
Mean PTI (%)
Time (h)
E

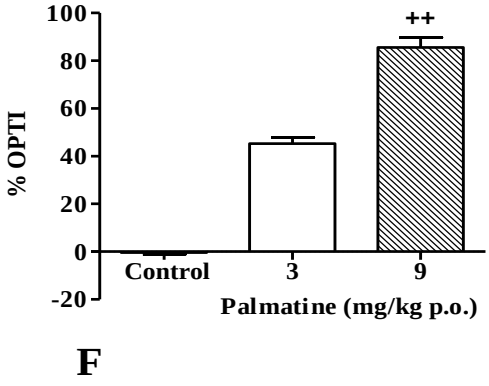
% OPTI
Control
Palmatine (mg/kg p.o.)
F

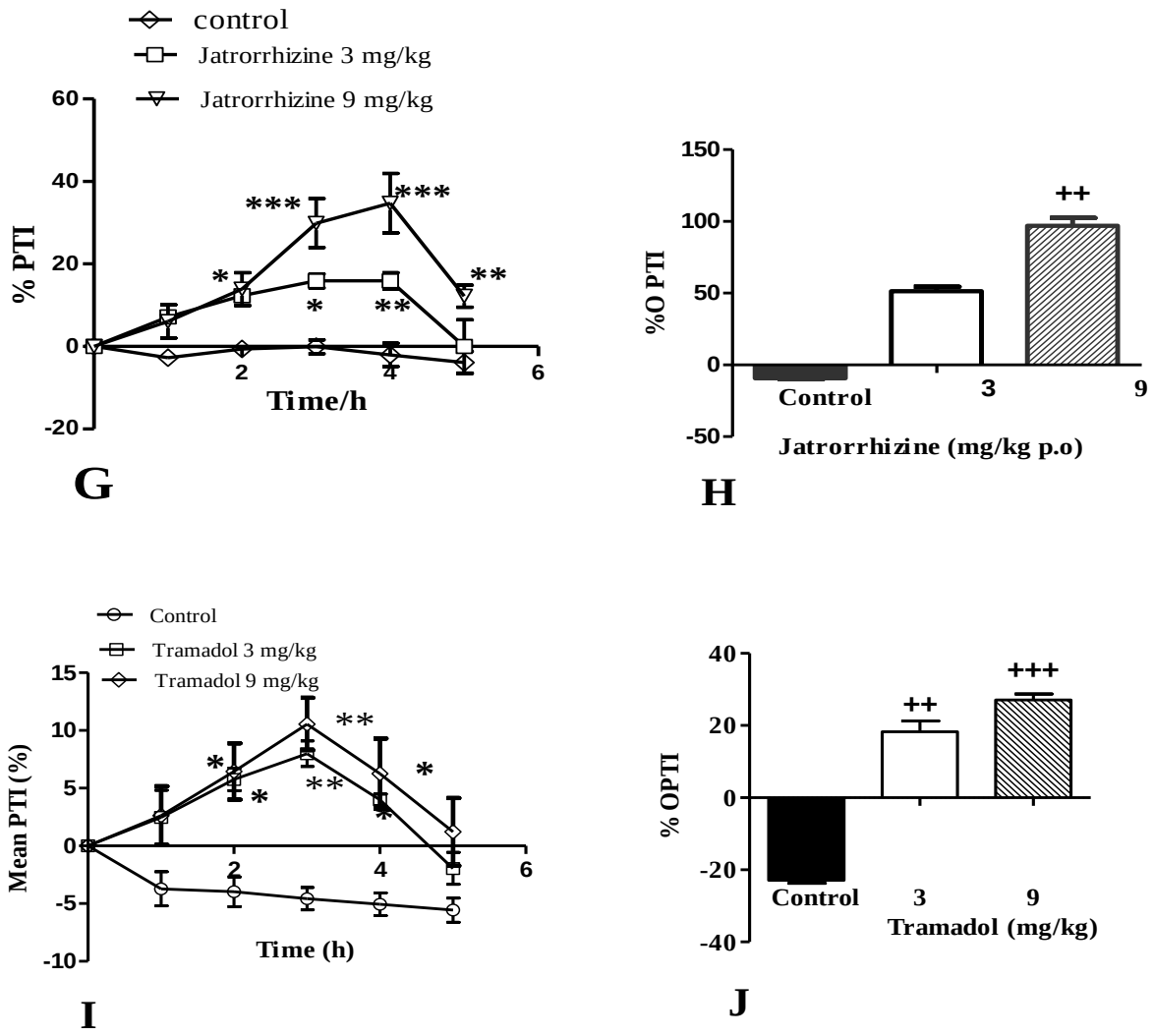

Figure 4.4: Analgesic effects of the isolated compounds; anisocoumarin B, xanthotoxol palmatine, jatrorrhizine or tramadol at (3-9 mg/kg p.o) respectively on time course curves (A, C, E, G, I) and Overall analgesic response, %OPTI (B, D, F, H, J) on thermally induced hyperalgesia in mice. Values are expressed as means ± SEM. (n= 4). *$p < 0.05$; **$p < 0.01$; ***$p < 0.001$ compared to vehicle treated control group (Two-way ANOVA followed by Bonferroni's *post hoc* test). $^{+}p < 0.05$; $^{++}p < 0.01$; $^{+++}p < 0.001$ compared to vehicle treated control group (One-way repeated measures ANOVA followed by Tukey's*post hoc* test.

Table 4.22: Analgesic activity (%) of some of the isolated compounds and tramadol on thermally induced pain in C57BL/6 mice.

	Compounds from *C. anisata*				Compounds from *A. polycarpa*					
Compounds	C1D	C1D	P2A	P2A	A6C	A6C	A8C	A8C	Tram	Tram
Dose (mg/kg p.o).	3	9	3	9	3	9	3	9	3	9
Analgesic activity (%OPTI)	30.13	50.40	25.95	25.34	45.22	85.56	51.35	93.87	18.27	27.13

C1D = Anisocoumarin B; P2A = Xanthotoxol; A6C = Palmatine; A8C = Jatrorrhizine; Tram = Tramadol

4.5.2 Acetic acid-induced writhing assay

4.5.2.1 *C. anisata* root and its fractions

Ethanol extract of the root of *C. anisata* (CRE)

The crude ethanol extract of the root of *C. anisata* (CRE) protected mice against acetic acid induced writhing cramp. The analgesic effect was statistically significant ($p < 0.05$ - 0.01) and dose-dependent with the highest analgesic effect (AE) of 48.05 % observed at 1000 mg/kg p.o. (Figure 4.5 A) which was similar to 47.65 % AE calculated for diclofenac at 10 mg/kg p.o. (Table 4.23).

Petroleum ether fraction (**PEF**)

The petroleum ether fraction (PEF) of CRE was the most active fraction among the three different fraction of *C. anisata* root extract. PEF exhibited inhibition of writhing responses induced by acetic acid in mice. The most analgesic response was calculated as 52.98 % at 1 000 mg/kg p.o (Figure 4.5 C and Table 4.23).

Chloroform fraction (CF)

The analgesic activity of the chloroform fraction (CF) of ethanol root extract of *C. anisata* was observed mostly at 100 mg/kg p.o. in the form of writhing inhibition (Figure 4.5 D). The calculated analgesic effect was 30.10 % at this dose which is comparable to that of diclofenac at 10 mg/kg p.o. (Table 4.23).

Aqueous fraction (EMF)

Aqueous fraction (EMF) of CRE also showed inhibition of writhing induced pain in mice. The analgesic response was almost the same at all the three dose levels with 39.50 % at 1 000 mg/kg p.o. being slightly higher than the other two dose levels (Figure 4.5 E; Table 4.23).

4.5.2.2 *A. polycarpa* and its fractions

Ethanol extract of *A. polycarpa* stem bark (ASE)

The ethanol extract of *A. polycarpa* stem bark (ASE) showed significant ($p < 0.05$ - 0.01) protection of mice against writhing responses induced by acetic acid (Figure 4.5). The most analgesic response (AE) of 44.3 % ($p < 0.01$) was produced by the 1 000 mg/kg p.o dose (Table 4.24).

Petroleum ether fraction (AP)

The petroleum ether fraction (AP) of the ethanol extract of *A. polycarpa* stem bark (ASE**)** was inactive (Figure 4.5; Table 4.24).

Chloroform fraction (AC)

The chloroform fraction (AC) of ASE showed significant ($p < 0.05$) inhibition of writhing responses against intraperitoneal (i.p.) administration of acetic acid at 10 mg/kg p.o (Figure 4.5). The most analgesic effect was 47.65 % at 10 mg/kg p.o. similar to 47.65 % calculated for diclofenac at the same dose (Table 4.24).

Aqueous fraction

The aqueous fraction of ASE also demonstrated significant ($p < 0.05$) inhibition of writhing responses in response to i.p. administration of acetic acid at 100 mg/kg p.o. with 40.33 % analgesic effect as the highest at this dose (Figure 4.5 I; Table 4.24).

Ethanol extract of *A. polycarpa* root bark (AR)

The ethanol extract of *A. polycarpa* root bark also exhibited significant ($p < 0.05$) analgesic activity in the acetic acid induced writhing assay with the highest analgesic activity of 41.04 % at a dose of 100 mg/kg p.o. (Figure 4.5 J; Table 4.25).

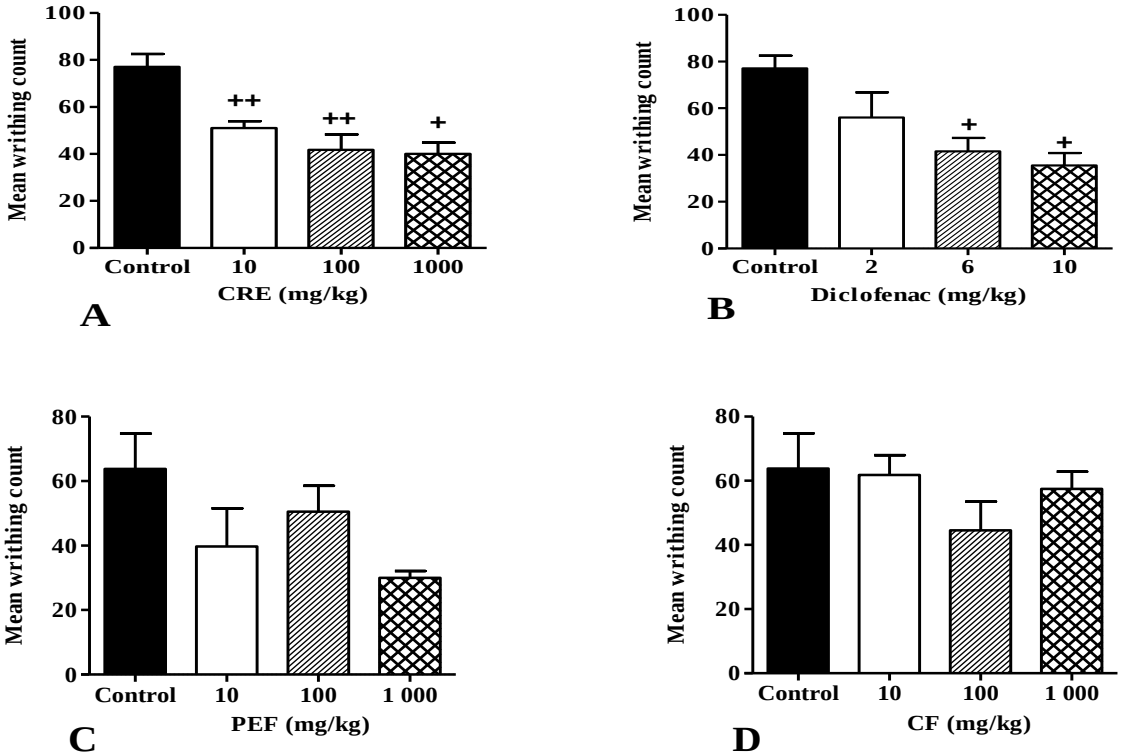

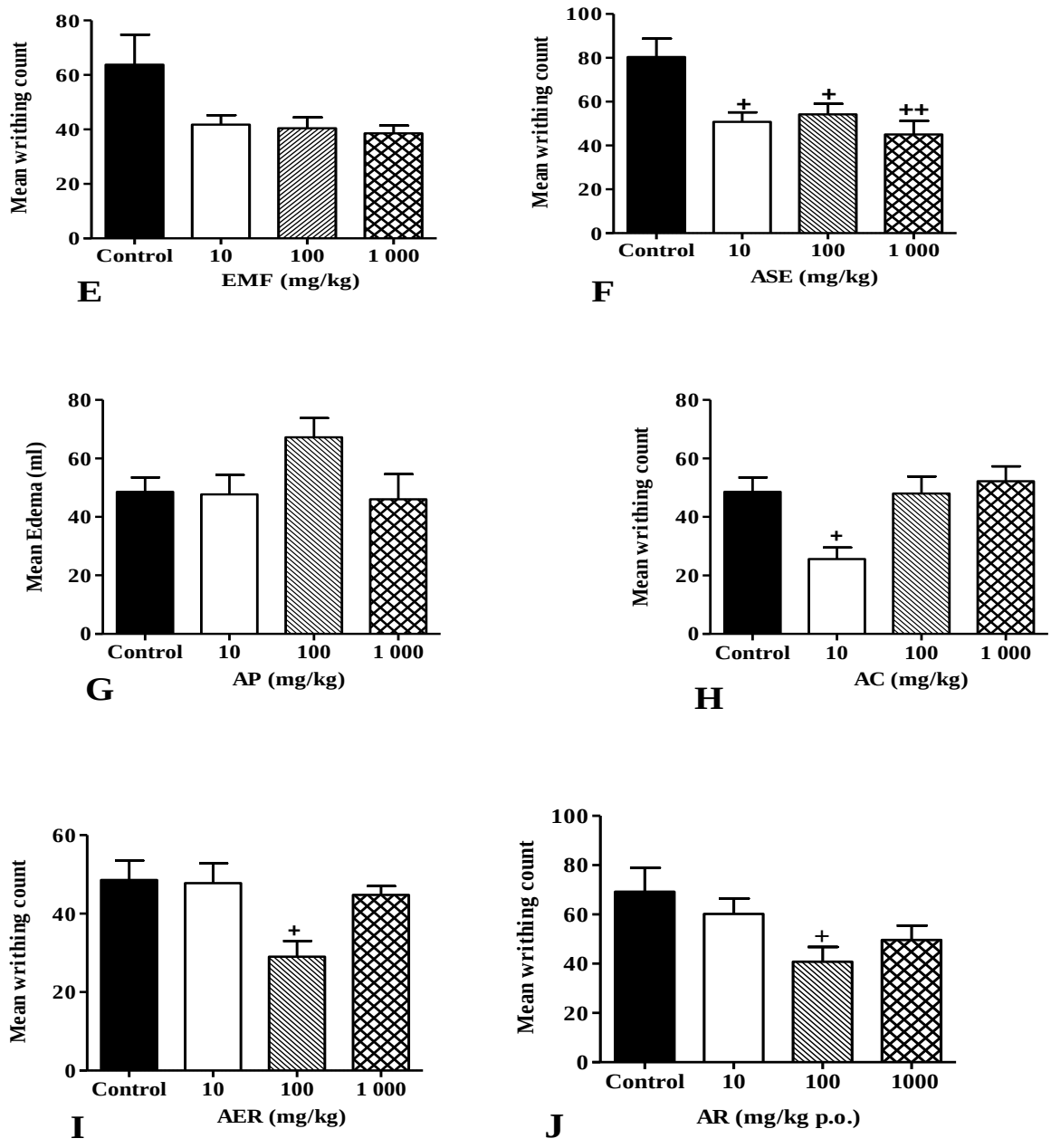

Figure 4.5: Antinociceptive effect of the ethanol extract of the root of *C. anisata* and *A. polycarpa* stem and root bark and their fractions on acetic acid induced writhing pain in mice; Values are expressed as mean ± S.E.M (n = 5) $^{+}p < 0.05$; $^{++}p < 0.01$ compared to the vehicle treated control group (One-way ANOVA followed by Tukey's Multiple Comparison Test).

Table 4.23: Analgesic activity of the ethanol extract of *C. anisata* root and its fractions in acetic acid-induced writhing test

Extract/ Fraction	CRE	CRE	CRE	PEF	PEF	PEF	CF	CF	CF	EMF	EMF	EMF	Diclo	Diclo	Diclo
Dose (mg/kg p.o)	10	100	1000	10	100	1000	10	100	1000	10	100	1000	2	6	10
Analgesic activity (%)	33.77	46.10	48.05	37.62	20.69	52.98	3.13	30.10	10.03	34.48	36.68	39.50	23.51	32.92	47.65

Table 4.24: Analgesic activity of *A. polycarpa* stem bark ethanol extract and its fractions in acetic acid-induced writhing test

Extract/ Fraction	ASE	ASE	ASE	AP	AP	AP	AC	AC	AC	ARE	ARE	ARE	Diclo	Diclo	Diclo
Dose (mg/kg p.o).	10	100	1000	10	100	1000	10	100	1000	10	100	1000	2	6	10
Analgesic activity (%)	36.81	32.59	44.03	i/a	-i/a	i/a	47.33	1.23	i/a	1.23	40.33	12.20	23.51	32.92	47.65

Keys: CRE = Ethanol extract of *C. anisata* root; PEF = Petroleum ether fraction of CRE; CF = Chloroform fraction of CRE; EMF = Aqueous fraction of CRE; ASE = Ethanol extract of *A. polycarpa* stem bark; AP = Petroleum ether fraction of ASE; AC = Chloroform fraction of ASE; AER = Aqueous fraction of ASE; Diclo = Diclofenac sodium chloride; i/a= inactive.

Table 4.25: Analgesic activity of *A. polycarpa* root bark ethanol extract in acetic acid-induced writhing test

Extract/ Fraction	AR	AR	AR	Diclo	Diclo	Diclo
Dose (mg/kg p.o).	10	100	1 000	2	6	10
Analgesic activity (%)	13.01	41.04	28.32	23.51	32.92	47.65

AR = Ethanol extract of *A. polycarpa* root bark

4.5.2.3 Isolated compounds

All the compounds and the reference drug, diclofenac, administered at 2 or 6 mg/kg p.o demonstrated various degrees of statistically significant ($p < 0.05 - 0.01$) analgesia by inhibiting the mean writhing count in response to intraperitoneal (i.p.) administration of acetic acid in mice. Except xanthotoxol which was inactive (Figure 4.6 A-F). At 6 mg/kg p.o., all the active compounds demonstrated higher analgesic activity than the reference drug, diclofenac. The most effective ones were heptaphyline, osthol, palmatine and jatrorrhizine with analgesic activity calculated to be 48.75, 46.52, 46.40, 47.13 and 44.25 % respectively at 6 mg/kg p.o. Diclofenac sodium also showed significant analgesic effect of 32.92 % at 6 mg/kg p.o. (Table 4.26). The analgesic effect of anisocoumarin B was not statistically significant at the doses used. Nevertheless, when the dose was increased to 10 mg/kg (p.o.) in the mechanism assay using the cholinergic antagonist atropine, anisocoumarin B produced a very significant ($p <. 0.01$) analgesia with 55.50 % analgesic effect (See Section 4.6.2.2: Figure 4.10 M; Table 4.26).

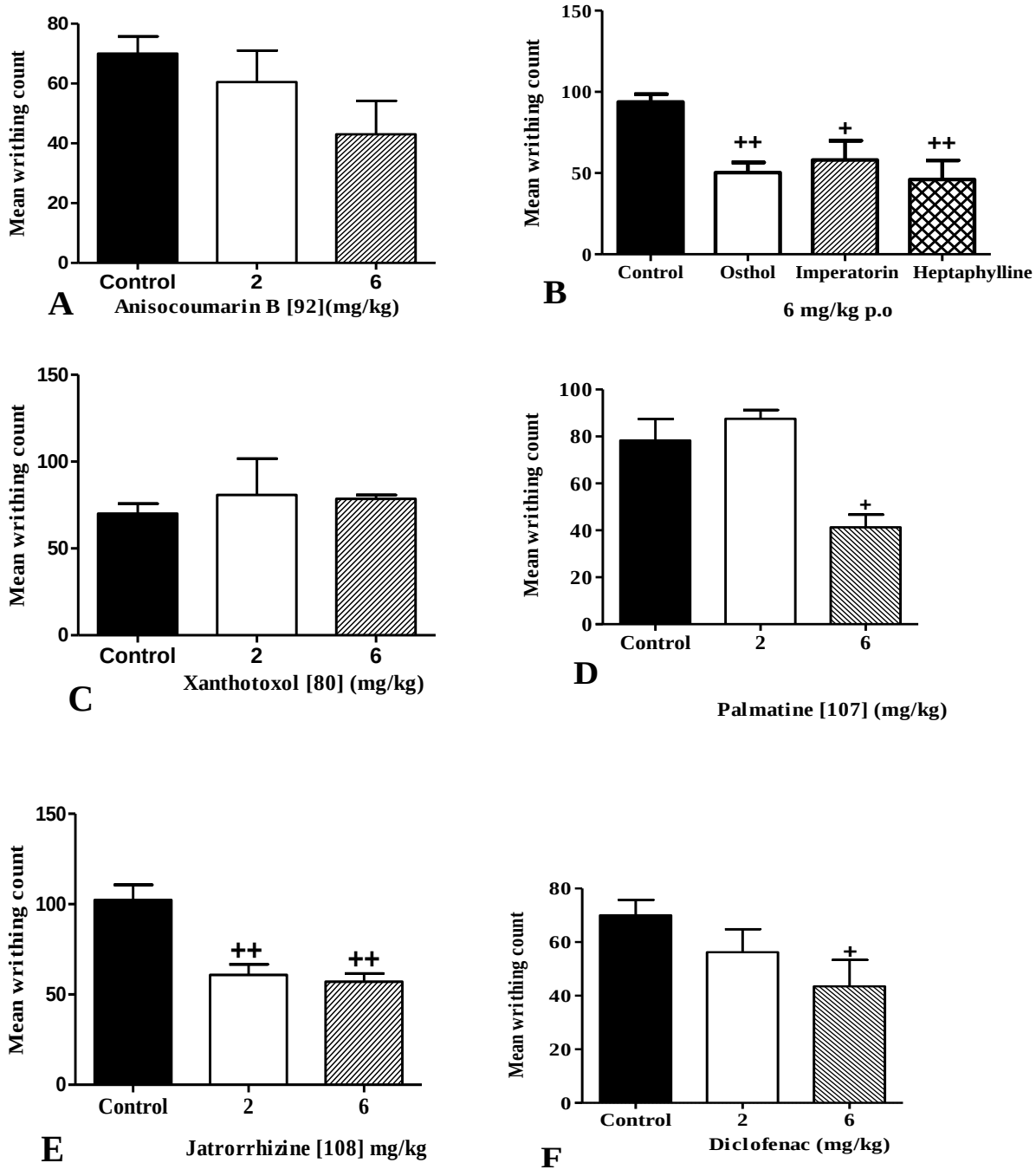

Figure 4.6: Analgesic effect of the isolates: anisocoumarin B, xanthotoxol, osthol, imperatorin, heptaphyline, palmatine, jatrorrhizine or diclofenac (A, B, C, D, E, F) on acetic acid induced writhing pain in mice; Values are expressed as mean ± S.E.M (n = 4) $^{+}p < 0.05$, $^{++}p < 0.01$ compared to the vehicle treated control group (One-way ANOVA followed by Tukey's Multiple Comparison Test).

Table 4. 26: Analgesic activity of the isolated compounds in the acetic acid-induced writhing assay

	Compounds from *C. anisata*							Compounds from *A. polycarpa*					
Compounds	C1D	C1D	P2A	P2A	C1F	C1G	C1-I	A6C	A6C	A8C	A8C	Diclo	Diclo
Dose (mg/kg p.o).	2	6	2	6	6	6	6	2	6	2	6	2	6
Analgesic activity (%)	1.07	38.57	i/a	i/a	46.40	38.13	48.75	i/a	47.28	40.59	44.25	19.64	32.92

C1D = Anisocoumarin B; P2A = Xanthotoxol; C1F = Osthol; C1G = Imperatorin; C1-I = Heptaphyline; A6C = Palmatine; A8C = Jatrorrhizine; Diclo = Diclofenac sodium chloride

4.6 MECHANISM OF ANTINOCICEPTIVE ACTION

The effects of the classical nonselective opioid receptor antagonist, naloxone and the typical nonselective cholinergic receptor antagonist, atropine on analgesic activities of the crude extracts and the isolated compounds of the medicinal plants used in this study were respectively evaluated in the hot plate and the acetic acid induced writhing assays in other to ascertain the kind(s) of nociceptors involved in mediating the analgesia induced by these agonists. These were done in other to be able to classify the tested extracts and compounds as an opioid analgesic agent or muscarinic cholinergic agonist type of analgesic substance. Four of the isolated compounds; anisocoumarin B, xanthotoxol, palmatine and jatrorrhizine were tested in these assays in exception to the others due to their paucity.

4.6.1 *C. anisata* root and *A. polycarpa* stem bark

4.6.1.1 Opioid mechanism

The ethanol extracts of *C. anisata* root (CRE) and *A. polycarpa* stem bark (ASE) produced significant analgesic effects when administered alone on both the time course curve and on the total analgesic response in mice at 10 mg/kg p.o respectively. However, administration of naloxone at 2 mg/kg i.p to mice 45 min after oral administration of CRE and ASE at 10 mg/kg p.o, significantly blocked the analgesia produced by these extracts when compared to the groups that were given the extract alone without naloxone (Figure 4.7 A- D). For instance, ASE at 10 mg/kg p.o alone group of mice produced a total analgesic response of 82.54 %. But the group in which ASE at 10 mg/kg p.o was given followed by naloxone at 2 mg/kg i.p the total analgesic response was substantially reduced to -44.72 % (Table 4.24).

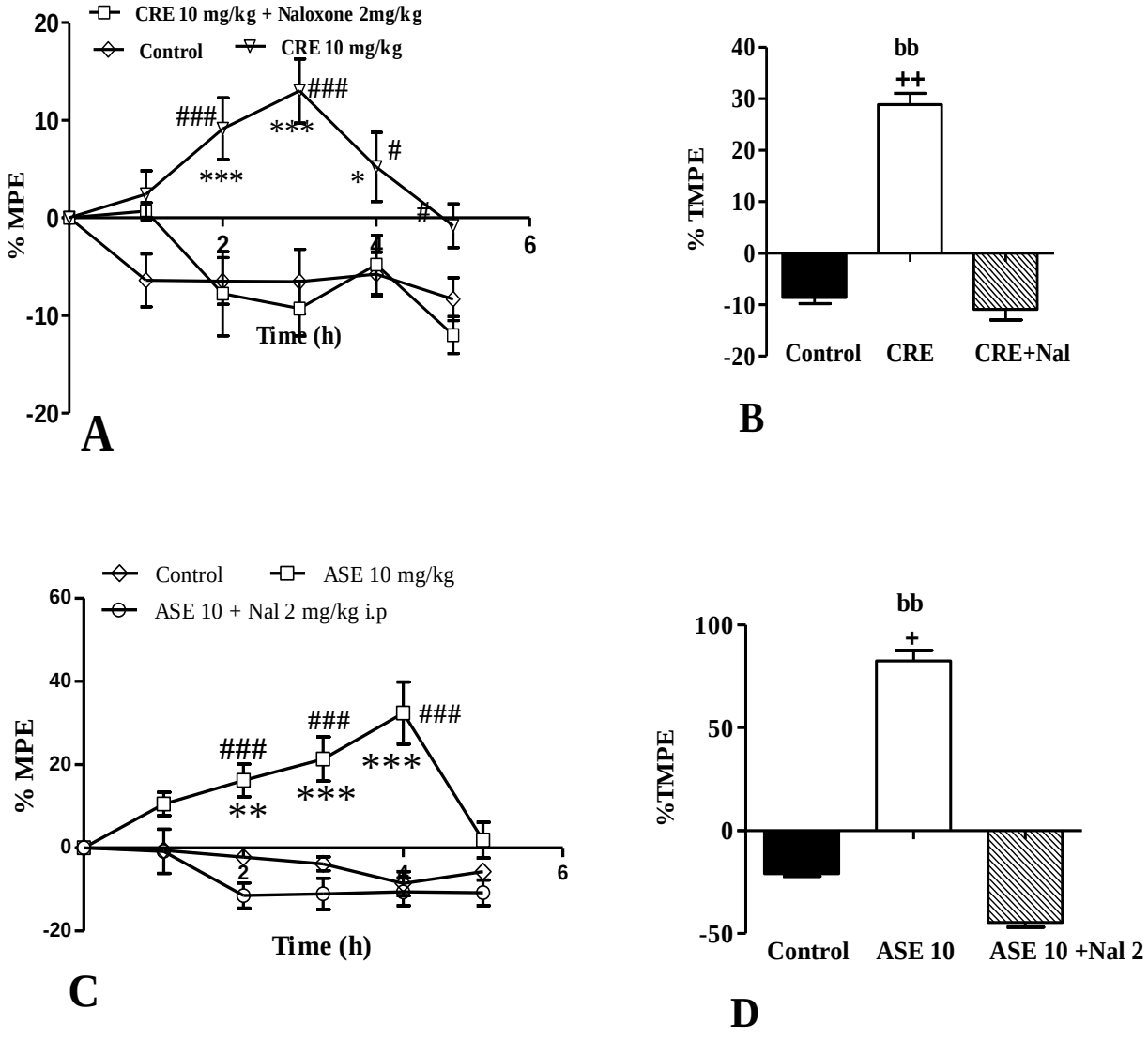

Figure 4.7: Effect of naloxone (2 mg/kg i.p) on the ethanol extracts of *C. anisata* (CRE) or *A. polycarpa* bark (ASE) (at 10 mg/kg p.o) thermal mediated antinociceptionon time course curve (A, C) and Overall analgesic activity (B, D). Values are expressed as means ± SEM. (n = 4): *p < 0.05; **p < 0.01 compared with vehicle treated control group: $^{\#}$p<0.05; $^{\#\#}$p <0.001 mg/kg p.o AC 10 mg/kg + Naloxone 2mg/kg i.p (Two- way ANOVA followed by Bonferroni's *post hoc* test). $^{++}$p<0.01compared with vehicle treated control (One-way repeated measures ANOVA followed by Tukey's *post hoc* test). ^{b}p<0.05, ^{bb}p<0.01 compared with AC 10 mg/kg p.o + naloxone 2 mg/kg i.p (One-way repeated measures ANOVA followed by Tukey's *post hoc* test).

4.6.1.2 Muscarinic cholinergic mechanism

In the writhing assay, atropine, the muscarinic cholinergic receptor antagonist, at 5 mg/kg i.p given to mice 30 min post administration of the ethanol extracts of *C. anisata* root (CRE) and *A. polycarpa* stem bark (ASE) had no significant ($p > 0.05$) effects on the analgesic effect of the extracts when compared with the group that took only the extracts (Figure 4.14 E; F: Table 4.24).

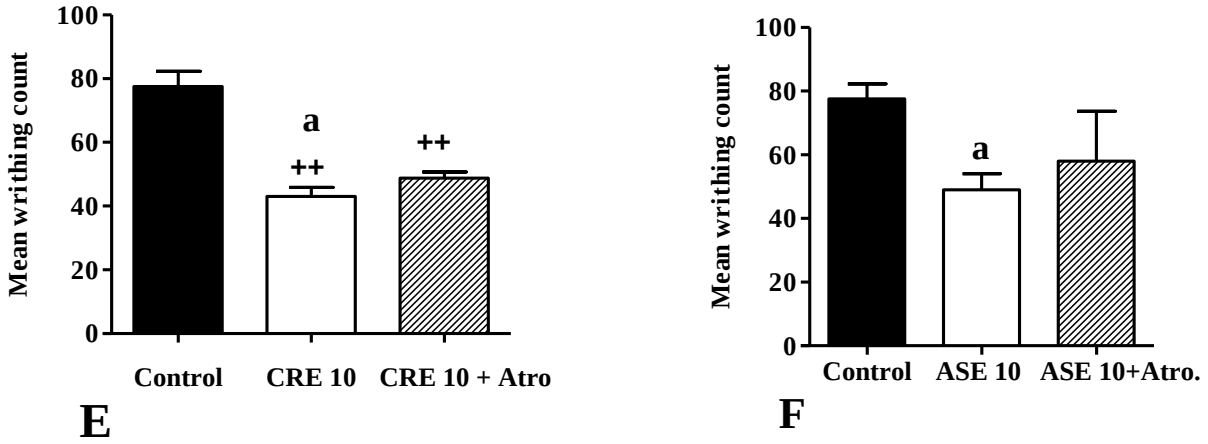

Figure 4.8: Effect of atropine (5 mg/kg i.p.) on antinociceptive action of the ethanol extract of *C. anisata* root and *A. polycarpa* stem bark. Values are expressed as mean ± SEM (n = 4). $^{++}p < 0.01$ compared with vehicle treated control (One-way repeated measures ANOVA followed by Tukey's post *hoc test*). $^{b}p < 0.05$, $^{bb}p < 0.01$, $^{a}p > 0.05$ compared with agonist 10 mg/kg p.o + atropine 5 mg/kg (i.p.) (One-way repeated measures ANOVA followed by Tukey's *post hoc* test).

4.6.2 Isolated compounds

4.6.2.1 Opioid mechanism

All the isolated compounds demonstrated considerable analgesic activity on the time course curve and on the total analgesic response in mice when alone at 9 mg/kg p.o in the hot plate assay (Figure 4.9; G - L). Yet, naloxone injected at 2 mg/kg i.p. 45 min post administration of these compounds resulted in the analgesic effects being totally abolished. For example, anisocoumarin B alone at 9 mg/kg p.o gave a total analgesic response of 30.13 % but when

it was co-administered with naloxone at 2 mg/kg i.p, the total analgesia vanished to - 6.37 % (Table 4.27).

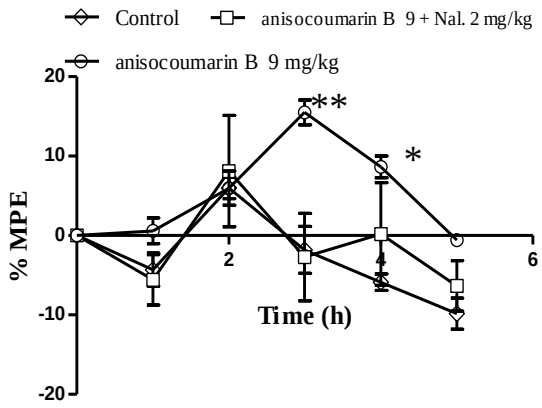

G

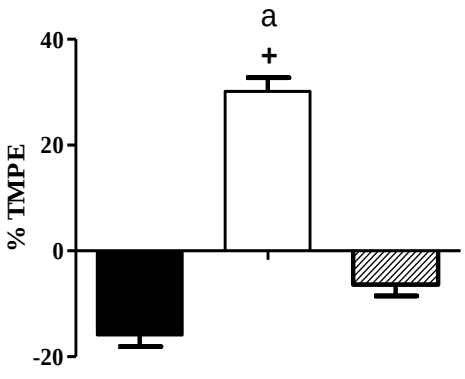

H

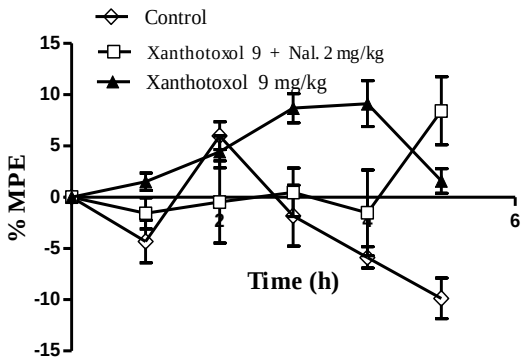

I

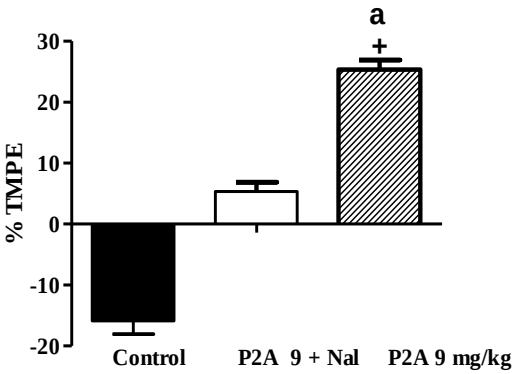

J

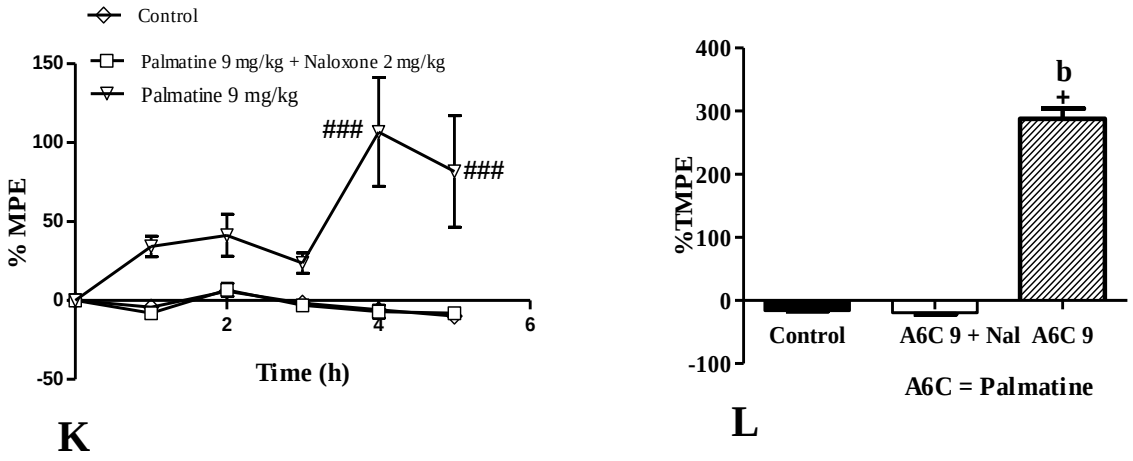

Figure 4.9: Effect of Naloxone (2 mg/kg i.p.) on analgesic effect of anisocoumarin B, xanthotoxol or palmatine on thermal mediated antinociception in mice on time course curve (G, I, K) and %OPTI (H, J, L). Values are expressed as means ± SEM. (n = 4): *p < 0.05; **p < 0.01 compared with vehicle treated control group: $^{\#}p < 0.05$; $^{\#\#}p < 0.001$ mg/kg p.o. Agonist 9 mg/kg + naloxone 2 mg/kg i.p. (Two - way ANOVA followed by Bonferroni's *post hoc* test). $^{++}p < 0.01$, $^{a}p > 0.05$ compared with vehicle treated control (One-way repeated measures ANOVA followed by Tukey's *post hoc* test). $^{b}p < 0.05$, $^{bb}p < 0.01$ compared with agonist 9 mg/kg p.o. + naloxone 2 mg/kg i.p. (One-way repeated measures ANOVA followed by Tukey's *post hoc* test).

4.6.2.2 Muscarinic cholinergic mechanism

In the acetic acid-induced writhing test, the muscarinic cholinergic antagonist, atropine at 5 mg/kg i.p. administered 30 min after the isolated compounds were given at 6 or 10 mg/kg p.o. respectively had no significant ($p > 0.05$) influence on their antinociceptive action when compared with the groups that were administered with only the isolated compounds without atropine for anisocoumarin B, palmatine or jatrorrhizine (Figure 4.10 M, N and O; Table 4.27). Effect of atropine on analgesic action of xanthotoxol was not assessed in the writhing test due to its inactivity in this assay.

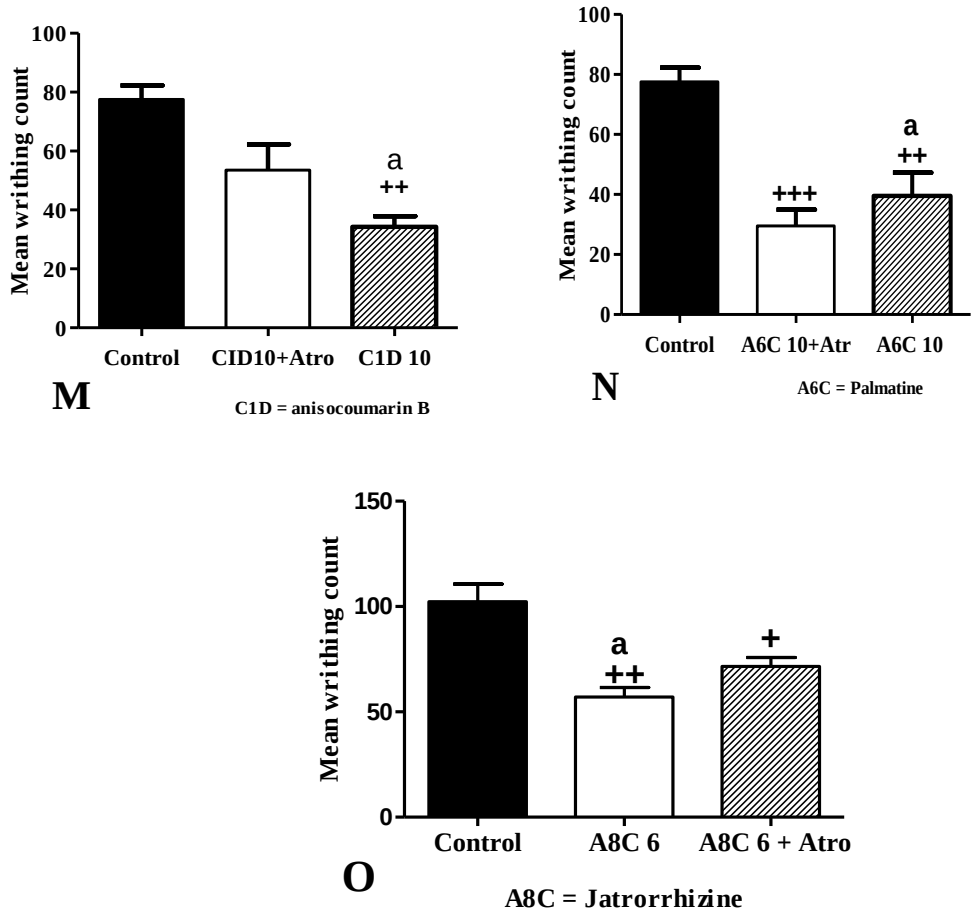

Figure 4.10: Effects of atropine (5 mg/kg i.p.) on analgesic effects of the anisocoumarin B, palmatine and jatrorrhizine in the mouse writhing test. Values are expressed as mean ± SEM (n = 4). $^{+}p < 0.05$, $^{++}p < 0.01$, compared with vehicle treated control (One-way repeated measures ANOVA followed by Tukey's *post hoc* test). $^{a}p > 0.05$, $^{b}p < 0.05$, $^{bb}p < 0.01$ compared with agonist 6/10 mg/kg p.o + atropine 5 mg/kg (i.p) (One-way ANOVA followed by Tukey's *post hoc* test).

Table 4.27: Effect of naloxone and atropine on analgesic activity of the extracts and some of the isolates in the hot plate and acetic acid-induced writhing assays respectively

	Hot plate assay			**Acetic acid induced- writhing assay**		
	Agonist alone	Agonist and Nalox		Agonist alone	Agonist and Atropine	
Agonist	**%TMPE**		**Inference**	**%AE**		**Inference**
CRE	28.87	-10.89	antagonized	44.52	37.1	no sig. effect
ASE	82.54	-44.72	antagonized	36.77	25.2	no sig. effect
Anisocoumarin B (C1D)	30.13	-6.37	antagonized	55.81	31.0	no sig. effect
Xanthotoxol (P2A)	25.34	5.34	antagonized	-	-	-
Palmatine Chloride (A6C)	84.91	-19.56	antagonized	35.63	30.36	no sig. effect
Jatrorrhizine Chloride (A8C)	-	-	-	44.25	30.07	no sig. effect

Nalox = naloxone; no sig. effect = had no significant effect on the antinociceptive action of the agonist; = was not active, so mechanism assay was not performed.

Note: all the isolates were administered at 6 mg/kg p.o. in the hot plate assay or 10 mg/kg p.o. in the acetic acid induced writhing assay; CRE and ASE were given at 10 mg/kg p.o in both assays.

4.7 ANTI-INFLAMMATORY ACTIVITY

The results of the anti-inflammatory activities of *C. anisata* root and *A. polycarpa* stem bark extracts and their respective petroleum ether, chloroform and aqueous fractions in addition to the anti-inflammatory effects of their isolated compounds on carrageenan induced edema in rats paw assay (Winter *et al.*, 1962) have also been described. The anti-inflammatory effect of *A. polycarpa* root bark was not tested. Figure 4.11 shows the results of the effects of the ethanol extracts of *C. anisata* root (CRE) and *A. polycarpa* and their various fractions on carrageenan-induced paw inflammation in rats on time course curve and on the overall induced inflammation over the 5 h duration of the experiment respectively.

4.7.1 Ethanol extracts of *C. anisata* root (CRE) and *A. polycarpa* stem bark (ASE)

C. anisata root (CRE)

CRE inhibited the induced inflammation in the paws of rat at all the three dose levels commencing at 1st h and become statistically significant ($p < 0.001$ for 100 mg/kg and $p < 0.01$ for 10 mg/kg) at the 5th h after its administration to the rats. The highest anti-inflammatory activity by 27.53 % was produced by the CRE at 1 000 mg/kg p.o. (Figure 4.11 B; Table 4.28) at 95 % confidence interval (C. I) of difference of 0.0265 - 0.1692. The effect was statistically significant ($p < 0.05$).

A. polycarpa stem bark

The time-course curve shows that, the anti-inflammatory action of ASE started from 1st h and turned significant ($p < 0.01$ - 0.001) till the 5th h (Figure 4.3C). ASE exhibited an inverse dose depended inhibition of the induced inflammation in rats' paw. The highest anti-inflammatory activity of 69.64 % (95 % CI of difference of 0.1787 - 0.4867) was produced by ASE 10 mg/kg p.o (Figure 4.11 D and Table 4.29) which was comparable to the anti-inflammatory activity of 67.71 % (95 % C.I of difference of 0.06849 - 0.3448) obtained for indomethacin at 15 mg/kg p.o. (Table 4.29). Among the two crude ethanol extracts administered orally (p.o.), ASE demonstrated the highest anti-inflammatory activity.

4.7.2 Fractions of ethanol extract of *C. anisata* root

The petroleum ether fraction (PEF)

PEF appears to exhibit dose dependent anti-inflammatory response which was very significant for the highest dose (1 000 mg/kg p.o) starting from the 1st h ($p < 0.05$) to the 5th h ($p < 0.001$) (Figure 4.11 E). It also showed a very significant ($p < 0.001$ at 95 % C.I interval of difference of 0.1774 - 0.4846) reduction in the overall mean oedema to 0.8 mL at 1 000 mg/kg p.o. compared to 2.8 mL of oedema formation in the vehicle treated control group (Figure 4.11 F). The maximum anti-inflammatory activity of 70.44 % was obtained for PEF at 1 000 mg/kg p.o. (Table 4.28).

Chloroform fraction (CF)

The reduction in the oedema of the rats treated with the chloroform fraction of the ethanol extract of *C. anisata* root (CF) commenced at 1 h after treatment and become significant ($p < 0.05$) at the 2 h till the 5th h ($p < 0.001$) at 100 mg/kg p.o. (Figure 4.11 G). The overall reduction in oedema formation for all the three dose levels of CF was significant compared to the control treated group with that of 100 mg/kg p.o. exhibiting extremely significant ($p < 0.001$) at 95 % C.I interval of difference of 0.1388 - 0.4748) reducing the oedema volume to 0.9 mL compared to 2.8 mL of the vehicle treated control set (Figure 4.11 H). The highest inhibition of the inflammation among the three doses of CF was 66.37 % at 100 mg/kg p.o. CF exhibited dose-dependent anti- inflammatory response. The response had reduced to 38.64 % at 1 000 mg/kg possibly because at that highest dose the extract might have exceeded its peak effect (Figure 4.11 G and H; Table 4.28).

Aqueous fraction (EMF)

EMF at 1 000 mg/kg p.o. (highest dose) showed significant ($p < 0.05$ - 0.001) inhibition of inflammation as early as at 1 h after it was administered till the 5 h (Figure 4.11 I). The maximum reduction of the overall oedema was 0.9 mL at 100 mg/kg p.o., which was very significant ($p < 0.001$) at 95 % C.I (difference of 0.1599 - 0.4554) compared to 2.8 mL of paw oedema formed in the control group. This accounted for maximum anti-inflammatory activity of 66.55 % at 1 000 mg/kg p.o. (Table 4.28).

4.7.3 Fractions of ethanol extract of *A. polycarpa* stem bark

Petroleum ether fraction of the ethanol extract of *A. polycarpa* stem bark (AP)

AP significantly reduced oedema formation to 1.8 ± 0.07 and 1.7 ± 0.06 mL at 10 and 100 mg/kg p.o. compared to 2.9 ± 0.11 mL oedema of the vehicle treated control (Figure 4.11 K and L). The highest overall inhibition of the inflammation was 40.30 % at 100 mg/kg p.o. (Table 4.29).

Chloroform fraction of the ethanol extract of *A. polycarpa* (AC)

AC exhibited the highest anti-inflammatory activity on the carrageenan induced paw inflammation among the three fraction of the ethanol stem bark extract of *A. polycarpa* by reducing the oedema significantly ($p < 0.01$) to 1.5 ± 0.07, 1.5 ± 0.08 and 1.4 ± 0.06 mL respectively at 10, 100 and 1 000 mg/kg p.o. compared to the control set of 2.9 ± 0.11 mL. AC exhibited the highest anti-inflammatory effect of 59.50 % which is comparable to 58.15 % exhibited by indomethacin at 9 mg/kg p.o. (Figure 4.3 M; N; Table 4.29).

Aqueous fraction of the ethanol extract of *A. polycarpa* (ARE)

ARE was inactive as an anti-inflammatory agent from 1 - 3 h after it was administered. It however showed significant ($p < 0.001$) inhibition of the inflammation from 4 - 5 h on the time course curve at 10 mg/kg p.o. (Figure 4.11 O). Yet these effects made no significant impact on the percentage overall inhibition of the inflammation (Figure 4.11 P and Table 4.29). Thus ARE was generally inactive as an anti-inflammatory substance at doses used in this assay.

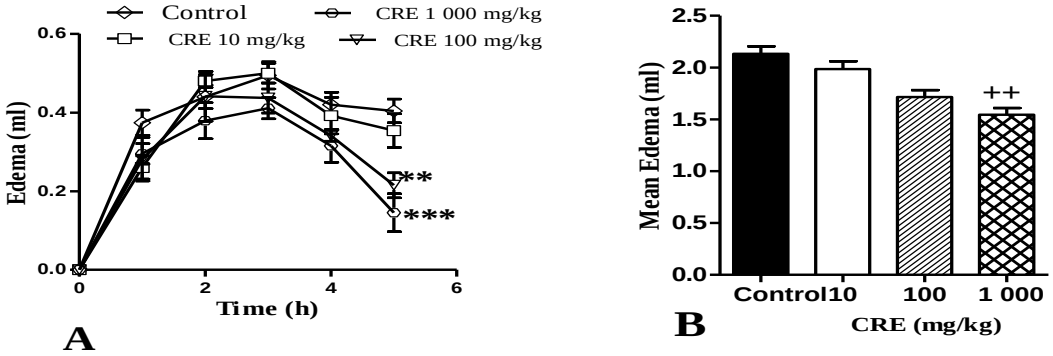

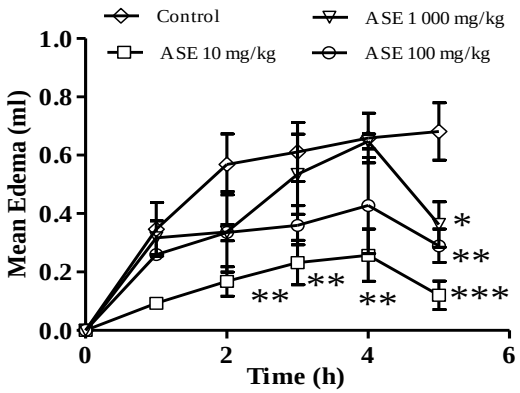

C *A. polycarpa* stem extract (ASE)

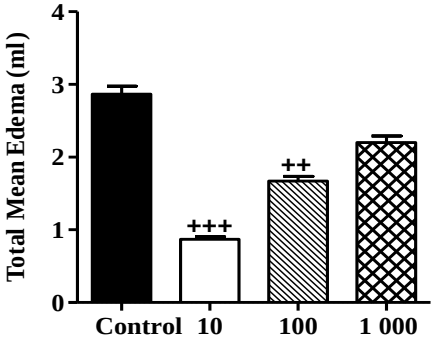

D *A. polycarpa* stem ASE (mg/kg)

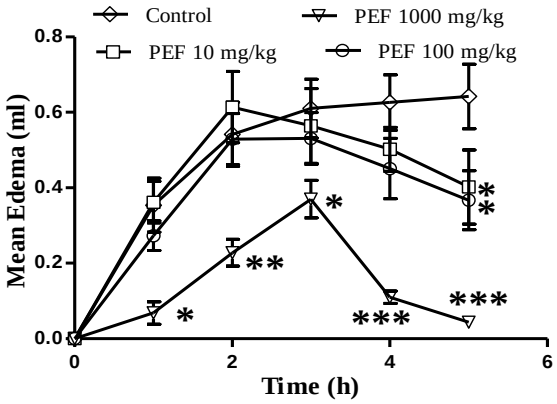

E

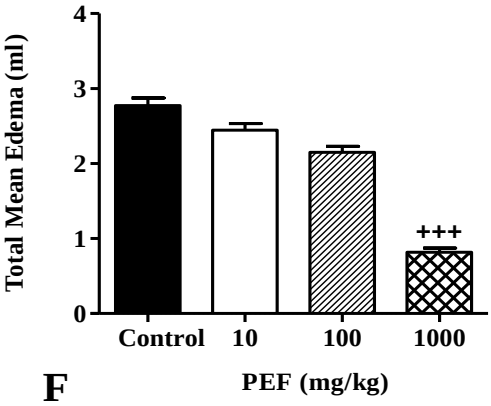

F

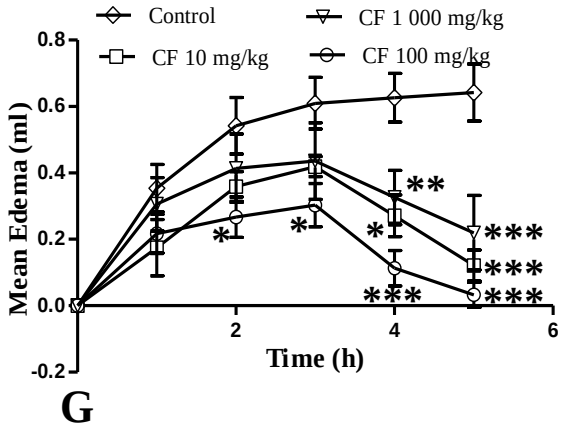

G

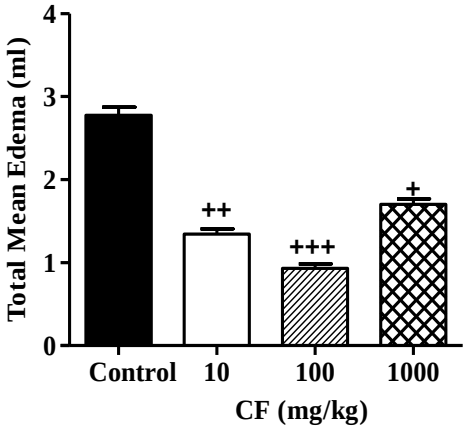

H

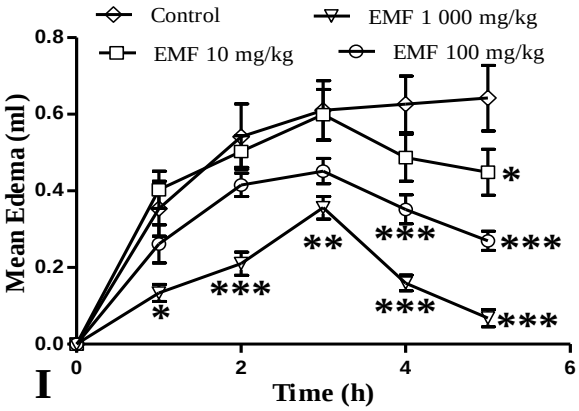
Control
EMF 1 000 mg/kg
EMF 10 mg/kg
EMF 100 mg/kg
Mean Edema (ml)
Time (h)

I

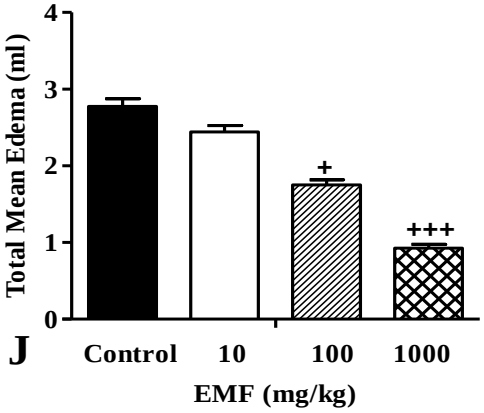
Total Mean Edema (ml)
Control
10
100
1000
EMF (mg/kg)

J

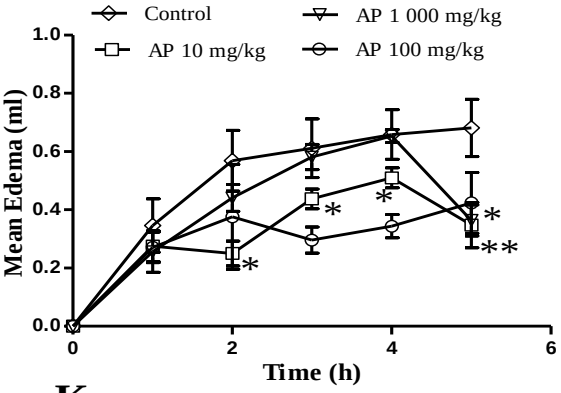
Control
AP 1 000 mg/kg
AP 10 mg/kg
AP 100 mg/kg
Mean Edema (ml)
Time (h)

K

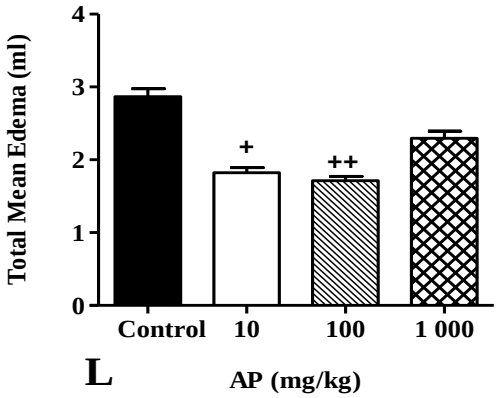
Total Mean Edema (ml)
Control
10
100
1 000
AP (mg/kg)

L

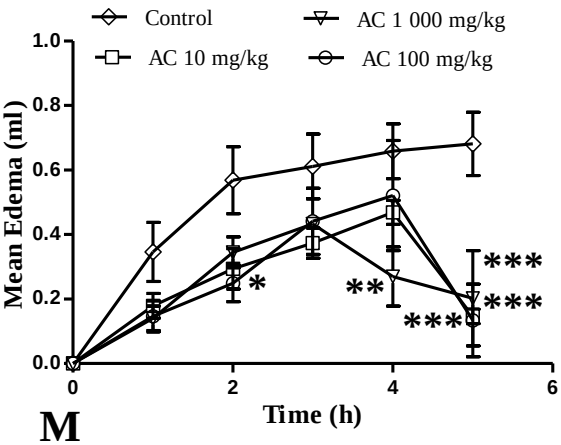
Control
AC 1 000 mg/kg
AC 10 mg/kg
AC 100 mg/kg
Mean Edema (ml)
Time (h)

M

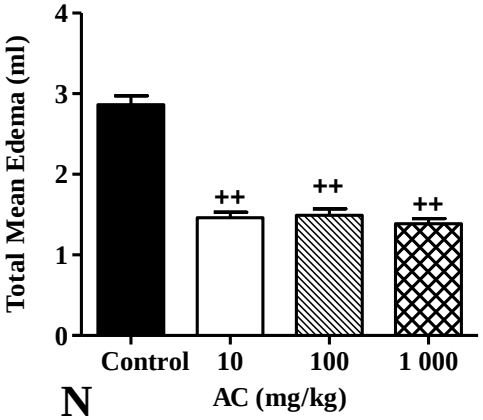
Total Mean Edema (ml)
Control
10
100
1 000
AC (mg/kg)

N

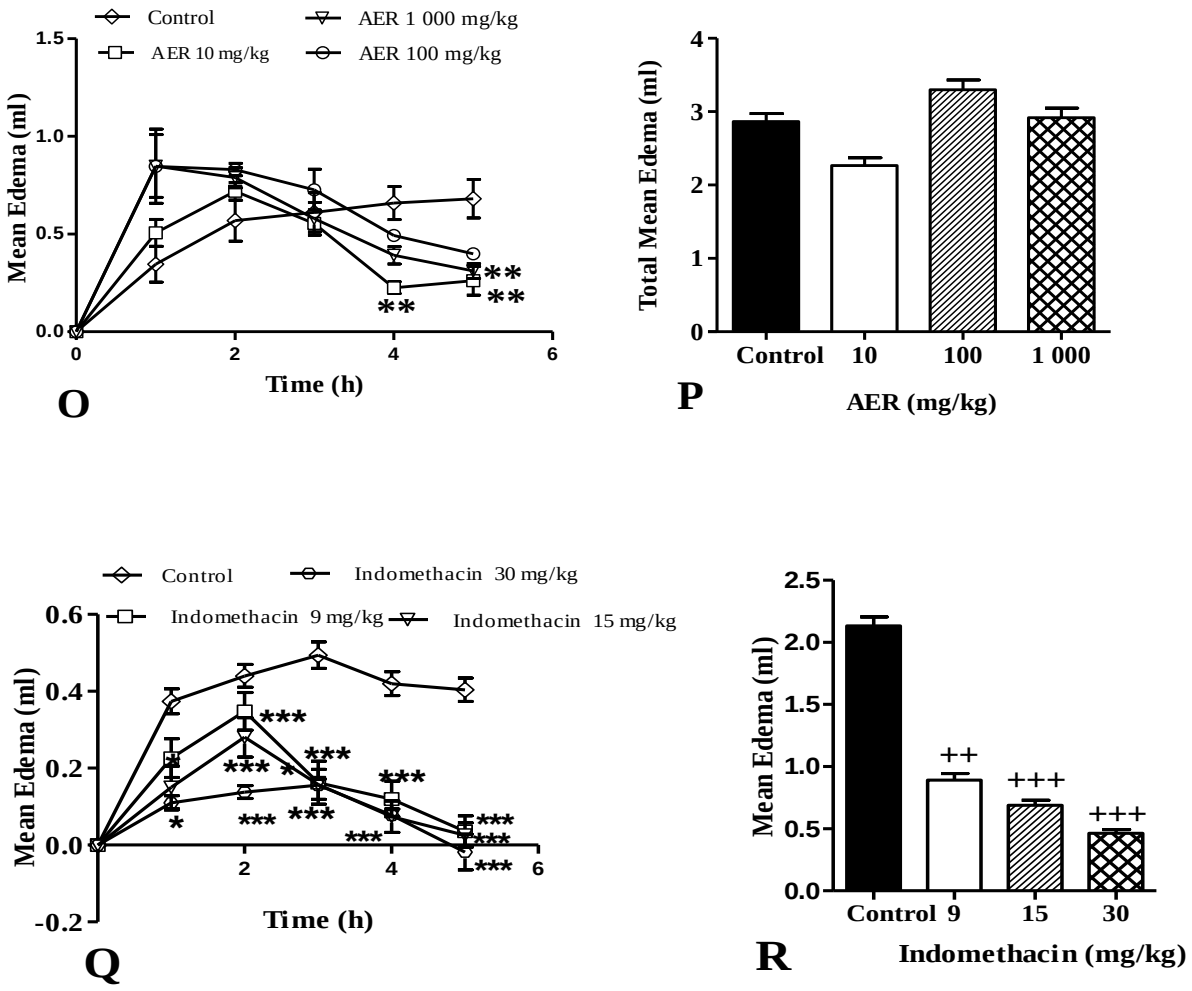

Figure 4.11: Anti-inflammatory effect of the ethanol extracts of *C. anisata* root (CRE), *A. polycarpa* stem bark (ASE); pet ether (PEF), chloroform (CF) and aqueous (EMF) fractions of the ethanol extracts of *C. anisata* root: pet ether (AP), chloroform (AC) or aqueous fraction (AER) of stem bark ethanol extract of *A. polycarpa* at (10 - 1000 mg/kg p.o.) and indomethacin (9 - 15 mg/kg p.o.) respectively on time course curves (A, C, E,G, I, K, M, O, Q) and total mean oedema response (B, D, F, H, J, L, N, P, R) respectively on carrageenan induced inflammation in rats' paw. Values are expressed as means ± SEM (n= 5). *p < 0.05; **p < 0.01; ***p < 0.001 compared to vehicle treated control group (Two-way ANOVA followed by Bonferroni's *post hoc* test). $^{+}$p < 0.05; $^{++}$p < 0.01; $^{+++}$p < 0.001 compared to vehicle treated control group (One-way repeated measures ANOVA followed by Tukey's *post hoc* test).

Table 4.28: Anti-inflammatory activity of the ethanol extract of *C. anisata* root and its fractions

Extract/ Fraction	CRE	CRE	CRE	PEF	PEF	PEF	CF	CF	CF	EMF	EMF	EMF	Indo	Indo	Indo
Dose (mg/kg p.o).	10	100	1000	10	100	1000	10	100	1000	10	100	1000	9	15	30
Anti-inflammatory activity (%)	6.84	19.50	27.53	11.46	22.90	70.44	51.51	66.37	38.64	12.00	36.84	66.55	58.15	67.71	78.23

Table 4.29: Anti-inflammatory activity of the ethanol extract of *A. polycarpa* stem bark and its fractions

Extract/ Fraction	ASE	ASE	ASE	AP	AP	AP	AC	AC	AC	ARE	ARE	ARE	Indo	Indo	Indo
Dose (mg/kg p.o).	10	100	1000	10	100	1000	10	100	1000	10	100	1000	3	9	15
Anti-inflammatory activity (%)	69.64	41.63	23.24	36.50	40.30	18.81	49.03	59.50	47.98	20.94	i/a	i/a	58.15	67.71	78.23

Keys: CRE = Ethanol extract of *C. anisata* root; PEF = Petroleum ether fraction of CRE; CF = Chloroform fraction of CRE; EMF = Aqueous fraction of CRE; ASE = Ethanol extract of *A. polycarpa* stem bark; AP = Petroleum ether fraction of ASE; AC = Chloroform fraction of ASE; AER = Aqueous fraction of ASE; Indo = indomethacin; i/a= inactive.

4.7.4 Anti-inflammatory activities of the isolated compounds

Anisocoumarin B (C1D)

Anisocoumarin B isolated from the root extract of *C. anisata*, demonstrated a dose-depended anti-inflammatory action against the carrageenan induced oedema in rat paws. The anti-inflammatory action of anisocoumarin B commenced from the 1 h at both doses and become statistically significant ($p < 0.05$) at 4 - 5 hour at 9 mg/kg p.o. (Figure 4. 12 A). This compound reduced the overall oedema to 0.1 ± 0.04 ($p < 0.05$) and 0.3 ± 0.08 mL in rat paws leading to 40.66 and 62.05 % overall inhibition of inflammation at 3 and 9 mg/kg p.o. respectively. The percentage overall inhibition of the inflammation by indomethacin was 16.47 and 75.86 % at the same doses (Figure 4.12 O and P; Table 4.30).

Xanthotoxol (P2A)

The anti-inflammatory effect of xanthotoxol from the root of *C. anisata* on carrageenan induced paw oedema in rats was dose-depended. Xanthotoxol at 3 and 9 mg/kg p.o exhibited statistically significant ($p < 0.05$) overall reduction in edema to 0.2 ± 0.05 and 0.1 ± 0.03 mL compared to the vehicle treated control group. Xanthotoxol demonstrated anti-inflammatory effect 1 h after it was administered but the effect only turned statistically significant on the 4^{th} h at 9 mg/kg p.o (Fig.4.12 C and D). Xanthotoxol produced maximum anti-inflammatory response of 57.97 % at 9 mg/kg p.o (Table 4.30).

Osthol (C1F)

Osthol exhibited potent anti-inflammatory action against carrageenan-induced inflammation in rat's paws. The highest overall anti-inflammatory response of 66.5 % was produced by the least dose of 3 mg/kg p.o (Table 4.30). The overall anti-inflammatory response was also statistically remarkable ($p < 0.01$) at 95 % CI of difference of 0.0161 - 0.1914 at 3 mg/kg p.o. (Figure 4.12 E). Osthol at this same dose produced statistically significant anti-inflammatory response from 1^{st} h ($p < 0.05$) through to the 5^{th} h ($p < 0.001$) on the time course curve (Figure 4.12 F).

Imperatorin (C1G)

Imperatorin showed a dose-depended inhibitory action on the carrageenan-induced inflammation in rats' paws (Figure 4.12 G and H). The highest response of 35.52 % was given by the higher dose of 9 mg/kg p.o. Imperatorin did not exhibit statistical significant overall anti-inflammatory response at the doses used in this experiment. The anti-inflammatory effect of imperatorin became statistically significant at 4^{th} h ($p < 0.05$) on the time course curve at the higher dose.

Heptaphyline (C1-I)

Heptaphyline inhibited the induced oedema at both dose levels of 3 or 9 mg/kg p.o. Although, at these doses the anti-inflammatory effects of heptaphyline was not statistically significant on the time course curve, the overall anti-inflammation response was significant ($p < 0.05$) at the higher dose of 9 mg/kg p.o. at 95 % CI of difference of 0.0151 to 0.1453 (Figure 4.12 I and J). The anti-inflammatory effect at 9 mg/kg p.o is 33.39 % (Table 4.30).

Palmatine (A6C)

Palmatine demonstrated dose-dependent anti-inflammatory activity by significantly inhibiting ($p < 0.05$ - 0.001) the carrageenan induced edema in rat paws from the 1^{st} h till the 5^{th} h on the time course curve (Figure 4.12 K). At 9 mg/kg p.o. Palmatine reduced the overall inflammation significantly to 0.04 - 0.2 and 1.5 ± 0.05 mL ($p < 0.001$) at 95 % C.I of difference of 0.1061-0.3025 and overall inhibition of inflammation of 48.39 % (Table 4.31).

Jatrorrhizine (A8C)

Jatrorrhizine produced a dose-dependent reduction of the induced inflammation in rat paws. The effect was statistically significant from 1 - 3 h after carrageenan injection compared to the vehicle treated control group at 9 mg/kg p.o (Figure 4.12 M). The overall inhibition of inflammation at 9 mg/kg p.o was immensely high ($p < 0.001$) (Figure 4.4 N), giving rise to anti-inflammatory effect calculated to be 50.25 % (Table 4.31). The overall oedema produced was 1.0 ± 0.04 mL at CI of difference off 0.0875 - 0.2025 at 9 mg/kg p.o.

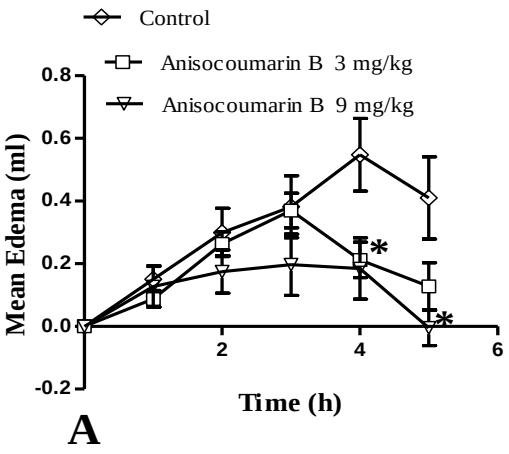
Control
Anisocoumarin B 3 mg/kg
Anisocoumarin B 9 mg/kg
Mean Edema (ml)
Time (h)
A

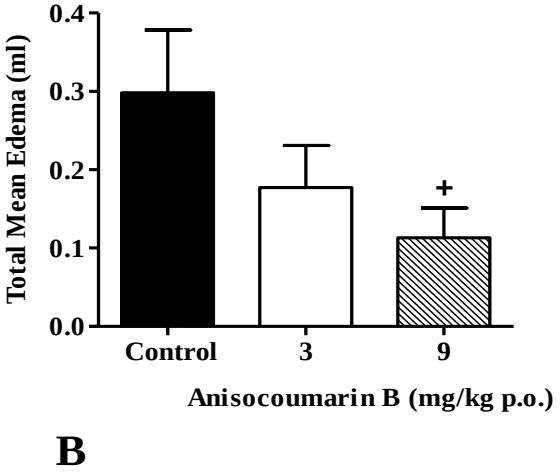
Total Mean Edema (ml)
Control
3
9
Anisocoumarin B (mg/kg p.o.)
B

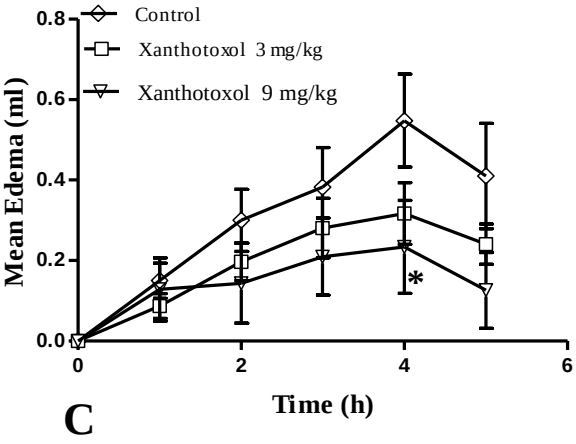
Control
Xanthotoxol 3 mg/kg
Xanthotoxol 9 mg/kg
Mean Edema (ml)
Time (h)
C

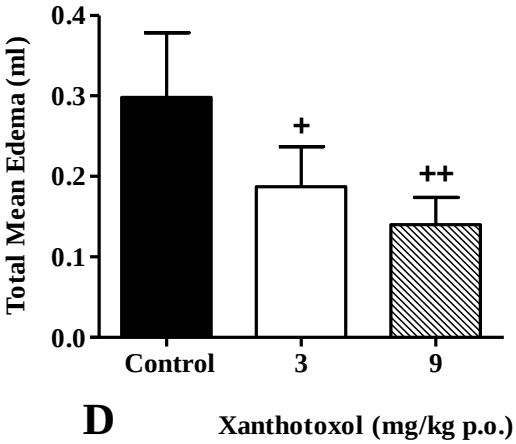
Total Mean Edema (ml)
Control
3
9
Xanthotoxol (mg/kg p.o.)
D

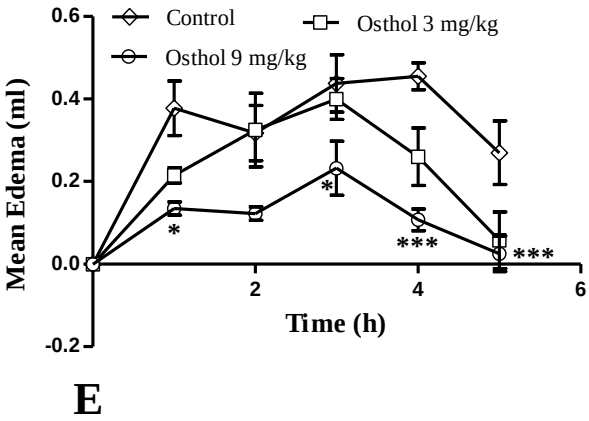
Control
Osthol 3 mg/kg
Osthol 9 mg/kg
Mean Edema (ml)
Time (h)
E

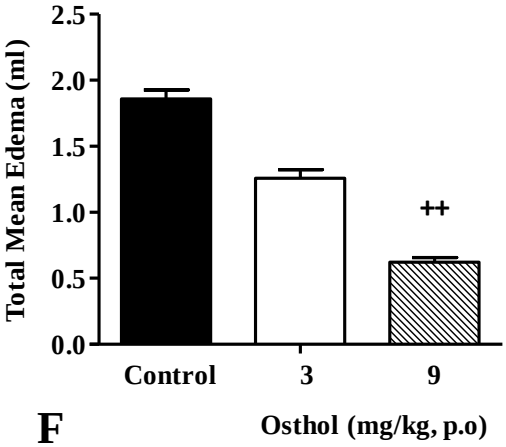
Total Mean Edema (ml)
Control
3
9
Osthol (mg/kg, p.o)
F

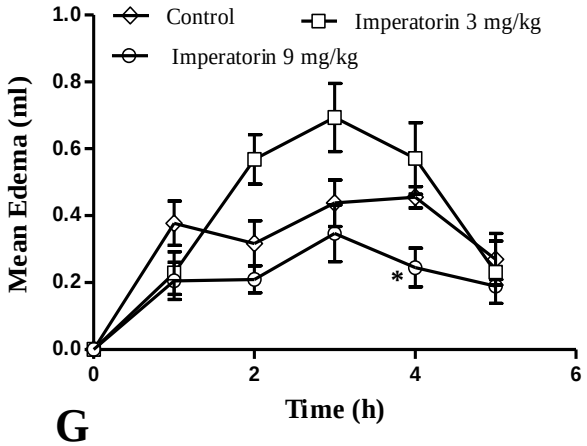
Control
Imperatorin 3 mg/kg
Imperatorin 9 mg/kg
Mean Edema (ml)
Time (h)
*

G

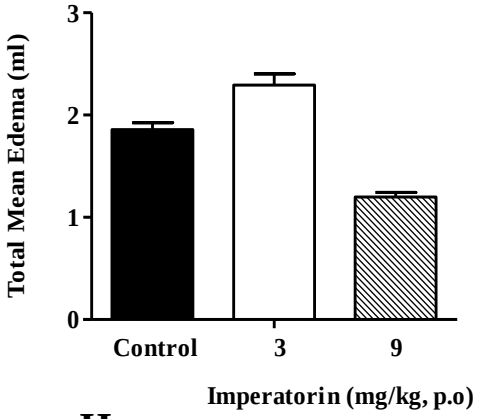
Total Mean Edema (ml)
Control
3
9
Imperatorin (mg/kg, p.o)

H

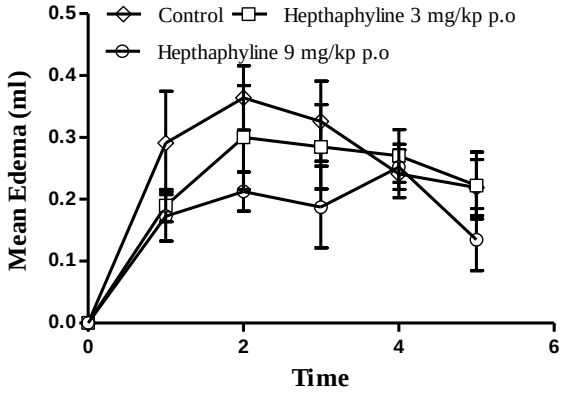
Control
Hepthaphyline 3 mg/kp p.o
Hepthaphyline 9 mg/kp p.o
Mean Edema (ml)
Time

I

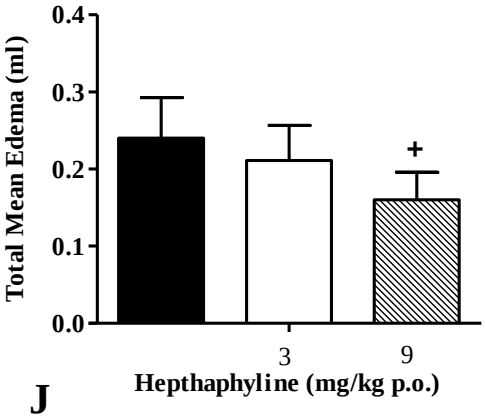
Total Mean Edema (ml)
+
3
9
Hepthaphyline (mg/kg p.o.)

J

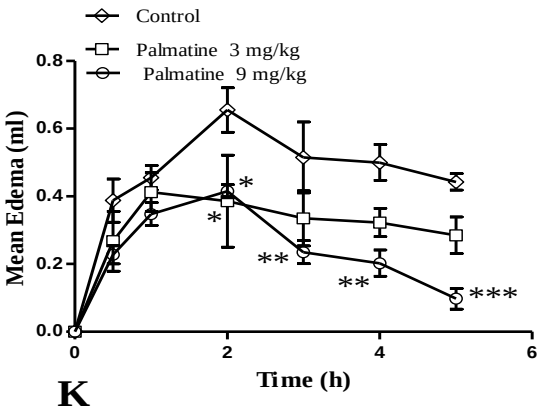
Control
Palmatine 3 mg/kg
Palmatine 9 mg/kg
Mean Edema (ml)
Time (h)
*
*
**
**
***

K

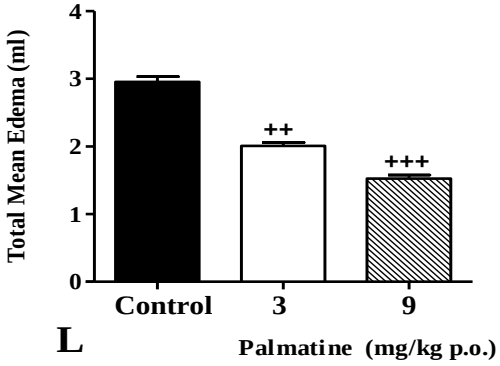
Total Mean Edema (ml)
++
+++
Control
3
9
Palmatine (mg/kg p.o.)

L

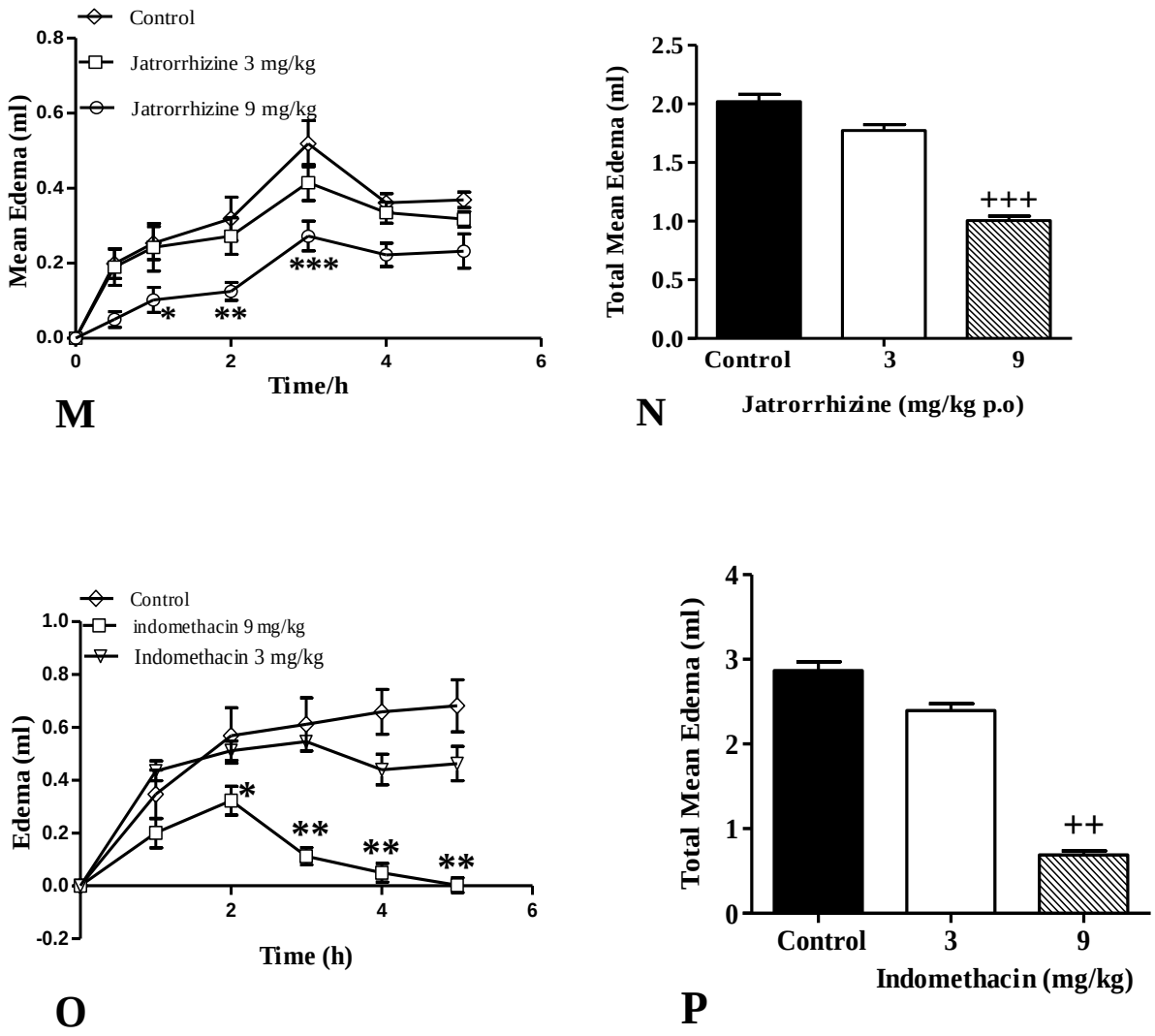

Figure 4.12: Anti-inflammatory effect of the isolated compounds: anisocoumarin B, xanthotoxol, osthol, imperatorin and heptaphyline from *C. anisata* root and palmatine, jatrorrhizine from *A. polycarpa* and the reference drug, indomethacin at (3 - 9 mg/kg p.o) respectively on time course curves (A, C, E, G, I, K, M, O) and total mean oedema response (B, D, F, H, J, L, N, P) respectively on carrageenan induced inflammation in rats' paw. Values are expressed as means ± SEM (n = 5). $^{*}p < 0.05$; $^{**}p < 0.01$; $^{***}p < 0.001$ compared to vehicle treated control group (Two- way ANOVA followed by Bonferroni's post hoc test). $^{+}p < 0.05$; $^{++}p < 0.01$; $^{+++}p < 0.001$ compared to vehicle treated control group (One-way repeated measures ANOVA followed by Tukey's post hoc test).

Table 4.30: Anti-inflammatory activity of compounds isolated from *C. anisata* root

Compounds	C1D	C1D	P2A	P2A	C1F	C1F	C1G	C1G	C1-I	C1-I	Indo	Indo
Dose (mg/kg p.o).	3	9	3	9	3	9	3	9	3	9	3	9
Ant-inflammatory activity (%)	40.66	62.05	37.24	57.97	32.30	66.50	i/a	35.52	12.03	33.39	16.47	75.86

Table 4.31: Anti-inflammatory activity of compounds isolated from *A. polycarpa*

Compounds	A6C	A6C	A8C	A8C	Indo	Indo
Dose (mg/kg p.o).	3	9	3	9	3	9
Ant-inflammatory activity (%)	32.05	48.39	12.23	50.25	16.47	75.86

Keys: C1D = Anisocoumarin B; P2A = Xanthotoxol; C1F = Osthol; C1G = Imperatorin; C1-I = Heptaphyline; A6C = Palmatine; A8C = Jatrorrhizine; Indo = indomethacin; i/a = inactive.

CHAPTER FIVE

DISCUSSIONS, CONCLUSIONS AND RECOMMENDATIONS

5.1 DISCUSSIONS

5.1.1 Phytochemical screening tests

The phytochemical screening tests revealed that the ethanol extract of *C. anisata* root contained coumarins, alkaloids, triterpenoids and free reducing sugars. Alkaloids, triterpenoids, saponins and free reducing sugars were also detected in the ethanol extract of *A. polycarpa* stem bark. Some phytoconstituents such as coumarins, alkaloids, triterpenoids and saponins among others are known to possess anti-inflammatory and analgesic activities (Yuan *et al.*, 2006; Perez, 2001). The presence of these secondary metabolites in the ethanol extract of *C. anisata* root, *A. polycarpa* stem bark and *A. polycarpa* root bark may therefore contribute to the remarkable anti-inflammatory and analgesic activities observed for these plant extracts. The results also showed that the phytoconstituents present in the plant extract should be the classes of compounds to be expected in the structural elucidation.

5.1.2 TLC profiles of the plants extracts

The chromatogram of the leaf, stem and root of *C. anisata* are quite similar (Figure 4.1 A). This indicates that the leaf and stem of *C. anisata* may also have some similarity in activity as its root. This deduction may also be true for *A. polycarpa* root and stem bark which also shows similar chromatograms. The leaf of this plant may also exhibit some activities similar as the root and stem since the upper blue spot is common to all chromatograms (Figure 4.1 B).

5.1.3 Acute toxicity assay

Sprague-Dawley rats and Swiss albino mice pre-treated with ethanol extracts of *C. anisata* root and *A. polycarpa* stem bark at 2 500 and 5 000 mg/kg p.o. respectively shows no signs of toxicity such as pilo-erection, motor impairment, sedation, salivation, hyperexcitability coma or death throughout the observation period. Hence the LD_{50} of these plant extracts is above 5 000

mg/kg p.o. These results indicate that *C. anisata* root and *A. polycarpa* stem bark may therefore be used as safe herbal remedies through the oral route in acute conditions.

5.1.4 Antinociceptive effects

5.1.4.1 Hot plate assay

Numerous neurotransmitters and receptors which are key targets for pain and inflammation are located in the spinal cord and the brain making them the principal modulators in central pain mechanism (McCurdy and Scully, 2005). The central analgesic effect of substances are evaluated using the hot plate test which is thermal-induced nociception model (Yong *et al.*, 2012), demonstrating narcotic participation (Okokon *et al.*, 2008).

***C. anisata* root**

The ethanol extract of *C. anisata* root (CRE) demonstrated significant ($p < 0.05$ - 0.001) dose-dependent antinociceptive effect in the hot plate test similar to ($p < 0.01$ - 0.001) tramadol, a known opioid analgesic drug. This result showed that CRE may possess remarkable central analgesic activity. The petroleum ether (PEF), chloroform (CF) and aqueous (EMF) fractions of the ethanol extract of *C. anisata* root all demonstrated elevation of latency of mice in response to thermal-induced pain with PEF producing the highest analgesic response of 96.23 % at 1 000 mg/kg p.o. The analgesic effect of EMF on pain stimulation in the hot plate model was the weakest among the three fractions of CRE. Thus the possible central analgesic effect of the ethanolic root extract of *C. anisata* is more concentrated in its petroleum ether and chloroform fractions. These results suggest that CRE and its fractions possess remarkable analgesic effects which could be opioid-like in nature. This appear to be the first report on the analgesic activity of *C. anisata* root.

The compounds isolated from the petroleum ether fraction also demonstrated remarkable analgesic effect in the hot plate assay. Anisocoumarin B and the furanocoumarin, xanthotoxol isolated from the petroleum ether fraction of *C. anisata* root produced potent analgesic response of 50.40 and 25.95 % respectively at 9 mg/kg p.o. This indicates that anisocoumarin B may also be acting as an analgesic agent through the central nervous system. This is the first time the analgesic activity of anisocoumarin B is being reported.

Furthermore, xanthotoxol also showed considerable analgesic action in the hot plate test similar to that of tramadol. It may be concluded that xanthotoxol exerts its analgesic effect through the central nervous system. However this effect of xanthotoxol is already known (Zhu, 1997).
The other compounds from *C. anisata* root were not tested in the hot plate assay due to their poor yield.

***A. polycarpa* stem bark**

The ethanol extract of *A. polycarpa* stem bark (ASE) exhibited very high analgesic activity of 82.54 % at 10 mg/ kg p.o in the hot plate test. This suggest that ASE possessed immense central analgesic activity and could be a good source of analgesic agent that act by exerting their effect on the central nervous system. The petroleum ether fraction (AP) of ASE also demonstrated substantial analgesia in the hot plate test. But the most analgesic response in this assay among the three factions of ASE was produced by its chloroform (AC) fraction. The aqueous fraction (AER) of ASE exhibited very weak analgesic activity. These outcomes show that the constituents responsible for the central analgesic actions of ASE mostly resides in the chloroform fraction (AC) of the ethanol extract of *A. polycarpa* stem bark (ASE). This is the first investigation reporting the analgesic effect of *A. polycarpa*. Palmatine or Palmatine chloride isolated from the chloroform fraction of ASE also demonstrated pronounced analgesia in the mouse hot plate test with analgesic activity of 85.56 % at 9 mg/kg p.o. Thus palmatine also possessed substantial central antinociceptive action. Jatrorrhizine also demonstrated immense analgesic activity of 93.87 % in the hot plate test indicating that this compound might also possess central antinociceptive activity. Therefore, the presence of palmatine and jatrorrhizine in the stem bark of this plant lend credence to the plant's use in the treatment of various ailments in traditional medicine. To the best of our knowledge this is the first study to report the central analgesic actions of palmatine and jatrorrhizine.

5.1.4.2 Acetic acid-induced writhing pain stimulation

The acetic acid induced writhing test is a very sensitive model and has the advantage of even detecting weak analgesics (Bars *et al.*, 2001). Injection of irritant substances such as acetic acid into intraperitoneal cavity of mice illicit stereotype response characterized by stretching of the hind limbs, abdominal contractions and twisting of dorsal abdominal muscles and these

occurrence per unit time are considered as abdominal cramps (Bars *et al.*, 2001) which are evidence of visceral pain (Vyklicky. L., 1979) induced by sensitization of nociceptors by prostaglandins (Yong *et al.*, 2012) since the level of prostaglandins in the peritoneal exudates of mice and rats increases after intraperitoneal injection of acetic acid (Derardt *et al.*, 1980). The stretchings and abdominal constrictions obtained in the acetic acid induced writhing test therefore, correlated with sensitization of nociceptors to the production of prostaglandins (Yong *et al.*, 2012).

***C. anisata* root and its isolates**

The results of this study showed that the ethanol extract of *C. anisata* root (CRE) produced analgesia by significantly ($p < 0.05$) inhibiting the writhing numbers again suggesting that CRE exert peripheral analgesic activity by inhibiting the production or actions of prostaglandins in the intraperitoneal cavity of mice. These results are consistent with those obtained in the carrageenan induced edematogenic test. In both assays, CRE demonstrated dose-dependent activity with the highest response at CRE 1 000 mg/kg p.o. It can therefore be concluded that the anti-inflammatory constituents of CRE were also responsible for its peripheral analgesic effect.

Anisocoumarin B which was successively isolated from ethanol root extract of *C. anisata* (CRE) by means of bioassay guided fractionation significantly ($p < 0.01$) inhibited the writhing responses in mice with 55.50 % analgesic activity at 10 mg/kg p.o. In addition, osthol, imperatorin and heptaphyline also produced significant analgesia in the acetic acid–induced writhing test. Therefore, the analgesic effect of anisocoumarin B, osthol, imperatorin and heptaphyline in the writhing assay could be attributed to their ability to suppress the synthesis or action of prostaglandins which is similar to the mechanism of action of the nonsteroidal anti-inflammatory drugs (NSAIDs). This finding also corroborates the result of the edematogenic assay using carrageenan. In both assays the anti-inflammatory response and the analgesic response of anisocoumarin B was dose-depended which further support the fact that the anti-inflammatory and peripheral analgesic effects of anisocoumarin B are the same and relates to those of NSAIDs. Anisocoumarin B which had been isolated from the pet ether fraction of ethanol root extract of *C. anisata* may account in parts for the use of *C. anisata* root in the treatment of some pain disorders mediated by the peripheral nervous system in ethnomedicine. This is the first report on the analgesic activity of anisocoumarin B.

Xanthotoxol which was also isolated from the pet ether fraction of CRE, failed to inhibit stomach constrictions and stretching induced by acetic acid at 2 and 6 mg/kg p.o respectively. Since xanthotoxol was active in the hot plate test it means it may possess central antinociceptive effect but not peripheral analgesic activity since it was inactive in the writhing test. This finding contradicted the report by Zhu, (Zhu, 1997) that xanthotoxol significantly inhibited pain stimulation by acetic acid. However, since the mean writhing counts of the mice decreased with increasing dose of xanthotoxol, xanthotoxol may perhaps show activity at very high doses.

A. polycarpa stem bark and it constituent compounds

A. polycarpa stem bark ethanol extract (ASE) demonstrated significant inhibition of writhing movements in the mouse writhing assay at all doses used in the experiment. The highest analgesic effect ($p < 0.01$) calculated for ASE was 44.03 % at 1 000 mg/kg p.o. Thus ASE possessed substantial analgesic effect and is a source of analgesic agent which act by inhibiting the cyclo-oxygenase enzyme and hence reducing the biosynthesis of prostanoids such as prostaglandins in the mass cells of mice abdominal cavity.

The petroleum ether fraction (AP) of ASE was virtually inactive as it failed to protect mice against acetic acid induced writhing responses. This showed that the compounds responsible for the analgesic effect of ASE in the writhing assay were not present in the non-polar fraction. The semi-polar chloroform fraction (AC) and the very polar aqueous fraction (AER) both showed antinociceptive activity with the most responses 47.33 and 40.33 % analgesic effects at 10 and 100 mg/kg p.o respectively. Thus AC and AER contained the constituents responsible for the antinociceptive action of ASE in the writhing test and the mode of action of these two fractions are the same as described for their mother extract (ASE). This is the first reported on the analgesic activity of *A. polycarpa*.

The results obtained for palmatine, which was there after isolated from the chloroform fraction (AC) of *A. polycarpa* stem bark (ASE), revealed that at 6 mg/kg p.o, palmatine produced statistically significant ($p < 0.05$) analgesic effect of 47.28 %. This indicates that palmatine exerts peripheral analgesic activity by inhibition of prostaglandins production or actions. This

finding is similar to that obtained from the carrageenan-induced edema assay. The effects were dose-depended in both assays. The result obtained for palmatine in the writhing test is similar to those reported by some earlier investigators (Liu *et al.*, 2010; Küpelia *et al.*, 2002). Jatrorrhizine at 2 or 6 mg/kg p.o also enhanced protection of mice against acetic acid-induced pain by significant ($p < 0.01$) inhibition of the mean writhing count compared with the vehicle treated control group. The highest analgesic effect of jatrorrhizine was 44.25 % at 6 mg/kg p.o. This indicates that jatrorrhizine also possessed peripheral analgesic effect.

This is the first report on this analgesic activity of jatrorrhizine to the best of our knowledge.

Root bark of *A. polycarpa*

The root bark of the ethanol extract of *A. polycarpa* (AR) exhibited significant anti-inflammatory activity in the acetic acid-induced writhing assay. AR produced the highest analgesic activity of 41.04 % ($p < 0.05$) at 100 mg/kg p.o. Thus, AR possessed analgesic effect and is a source of analgesic agent which act by inhibiting the cyclo-oxygenase enzyme and hence reducing the biosynthesis of prostanoids such as prostaglandins in the inflammatory reaction.

Furthermore, palmatine was isolated from the root bark of *A. polycarpa* which had also been isolated from the stem bark in this study. Palmatine exhibited anti-inflammatory activity in the carrageenan induced assay. In addition, it has been established in this study that the analgesic activity of palmatine was mediated by the central opioidergic nociceptors in the hot assay. It can therefore be concluded that *A. polycarpa* root bark may have all these properties that palmatine showed in this research. This is the first report on anti-inflammatory and analgesic activity of *A. polycarpa* root.

5.1.5 Mechanism of antinociceptive action

Opioid analgesics such as morphine and its analogues are used in the treatment of moderate or severe pain. This class of analgesic drug elicits antinociceptive action by excitation of the mu-opioid nociceptors (Lamberts *et al.*, 2011).When mu-opioid receptors (MOR) are stimulated: voltage sensitive calcium channels (VSCC) are closed; potassium efflux leading to hyperpolarization is stimulated and cyclic adenosine monophosphate (cAMP) synthesis is decreased due to inhibition of adenylyl cyclase; the overall effect of these processes is decrease in responsiveness of neuronal cell which finally cut back transmission of nerve impulses in addition to prohibiting the liberation of neurotransmitter (McDonald and Lambert, 2005). This prevents the nociceptive stimuli from getting to the brain to be felt as pain and hence inducing analgesia.

Acetylcholine (ACh) is capable of exciting sensory neurons through nicotinic receptors (Bernardini *et al.*, 2001; Jinks and Carstens, 1999; Steen and Reeh, 1993). Nicotinic agonists generate feelings of irritation or pain when applied to the skin or the oral mucosa (Dessirier *et al.*, 1997; Dessirier *et al.*, 1998). These effects are reversed with distinctive antagonists and show desensitization with substitutive application. Moreover, muscarinic receptors are conveyed by many sensory neurons (Bernardini *et al.*, 1999; Tata *et al.*, 2000). In addition, activation of muscarinic receptor, mainly through M2 receptors, leads to desensitization of sensory neurons (Bernardini *et al.*, 2001; Bernardini *et al.*, 2002). Hence, certain cholinergic receptor agonists could probably be peripheral analgesic agents (Jana, 2003). For instance, intra-articular injection of the cholinesterase inhibitor, neostigmine directly into rats' knee joint partly inhibited mechanical-induced pain (Buerkle *et al.*, 1998) and cause a range of postoperative pain relief in patients who undertook knee operations (Yang *et al.*, 1998). Generation of analgesic effect in animals by stimulation of the central cholinergic receptors had also been established by various researchers (Paxinos and Watson, 1986; Jensen and Yaksh, 1986; Karlsson, 1979; Pedigo *et al.*, 1975; Harris and Dewey W. L., 1972). Excitation of cholinergic nociceptors with nicotine and nicotinic agonists has been demonstrated to bring about antinociceptive actions in different kinds of animal and pain assays (Chen *et al.*, 2006). The cholinergic pathway is therefore involved in mediating both central and peripheral antinociceptive action.

***C. anisata* root**

The results of the experiments showed that the ethanol extract of the root of *C. anisata* (CRE) produced significant analgesic action of 28.87 % in the hot plate test at 10 mg/kg p.o. However, that effect was completely abolished by naloxone to - 10.89 %. Indicating that the non-selective opioid receptor inverse agonist, naloxone antagonized CRE induced analgesia. Atropine, on the other hand, had no substantial effect on the analgesic activity of CRE in the acetic acid induced writhing assay as the analgesic effect of as of the two groups of mice did not differ significantly when compared to each other. Since naloxone antagonized the analgesia induced by CRE in the hot plate test whereas atropine could not, it implies that CRE elicits antinociceptive action by binding to the central endogenous opioid nociceptor system and deactivate it and thereby preventing the neurotransmitters from transmitting the nociceptive stimuli to the brain to be detected as pain.

The two coumarins, anisocoumarin B and xanthotoxol, isolated from the most active fractions of CRE also had their antinociceptive actions being blocked by naloxone in the hot plate assay whereas atropine could not antagonize their effects in the mouse writhing assay. Thus the central endogenous opioidergic nociceptors also involved in mediating the analgesic actions of anisocoumarin B and xanthotoxol just as their mother extract from which they were isolated. Therefore, the ethanol extract of the root of *C. anisata* and its isolated constituents; anisocoumarin B and xanthotoxol could be classified as opioid analgesic agents. Anisocoumarin B and xanthotoxol in *C. anisata* root contributes to the opioid analgesic character of the ethanol extract of the root of *C. anisata* (CRE) observed in this study. This further, lend credence to the use of the root of this plant in the management of various pain disorders in traditional medicine as reported earlier in Chapter 2.

This is the first study to report the mechanism of antinociceptive action on the root of *C. anisata* (CRE) and anisocoumarin B. The result obtained for xanthotoxol was in agreement with what has been reported that naloxone did antagonize its analgesic effect (Zhu, 1997). The presence of xanthotoxol in *C. anisata* root therefore contributres to the analgesic activity of this medicinal plant.

***A. polycarpa* stem bark**

The ethanol extract of *A. polycarpa* stem bark (ASE) at 10 mg/kg p.o alone exhibited remarkable overall analgesic effect of 82.54 % which was effectively blocked by co-administration of naloxone at 2 mg/kg i.p to -44.72 % in the hot plate test. However, effect of atropine on antinociceptive effect of ASE was not statistically insignificant ($p > 0.05$) although the analgesia produced by ASE alone was 36.77 % which was reduced to 25.20 % upon co- administration with large dose of atropine. Hence atropine could not be deemed to have any remarkable influence on the analgesic effect of the ethanol extract of *A. polycarpa* stem bark in the writhing assay. These results are indicative of the fact that naloxone did antagonize the antinociceptive action of ASE in the hot plate test but atropine did not in the writhing assay. And hence, the ethanol extract of *A. polycarpa* stem bark (ASE) produces analgesia by exerting its action on the endogenous opioid peptide nociceptors in the central nervous system.

The analgesic effect of palmatine which has been isolated from the stem bark extract of *A. polycarpa* was also substantially antagonized by naloxone in the hot plate assay in this study. Thus suggesting that palmatine elicits analgesic effect by excitation of the central endogenous opioid nociceptors. Atropine on the other hand did not show any effect on the antinociceptive action of palmatine in the writhing test. These results indicate that *A. polycarpa* stem bark and its isolated constituent, palmatine act through the central opioidergic system to induce analgesia. The effect of naloxone on the analgesic activity of jatrorrhizine was not tested. However, atropine did not antagonize the analgesic activity of jatrorrhizine in the writhing assay. But since jatrorrhizine and palmatine have similar structures, it could be assumed that jatrorrhizine could also acted through the central opioidergic system to produce analgesia.

5.1.6 Anti-inflammatory effects

Carrageenan-induced edema in rat paws is a notable test used to screen anti-inflammatory substances (Winter *et al.*, 1962) and had been established to be a three phase process mediated by sequential release of several mediators (Di Rosa, 1972). The 0 - 1.5 h after carrageenan injection involves the release of histamine and serotonin and constitute phase 1. It is followed by

phase 2 mediated by liberation of bradykinin from the 1.5 to 2.5 hours (Antonio and Brito, 1998) and the final phase mediated by prostaglandins (PGI_2) and slow reaction agents release from 2.5 to 6 hours (Spector, 1960). These inflammatory mediators are effective vasodilators which enhance vascular permeability and consequently lead to edema formation during acute inflammation (Vasudeva *et al.*, 2007). The plant extracts and their fractions together with their isolated constituents produced various degrees of inhibition of edema in this assay.

***C. anisata* root and its isolated constituents**

The results of the anti-inflammatory studies of the ethanol root extract of *C. anisata* (CRE) and its fractions showed that they possessed anti-inflammatory properties which could be mostly due to their ability to inhibit the production or action of prostaglandins and other pro inflammatory mediators. This is because all the fraction showed significant ($p < 0.05$) inhibition of the carrageenan induced edema in rats' paws starting from the 1^{st} h (PEF) or 2^{nd} h (CF and EMF) and were maintained till the 5^{th} h on their respective time course curves. The crude ethanolic root extract of this plant showed the maximum significant ($p < 0.001$) inhibition of edema only at the 5^{th} h with an overall inhibition of inflammation of 27.53 % at 10 mg/kg p.o. The maximum overall anti-inflammatory activity of the pet ether (PEF), chloroform (CF) and aqueous (EMF) fractions of CRE were 70.44, 66.37 or 66.55% at 1000, 100 or 100 mg/kg p.o respectively which compares with those of indomethacin at 9-30 mg/kg p.o. These results also indicated that the various fractions of CRE were more potent when they were separated than when they were together as crude extract. This is the first report on anti-inflammatory activity of the root of *C. anisata*.

The compounds isolated from the root also showed very significant anti-inflammatory effects.

Anisocoumarin B (C1D)

The prenyloxy coumarin, 5-hydroxy-7-(3,3-dimethylallyloxy)coumarin also known as anisocoumarin B exhibited considerable anti-inflammatory action 62.05% overall anti-inflammatory effect at 9 mg/kg p.o. Anisocoumarin B significantly ($p < 0.05$) inhibited the carrageenan-induced edema in rat paws from the 4^{th} - 5^{th} h. This indicates that the anti-inflammatory action of anisocoumarin B may involve its ability to inhibit the biosynthesis or action on target site of prostaglandin and slow reacting substances. This is consistent with the

observed possible mechanism of anti-inflammatory effect of the crude ethanol root extract of *C. anisata*. This is the first report on anti-inflammatory activity of anisocoumarin B.

Xanthotoxol (P2A)

Xanthotoxol also showed statistical significant ($p < 0.05$) inhibition of the edema on the 4^{th} h on the time course curve with the highest overall inhibition of the inflammation by 57.97 %. Therefore, the mechanism of anti-inflammatory action of xanthotoxol may be related to inhibition of prostaglandin synthesis and may be similar to that of anisocoumarin B and the crude ethanol root extract.

Previous studies reported that xanthotoxol possessed anti-inflammatory effect in both acute and chronic inflammation models in rats and mice and also lowered the prostaglandin E content in the inflammatory tissue exudate from rat hind paw induced by means of carrageenan (Qishen *et al.*, 1998). Thus the present study on anti-inflammatory activity of xanthotoxol is consistent with the earlier report. Free radicals are generated in organisms during biochemical processes and are eliminated by redox reactions in the body. However failure to remove excess free radicals from the body can result in injury to healthy tissues and activation of inflammatory intermediaries (Yong *et al.*, 2012). Removal of free radicals results in decline in inflammatory mediators and inhibition of prostaglandins (Yong *et al.*, 2012). Substances with antioxidant properties can be potent scavengers of free radicals and may therefore be able to inhibit inflammation. Xanthotoxol was also reported to demonstrate effective antioxidant activity in both lipid peroxidation and hemolysis tests (Ng *et al.*, 2000). Hence the anti-inflammatory effect of xanthotoxol may also be due to its ability to scavenge free radicals which causes oxidative stress.

Osthol (C1F)

The results obtained from the anti-inflammatory assay of osthol indicates that it possessed substantial anti-inflammatory activity. The overall anti-inflammatory response of 66.5 % produced by osthol at 9 mg/kg p.o was the highest obtained amoung the compounds isolated from the two plants. Moreover, osthol displayed statistically significant anti-inflammatory response on all the three phases of carrageenan induced edematogenic assay ($p < 0.05$ from 1^{st} - 5^{th} h, $p < 0.001$) on the time course curve. This indicates that osthol attenuates inflammation by

possibly inhibiting the action of all the inflammation mediators such as histamine, serotonin, bradykinin, prostaglandins (PGI_2) and slow reaction substances which initiate and sustain the inflammation reaction at all the three stages.

Imperatorin (C1G)

The prenyloxy furanocoumarin, imperatorin, showed a dose-depended anti-inflammatory action. The highest anti-inflammatory response of 35.52 % given by the higher dose of 9 mg/kg p.o. was remarkable. Since imperatorin produced dose dependent anti-inflammatory response, it shows that the overall anti-inflammatory response will become statistically significant at doses greater than 9 mg/kg p.o. The anti-inflammatory effect of imperatorin became statistically significant at 4^{th} h ($p < 0.05$) on the time course curve. This period corresponds to the 3^{rd} phase of inflammation which involves the release of prostaglandins (PGI_2). Hence the mechanism of anti-inflammatory action of imperatorin may be due to its ability to inhibit synthesis and/or action of prostaglandins.

Huang *et al.*, 2012 showed that imperatorin demonstrated anti-inflammatory activity in lipopolysaccharide-stimulated mouse macrophage *in vitro* and in carrageenan-induced mouse paw oedema assay. In addition, imperatorin inhibited protein expression of inducible nitric oxide (NO) synthase and cyclooxygenase-2 in lipopolysaccharide-stimulated RAW264.7 cell (Huang *et al.*, 2012). The mechanism of anti-inflammation action of imperatorin may therefore not only be due to its ability to inhibit cyclo-oxygenase enzyme but also to its inhibitory effect on other inflammation mediators such as nitric oxide (NO).

The result obtained for the anti-inflammatory study of imperatorin is consistent with that obtained by Huang *et al.*, 2012.

Heptaphyline (C1-I)

Heptaphyline also demonstrated anti-inflammatory activity by inhibiting carrageenan induced oedema in rats' paws. Although, heptaphyline did not exhibit statistically significant ($p > 0.05$) inhibition of inflammation at any phase of the inflammation process, its overall anti-inflammatory response at 9 mg/kg p.o. was significant ($p < 0.05$). This may be because the doses

used in this experiment were too small. This is the first report on the anti-inflammatory activity of the carbazole alkaloid heptaphyline to the best of my knowledge.

Anisocoumarin B, xanthotoxol and imperatorin, unlike osthol and heptaphyline, all demonstrated significant anti-inflammatory activity at the 3rd phase of the acute inflammatory process just like the crude ethanol extract of *C. anisata* root (CRE). This indicates that these three compounds (anisocoumarin B, xanthotoxol and imperatorin) controls the anti-inflammatory activity of CRE than the other two (osthol and heptaphyline).

The anti-inflammatory activities described for anisocoumarin B and xanthotoxol, osthol, imperatorin and heptaphyline isolated from the pet ether fraction of ethanol extract of *C. anisata* root were responsible in parts for the anti-inflammatory activity of *C. anisata* root.

A. polycarpa stem bark and its isolates

The crude ethanol extract of the stem bark of *A. polycarpa* (ASE) showed maximal overall inhibitory effect of 69.64 % of the carrageenan induced inflammation in rat paws and extremely significant ($p < 0.001$) reduction in total mean edema at 10 mg/kg p.o. which is similar to those obtained for indomethacin (58.15 - 78.23 %) at 9 - 15 mg/kg p.o. This indicates that *A. polycarpa* stem bark possessed considerable anti-inflammatory activity. The pet ether fraction (AP) of the ethanol extract of the stem bark (ASE) of this plant demonstrated significant reduction in total mean edema at 10 mg/kg p.o. ($p < 0.05$) and 100 mg/kg p.o. ($p < 0.01$) with 36.50 and 40.30 % anti-inflammatory activity respectively. The chloroform fraction (AC) also showed $p < 0.01$ inhibition of total edema with 49.03 - 59.50 % overall inhibition of inflammation at 10 and 100 mg/kg p.o. respectively. These results showed that the anti-inflammatory activity of ASE resides in its pet ether and chloroform fractions.

The aqueous fraction (ARE), although showed some significant ($p < 0.001$) inhibition of the inflammation from 4 - 5 hours on the time course curve at 10 mg/kg p.o. did not make significant ($p > 0.05$) impact on the percentage overall inhibition of the inflammation. Thus ARE was generally inactive in the anti-inflammatory assay.

Furthermore, the time course curve which showed the three phase process involved in the carrageenan induced edema assay for the extract and its fractions indicates that ASE, AP and AC

all demonstrated significant ($p < 0.05 - 0.001$) anti-inflammatory action starting from the 2 hour to the 5 hour. These periods correspond to the phase 2 and phase 3 of the acute inflammatory process mediated by bradykinins and prostaglandins (Antonio and Brito, 1998; Spector, 1960). Therefore, the mechanism of anti-inflammatory action of ASE, AC and AP may be due to their inhibition of bradykinins and prostaglandins synthesis or action. Whereas the anti-inflammatory effect of AER, which only took effect ($p < 0.01$) from 4 - 5 hour, may be due to inhibition of prostaglandins biosynthesis. This is the first report on the anti-inflammatory activity on any morphological part of *A. polycarpa*.

Palmatine (A6C)

Palmatine isolated from the chloroform fraction (AC) of the ethanol extract of the stem (ASE) and root barks (AR) of *A. polycarpa* exhibited a very significant ($p < 0.001$) reduction in total edema formation with an overall inhibition of inflammation of 48.39 % at 9 mg/kg p.o. This indicates that palmatine possess anti-inflammatory activity. Besides, palmatine commenced significant ($p < 0.05 - 0.001$) inhibition of the edema from the period of 2 - 5 hour on the time course curve which also correlate with the inhibition of the 2nd and 3rd phases of the acute inflammation process. Indicating that, the anti-inflammatory effect of palmatine may be due to its ability to inhibit bradykinins and prostaglandins synthesis or actions. This result agreed with those obtained for ASE and AC from which palmatine was isolated.

The anti-inflammatory activity of palmatine was well documented as demonstrated in its ability to significantly inhibit xylene-induced ear inflammation (Liu *et al.*, 2010), acetic acid-induced increase in vascular permeability and serotonin-induced hind paw edema (Küpelia *et al.*, 2002). This compound was also reported to exhibit antioxidant properties (Kim *et al.*, 2009). Xylene-induced ear edema and increased vascular permeability assays involve release of inflammation mediators subsequent to induction. This promotes dilation of arterioles and venules in addition to increased vascular permeability (Vogel and Vogel, 1997). Thus the anti-inflammatory effects of palmatine is not only due to its inhibitoin of mediators such as bradykinins and prostaglandins, as described here in the carrageenan induced test, or serotonins (Küpelia *et al.*, 2002) but may also be due to its membrane-stabilizing property that reduces capillary permeability and/or antioxidant actions.

Jatrorrhizine (A8C)

The result from the anti-inflammatory studies indicates that jatrorrhizine is a potent anti-inflammatory agent. The anti-inflammatory action of jatrorrhizine became statistically significant on the time-course curve between 1 - 3 h. This period corresponds to the first and the second phase of inflammatory response. Hence the anti-inflammatory action of jatrorrhizine may be mainly due to inhibition of histamine, serotonin and bradykinin production by the injured cells. The anti-inflammatory activity of jatrorrhizine isolated from *Plagiorhegma dubium* cell culture was already known (Arens *et al.*, 1985). In addition, jatrorrhizine also exhibited anti-oxidant activity in various test models (Luoa *et al.*, 2011). Therefore, the presence of Jatrorrhizine in the stem bark of *A. polycarpa* may also contribute to its anti-inflammatory action. *A. polycarpa* stem bark is mostly employed in traditional medicine as antibacterial and wound healing agent (Ajali, 2000; Irvine, 1961), although there was no literature report on it's use as an analgesic or anti-inflammatory substance. However inflammation and pain are rigorously associated with wound healing (Das and Maulik, 1994). Thus the anti-inflammatory effects of palmatine and jatrorrhizine present in *A. polycarpa* stem bark contribute greatly to its wound healing properties. Malaria and pyrexia are also treated with the stem bark of *A. polycarpa* (Atindehou *et al.*, 2004; Bep, 1986). The anti-malaria, anti-trypanosomiasis, anti-leishmaniasis (Malebo *et al.*, 2013), anti-microbial and anti-bacterial activities (Volleková *et al.*, 2003; Ali *et al.*, 2013) of the quaternary protoberberine alkaloids, palmatine and jatrorrhizine are well documented. Therefore, palmatine and jatrorrhizine in the stem bark of *A. polycarpa* justify their use in traditional medicine in treating various ailments.

5.2 CONCLUSIONS

This study showed that the ethanol extract of *C. anisata* root and *A. polycarpa* stem bark exhibited considerable anti-inflammatory and analgesic activity in various animal models. In addition, it also showed that the extract of *A. polycarpa* root bark had significant analgesic activity. These extracts were also found to act through the central opioidergic norciceptors to attenuate pain. Bioassay-guided fractionation of the extracts for anti-inflammatory and analgesic constituents result in isolation of seven (7) compounds from these plant parts. Five (5) of the compounds were isolated from the most active pet ether fraction of *C. anisata* root. Four (4) of these were coumarins, namely: anisocoumarin B, osthol, imperatorin, xanthotoxol and a carbazole alkaloid, heptaphyline. The other two compounds were quaternary protoberberine alkaloids namely, palmatine and jatrorrhizine isolated from the most active chloroform fraction of *A. polycarpa* stem bark. Palmatine was also isolated from the chloroform fraction of the root bark of *A. polycarpa* in this study. These seven compounds exhibited significant anti-inflammatory activity in the carrageenan induced paw oedema assay. Furthermore, the compounds also demonstrated analgesic activity in the acetic acid-induced writhing assay except xanthotoxol which was inactive at the doses used in this model of analgesic test.

Anisocoumarin B**,** xanthotoxol, palmatine and jatrorrhizine also showed significant analgesic activity in the hot plate assay and were also found to be opioid analgesic agents. However, osthol, imperatorin and heptaphyline were not tested in the hot plate assay.

The isolated compounds therefore contributed significantly to the anti-inflammatory and analgesic activities of the plants.

The anti-inflammatory and analgesic activities and the mechanism of antinociceptive action of *C. anisata* root, *A. polycarpa* anisocoumarin B and heptaphyline are being reported for the first time by this study. In addition, the analgesic activities of jatrorrhizine and the mechanism of antinociception of palmatine are also being reported for the first time by this study to the best of our knowledge.

This study has therefore provided scientific justification for the use of these plants as anti-inflammatory and analgesic agents in traditional medicine.

5.3 RECOMMENDATIONS

- Since this is the only reported studies on any biological activity of anisocoumarin B, it is therefore recommended that other *in vivo* and *in vitro* pharmacological and antimicrobial activities that relate to the ethnopharmacological uses of *C. anisata* root be scientifically investigated for this compound.

- Efforts should also be made to isolate any other compound(s) that may be present in the chloroform fraction of *A. polycarpa* stem bark and their anti-inflammatory and analgesic activities together with their mechanism(s) of antinociceptive action tested.

- Further research should also be conducted on the isolated compounds for possible development into analgesic and anti-inflammatory drugs.

- Finally, further work should be carry out on *A. polycarpa* root to isolate its constituents since only one compound was isolated from it during this study.

REFERENCES

Adesina, S. K. and Adewunmi, C. O. (1985). Molluscicidal agents from the root of *Clausena anisata*. *Fitoterapia,* 56**,** 289-292.

Ajali, U. (2000). Antibacterial activity of *Enantia polycarpa* bark. *Fitoterapia,* 71(3)**,** 315-316.

Ali, S., Igoli, J., Clements, C., Semaan, D., Alamzeb, M., Rashid, M. U., Shah, S. Q., Ferro, V. A., Gray, A. I. and Khan, M. R. (2013). Antidiabetic and antimicrobial activities of fractions and compounds isolated from *Berberis brevissima* Jafri and *Berberis parkeriana* Schneid. *Journal of the Bangladesh Pharmacological Society,* 8**,** 336-342.

Almeida, T. F., Roizenblatt, S. and Tufik, S. (2004). Afferent pain pathways: a neuroanatomical review. *Brain Research,* 1000**,** 40-56.

Almudena B., Philippe P. M., K., A. B., Sundar, R. M., Carmen, Z. and Diego, C. (1995). Dopaminergic Isoquinoline Alkaloids from Roots of *Xylopia papuana*. *Natural Product Letters,* 6 (1)**,** 57- 62.

Alves, C. Q., Lima, L. S., David, J. M., Lima, M. V. B., David, J. P., Lima, F. W. M., Pedroza, K. C. M. C. and Queiroz, L. P. (2013). In vitro acetylcholinesterase activity of peptide derivatives isolated from two species of Leguminosae. *Pharmaceutical Biology,* 51 (7)**,** 936-939.

Ankier, S. I. (1974). New hot plate tests to quantify antinociceptive and narcotic antagonist activities. *European Journal of Pharmacology* 27**,** 1–4.

Antonio, M. A. and Brito, A. R. M. S. (1998). Oral anti-inflammatory and antiulcerogenic activities of hydroalcoholic extract and partitioned fractions of *Turnera ulmifolia* (Turneraceae). *Journal of Ethnopharmacology,* 61**,** 215–228.

Apkarian, A. V., Bushnell, M. C., Treede, R. D. and Zubieta, J. K. (2005). Human brain mechanisms of pain perception and regulation in health and disease. *European Journal of Pain,* 9**,** 463 - 84.

Archer, S., Glick, S. D. and Bidlack, J. M. (1996). Cyclazocine Revisited. *Neurochemical Research,* 21 (11)**,** 1369–1373.

Arens, H., Fisher, H., Leyck, S., Romer, A. and Ulbrich, B. (1985). Anti-inflammatory compounds from *Plagiorhegma dubium* cell culture. *Planta Medica***,** 52–56.

Atindehou, K. K., Schmid, C., Brun, R., Kone M.W. and Traore, D. (2004). Antitrypanosomal and antiplasmodial activity of medicinal plants from Cote d'Ivoire. *Jounal of Ethnopharmacology,* 90 221-227.

Ayensu, E. S. (1978). Medicinal Plants of West Africa, Chicago, Reference publications INC., 233.

Azhar, R., Muhammad K., Bo Y., Tonghui M. and Hong Y. (2011). Xanthoxyletin, a coumarin induces s phase arrest and apoptosis in human gastric Adenocarcinoma SGC-7901 Cells. *Asian Pacific Journal Cancer Prevention* 12**,** 1219-1223.

Baek, N. I., Ahn, E. M., Kim, H. Y. and Park, Y. D. (2000). Furanocoumarins from the root of *Angelica dahurica*. *Archives of Pharmacal Research,* 23 (5)**,** 467–470.

Ballesta-Acosta, M. C., Pascual-Villalobos, M. J. and Rodríguez, B. (2008). Short communication. The antifeedant activity of natural plant products towards the larvae of *Spodoptera littoralis*. *Spanish Journal of Agricultural Research* 6 (1)**,** 85-91.

Bankier, B., Barajas, J., Martinez-Rumayor, A. and Januzzi, J. L. (2008). Association between C-reactive protein and generalized anxiety disorder in stable coronary heart disease patients. *European Heart Journal* 29**,** 2212–2217.

Bars, D. L., Gozariu, M. and Cadden, W. S. (2001). Animal Models of Nociception. *Pharmacological Reviews,* 53 (4)**,** 597–652.

Basbaum, A. I., Bautista, D. M., Scherrer, G. and Julius, D. (2009). Cellular and Molecular mechanism of pain. *Cell,* 139**,** 267 - 284.

Battinelli, L., Mengoni, F., Lichtner, M., Manzzati, G., Saija, A., Mastroianni, C. M. and Vullo, V. (2003). Effects of limoni and nomilin on HIV-1 replications on infected human mononuclear cell. *Planta Medica,* 69**,** 910-913.

Beecher, H. K. (1957). The measurement of pain: prototype for the quantitative study of subjective responses. *Pharmacological Reviews,* 9**,** 59–209.

Beibei, Z., Aili, C., Jiyan, Z., Zhibi, H. and Dazheng, W. (2012). Effect of jatrorrhizine on delayed gastrointestinal transit in rat postoperative ileus. *Journal of Pharmacy and Pharmacology,* 64 (3)**,** 413 - 419.

Bennett, G. J. (2000). Update on the neurophysiology of pain transmission and modulation:focus on the NMDA-receptor. *Journal of Pain Symptom Management,* 19 : S2-6.

Bep, O. B. (1986). Medicinal plants in tropical West Africa, London University Press.

Bernardini, N., Levey, A. I. and Augusti-Tocco, G. (1999). Rat dorsal root ganglia express M1-M4 muscarinic receptor proteins. *Journal of Peripheral Nervous System* 4**,** 222 - 232.

Bernardini, N., Roza, C., Aauer, S. K., Gomeza, J., Wess, J. and Reeh, P. W. (2002). Muscarinic M2 receptors on peripheral nerve endings: a molecular target of antinociception. *Jounal of Neuroscience* (RC229): 22**,** 1–5.

Bernardini, N., Sauer, S. K., Harberberger, R., Fischer, M. J. M. and Reeh, P. W. (2001). Excitatory nicotinic and desensitizing muscarinic (M2) effects on C-nociceptors in isolated rat skin. *Journal of Neuroscience* 21**,** 3295 – 3302.

Bettarinia, F., Borgonovia, G. E., Fiorania, T., Gagliardia, I., Capriolia, V., Massardoa, P., J. I. J. Ogochea, J. I. J., Hassanalia, A., Nyandata, E. and Chapyaa, A. (1993). Antiparasitic compounds from East African plants: Isolation and biological activity of anonaine, matricarianol, canthin-6-one and caryophyllene oxide. *International Journal of Tropical Insect Science,* 14 (1)**,** 93-99.

Bhattacharyya, P. and Chakraborty, D., P., (1987). Progress in the Chemistry of Organic Natural Products. *In:* Herz, W., Grisebach, H., Kirby, G. W. & Tamm, C. (eds.). Springer-Verlag, Wien, 52; 159.

Bing-Hung, C., Hsueh-Wei, C., Hsuan-Min, H., Inn-Wen, C., Jia-Shing, C., Chung-Yi, C. and Hui-Min, W. (2011). (−)-Anonaine Induces DNA Damage and Inhibits Growth and Migration of Human Lung Carcinoma H1299 Cells. *Journal of Agriculture and Food Chemistry,* 59 (6)**,** 2284 - 2290.

Bloom, D. E., Cafiero, E. T., Jane- Llopis, E., Abrahams-Gessel, S., Bloom, L. R., Fathima, S., Feigl, A. B., Gaziano, T., Mowafi, M., Pandya, A., Prettner, K., Rosenberg, L., Seligman, B., Stein, A. Z. and Weinstein, C. (2011). The Global Economic Burden of Non-Communicable Diseases. *Geneva : World Economic Forum*.

Bolou, G. E. K., Bagré, I., Ouattara, K. and Djaman, A. J. (2011). Evaluation of the Antibacterial Activity of Fourteen Medicinal Plants in Côte d'Ivoire. *Tropical Journal of Pharmaceutical Research,* 10 (3)**,** 355-340.

Bouquet, A. and Debray, M. (1974). Medicinal plants in Cote d'Ivoire. *Mémoires* Paris, O.R.S.T.O.M., O.R.S.T.O.M. (éd).

Bowersox, S. S., Singh, T., Nadasdi, L., Zukowska-Grojec, Z., Valentino, K. and Hoffman, B. B. (1992). Cardiovascular effects of omega-conopeptides in conscious rats: mechanism of action. *Journal of Cardiovascular Pharmacology*, 20: 756-764.

Buerkle, H., Boschin, M., Marcus, M. A. E., Brodner, G., Wu Sten, R. and Van Aken, H. (1998). Central and peripheral analgesia mediated by the acetylcholinesterase inhibitor neostigmine in the rat inflamed knee joint model *Anesthesia and Analgesia,* 86**,** 1027–1032.

Burkill, I. H. (1966). A dictionary of the economic products of the Malay Peninsula, Ministry of Agriculture and Cooperation, Government of Malaysia and Singapore.

Buzas, A., Osowiecki, M. and Regnier, C. (1965). On the presence of quinidine in addition to berberine alkaloids in the barks of *Enantia pilosa* and *Enantia polycarpa* (Annonaceae). *Annales Pharmaceutiques,* France; 23 (5): 351-354.

Cai, Y., Baer-Dubowska, W., Ashwood-Smith, M. and Digiovanni, J. (1997). Inhibitory effects of naturally occurring coumarins on the metabolic activation of benzo[a]pyrene and 7, 12-dimethylbenz[a] anthracene in cultured mouse keratinocytes. Carcinogenesis. 18**,** 215-222.

Cannell, R. J. P. (1998). How to approach the isolation of a natural product. *In:* Cannell, R. J. P. (ed.) *Natural Products Isolation.* New Jersey: Humana Press, 1, 1–51.

Caterina, M. J., Schumacher M. A., Tominaga M., Rosen T. A., Levine J. D. and Julius, D. 1997. The capsaicin receptor: a heat-activated ion channel in the pain pathway. *Nature*, 389, 816-824.

Cernakova, M., Kostalova, D., Kettmann, V., Plodova, V., Toth, J. and Drimal, J. (2002). Potential antimutagenic activity of berberine, a constituent of *Mahonia aquifolium*. *BMC Complementary and Alternative Medicine*, 2 (2), 1 - 6.

Chaichantipyuth, C., Pummangura, S., Naowsaran., K., Thanyavuthi, D. (1988). Two new bioactive carbazole alkaloids from the root bark of *Clausena harmandiana*. *Journal of Natural Products*, 51 (6). 1285-1288.

Chakraborty, A., Chowdhury, B. K. and Bhattacharyya, P. (1995). Clausenol and clausenine - two carbazole alkaloids from *Clausena anisata. Phytochemistry*, 1 (40), 295–298.

Chakraborty, D. P. and Roy, S. (1991). Progress in the Chemistry of Organic Natural Products. *In:* Herz, W., Grisebach, H., Kirby, G. W., Steglich, W. and Tamm, C. (eds.). Springer-Verlag, Wien, 57; 71.

Chen, R. and Robinson, S. E. (1990). Effect of cholinergic manipulations on the analgesic response to cobrotoxin in mice. *Life Sciences*, 1949 – 1954.

Chen, Z.-X., Zhang, H.-L., Gu, Z.-L., Chen, B.-W., Han, R., Reid, P. F., Raymond, L. N. and Qin, Z.-H. (2006). A long-form α-neurotoxin from cobra venom produces potent opioidindependent analgesia. *Acta Pharmacologica Sinica,* 27 (4), 402–408.

Chi, H. J. and Kim, H. S. (1970). Pharmacological study of isoimperatorin and oxypeucedanin. *Korean Journal of Physiology and Pharmacology*, 14, 21-27.

Chimienti, M., Panciroli, C., Salerno, J. A., Regazzj-Bonora, M., Previtali, M., Cristiani, D., Rondanelli, R. and Bobba, P. (1984). Dihydroquinidine versus disopyramide: efficacy in patients with chronic stable ventricular ectopy. *Clinical Cardiology,* 7, 538-546.

Chitchang, S., Piamjinda, T., Yodmani, B. and Radomyos, P. (1985). Relationship between severity of the symptom and the number of *Hymenolepis nana* after treatment. *Journal of Medical Association of Thailand,* 68, 423 - 426.

Chulia, S., Ivorra, M. D., Cave, A., Cortes, D., Noguera, M. A. and D'ocon, M. P. (1995). Relaxant activity of three aporphine alkaloids from Annona cherimolia on isolated aorta of rat. *Journal of Pharmacy and Pharmacology,* 47, 647- 650.

Cordell, G. A. (ed.) (2008). The Alkaloids, *Chemistry and Biology,* Evanston, Illinois: Academic Press, Elsevier, 65, 1-430.

Corson, T. W. and Crews, C. M. (2007). Molecular understanding and modern application of traditional medicines: triumphs and trials, *Cell,* 130, 769–774.

Cortes, D., Torrero, M. Y., Pilar D'ocon, M., Luz Candenas, M., Cavé, A. and Hadi, A. H. (1990). Norstephalagine and atherospermidine: two smooth muscle relaxant aporphines from *Artabotrys maingayi Journal of Natural Products* 53 (2), 503 - 508.

Cunningham, A. B. (1993). African Medicinal Plants: Setting priorities at the interface between conservation and primary health Care. *People and Plants Working Paper 1,* 1-54.

Dalisay, D. S., Lievens, S. L., Saludes, J. P. and Molinski, T. F. (2008). *Nature Reviews Drug Discovery,* 8, 69

Das, D. K. and Maulik, N. (1994). Antioxidant effectiveness in ischemia-reperfusion tissue injury. *Methods in Enzymology,* 233**,** 601–610.

De Zoeten, K., Van Meel, J. C., Van Kemenade, J. E., Batink, H. D., Timmermans, P. B. and Van Zwieten, P. A. (1982). Postsynaptic alpha 1-and alpha 2-adrenoceptor blocking properties of (dihydro) quinidine and (dihydro) quinine. *Arzneimittel-Forschung,* 33 (5)**,** 694 - 698

Deleu, D., Hanssens, Y. and Northway, M. G. (2004). Subcutaneous apomorphine: an evidence-based of its use in Parkinson's disease. *Drugs and Aging,* 21 (11), 687 - 789.

Derardt, R., Jougney, S., Delevalcee, F. and Falhout, M. (1980). Release of prostaglandins E and F in analgogenic reaction and its inhibition. *European Journal Pharmacology*, (61)17-24.

Dessirier, J. M., O'mahony, M. and Carstens, E. (1997). Oral irritant effects of nicotine psychophysical evidence for decreased sensation following repeated application and lack of cross-desensitization with capsaicin. *Chem Senses,* 22**,** 483 - 492.

Dessirier, J. M., O'mahony, M., Sieffermann, J. M. and Carstens, E. (1998). Mecamylamine inhibits nicotine but not capsaicin irritation on the tongue: psychophysical evidence that nicotine and capsaicin activate separate molecular receptors. *Neuroscience Letters,* 40**,** 2 65–68.

Devakumar, C. and Sukh, D. (1996). "Chemistry", neem research and development *In:* Randhawa, N. S. and Parmar, B. S. (eds.). New Delhi, India: Society of Pesticide Science, 63 - 99.

Di Rosa, M. (1972). Biological properties of carrageenin. *Journal of Pharmaceutics and Pharmacology,* 24**,** 89–102.

Di Rosa, M., Giround, J. P. and Willoughby, D. A. (1971). Studies of acute inflammatory response induced in rats in different sites by carrageenan and turpentine. *Journal of Pathology* 104, 15-29.

Dickenson, A. H., Chapman, V. and Green, G. M. (1997). The pharmacology of excitatory and inhibitory amino acid-mediated events in the transmission and modulation of pain in the spinal cord. *General Pharmacology* 28**,** 633-638.

Dikshit, M., Rastogi, L., Shukla, R. and Srimal, R. C. (1995). Prevention of ischaemia-induced biochemical changes by curcumin and quinidine in the cat heart. *Indian Journal of Medical Research,* 101, 31-35.

Dvorak, H. F. 1986. Tumors: wounds that do not heal. Similarities between tumor stroma generation and wound healing. *New England Journal of Medicine,* 315, 1650–1659.

Eckhardt, E. T., Cheplovitz, F., Lipo, N. and Govier, W. M. (1958). Etiology of chemically induced writhing in mouse and rat. *Proceedings of the Society for Experimental Biology and Medicine,* 98, 186 - 188.

Eddy, N. B. and Leimbach, D. (1953). Synthetic analgesics. II. Dithienylbutenyl - and dithienylbutylamines, *Journal of Pharmacology and Experimental Therapeutics,* 107, 385–93.

Ekuadzi, E. (2013). *Antibacterial, antioxidant and anti-inflammatory agents of Margaritaria discoidea, Gouania longipetala, Glyphaea brevis and Euadenia eminens.* Doctor of Philosophy (PhD) Thesis, Kwame Nkrumah University of Science and Technology, Kumasi, 25 - 151.

El Tahir, K. E. H. (1991). Pharmacological Actions of Magnoflorine and Aristolochic Acid-1 Isolated from the Seeds of *Aristolochia bracteata*. *Pharmaceutical Biology,* 29 (2) 101-110

Emele, J. F. and Shanaman, J. (1963). Bradykinin writhing: a method for measuring analgesia. *Proceedings of the Society for Experimental Biology and Medicine,* 114, 680 - 682.

Emerole, G., Thabrew, M. I., Anosa, V. and Okorie, D. A. (1981). Structure-activity relationship in the toxicity of some naturally occuring coumarins – chalepin, imperatorin and oxypeucedanine *Toxicology,* 71-80.

Endo, T., Kita, M., Shimada, T., Moriguchi, T., Hidaka, T., Matsumoto, R., Hasegawa, S. and Omura M. (2002). *Plant Biotechnology*, 19, 397- 403.

Fabricant, D. S. and Farnsworth, N. R. (2001). The value of plants used in traditional medicine for drug discovery. *Environmental Health Perspectives,* 109 (Supplmentery 1)**,** 69 - 75.

Fang, Y.-T., Chou, Y.-J., Pu, C., Lin, P.-J., Liu, T.-L., Huang, N. and Chou, P. (2013). Prescription of atropine eye drops among children diagnosed with myopia in Taiwan from 2000 to 2007: a nationwide study. *Nature; Eye*, 27, 418–424.

Farnsworth, N. R. and Dobberstein, R. H. (1977). Phytochemical screening methods,, Chicago, Illinois, College of Pharmacy, University of Illinois, 6-85.

F.B.R., Foundation for Biomedical Research*: The biomedical investigator's handbook for researchers using animal models*. (1987), Washington, D.C.

Fischl, M. A., Richman, D. D., Hanse, N., Collier, A. C., Carey, J. T., Para, M. F., Hardy, W. D., Dolin, R., Powderly, W. G., Wong, B., Merigan, T. C., Mcauliffe, V. J., Hyslop, E. N., Rhame, F. S., Spector, A. S., Volberdi, P. and Anderson, J. (1990). The safety and efficacy of zidovudine (azt) in the treatment of subjects with mildly symptomatic Human Immunodeficiency Virus Type 1 (HIV) Infection: double-blind, placebo-controlled trial. *Annals of Internal Medicine*, 112 (10), 727-737.

Fu, Y., Hu, B., Tang, Q., Fu, Q. and Xiang, J. (2005). Hypoglycemic activity of jatrorrhizine. *Journal of Huazhoug University of Science and Technology Medical Science*, 25 (5)**,** 491-493.

Georgievski, Z., Koklanis, K. and Leone, J. (2008). Fixation behavior in the treatment of amblyopia using atropine. *Clinical and Experimental Ophthalmology*, 36 (Suppl 2), A764–A765.

Gerhard Vogel, H., Wolfganga, H. V., Bernward, A. S., Jurgen, S., Gunter, M. and Wolfganga, F. V. (2002). *Drug discovery and evaluation pharmacological assays*, Edition, 2; Berlin, Germany Spinger, 725-71.

Ghana Herbal Pharmacopoeia, G. H. P. (1992). *Clausena anisata*, Accra, Ghana, The Advent Press, 31-33.

Gill, J. M., Saligan, L., Woods, S. and Page, G. (2009). PTSD is associated with an excess of inflammatory immune activities, *Perspectives in Psychiatric Care*, 262–277.

Gordon, A. N., Fleagle, J. T., Guthrie, D., Parkin, D. E., Gore, M. E. and Lacave, A. J. (2001). Recurrent epithelial ovarian carcinoma: A Randomized Phase III study of pegylated liposomal doxorubicin versus topotecan. *Journal of Clinical Oncology*, 19, 3312-3322.

Govindasamy, R., Simon, J., Puduriv. S., Juliani H. R., Asante-Dartey, J., Arthur, H., Diawuo B., Acquaye, D. and Hitimana N. (2007). Issues in new crops and new uses: Retailers and wholesalers of African herbal and natural products: Case Studies from Ghana and Rwanda, Janick, J and Whipkey, A., (eds), Alexandria, VA, ASHS Press.

Graham, D. J. (2006). COX-2 Inhobitors, other NSAIDs and cardiovascular risk; the seduction of common sense. *JAMA: The Journal of America Medical Association,* 296 (13)**,** 1653 - 1656.

Graziose, R., Rathinasabapathy, T., Lategan, C., Poulev, A., Smith, P. J., Grace, M., Lila, M. A. and Raskin, I. (2011). Antiplasmodial activity of aporphine alkaloids and sesquiterpene lactones from *Liriodendron tulipifera* L. *Journal of Ethnopharmacology,* 133, 26 - 30.

Grycova, L., Dosta, J.and Marek, R. (2007). Quaternary protoberberine alkaloids. *Phytochemistry,* 68, 150–175.

Hamilton, G. R. and Baskett, T. F. (2000). In the arms of morpheus the development of morphine for postoperative pain relief. *Canadaian Journal of Anaesthesia*, 47, 367.

Hamza, O. J., Van Den Bout-Van Den Beukel, C. J. and Matee, M. I. E. A. (2006). Antifungal activity of some Tanzanian plants for the treatment of fungal infections. *Journal of Ethnopharmacolology,* 108 (1), 124-132.

Han, H., Fang, D. C. and Zhonggu, Y. (1989). The blocking and partial agonistic actions of jatrorrhizine on alpha-adrenoceptors, *Acta Pharmacologica Sinica,* 10 (5)**,** 385 - 389.

Harris, L. S. and Dewey W. L. (1972). Role of cholinergic systems in the central action of narcotic agonists and antagonists. *In:* Kosterlitz, H. W., Collier, H. O. J. and Villareal, J. E. (eds.), *Agonist and antagonist actions of narcotic analgesic drugs.* London: Macmillan, 198 – 206.

Harsh, M. (2005). *Text book of Pathophysiology,* New Delhi, Jaypee publication; Edition 5; 126 - 34.

Harvey, A. (2000). Strategies for discovering drugs from previously unexplored natural products. *Drug Discorvery Today,* 5 (7) 293 - 300.

Hawthorne, W. D. and Gyakari, N. (2006). *Photoguide for the Forest Trees of Ghana. A tree's spotter's field guide for identifying the largest tress,* U.K., Oxford Forestry Institute, Department of Plant Science, Ghana Forestry Commission, United Kingdom Department for International Development (DFID), Forestry Research Programme (FRP), 268.

He, W., Chen, W., Ye, H., Zhou, Y., and Huang, X. (2009). Inhibitory effects of xanthotoxol on neutrophil infiltration and brain edema induced by focal cerebral ischemia-reperfusion injury in rats. *Pharmacology and Clinics of Chinese Materia Medica* 05.

Hendershot, L. C. and Forsaith, J. (1959). Antagonism of the frequency of phenylquinone-induced writhing in the mouse by weak analgesics and non analgesics. *Journal of Pharmacology and Experimental Therapeutics,* 125, 237 - 240.

Hesse, M., Meier, H., Zeeh, B., Translated By, Dunmur, R. and Murray, M. (2008). *Spectroscopic Methods in Organic Chemistry,* Stuttgart. New York, Thieme.

Higgs, G. A. (1989). Use of Inplanted sponges to study the acute inflammatory respons*e,* edn. New York, Alan R. Liss, Inc.

Himmelfarb, J., Stenvinkel, P., Ikizler, T. A., Hakim, R. M. (2002). The elephant in uremia: oxidant stress as a unifying concept of cardiovascular disease in uremia. *Kidney International* 62, 1524 – 1538.

Hoch, P. H. (1957). New Drug therapy in psychiatry clinical uses and abuse in mental disorders. *Bulletein of the New York Academy of Medicine*, 474 - 486.

Hoge, E. A., Brandstetter, K., Moshier, S., Pollack, M. H., Wong, K. K. and Simon, N. M. (2009). Broad spectrum of cytokine abnormalities in panic disorder and posttraumatic stress disorder. *Depress Anxiety*, 26 (5), 447 – 455.

Hong-Fang, J., Xue-Juan, L. and Hong-Yu, Z. (2009). Natural products and drug discovery: Can thousands of years of ancient medical knowledge lead us to new and powerful drug combinations in the fight against cancer and dementia? *European Molecular Biology Organization (EMBO) Reports*, 10 (3), 194 - 200.

Hotamisligil, G. S. (2004). Inflammation, TNF alpha and insulin resistance. In Diabetes mellitus: a fundamental and clinical text *(Eds. LeRoith, D.T.S., Olefsky, J.M.,) 3rd edition,* New York, USA, Lippincott, Williams and Wilkins, New York.

Hsieh, M. T., Su, S. H., Tsai, H. Y., Peng, W. H., Hsieh, C. C. and Chen, C. F. (1993). Effects of palmatine on motor activity and the concentration of central monoamines and its metabolites in rats. *Japanese Journal of Pharmacology*, 61 (1), 1- 5.

Huang, G. J., Deng, J. S. and Liao, J. C. E. A. (2012). Inducible nitric oxide synthase and cyclooxygenase-2 participate in antiinflammatory activity of imperatorin from Glehnia littoralis. *Journal of Agricultural and Food Chemistry*, 60 (7), 1673 – 1681.

Huasain, R. A., Kim, J., Beeher, W. W. C. and Kinghorn, A. D. (1989). Unambiguous carbon-13 NMR assignments of some biologically active protoberberine alkaloids. *Heterocycles,* 29 (12)**,** 2257 - 2260.

Hughes, B. (2008). 2007 FDA drug approvals: a year of flux. *Nature Reviews Drug Discovery*, 7, 107–109.

Hung, T. M., Lee, J. P., Min, B. S., Choi, J. S., Na, M. K., Zhang, X. F., Ngoc, T. M., Lee, I. S. and Bae, K. H. (2007). Magnoflorine from *Coptidis rhizoma* Protects High Density Lipoprotein during Oxidant Stress. *Biological and Pharmaceutical Bulletein,* 30 (6), 1157 - 1160.

Hunskaar, H. S., Fasmer, O. B. and Hole, K. (1985). Formalin test in mice, a useful technique for evaluating mild analgesics. *Journal of Neuroscience Methods,* 14, 69 - 76.

Hutchings, A., Scott, A. H., Lewis, G. and Cunningham, A. (1996). *Clausena anisata* (Wild.) Hook. F. ex Benth. Zulu medicinal plants: An Inventory, Pietermaritzburg, South Africa, University of Natal Press, 153-154.

Irvine, F. R. (1961). *Woody Plants of Ghana,* London, Oxford University, 8-9.

Issekutz, C. A. and Issekutz, T. B. (1989). Quantization of blood cell accumulation and vascular responses in inflammatory reactions.New York, edn., Alan R. Liss, Inc.

Isshiki, K., Asai, Y., Tanaka, S., Nishio, M., Uchida, T., Okuda, T., Komatsubara, S. and Sakurai, N. (2001). Aurantiamide acetate, a selective cathepsin inhibitor, produced by *Aspergillus penicilloides*. *Bioscience, Biotechnology and Biochemistry,* 65 (5), 1195-1197.

Ito, C., Itoigawa, M., Aizawa, K., Yoshida, K., Ruangrungsi, N. and Furukawa, H. (2009). γ-lactone carbazoles from *Clausena anisata*. *Journal of Natural Products,* 72 (6)**,** 1202–1204.

Ito, C., Katsuno, S., Itoigawa, M., Ruangrungsi, N., Mukainaka, T., Okuda, M., Kitagawa, Y., Tokuda, H., Nishino, H. and Furukawa, H. (2000). New carbazole alkaloids from *Clausena anisata* with antitumor promoting activity. *Journal of Natural Products* 63 (1)**,** 125-128.

Ito, C., Katsuno, S., Ruangrungsi, N. and Furukawa, H. (1998). *Chemical and Pharmarceutical Bulletin,* 46, 344-346.

Iwata, H., Tezuka, Y., Kadota, S., Hiratsuka, A. and Watabe, T. (2005). Mechanism-based inactivation of human liver microsomal CYP3A4 by rutaecarpine and limonin, *Drug Metabolism and Pharmacokinetics,* 20 (1), 34 - 45.

Jana, S. (2003). Topical and Peripherally Acting Analgesics. *Pharmacological Reviews,* 55, 2.

Jash, S. S., Biswas, G. K., Bhattacharyya, S. K., Bhattacharyya, P., Chakraborty, A. and Chowdhury, B. K. (1992). Carbazole alkaloids from *Glycosmis pentaphylla. Phytochemistry,* 31 (7), 2503-2505.

Jensen, T. S. and Yaksh, T. L. (1986). Comparison of antinococeptive action of morphine in the periaqueductal gray, medial and puramedial medulla in rat. *Brain Research,* 363, 99 – 113.

Ji, H.-F. and Zhang, H.-Y. (2008). Multipotent natural agents to combat Alzheimer's disease. Functional spectrum and structural features. *Acta Pharmacologica Sinica,* 29, 143–151.

Jia-Quan, C., Ji-Guang, W., Chang - Chun, L., Yi - De, S., Yin - Quan, P., Ming - Ying, J., Tao, L. and Duan-Zheng, X. (1964). Pharmacological studies on magnoflorine, a hypontensive principle from Tu Qing Mu Xiang. *Acta Pharmaceutica Sinica,* 1964, 01.

Jinks, S., L., and Carstens, E. (1999). Activation of spinal wide dynamic range neurons by intracutaneous microinjection of nicotine. *Journal of Neurophysiology,* 82**,** 3046 – 3055.

Johnson, I. S., Armstrong, J. G., Gorman, M. and Burnett, J. P. (1963). The Vinca Alkaloids: A New Class of Oncolytic Agents. *Cancer Research,* 23, 1390 - 1427.

Joshi, B. S. Kamat, V. N Saksena, A. K. and Govindachari, T. R. (1967). Structure of heptaphylline, a carbazole alkaloid from *Clausena heptaphylla. Tetrahedron Letters*, 4019-4022.

Joshi, B. S., Kamat, V. N., Gawad D. H. and Govindachari, T. R. (1972). Structure and synthesis of heptaphyline. *Phytochemistry*, 11, 2065 - 2071.

Jossang, A., Leboeuf, M. and Cave, A. (1977). Alkaloids of *Enantia polycarpa* Engl. and Diels. *Planta Medica,* 32 (7), 249 - 257.

Kang, T. J., Lee, S. Y., Singh, R. P., Agarwal, R. and Yim, D. S. (2009). Anti-tumor activity of oxypeucedanin from *Ostericum koreanum* against human prostate carcinoma DU145 cells. *Acta Oncologica,* 48, 895 - 900.

Karim M. R. and Hashinaga F. (2001). Screenig and some properties of limonoid glucosyltransferase from selected citrus varieties. *Pakistan Journal of Biological Science,* 4, 486 - 483.

Karlsson, E. (1979). Chemistry of protein toxins in snake venoms. *In:* Lee, C. Y. (ed.) *Handbook of experimental pharmacology.* New - York: Springer-Verlag, 159 – 83.

Katz, W. A. and Rothenberg, R. (2005). The nature of pain pathophysiology. *Journal Clinical Rheumatology,* 3 (11), 11 - 15.

Keh-Shaw, C., Feng-Nien K., Che-Ming, T. and Yang-Chang, W. (1996). Antiplatelet and Vasorelaxing Actions of Some Aporphinoids. *Planta Medica* 62 (2), 133 - 136.

Kenechukwu, F. C., Mbah, C. J., Momoh, M. A., Chime, S. A., Umeyor, C. E. and Ogbonna, J. D. N. (2012). Pharmacological justification for the ethnomedical use of *Clausena anisata* root-bark extract in the management of epilepsy. *Journal of Applied Pharmaceutical Science,* 2 (9), 36 - 40.

Kidd, B. L. and Urban, L. A. (2001). Mechanism of infammatory pain. *British Journal of Anaesthesia,* 87 (1), 3.

Kim, Y. M., Haa, Y. M., Jin, Y. C., Shi, L. Y., Lee, Y. S., Kim, H. J., Seo, H. G., Choi, J. S., Kim, Y. S., Kang, S. S., Lee, J. H. and Chang, K. C. (2009). Palmatine from *Coptidis rhizoma* reduces ischemia–reperfusion-mediated acute myocardial injury in the rat. *Food and Chemical Toxicology,* 47, 2097 – 2102.

Kinghorn, A. D. (1994). The discovery of drugs from higher plants. *Biotechnology,* 26, 81 - 108.

Klayman, D. L., Lin, A. J., Acton, N., Scovill, J. P., Hoch, J. M., Milhous, W. K., Theoharides, A. D. and Dobek, A. S. (1984). Isolation of artemisinin (qinghaosu) from *Artemisia annua* growing in the United States. *Journal of Natural Products* 4, 715 - 717.

Komis, T. and Samuel, S. (2005). Tiotropium bromide; a new long acting bronchodilator for the treatment of chronic obstructive pulmonary disease. *Clinical Therapeutics,* 27 (4), 377 - 392.

Koster, R., Anderson, M. and De Beer, E. J. (1959). Acetic acid for analgesic screening *Federation Proceedings,* 18, 412–417.

Küpelia, E., Koşarb, M., Yeşilada, E., Hüs, K. and Başerb, C. (2002). A comparative study on the anti-inflammatory, antinociceptive and antipyretic effects of isoquinoline alkaloids from the roots of *Turkish Berberis species*. *Life Sciences,* 72 (6), 645 – 657.

Lakshmi, V., Prakash, D., Raj, K., Kapil, R. S. and Popli, S. P. (1984). Monoterpenoid furanocoumarin lactones from *Clausena anisata*, *Phytochemistry,* 23 (11), 2629 – 2631.

Lam, L. K. T., Li, Y. and Hasegawa, S. (1989). Effects of citrus limonoids on glutathione S-transferes activity in mice. *Journal of Agriculture and Food Chemistry,* 37, 878 - 880.

Lam, L. K. T., Zhang, J., Hasegawa, S. and Schut, H. A. J. 1994. Inhibition of chemically induced carcinogenesis by citrus limonoids. *In:* Huang, M. T., Osawa, T., Ho, C., T., & Rosen, R. T. (eds.) *Food phytochemicals for cancer prevention I,* Washington, DC: *Americal Chemical Society,* 209 - 219.

Lamberts, J. T., Jutkiewicz, E. M., Mortensen, R. M. and Traynor, J. R. (2011). Mu-opioid receptor coupling to gao plays an important role in opioid antinociception. *Neuropsycho Pharmacology,* 36, 2041 – 2053.

Laube, H. (2013). Acarbose. *Clinical Drug Investigation,* 33 (4), 1 - 4.

Lee, J. W., Mase, N., Yonezawa, T., Seo, H. J., Jeon, W. B., Cha, B. Y., Nagai, K. and Woo, J. T. (2010a). Palmatine attenuates osteoclast differentiation and function through inhibition of receptor activator of nuclear factor-kB ligand expression in osteoblast cells. *Biological and Pharmaceutical Bulletin,* 33 (10), 1733 - 1739.

Lee, S. S., Kim, H. O. and Lee, M. K. (1999). Inhibition of monoamine oxidase by palmatine. *Archives of Pharmacal Research,* 22 (5), 529 - 531.

Lee, W., Kim, J., Kang, J., Oh, W., Jung, J., Kim, Y. S., Jung, H. A., Choi, J. S. and Lee, S. (2010b). Palmatine attenuates D-galactosamine/lipopolysaccharide-induced fulminant hepatic failure in mice. *Food and Chemical Toxicology,* 48, 222 – 228.

Levine, J. D., Fields, H. L. and Basbaum, A. I. (1993). Peptides and the primary afferent nociceptor. *Journal of Neuroscience,* 13, 2273 - 2286.

Levrier, C., Balastrier, M., Beattie, K. D., Carroll, A. R., Martin, F., Choomuenwai, V. and Davis, R. A. (2013). Pyridocoumarin, aristolactam and aporphine alkaloids from the Australian rainforest plant *Goniothalamus australis. Phytochemistry,* 86, 121-126.

Li, J. W. and Vederas, J. C. (2009). Drug discovery and natural products: end of an era or an endless frontier? *Science,* 325 (161) 161 - 165.

Liang, Y., Liu, D., Hung, L., Lin, P., Chen, N. and Chen, Y. (2012). *Hypoclycemic activity of osthole*. United States, US 8, 198, 320 B2 patent application.

Light, A. R. and Perl, E. R. (1979). Reexamination of the dorsal root projection to the spinal dorsal horn including observations on the differential termination of coarse and fine fibers. *Journal of Complementary Neurology,* 186**,** 117-131.

Light, A. R. and Perl, E. R., J. (1979). Spinal termination of functionally identified primary afferent neurons with slowly conducting myelinated fibers. *Journal of Complementary Neurology,* 186, 133-50.

Light, A. R., Trevino, D. L. and Perl, E. R. (1979). Morphological features of functionally defined neurons in the marginal zone and substantia gelatinosa of the spinal dorsal horn. *Journal of Comp Neurology,* 186, 151-171.

Lim, L., Suhler, E. B. and Smith, J. R. (2006). Biologic therapies for inflammatory eye disease. *Clinical and Experemental Ophthalmology,* 34 (4)**,** 365 - 374.

Lineberry, C. G. (1981). Laboratory animals in pain research, in Methods in animal experimentation. New York, *Academic Press,* 6, 237 - 311.

Liu, J., Lee, J., Hernandez, M. A. S., Mazitschek, R. and Ozcan U. (2015). Treatment of Obesity with Celastrol. *Cell Press,* 161, 999 - 1011.

Liu, X., Hu, Z., Shi, Q., Zeng, H., Shen, Y., Jin, H. and Zang, W. (2010). Anti-inflammatory and antinociceptive compounds from *Tinospora sagittata* (Olive) Gagnep. *Archives of Pharmacal Research,* 33 (7), 981 - 987.

Loeser, J. D., Butler, S. H., Chapman, C. R. and Turk, K. C. (eds.) (2001). Bonica's management of pain, Philadelphia: Lippincott.

Lomovskaya, N., Otten, S. L., Doi-Katayama, Y., Fonstein, L., Liu, X. L., Takatsu, T., Inventi-Solari, A., Filippini, S., Torti, F., Colombo, A. L. and Hutchinson, C. R. (1999). Doxorubicin overproduction in Streptomyces peucetius: cloning and characterization of the dnrU ketoreductase and dnrV genes and the doxA cytochrome P-450 hydroxylase gene. *Journal of Bacteriology,* 181 (1), 305 - 318.

Lopez-Lazaro, M., Pastor, N., Azrak, S. S., Ayesu, M. J., Austin, C. A. and Cortes, F. (2005). Digitoxin inhibits the growth of cancer cell lines at concentrations commonly found in cardiac patients. *Journal of Natural Products,* 68 (11), 1642 - 1645.

Loux, J. J., Smith, S. and Salem, H. (1978). Comparative analgesic testing of various compounds in mice using writhing techniques. *Arzneim Forsch,* 28, 1644 - 1647.

Luoa, T., Zhangb, H., Zhangc, W.-W., Huanga, J.-T., Songd, E.-L., Chena, S. G., Hee, F., Xua, J. & Wang, H. Q. (2011). Neuroprotective effect of Jatrorrhizine on hydrogen peroxide-induced cell injury and its potential mechanisms in PC12 cells. *Neuroscience Letters,* 498 (3) 227- 231.

Luszczki, J. J., Wojda, E., Andres-Mach, M., Cisowski, W., Glensk, M., Glowniak, K. and Czuczwar, S. J. (2009). Anticonvulsant and acute neurotoxic effects of imperatorin, osthole and valproate in the maximal electroshock seizure and chimney tests in mice: A comparative study. *Epilepsy Research,* 85 (2-3), 293 - 299.

Malan, D. F. and Neuba, D. F. R. (2011). Traditional Practices and Medicinal Plants Use during Pregnancy by Anyi-Ndenye Women (Eastern Côte d'Ivoire). *Africa Journal of Reproductive Health,* 15 (1), 85 - 93.

Malebo, M. H., Wenzler, T., Cal, M., Swaleh, S. M., Omolo, O. M., Hassanali, A., Séquin, U., Häussinger, D., Dalsgaard, P., Hamburger, M., Brun, R. and Ndiege, I. O. (2013). Anti-protozoal activity of aporphine and protoberberine alkaloids from *Annickia kummeriae (*Engl and Diels) Setten and Mass (Annonaceae). *BMC Complementary and Alternative Medicine* 13 (48), 1473 - 6882.

Maneerat, W., Prawat, U., Saewanc, N. and Laphookhieo, S. (2010). New Coumarins from *Clausena lansium* Twigs. *Journal of Brazilian Chemical. Society.,* 21 (4), 665 - 668.

Matsuda, H., Yoshikawa, M., Linuma, M. and Kubo, M. (1998). Antinociceptive and anti-inflammatory activities of limonin isolated from the fruits of *Evodia rutaecarpa* var. bodinieri, *Planta Medica,* 64 (4) 339 - 342.

Mccurdy, C. R. and Scully, S. S. (2005). Analgesic substances derived from natural products (natureceuticals). *Life Sciences,* 78 (5)**,** 476–484.

Mcdonald, J. and Lambert, D. G. (2005). Opioid receptors. Continuing Education in Anaesthesia, *Critical Care and Pain,* 5 (1), 22 - 25.

Mcgivern, J. G. (2007). Ziconotide: a review of its pharmacology and use in the treatment of pain. *Neuropsychiatric Disease and Treatment,* 3 (1) 69 – 85.

Meimei, B., Zhifei, C., Di, Y., Shilong, F., Gaochuan, Z., Ping, Y., Yanyan, P., Bo, Y., Hongyan, H. and Quansheng, Z. (2012). Columbamine suppresses the proliferation and neovascularization of metastatic osteosarcoma U2OS cells with low cytotoxicity. *Toxicology Letters,* 215 (3)**,** 174 – 180.

Mester, I. and Reisch, J. (1977). Constituents of *Clausena anisata* (Willd.) Oliv. (Rutaceae), Isolation and structure of mupamine, a new carbazole alkaloid. Justus Liebigs Ann. *Chemie*, 1725 - 1729.

Misik, V., Bezáková, L., Malekova, L. and Kostalova, D. (1995). Lipoxygenase inhibition and antioxidant properties of protoberberine and aporphine alkaloids isolated from *Mahonia aquifolium, Planta Medica*, 61 (4), 372 - 373.

Miskia, M., Shena, X., Coopera, R., Gillumb, A. M., Fisherc, D. K., Millerc, R. W. and Higginsc, T. J. (1995). Aporphine alkaloids, CD45 protein tyrosine phosphatase inhibitors, from *Rollinia ulei*. *Bioorganic and Medicinal Chemistry Letters*, 5 (14), 1519 - 1522.

Mitul, P., Murugananthan and Shivalinge G. K. P. (2012). *In vivo* animal models in preclinical evaluation of anti-inflammatory activity - a review. *International Journal of Pharmaceutical Research and Allied Science*, 1 (2), 1 - 5.

Mitul P., Murugananthan & Shivalinge G. K. P. (2012). *In vivo* animal models in preclinical evaluation of anti-inflammatory activity-a review. *International Journal of Pharmaceutical Research and Allied Science*, 1 (2), 1 - 5.

Mogil, J. S., Davis, K. D. and Derbyshire, S. W. (2010). The necessity of animal models in pain research. *Pain*, 151, 12 - 17.

Montenegro, H., Gutierrez, M., Romero, L. L., Ortega - Barna, E., Capson, T. L. and Rios, L. C. (2003). Aporphine alkaloids from *Guatteria spp* with leishminicidal activity. *Planta Medica*, 69, 677 - 679.

Moshi, M. J., Kagashe, G. A. and Mbwambo, Z. H. (2005). Plants used to treat epilepsy by Tanzanian traditional healers. *Journal of Ethnopharmacology*, 97 (2), 327 - 363.

Moss, S. F. and Blaser, M. J. (2005). Mechanisms of Disease: inflammation and the origins of cancer. *Clinical Practice Oncology*, 2 (2).

Mshana , N. R., Abbiw, D. K., Addae-Mensah, I., Adjanouhoun, E., Ahyi, M. R. A., Ekpere, J. A., Enow-Orock, E. G., Gbile, Z. O., Noamesi, G. K., Odei, M. A., Odunlami, H., Oteng-Yeboah, A. A., Sarpong, K., Soforowa, A. and Tackie, A. N. (2000). *Traditional Medicine and Pharmacopoiea: Contribution to the Revision of Ethnobotanical and Floristic Studies in Ghana*, Organisation of Africa Unity/Scientific, Technical and Reseach Commission (OAU/STRC), 535.

Mukherjee, D., Nissen, S. E. and Topol, E. J. (2001). Risk of cardiovascular events associated with selective COX - 2 inhibitors. *JAMA: The Journal of America Medical Association*, 286 (8), 954 - 959.

Muller, M. Byres, M. Jaspars, M. Kumarasahy, Y. Middleton, M. Nahar, L. Shoed, M. Sarker, S. D. (2004). 2D NMR spectroscopic analyses of archangelicin from the seeds of *Angelica archangelica. Acta Pharmaceutica,* 54, 277–285.

Nakatani, M., Ishiba, K., Tsunao, K. and Hase, T. (1991). Coumarins and triterpenes from *Skimmia japonica* Thunb. *Repositry of Faculty of Science, Kagoshima University (Mathematics, Physics and Chemistry),* 24, 81 - 86.

Neuwinger, H. D. (1998). Alkaloids in Arrow Poisons, Roberts and Winks (eds.), New York, *Plenum Press*, 45 - 84.

Newman, D. J. (2008). Natural products as leads to potential drugs: an old process or the new hope for drug discovery? *Journal of Medicinal Chemistry,* 51, 2589 – 2599.

Newman, D. J. and Cragg, G. M. (2004). Advanced preclinical and clinical trials of natural products and related compounds from marine sources. *Current Medicinal Chemistry,* 11 (13), 1693 - 1713.

Ng, T. B., Liu, F. and Wang, Z. T. (2000). Antioxidative activity of natural products from plants. *Life Sciences,* 66 (8), 709 - 723.

Ngadjui, B. T., Ayafor, J. F., Sondengam, B. L. and Connolly, D. J. (1989a). Coumarins from *Clausena anisata*. *Phytochemistry*, 28 (2), 585 - 589.

Ngadjui, B. T., Ayafor, J. F., Sondengam, B. L. and Connolly, D. J. (1989b). Limonoids from *Clausena anisata*. *Journal of Natural Products,* 52 (4), 832 - 836.

Ngadjui, B. T., Ayafor, J. F., Sondengam, B. L. and Connolly, D. J. (1989c). Prenylated coumarins from the leaves of *Clausena anisata*. *Journal of Natural Products,* 52, (2), 243 - 247.

Ngadjui, B. T., Ayafor, J. F., Sondengam, B. L. and Connolly, D. J. (1989d). Quinolone and carbazole alkaloids from *Clausena anisata*. *Phytochemistry,* 28 (5), 1517 – .

Niemegeers, C. J., Van Bruggen, J. A. and Janssen, P. A. (1975). Suprofen, a potent antagonist of acetic acid-induced writhing in rats. *Arzneim Forsch,* 25, 1505 - 1509.

O'callaghan, J. P. and Holzman, S. G. (1975). Quantification of the analgesic activity of narcotic antagonists by a modified hot plate procedure. *Journal of Pharmacology and Experimental Therapeutics,* 192, 497 – 505.

OECD/OCDE. (2001). Guideline for testing of chemicals; Acute oral toxicity – fixed dose procedure No. 420, 1 - 14.

Oh, H., Lee, H. S., Kim, T. W., Chai, K. Y., Chung, H. T., Kwon T. O., Jun, Y. J., Jeong, O. S., Kim, Y. S., Yun, Y. G., (2002). Furocoumarins from *Angelica dahurica* with

hepatoprotective activity on tacrine-induced cytotoxicity in Hep G2 cells. *Planta Medica*, 463 - 464.

Ojewole, J. A. (2002). Hypoglycaemic effect of *Clausena anisata* (Willd.) Hook methanolic root extract in rats. *Journal of Ethnopharmacology*, 81, 2**,** 231-237.

Okokon, J. E., Antia, B. S. and Umoh, E. (2008). Analgesic and anti-inflammatory effects of ethanolic root extract of Hippocratea. *Africana International Journal of Pharmacology,* 4, 51-55.

Okokon, J. E., Udoh, A. E., Andrew, U. E. and Amazu, L. U. (2012). Antiinflammatory and antipyretic activities of *Clausena anisata*. *Molecular and Clinical Pharmacology* 3,1, 47-54.

Okorie, D. A. (1975). A new carbazole alkaloid and coumarins from rootsof *Clausena anisata Phytochemistry,* 14, 2720

Okunade, A. L. (1987). Estragole: An acute toxic principle from the volatile oil of the leaves of *Clausena anisata*. *Journal of Natural Products,* 50 (5), 990 - 991.

Patwardhan, B., Ashok, D. B., Vaidya A. D. B., Chorghade, M., and Joshi S. P., (2008) Reverse pharmacology and systems approaches for drug discovery and development. *Current Bioactive Compounds, 4,* 201 - 212.

Paulo Mde, Q., Barbosa-Filho, J. M., Lima, E. O., Maia, R. F., Barbosa Rde, C. and Kaplan, M. A. (1992). Antimicrobial activity of benzylisoquinoline alkaloids from *Annona salzmanii* D.C. *Journal of Ethnopharmacology*, 36 (1), 39 - 41.

Paxinos, G. and Watson, C. (1986). The rat brain in stereotaxic coordinates, New York, Academic Press, 2nd edition.

Pearl, J., Aceto, M. D. and Harris, L. S. (1968). Prevention of writhing and other effects of narcotics and narcotic antagonists in mice. *Journal of Pharmacology and Experimental Therapy*, 160, 217 - 230.

Pedigo, N. W., Dewey, W. L. and Harris, L. S. (1975) Determination and characterization of the antinociceptive activity of intraventricularly administered acetylcholine in mice. *Journal of Pharmacology and Experimental Therapy* 193, 845 – 52.

Perez, G. R. M. (2001). Anti-Inflammatory activity of compounds isolated from plants. *The Scientific World,* 1, 713 - 784.

Philipsa, R. E., Warrell, D. A., White, N. J., Loomwn, S. and Karbwang, J. (1985). Intravenous quinidine for the treatment of severe faciparum malaria: clinical and pharmacokinetics studies. *New England Journal of Medicine,* 312, 1273 - 1278.

Phillips, R. E., Looareesuwan, S., White, N. J., Chanthavanich, P., Karbwang, J., Supanaranand, W., Turner, R. C. and Warrell, D. A. (1986). Hypoglycaemia and antimalarial drugs: quinidine and release of insulin. *British Medical Journal,* 292, 1319 - 1321.

Phuwapraisirisan, P., Surapinit, S. and Tip-Pyang, S. (2006). A novel furanocoumarin from *Feroniella lucida* exerts protective effect against lipid peroxidation. *Phytotherapy Research,* 20, 708 - 710.

Poulose, S. M., Harris, E. D. and Patil, B. S. (2006). Antiproliferative effects of citrus limonoids against human neuroblastoma and colonic adenocarcinoma cells. *Nutrition and Cancer,* 56, 103 - 112.

Prommer, E. (2007). "Levorphanol: the forgotten opioid " *Supportive Care in Cancer,* 15 (3), 259 – 264.

Pujol, J. (1990). Natur Africa: The herbalist handbook, Durban, Jean Pujol Natural Healers Foundation.

Qishen, L., Zhizu, Zhu, S., Li, Z., Rongbiao, P., Rende, X., Ying, H. and Xinyong, Z. (1996). Studies on the anti-arrhythmic effect of xanthotoxol in experimental animals. *Europe PubMed Central; Chinese Traditional and Herbal Drugs* 27 (6), 347 - 349.

Qishen, L., Zhizu, Z., Xiao, H., Li, Z., Heyang, Y., Wei, H. and Zunping, Z. (1998). Studies on the Anti-inflammatory Effect of Xanthotoxol in Experimental Animals. *Europe PubMed Central-Chinese Traditional and Herbal Drugs* 29 (2), 102 - 104.

Qu, Y., Liu, M., Wu, Z., Gao, H., Sun, B., Su, Q. and Wu, L. (2007). 2, 3, 9, 10-tetraoxygenated protoberberine alkaloids from *Corydalis yanhusuo* W. T. Wang. *Asian Journal of Traditional Medicines,* 2 (2), 61 - 65.

Rang, H. P. and Dale, M. M. (1987). Phamacology, Singapore, *Longman Group U.K. Ltd.*, 4 - 610.

Rates, S. M. K. (2001). Plants as source of drugs. *Toxicon,* 39, 603 – 613.

Ravi, S. K., Vasantha, P. S. and Janardhan, R. K. (2012). Studies on mosquito larvicidal activity of *Chloroxylon swietenia* DC. *Journal of Pharmacognosy,* 3 (2), 123 - 125.

Razavi, S. M., Zahri, S., Motamed, Z. and Ghasemi, G. (2010). Bioscreening of oxypeucedanin, a known furanocoumarin. *Iranian Journal of Basic Medical Sciences,* 13 (3), 133 - 138.

Razdan, T. K., Kachroo, V., Harkar, S. and Koul, G. L. (1982). Furanocoumarins from *Heracleum canescens*. *Phytochemistry,* 21 (4), 923 - 927

Ringman, J. M., Fraustchy, S. A., Teng, E., Begum, A. N., Bardens, J., Beigi, M., Gylys, K. H., Heath, D. D., Badmaev, G., Apostolova, L. A., Porter, V., Vanek, Z., Marshall, G. A., Hellemann, G., Sugar, C., Masterman, D. L., Montine, T. J., Cummings, J., L., and Cole,

G. M. (2012). Oral curcumin for Alzheier's disease: tolerability and efficacy in a 24-week randomized, double-blind placebo controlled study. *Alzheimer's Research and Theraphy,* 4, 1 - 8.

Robbins and Cortran (2004). Acute and chronic inflammation. Pathologic Basis of Disease. *Elsevier Publication,* Ed 7, 47 - 87.

Roberts, M. F. and Wink, M. (1998). Biochemistry, ecology, and medicinal applications. *In:* Roberts, M. F. and Wink, M. (eds.) *Alkaloids.* New York, London: Plenum Press.

Rong-Jyh, L., Mei-Hsuan, W., Yi-Hsuan, M., Li-Yu, C., Chung-Yi, C. and Chuan-Min, Y. (2014). Anthelmintic activities of aporphine from *Nelumbo nucifera* Gaertn. cv. Rosa-plena against *Hymenolepis nana*. *International Journal of Molecular Sciences,* 15, 3624 - 3639.

Rosenthal, P. J. (2003). Review: Antimalarial drug discovery: old and new approaches. *Journal of Experemental Biology,* 206, 3735-3741.

Roy, A. and Saraf, S. (2006). Limonoids: Overview of significant bioactive triterpenes distributed in plants kingdom. *Biological and Pharmaceutical Bulletin,* 29 (2), 191 - 201.

Ruberto, G., Renda, A., Tringali, C., Napoli, E. M. and Simmonds, M. S. (2002). Citrus limonoids and their semisynthetic derivatives as antifeedant agents against *Spodoptera frugiperda* larvae. A structure-activity relationship study, *Journal of Agriculture and Food Chemistry,* 50, 6766 - 6774.

Sajjadi, S.E., Zeinvand, H. and Shokoohinia, Y. (2009). Isolation and identification of osthol from the fruits and essential oil composition of the leaves of *Prangos asperula* Boiss. *Research in Pharmaceutical Sciences,* 4 (1), 19 - 23.

Samuelsson, G. (1999). Drugs of natural origin: A Textbook of Pharmacognosy, Stockholm, Sweden, *Swedish Pharmaceutical Press*, 4.

Sarker, S. D., Latif, Z. and Gray, A. I. (2006a). Methods in biotechnology; natural products isolation. *In:* Sarker, S. D., Latif, Z. and Gray, A. I. (eds.), Natural Products Isolation, An Overview. Totowa; NJ: *Humana Press Inc.* 1 - 500.

Sarker, S. D., Latif, Z. and Gray, A. I. (2006b). Super critical fluid extraction *In:* Nahar, L. and Sarker, S. D. (eds.) Methods in Biotechnology; Natural Products Isolation. Totowa; NJ: *Humana Press Inc*. 20 (2), 63 - 74.

Sarulkah, A., Sarda, S. P., Ghaisas, M. M., Thakare, V. N. and Deshpande, A. V. (2008). In vivo animal models for evaluation of anti-inflammatory activity. *Pharmaceutical Informations; Latest Reviews available on line at Pharmainfo.net,* 6 (2).

Sawynok, J. (2003). Topical and peripherally acting analgesics. *Pharmacological Reviews,* 55, 2.

Schimmer, B. P. and Parker, K. L. (2001). Adrenocorticotropic hormone; adrenocortical steroids and their synthetic analogs; Inhibitors of the synthesis and actions of adrenocortical hormones., (eds)., Hardman, J. G., Limbird, I. E., Gilman, A. G., Goodmanof and Gilmans The pharmacological basis of therapeutics, Vol. 10, USA, McGraw, 1649 - 1677.

Schmid, B., Kotter, I. and Heide, I. (2001). Pharmacokinetics of salicine after oral administration of a standardized willow bark extract. *European Journal of Clinical Pharmacology*, 57**,** 387 - 391.

Selim, Y. A. and Ouf, N. H. (2012). Anti-inflammatory new coumarin from the *Ammi majus* L. *Organic and Medicinal Chemistry Letters*, 2 (1), 2 - 4.

Serhan, C. N. and Savill, J. (2005). Resolution of inflammation: the beginning programs the end *Nature, Immunology*, 6, 1191 − 1197.

Sethi, O. P., Anandb, K. K. and Gulati, O. D. (1992). Evaluation of xanthotoxol for central nervous system activity. *Journal of Ethnopharmacology*, 36 (3), 239 - 247.

Shah, B. N., Nayak, B. S., Seth, A. K., Jalalpure, S. S., Patel, K. N., Patel, M. A., and Mishra, A. D. (2006). Search for medicinal plants as source of anti-inflammatory and anti-arthritic agents. A review. *Pharmacognosy Magazine*, 2, 77 - 86.

Shi, G.-N., Liu, Y.-L., Lin, H.-M., Yang, S.-L., Feng, Y.-L., Reid, P. F. and Qin, Z.-H. (2011). Involvement of cholinergic system in suppression of formalin-induced inflammatory pain by cobratoxin. *Acta Pharmacologica Sinica*, 32, 1233 – 1238.

Siegmund, E., Cadmus, R. and Lu, G. (1957). A method for evaluating both non-narcotic and narcotic analgesics. *Proceedings of the Society of Experimental Biology and Medicine*, 95, 729 - 731.

Singh, J. A., Wells, G. A., Christensen, R., Tanjong Ghogomu, E., Maxwell, L., Macdonald, J. K., Filippini, G., Skoetz, N., Francis, D. K., Lopes, L. C., Guyatt, G. H., Schmitt, J., La Mantia, L., Weberschock, T., Roos, J. F., Siebert, H., Hershan, S., Cameron, C., Lunn, M. P. T., Tugwell, P. and Buchbinder, R. (2011). Adverse effects of biologics: a network meta-analysis and Cochrane overview. *Cochrane Database of Systematic Reviews*, 2, 1 - 82.

Singh, S. B., Kumar, S., Dewan, S. and Kumar, V. L. (2000). Inflammation induced by latex of *Calotropis procera* - a new model to evaluate anti-inflammatory drugs. *Journal of Pharmacological and Toxicological Methods*, 43, 219 - 224.

Singh, A., Singh, S., Kesherwani, M., Singh, T. D., Singh, V. P., Pandey, V. B. and Singh, U. P. (2010). Jatrorrhizine and columbamine alkaloids isolated from *Argemonemexicana* are inhibitory to spore germination of some plant pathogenic fungi. *Archives of Phytopathology and Plant Protection*, 43 (15), 1450 - 1453.

Slotkin, T. A. (1974). Piosons of Plant Origin, *Spriger*, 1 - 60

Smith, M. T., Cabot, P. J., Ross, F. B., Robertson, A. D. and Lewis, R. J. (2002). The novel N-type calcium channel blocker, AM336, produces potent dose-depended antinociception after intrathecal dosing in rats and inhibits substance P release in rats spinal cord slices. *Pain*. 96: 119 - 127

Sneader, W. (1985). Drug discovery*:* The evolution of modern medicines, New York, Wiley.

Sneader, W. (ed.) (2005). Drug discorvery: a history John Wiley and Sons Ltd.

Songue, J., L.,, Kouman, Dongo, E., Mpondo, T. N. and White, R. L. (2012). Chemical constituents from stem bark and roots of *Clausena anisata*. *Molecules*, 17, 13673-13686.

Spector, W. G. (1960). The inflammation response. *Journal of Pathology of Bacteria*, 84, 391-403.

Spitzer, C., Barnow, S., Volzke, H., Wallaschofski, H., John, U. and Freyberger Hj *etal*. (2010). Association of posttraumatic stress disorder with low-grade elevation of C-reactive protein: evidence from the general population. *Journal of Psychiatric Research*, 15 – 21.

Steck, W. and Bailey, B. K. (1969). Leaf coumarins of *Angelica archangelical*. *Canadian Journal of Chemistry*, 47, 2425 - 2429.

Steen, K. H. and Reeh, P. W. (1993). Actions of cholinergic agonists and antagonists on sensory nerve endings in rat skin in vitro. *Journal of neurophysiology*, 70, 397 – 405.

Strand, V., Kimberly, R. and Isaacs, J. D. (2007). Biologics therapy in rheumatology: lessons learned, future directions. *Nature reiews; drug discovery*, 6 (1), 75 - 92.

Stucky, C. L., Gold, M. S. and Zhan, X. (2001). Mechanisms of pain. *Proceedings of the National Academy of Sciences*, 98 (21), 11845 – 11846.

Sua, M. R., Silva, V. and Valpuesta, M. (1993). Quaternary protoberberine alkaloids from *Ceratocapnos heterocarpa*. *Phytochemistry*, 34 (2), 559 - 561.

Suckling, C. J. (1991). Chemical approaches to the discovery of new drugs. *Science Progress*, 75, 323 - 359.

Sunthitikawinsakul, A., Kongkathip, N., Kongkathip, B., Phonnakhu, S., Daly, J. W., Spande, T. F., Nimit, Y., Napaswat, C., Kasisit, J. and Yoosook, C. (2003). Anti-HIV-1 limonoid: first isolation from *Clausena excavata*. *Phytotherapy Research*, 17 (9) 1101 - 1103.

Swingle, R. W. (1974). Evaluation for antiinflammatory activity. Anti-inflammatory Agents: Chemistry and Pharmacology,. *In:* Scherer, R. A. and Whitehouse, M. W. (eds.). New York: Academic Press, 34 – 122.

Syam, M., Siddig I. A., Shiau-Chuen C., Mohd, A. S., Suvitha, S., Noorasyikin, S. and Mohd R. (2013). Apoptosis effect of girinimbine isolated from *Murraya koenigii* on lung cancer cells in vitro. *Hindawi-Evidence-Based Complementary and Alternative Medicine,* 2013, 12 pages.

Takahara, A., Koganei, H., Takeda, T., Iwata, S. (2002). Anti-sympathetic and hemodynamic properties of a dual L/N type Ca^{2+} blocker channel blocker cilnidipine in rats. *European Journal of Pharmacology,* 434: 43 - 47.

Tamokou, J. D., Mpetga, D. J. S., Lunga, P. K., Tene, M., Tane, P. and Kuiate, J. R. (2012). Antioxidant and antimicrobial activities of ethyl acetate extract, fractions and compounds from stem bark of *Albizia adianthifolia* (Mimosoideae). *BMC Complementary and Alternative Medicine,* 99.

Tanahashi, T., Su, Y., Nagakura, N. and Nayeshiro, H. (2000). Quaternary isoquinoline alkaloids from *Stephania cepharantha*. *Chemical and Pharmaceutical Bulletin,* 48 (3), 370 - 373

Tanaka, A., Maeda, M., Kohno, A., Murakami, M., Kagami, S., Miyake, M. and Wada, K. (2000). inhibition of azoxymethane-induced colon carcinogenesis in male F344 rats by citrus limonoids abacunone and limonin. *Carcinogenesis,* 22 (1), 193 - 198.

Tata, A. M., Vilaro, M., T., and Mengod, G. (2000). Muscarinic receptor subtype expression in rat and chick dorsal root ganglia. *Molecular Brain Research,* 82, 1 - 10.

Tringali, C., Spataforaa, C., Calìa, V., Simmondsb, M. S. J. and Tringali, C. (2001). Antifeedant constituents from *Fagara macrophylla*. *Fitoterapia,* 72 (5), 538 - 543.

Tsassi, V. B., Hussain, H. and Meffo B. Y., Kouam S. F., Dango, E., Schuzl, B., Greene, I. R., and Krohn, K. (2010). Antimicrobial coumarins from the stem bark of *Afraegle paniculata*. *Natural Product Communication,* 5, 559 - 561.

Tzong-Cherng, C., Shoei-Sheng, L. and Ming-Jai, S. (2006). Antihyperglycemic Effect of Aporphines and their Derivatives in Normal and Diabetic Rats. *Planta Medica,* 72 (13), 1175 - 1180.

Ubeda, A., Montesinos, C., Paya, M., Terencio, C. and Alcaraz, M. J. (1993). Antioxidant action of benzylisoquinoline alkaloids. *Free Radical Research Communications,* 18, 167 - 175.

Uwaifo, A. O. (1984). The mutagenicities of seven coumarin derivatives and a furan derivative (nimbolide) isolated from three medicinal plants. *Journal of Toxicology and Environmental Health* 13, 521 - 530.

Van Der Wende, C. and Margolin, S. (1956). Analgesic tests based upon experimentally induced acute abdominal pain in rats. *Federal Proceedings*, 15, 494.

Vane, J. and Botting, R. (1987). Inflammation and the mechanism of action of anti-inflammatory drugs. *The Fedaration of America Societies of Experimental Biology Journal,* 1, 89 - 96.

Vane, J. R. (1982). Adventures and excursions in bioassay: the stepping stones to prostacyclin. In Les Prix Nobel: Nobel Prizes, Presentations, Biographies and Lectures *Stockholm: Almqvist and Wiksell*, 181 – 206.

Vasudeva, M., Gunnam, K. K. and Parle, M. (2007). Anti-inflammatory and antiniciceptive effects of *Thespesia populenea* bark extract. *Journal of Ethnopharmacology,* 109 (2), 264 - 270.

Vieira, P. C., Mafezoli, J., Pupo, M. T., Fernandes, J. B., Fátima Das Da Silva, M. G. F., Sérgio De Albuquerque, Oliva, G. and Pavão, F. (2001). Strategies for the isolation and identification of trypanocidal compounds from the Rutales. *Pure and Applied Chemistry*, 73 (3), 617 – 622.

Villar, A., M., , Rios, J. L., Canton, E. and Gobernado, M. (1987). Antimicrobial activity of benzylisoquinoline alkaloids. *Die Pharmazie* 42 (4), 248 - 250

Vogel, H. G. and Vogel, W. H. (1997). Drug Discovery and Evaluation, Pharmacological Assays, Berlin, *Springer*, 402 – 403.

Volleková, A., Košt'álová, D., Kettmann, V. and Tóth, J. (2003). Antifungal activity of Mahonia aquifolium extract and its major protoberberine alkaloids. *Phytotherapy Research,* 17 (7), 834 - 837.

Vyklicky. L. (1979). Techniques for the study of pain in animals, in Advances in pain research and therapy (eds. Bonica JJ, Liebeskind JC, and Albe-Fessard DG) (3), New York, Raven Press.

Wall, M. E., Wani, M. C., Manikumar, G., Hughes, T. J., Taylor, H., Mcgivney R. and Warner, J. (1988). Plant antimutagenic agents, 3. Coumarins. *Journal of Natural Products,* 51, 1148 - 1152.

Wang, C. M., Zhou, W., Li, C. X., Chen, H., Shi, Z. Q. and Fan, Y. J. (2009). Efficacy of osthol, a potent coumarin compound, in controlling powdery mildew caused by *Sphaerotheca fuliginea*. *Asian Journal of Natural Products Research,* 11 (9), 783 - 791.

Wang, L. X. and Wang, Z. J. (2003). Animal and cellular models of chronic pain. *Advanced Drug Delivery Reviews,* 55, 949 - 965.

Wang, R., Yan, H. and Tang, X. C. (2006). Progress in studies of huperzine A, a natural cholinesterase inhibitor from Chinese herbal medicine. *Acta Pharmacological Sinica,* 27, 1 - 26.

Wang, Y., Lu, J.-J., He, L. and Yu, Q. (2011). Triptolide (TPL) inhibits global transcription by inducing proteasome-dependent degradation of RNA polymerase II (Pol II). *Plos One,* 9, 23993.

Weiss, U. (2008). Inflammation. *Nature*, 454, 427.

Wen, Q., Yu, G., Li, Y., Yan, L. and Gong, Z. (2011). Pharmacological mechanisms underlying the antinociceptive and tolerance effects of the 6,14-bridged oripavine compound 030418. *Acta Pharmacologica Sinica*, 32, 1215 – 1224.

WHO, (2005). WHO Model List of Essential Medicines. [Accessed online -12 - 3 - 2006].

Winter, C. A., Riselay, E. A. and Nuss, G. W. (1962). Carrageenan induced oedema in the hind paw of the rats as an assay for anti-inflammatory drugs. *Proceedings of the Society for Experimental Biology and Medicine*, 111, 544 - 547.

Wisanu, M., Uma P., Nisakorn S. and Surat L. (2010). New Coumarins from *Clausena lansium* Twigs. *Journal of the Brazilian Chemical Society*, 21 (4), 665 - 668.

Woolfe, G. and Macdonald, A. L. (1944). The evaluation of the analgesic action of pethidine hydrochloride (Demerol). *Journal of Pharmacology and Experimental Therapuetics*, 80, 300 - 307.

Wright, C. E., Robertson, A. D., Whorlow, S. L. and Angus, J. A.. (2000). Cardiovascular and autonomic effects of omega-conotoxin MVIIA and CVID in conscious rabbits and isolated tissue assays. *British Journal of Pharmacology*, 131(7), 325 - 1336.

Wu, T. S., Chan, Y. Y., Liou, M. J., Lin, F. W., L.-S. Shi, L. S. and Chen, K. T. (1998). Platelet aggregation inhibitor from *Murraya euchrestifolia. Phytotherapy Research*, 12, S80 - 82.

Wu, T. S. and Huang, S. C. (1992). Alkaloidal and other constituents from the root bark of *Clausena excavata* . *Chemical and Pharmaceutical Bulletin*, 1069.

Wu, T. S., Huang, S. C., Wu, P. L. and Teng, C. M. (1996). Carbazole alkaloids from *Clausena excavata* and their biological activities. *Phytochemistry*, 133.

Xiao, H., Xianghua, H., Fei, L., Qing, Z. and Qishen, L. (2006). Studies on antitussive,antiasthmatic and expectorant action of xanthotoxol. *Pharmacology and Clinics of Chinese Materia Medica* Z1.

Ya-Fei, K., Chi-Ming, L., Chiu-Li, K. and Chung-Yi, C. (2014). Antioxidant and anticancer constituents from the leaves of *Liriodendron tulipifera*. *Molecules*, 19, 4234 - 4245.

Yacoubian, S. and Serhan, C. N. (2007). New endogenous anti-inflammatory and proresolving lipid mediators: implications for rheumatic diseases. *Nature Clinical Practice-Rheumatology*, 3 (10), 570 - 579.

Yang, D., Gu, T., Wang, T., Tang, Q. and Ma, C. (2010). Effects of osthole on migration and invasion in breast cancer cells. *Bioscience, Biotechnology and Biochemistry*, 74 (7), 1430 – 1434.

Yang, L. C., Chen, L. M., Wang, C. J. and Buerkle, H. (1998). Postoperative analgesia by intra-articular neostigmine in patients undergoing knee arthroscopy. *Anesthesiology,* 88, 334 - 339.

Yang, Y., Ye, X.-L. and Li, X.-G. (2007). Antimicrobial Effect of Four Alkaloids from Coptidis Rhizome. *Lishizhen Medicine and Materia Medica Research,* 12.

Yenjai, C., Sripontan, S., Sriprajun, P., Kittakoop, P., Jintasirikul, A., Tanticharoen, M. and Thebtaranonth, Y. (2000). Coumarins and carbazole alkaloids with anti-plasmodial activity from *Clausena harmandiana. Planta Medica,* 66, 277 - 279.

Yi - Chen, C., Fang - Rong, C., Chao - Miing, L. and Yang - Chang, W. (1998). Protoberberine alkaloids from *Fissistigma balansae*. *Phytochemistry,* 48 (2), 367 - 369.

Ying-Lin, C., Sunichi, U., Ming-Tsuen, H. and Meei, J. J. (1999). Effects of palmatine on isometric force and intracellular calcium levels of arterial smooth muscle. *Life Sciences,* 64 (8), 597 – 606.

Yong, Y., Ya, G. and Yue-Ting, L. (2012). Anti-inflammatory and analgesic activities of a novel biflavonoid from shells of *Camellia oleifera*. *International Journal of Molecular Sciences,* 13, 12401 - 1241.

Yuan, G., Wahlqvist, M. G., He, G., Yang, M. and Li, D. (2006). Natural products and anti-inflammatory activity. *Asia Pacific Journal of Clinical Nutrition,*15 (2), 143 - 152.

Yuana, J., Zhoua, J., Hua, Z., Jic, G., Xied, J. and Wu, D. (2011). The effects of jatrorrhizine on contractile responses of rat ileum. *European Journal of Pharmacology, Pulmonary, Gastrointestinal and Urogenital Pharmacology,* 663 (1-3), 74 - 75.

Zhang, W., Kim, D., Philip, E., Miyan, Z., Barykina, I., Schmidt, B., Stein, H. and Gluco Vip Study.(2013). A multinational, observational study to investigate the efficacy, safety and tolerability of acarbose as add-on or monotherapy in a range of patients: the Gluco VIP study. *Clinical Drug Investigation,* 33 (4), 263 - 274.

Zhu, S. (1997). An experimental study for the analgesic effect of xanthotoxol. *Journal of Gannan Medical College,* 3.

APPENDICES

Appendix 1: ^{1}H NMR spectrum of C1D (Anisocoumarin B) in chloroform-d

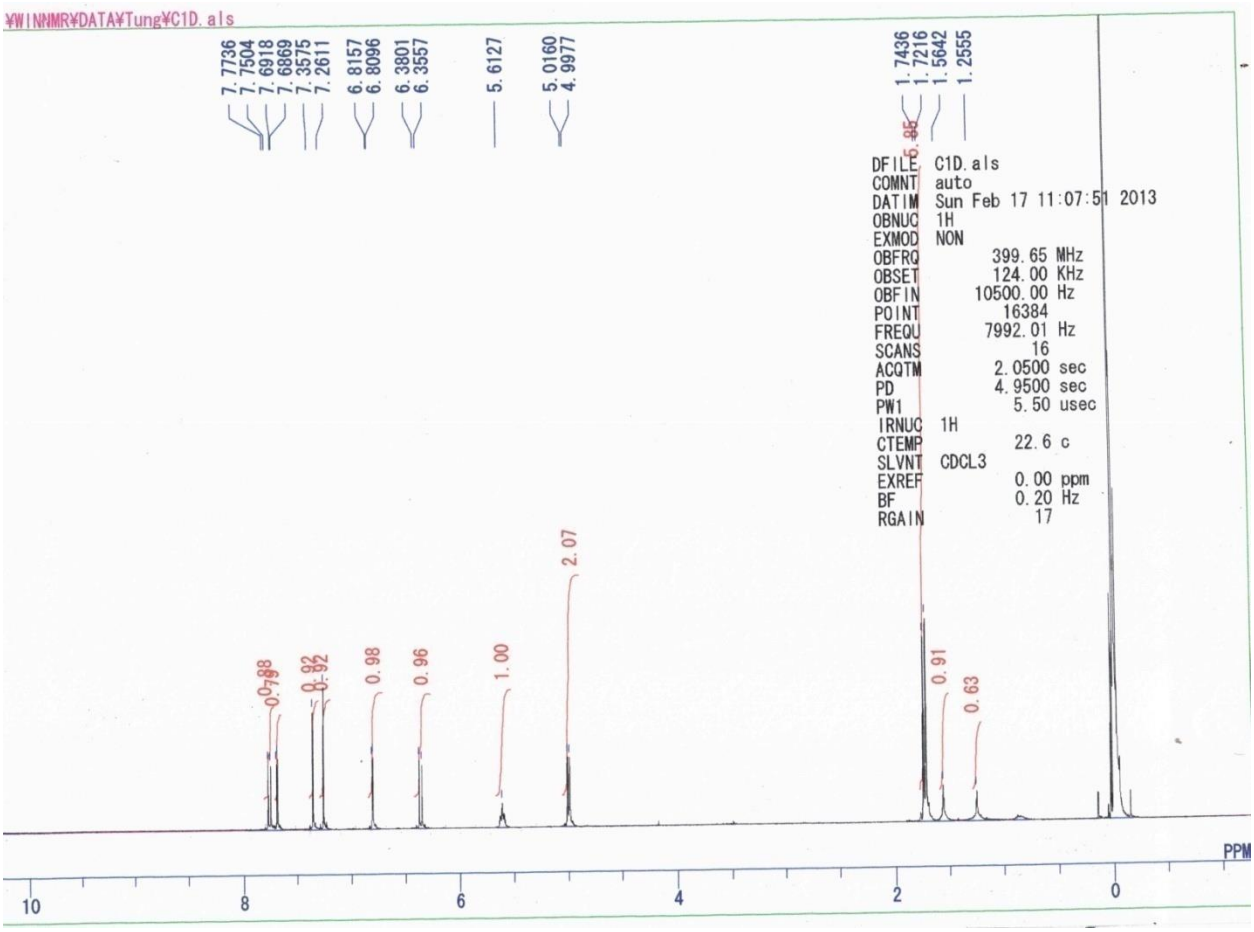

Appendix 2: ^{13}C NMR spectrum of C1D (Anisocoumarin B) in chloroform-d

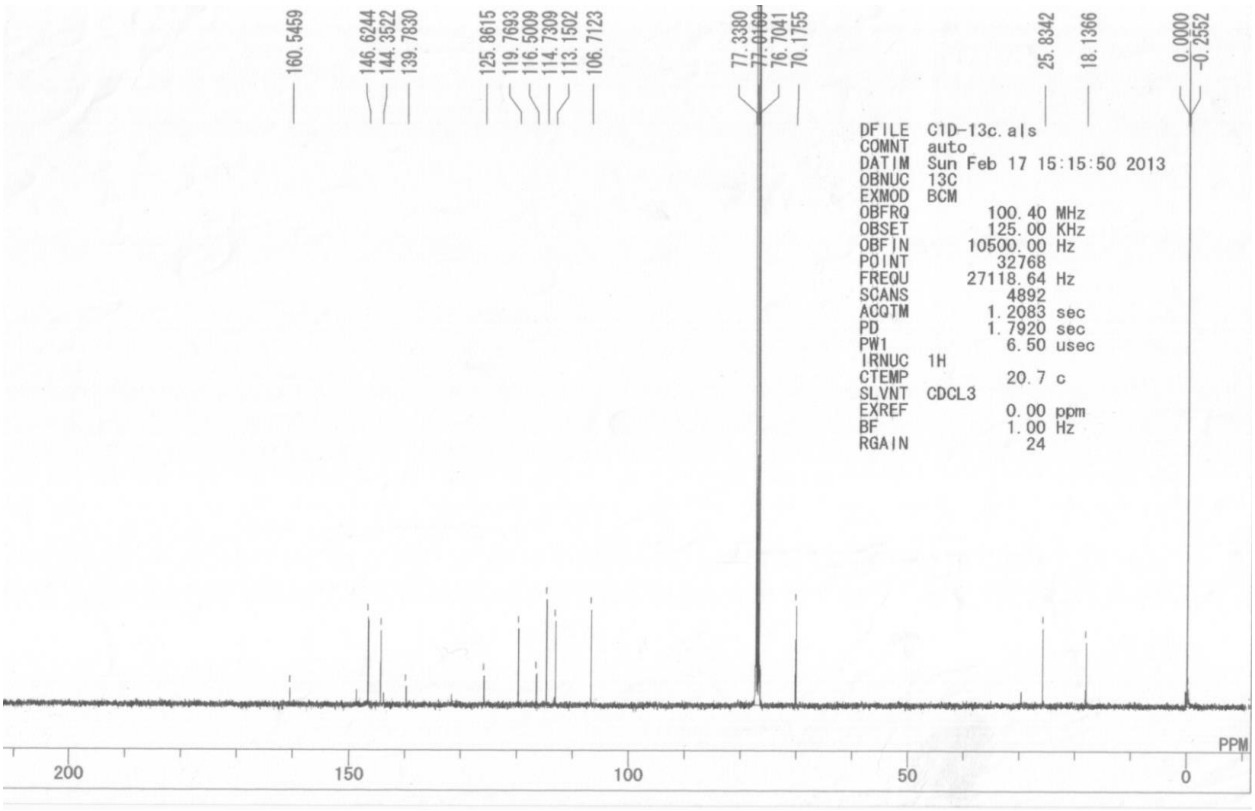

Appendix 3: GC-MS spectrum of C1D (Anisocoumarin B) in chloroform

Spectrum 1A Plot - 6/6/2016 10:27 AM

1 A Scan 1956 from .... 1 (2016-06-01)\886-pes2-16 - c1d 6-1-2016.sms

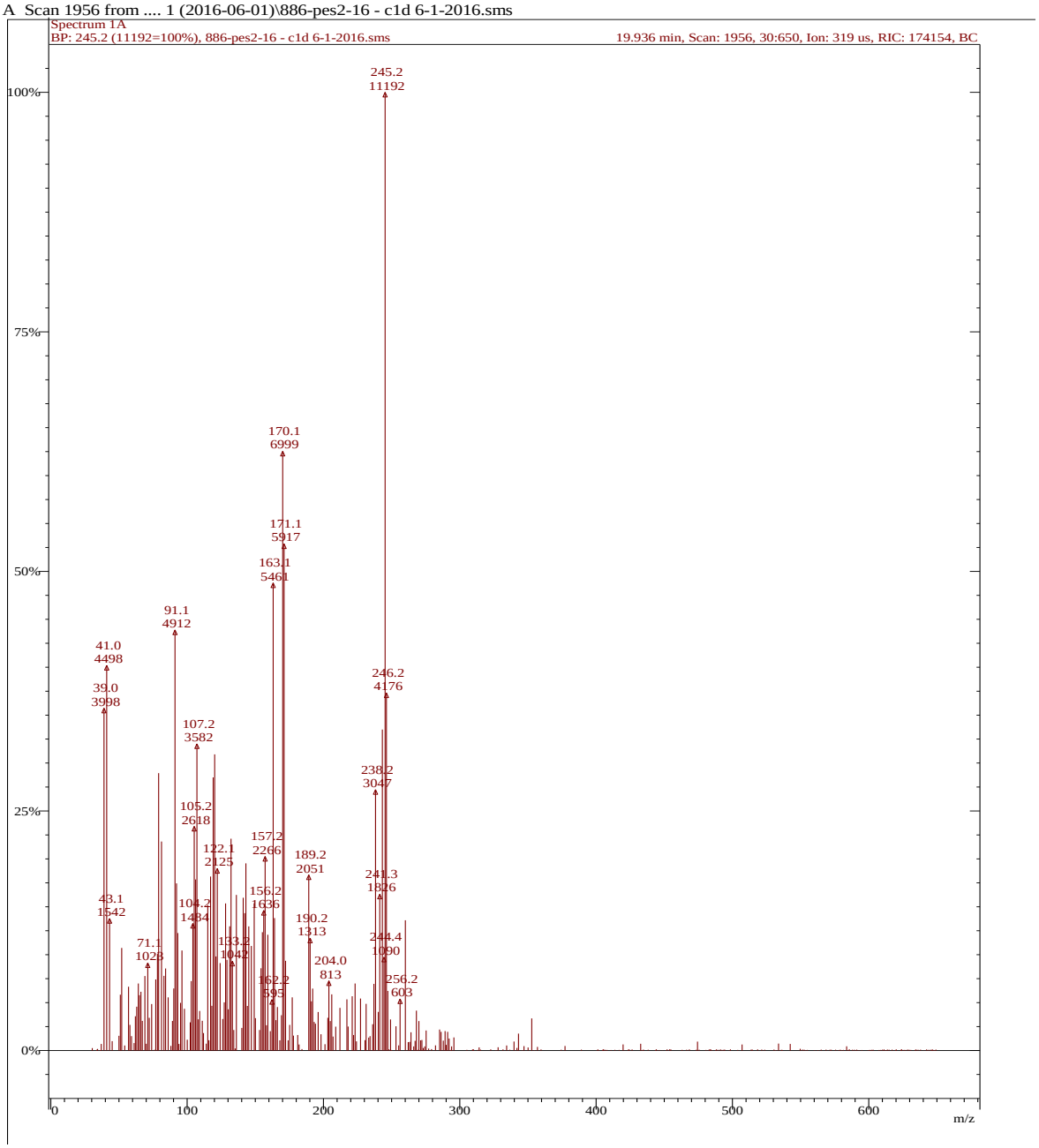

Appendix 4: I.R spectrum of C1D (Anisocoumarin B) in potassium bromide

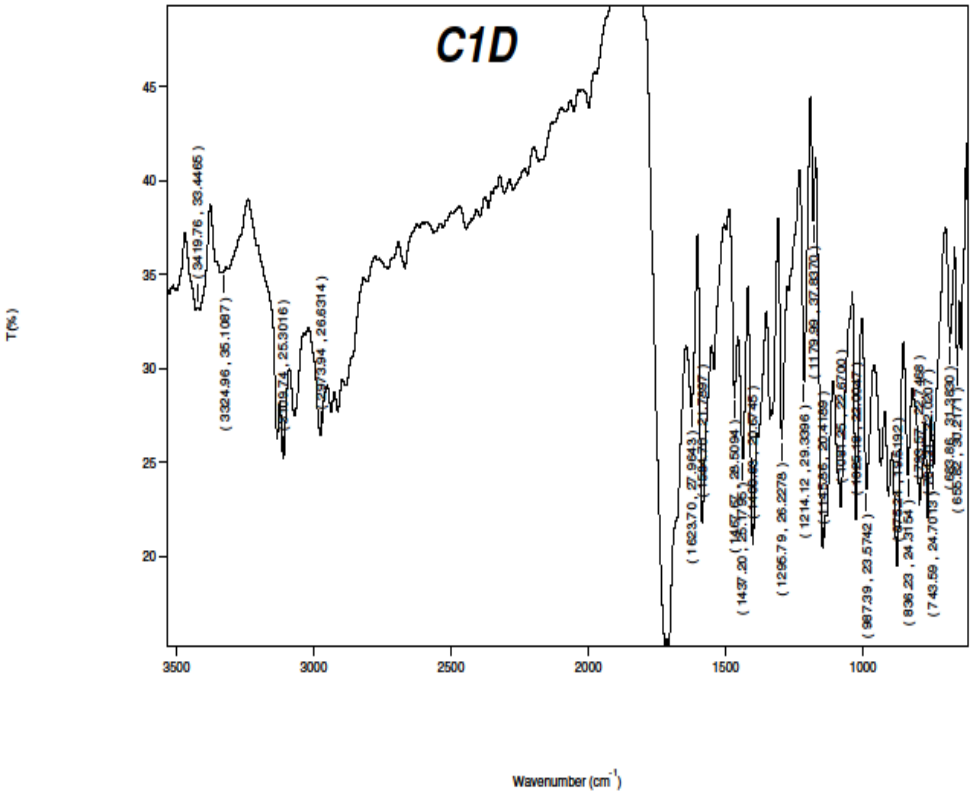

Appendix 5: ^{1}H NMR spectrum of P2A (Xanthotoxol) in methanol-d at 400 MHz

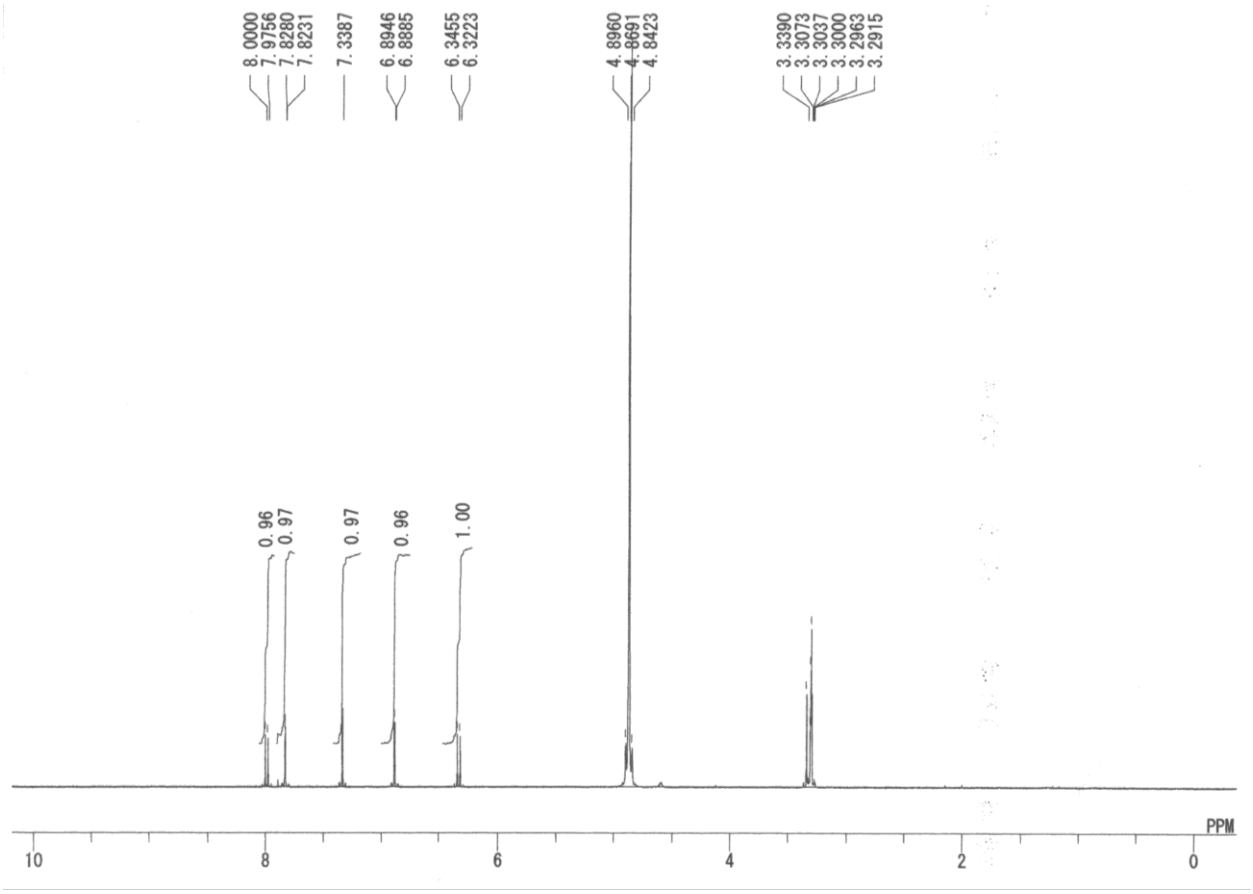

Appendix 6: ^{13}C NMR spectrum of P2A (Xanthotoxol) in chloroform-d at 100 MHz

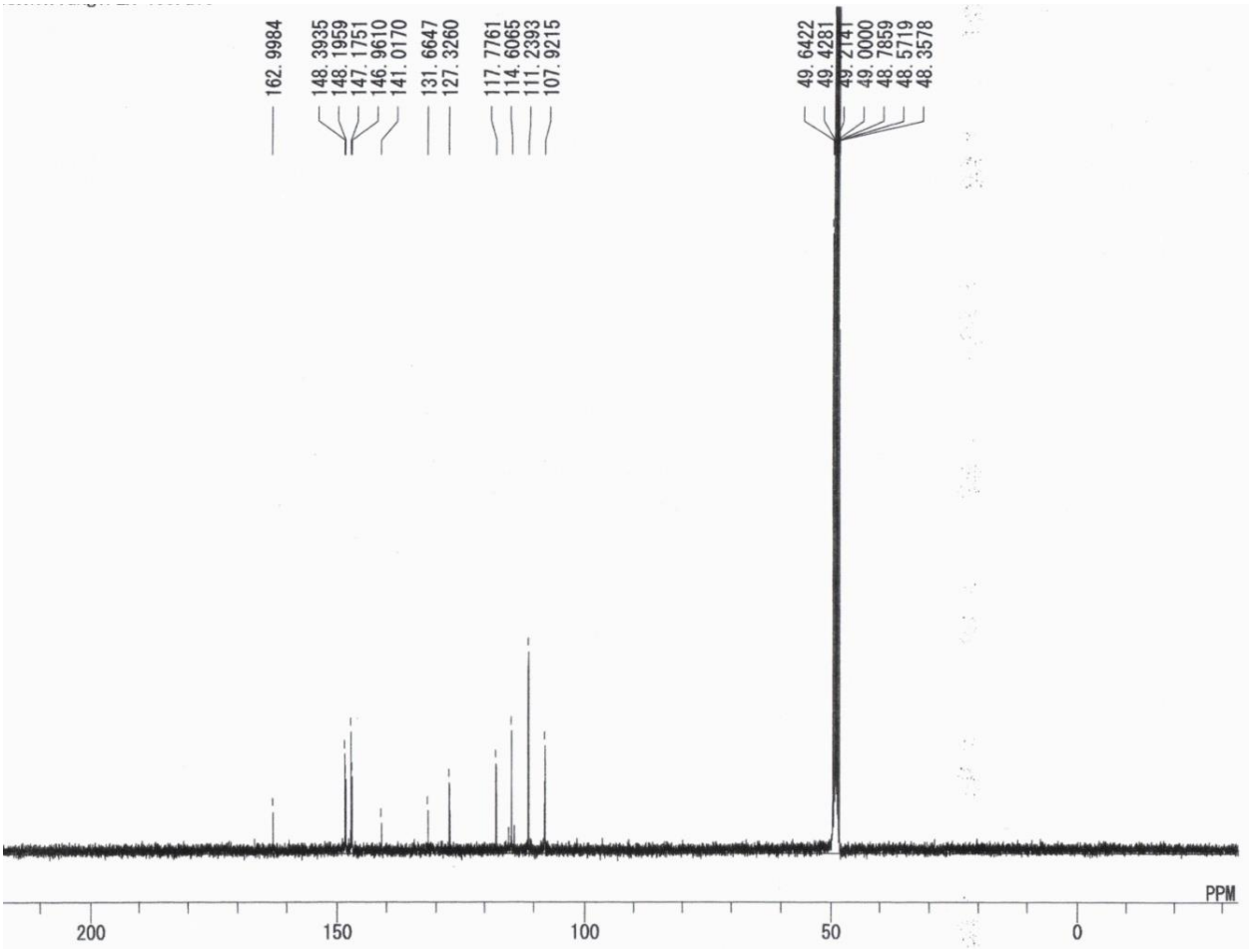

Appendix 7: GC-MS spectrum of P2A (Xanthotoxol) in methanol

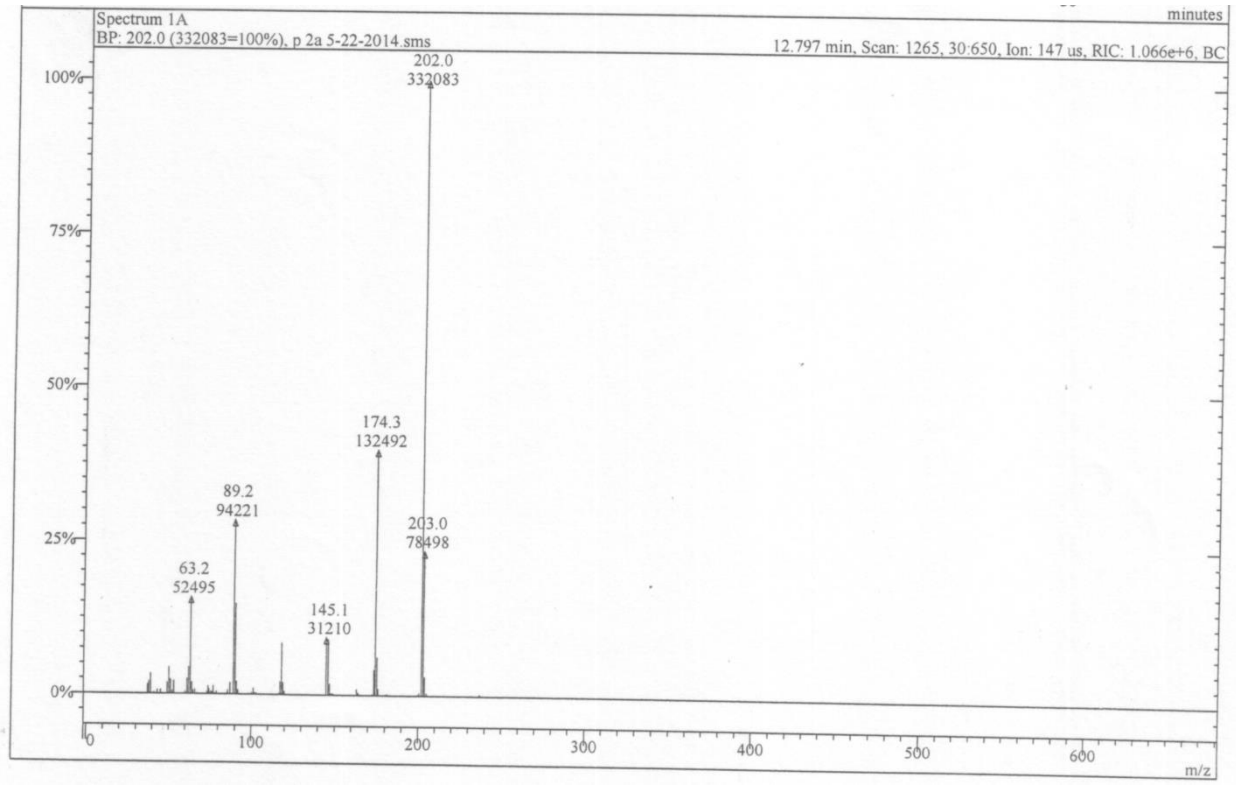

Appendix 8: I.R spectrum of P2A (Xanthotoxol) in potassium bromide

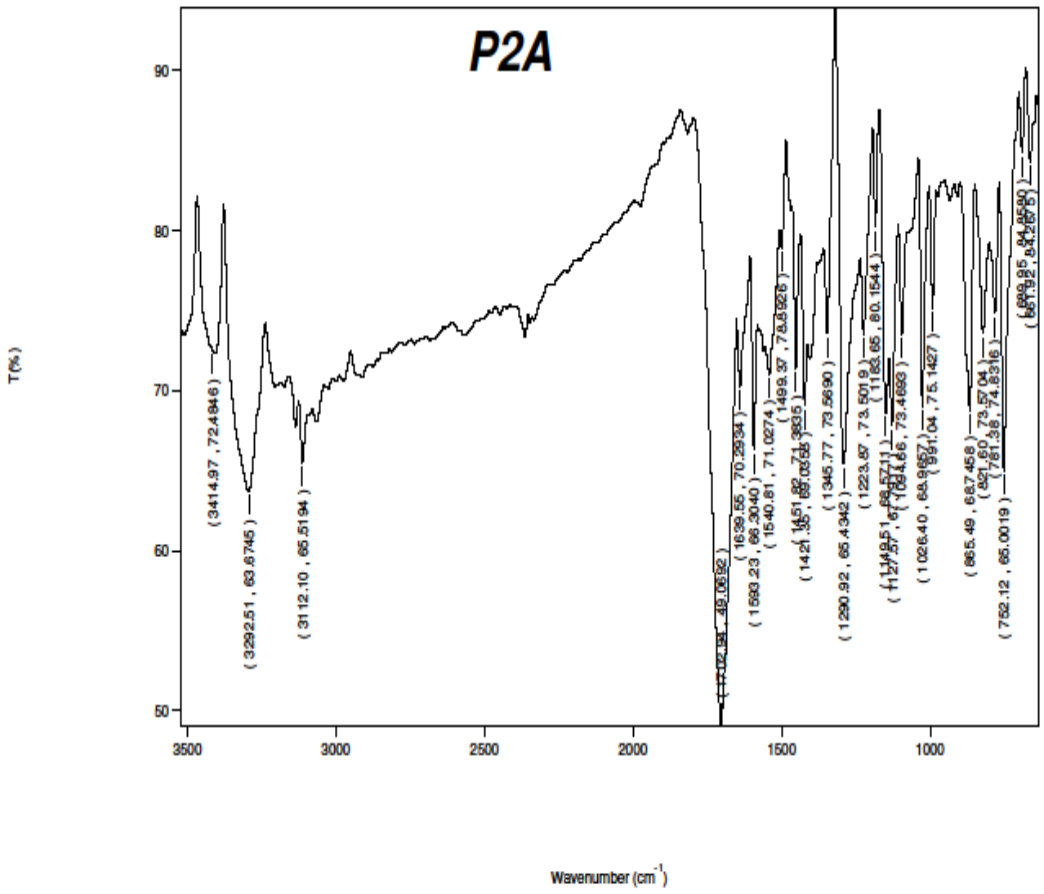

Appendix 9: ^{1}H NMR spectrum of C1F (Osthol) in chloroform-d at 500 MHz

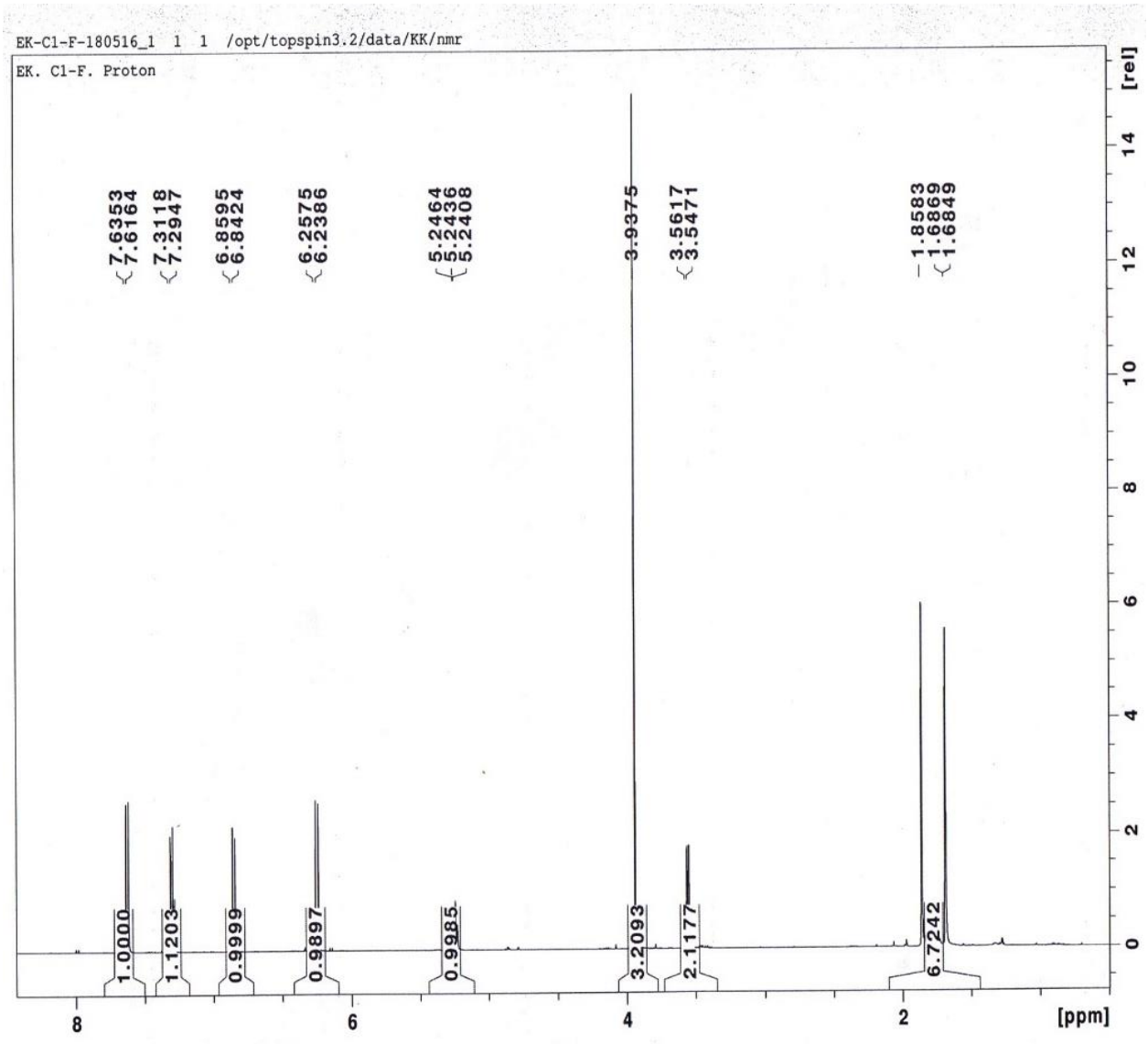

Appendix 10: ^{13}C NMR spectrum of C1F (Osthol) in chloroform-d at 500 MHz

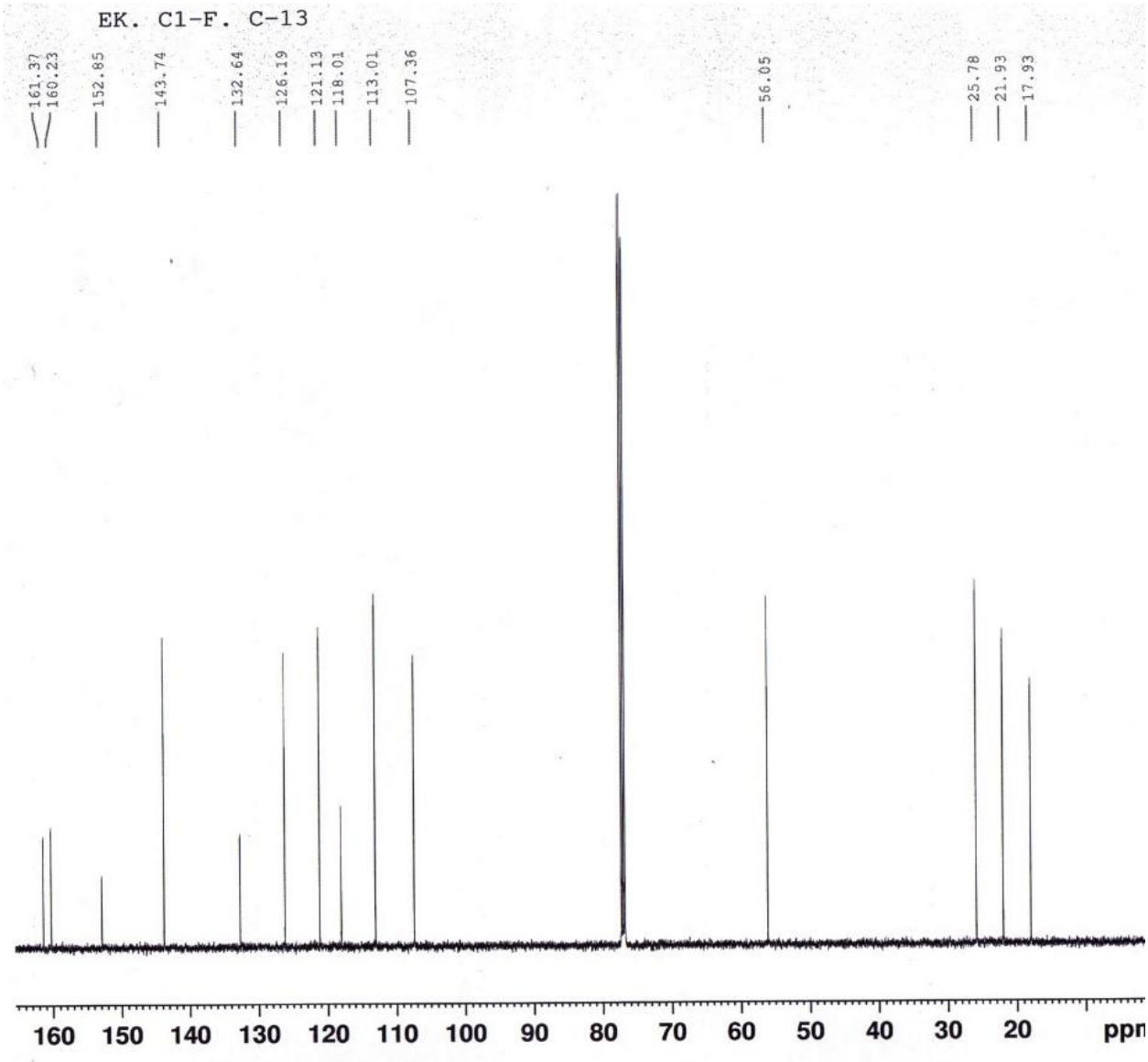

Appendix 11: G.C-MS spectrum of C1F (Osthol) in chloroform

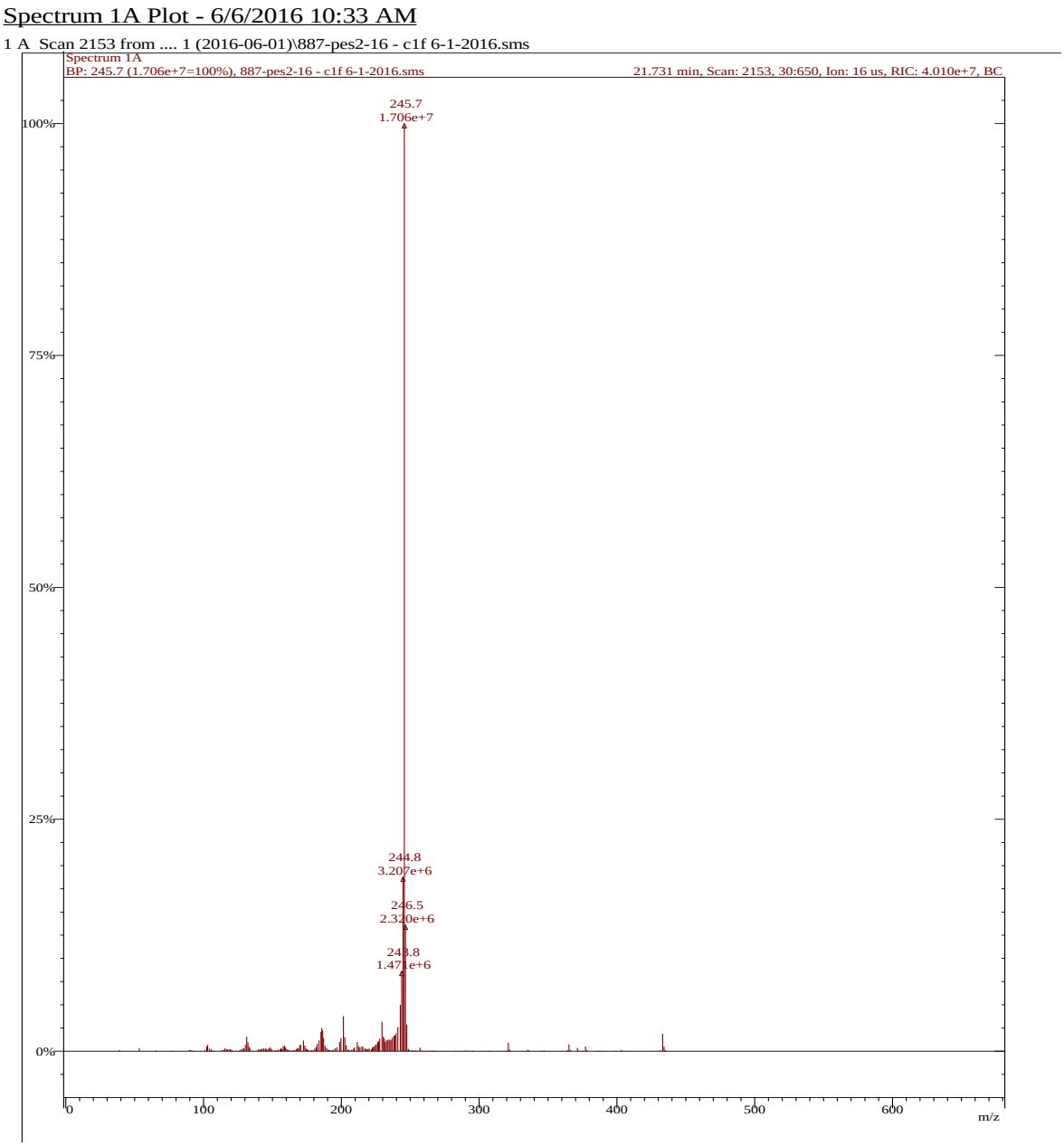

Appendix 12: I.R spectrum of C1F (Osthol)

Sample Description C1F

Spectrum Graph

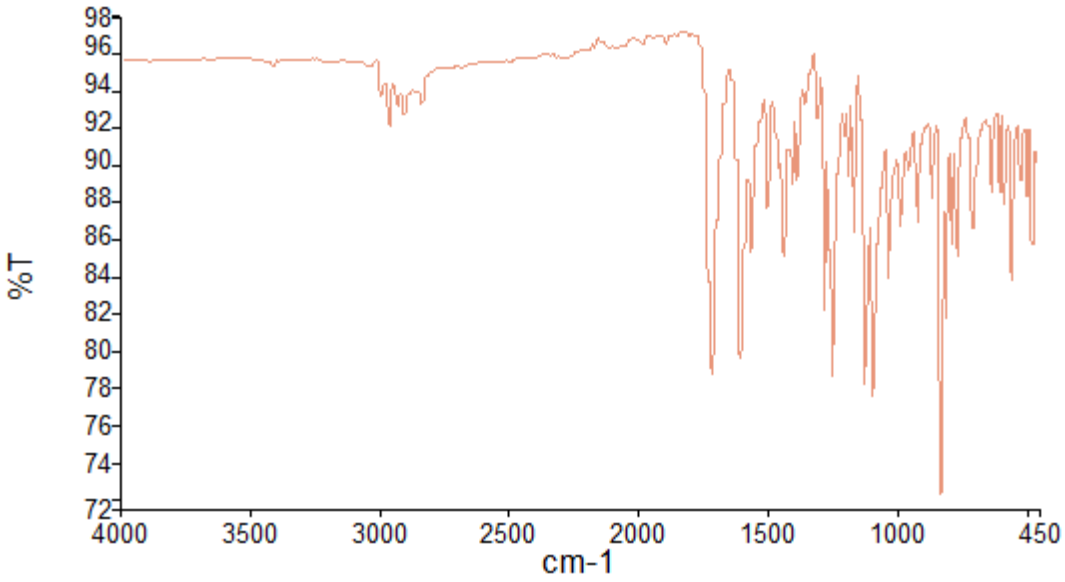

Appendix 13: ^{1}H NMR spectrum of C1G (Imperatorin) in chloroform-d at 500 MHz

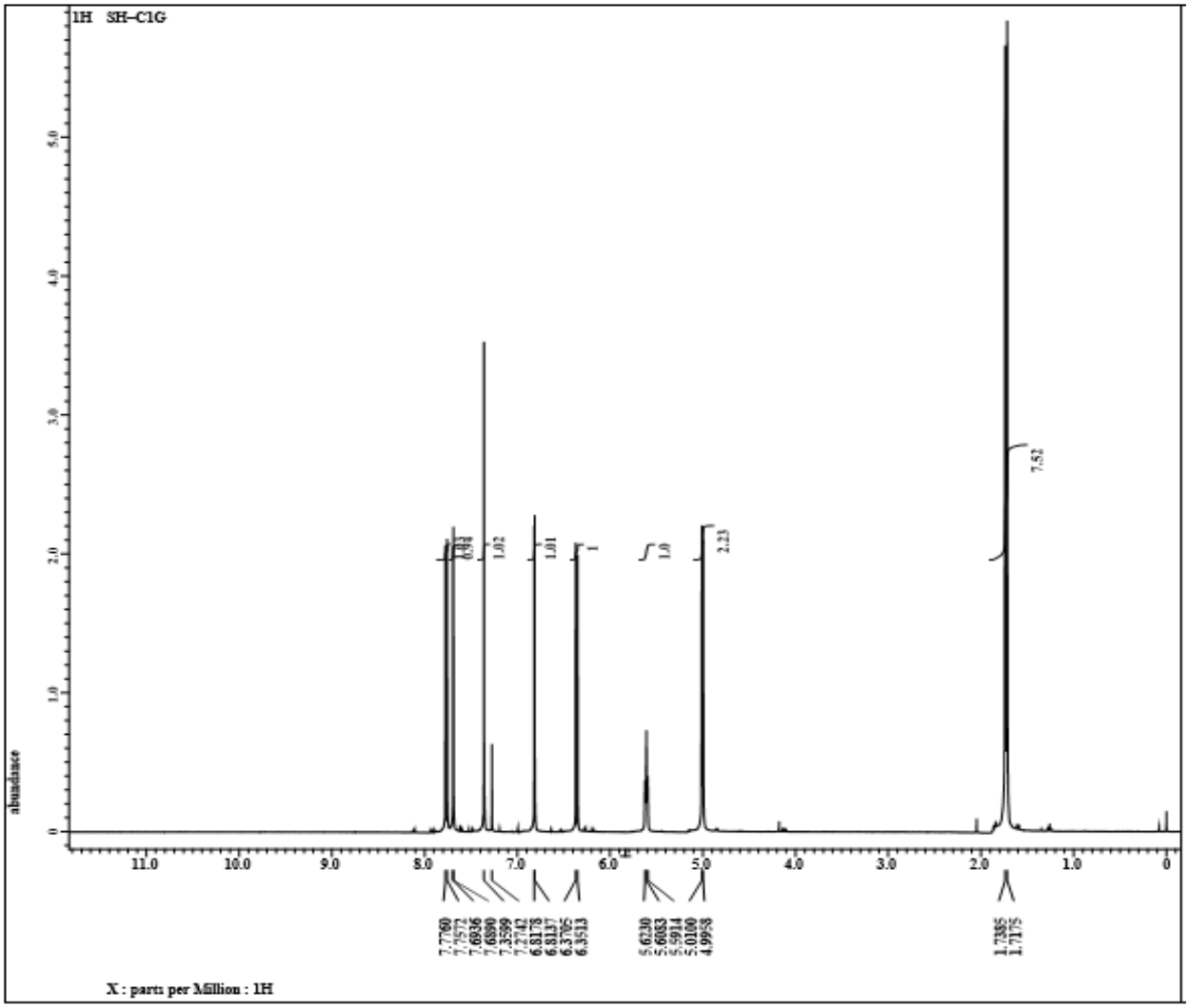

Appendix 14: ^{13}C NMR spectrum of C1G (Imperatorin) in chloroform-d at 500 MHz

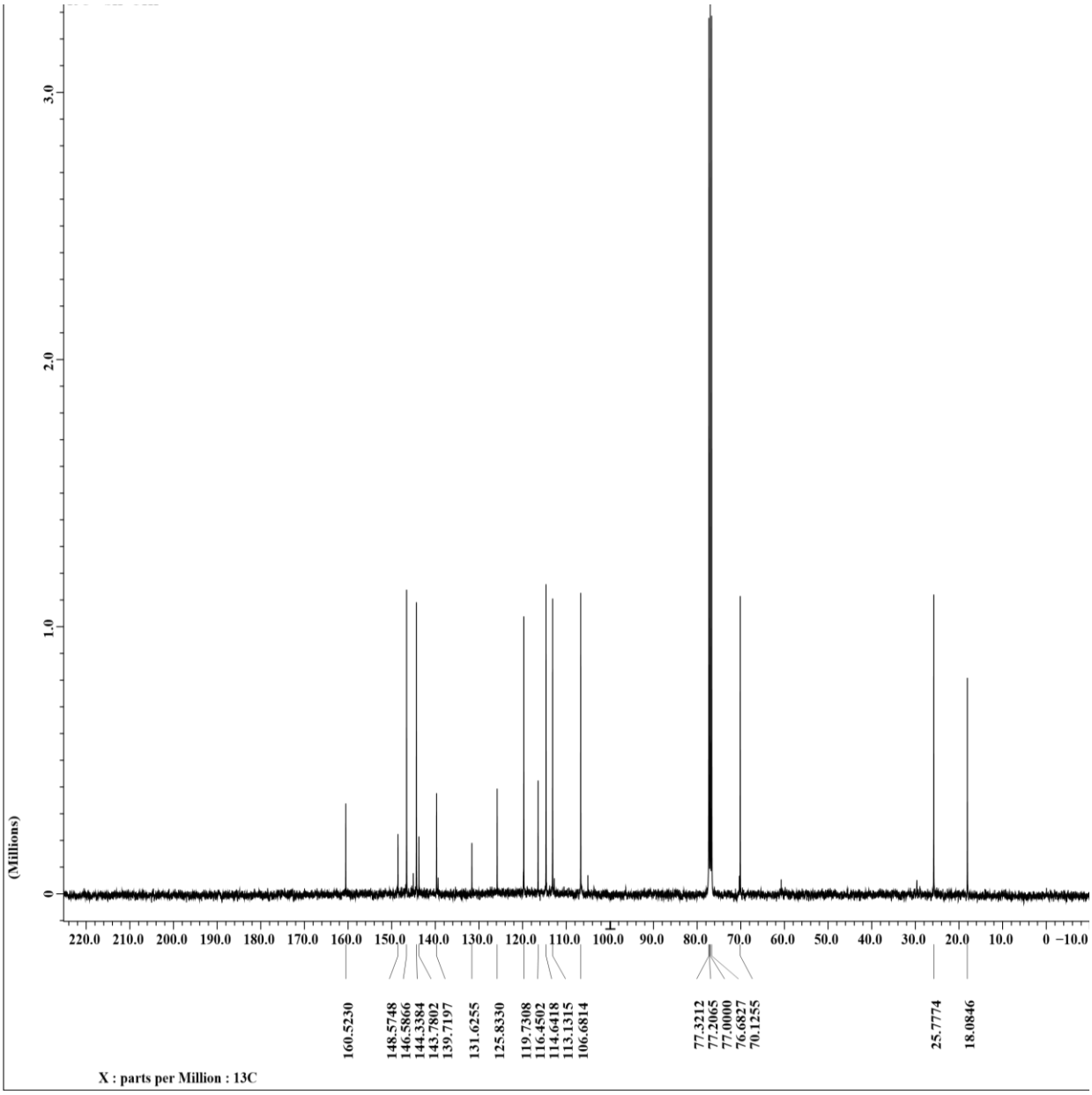

Appendix 15: GC-MS spectrum of C1G (Imperatorin) in chloroform

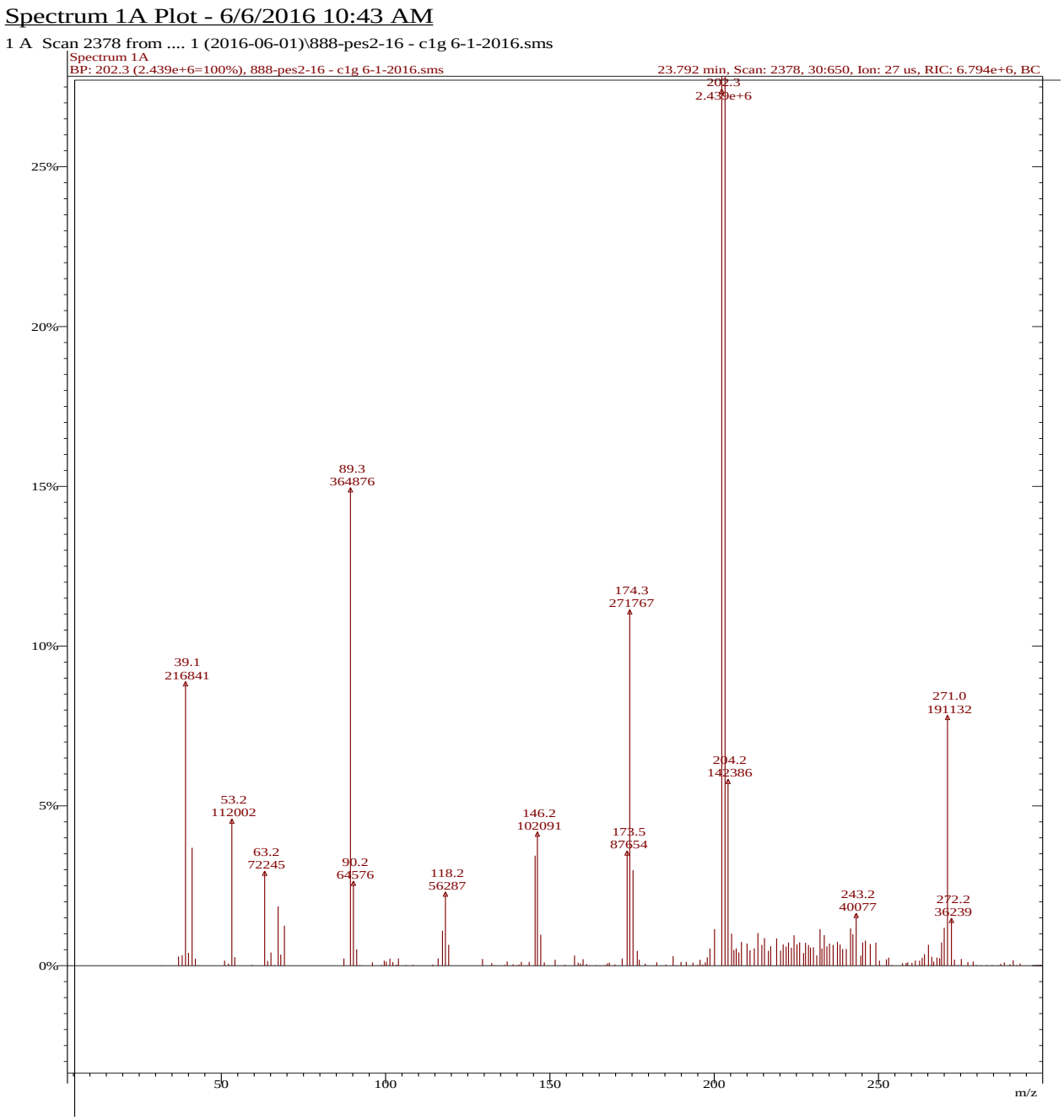

Appendix 16: I.R spectrum of C1G (Imperatorin)

Sample Description C1G

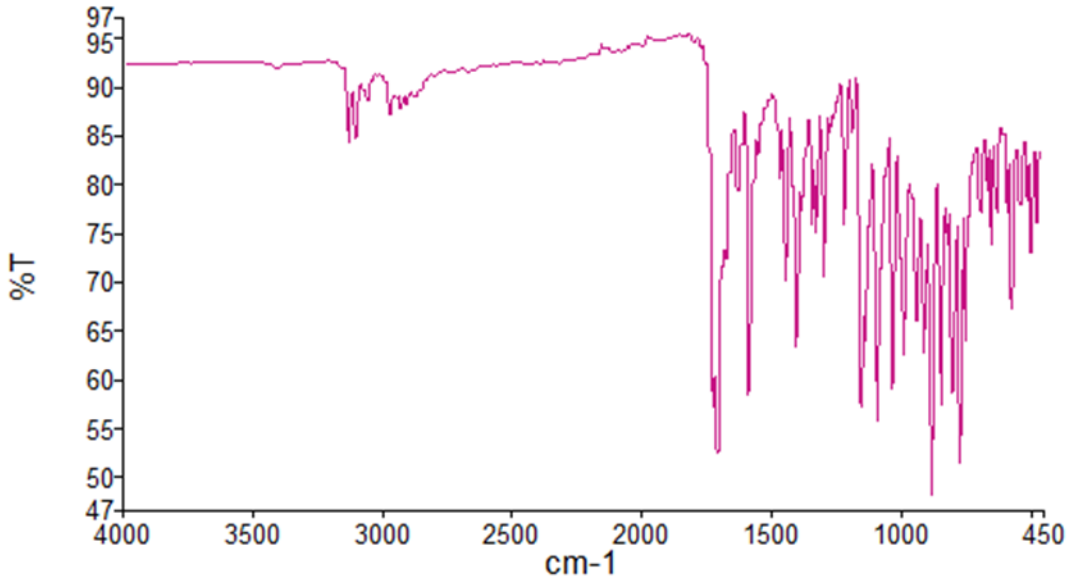

Appendix 17: ^{1}H NMR spectrum of C1-I (Heptaphyline) in chloroform-d at 500 MHz

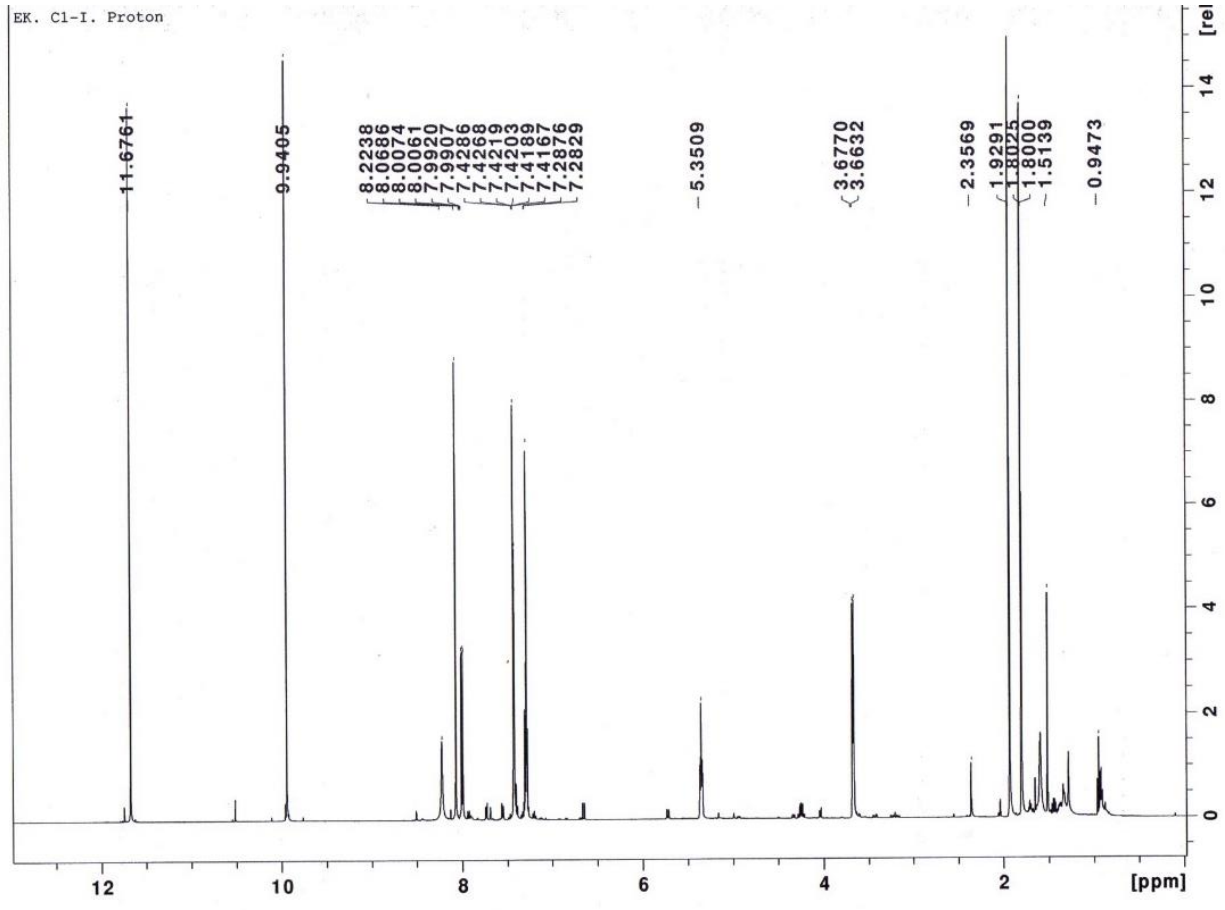

Appendix 18: ^{13}C NMR spectrum of C1-I (Heptaphyline) in chloroform-d at 500 MHz

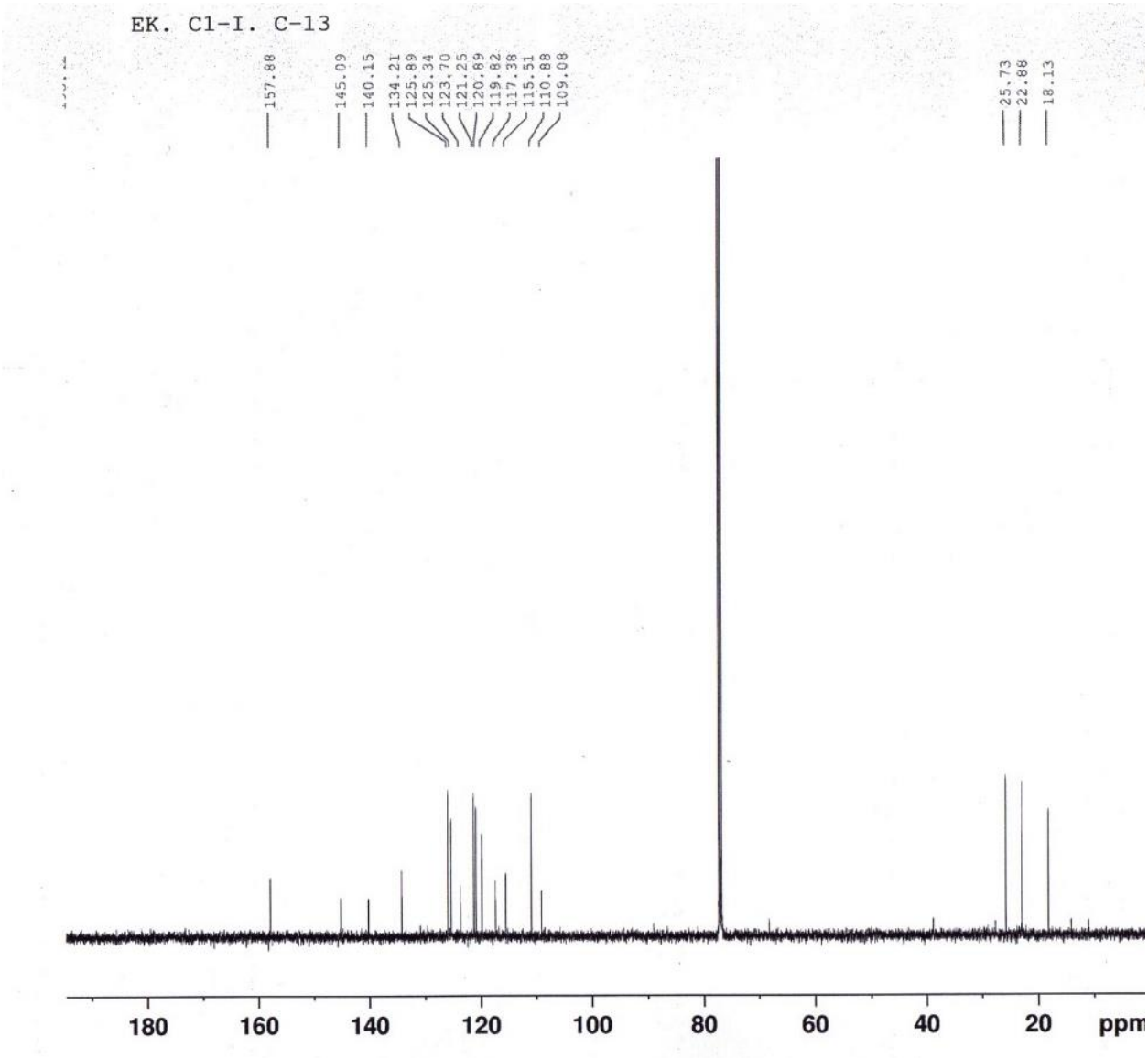

Appendix 19: GC-MS spectrum of C1-I (Heptaphyline) in chloroform

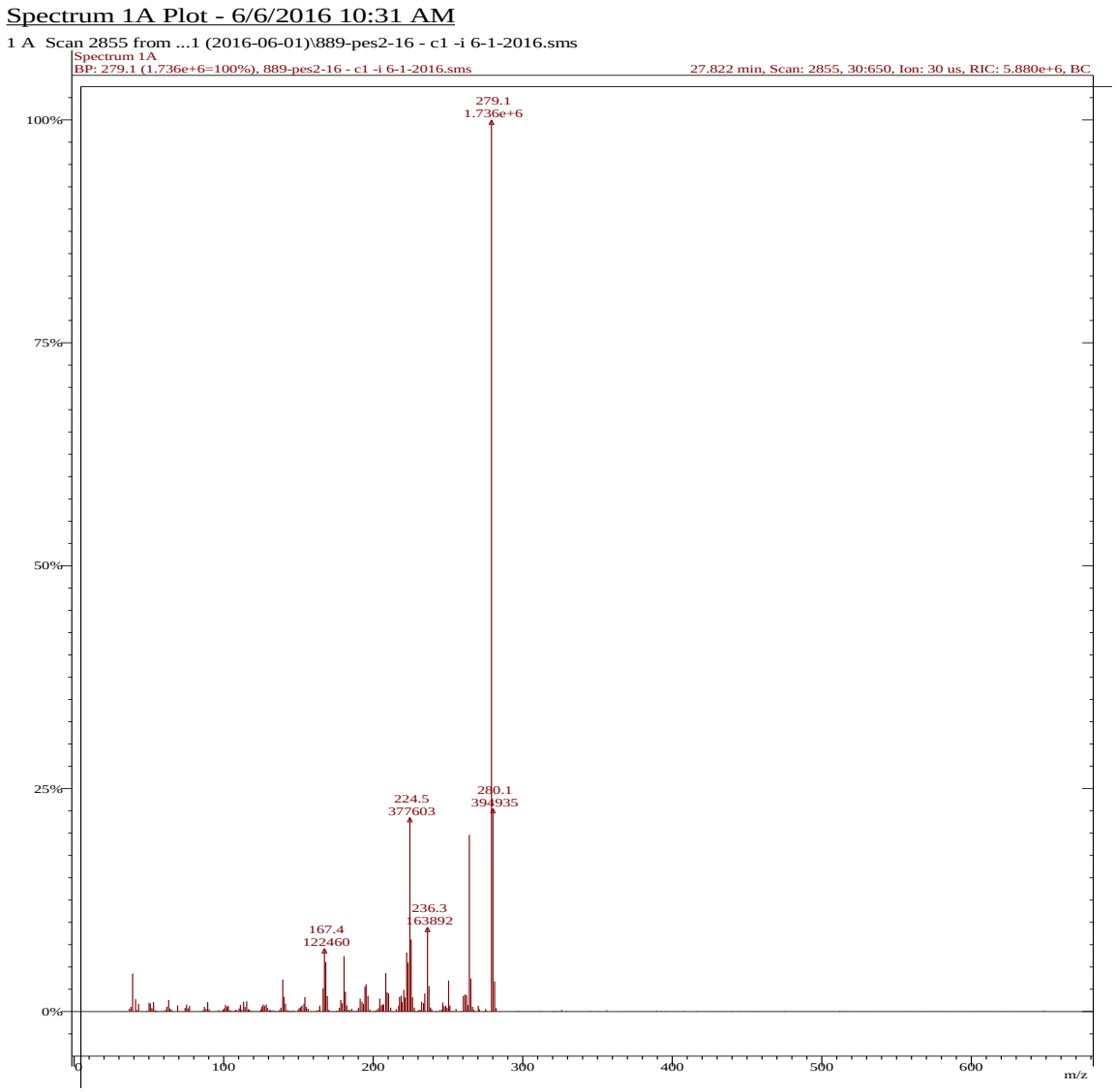

Appendix 20: I.R spectrum of C1-I (Heptaphyline)

Sample Name C1-I

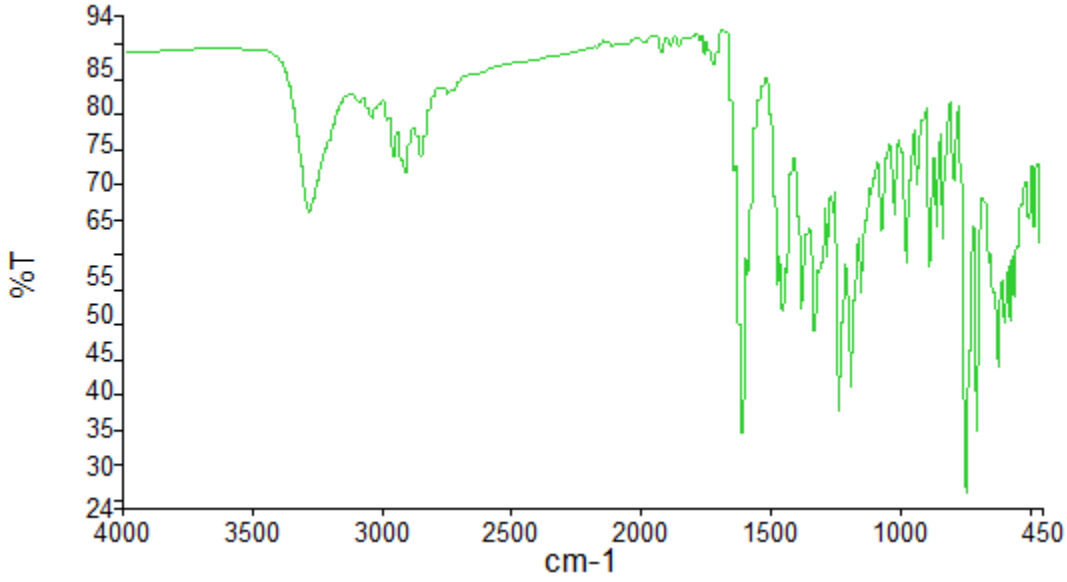

Appendix 21: ^{1}H NMR spectrum of A6C (Palmatine) in methanol-d at 400 MHz

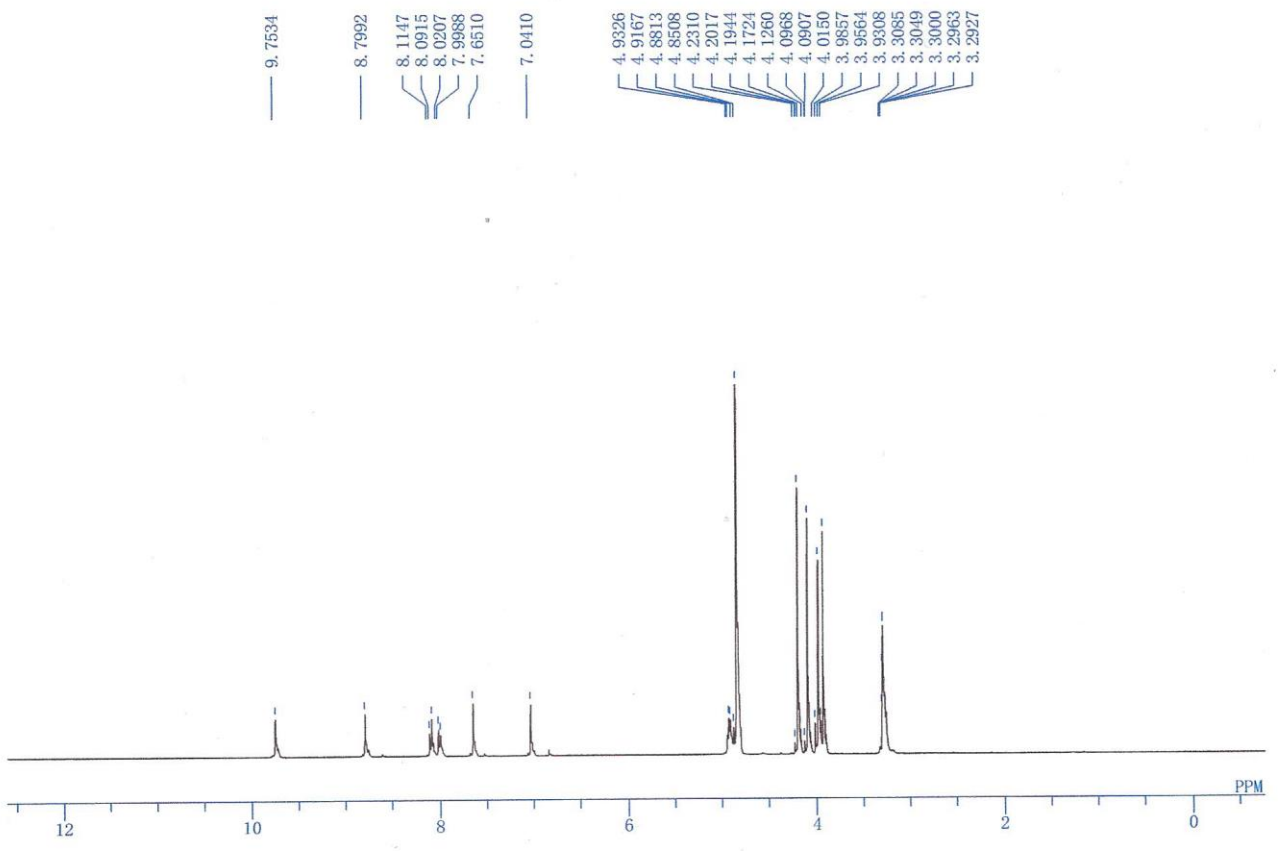

Appendix 22: ^{13}C NMR spectrum of A6C (Palmatine) methanol-d at 100 MHz

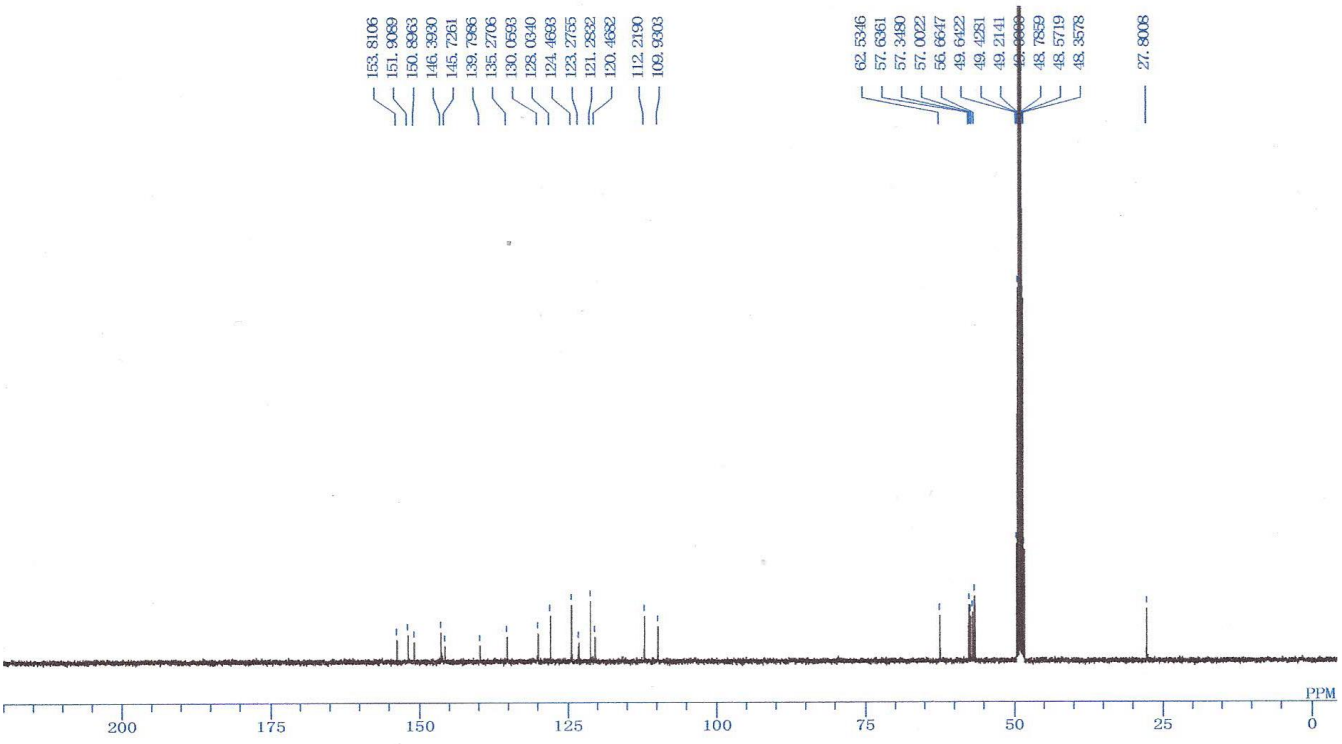

Appendix 23: GC-MS spectrum of A6C (Palmatine) in methanol

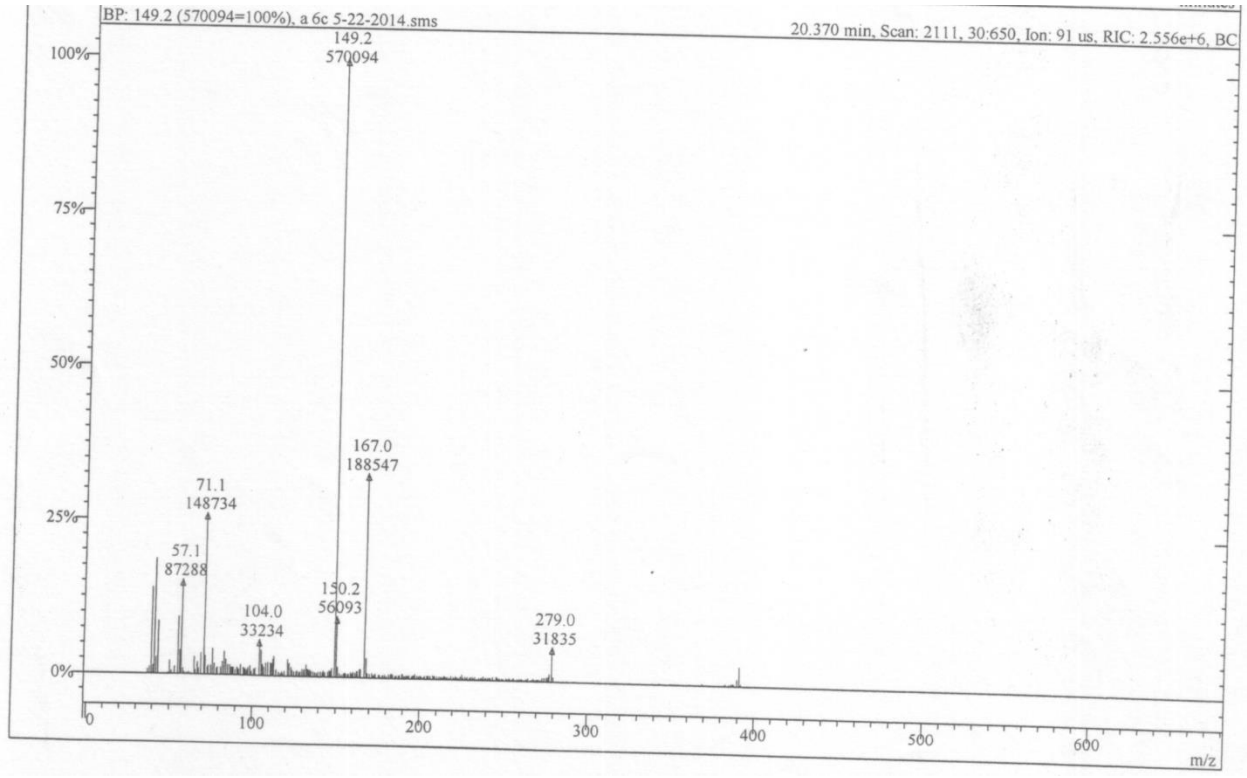

Appendix 24: I.R spectrum of A6C (Palmatine) in potassium bromide

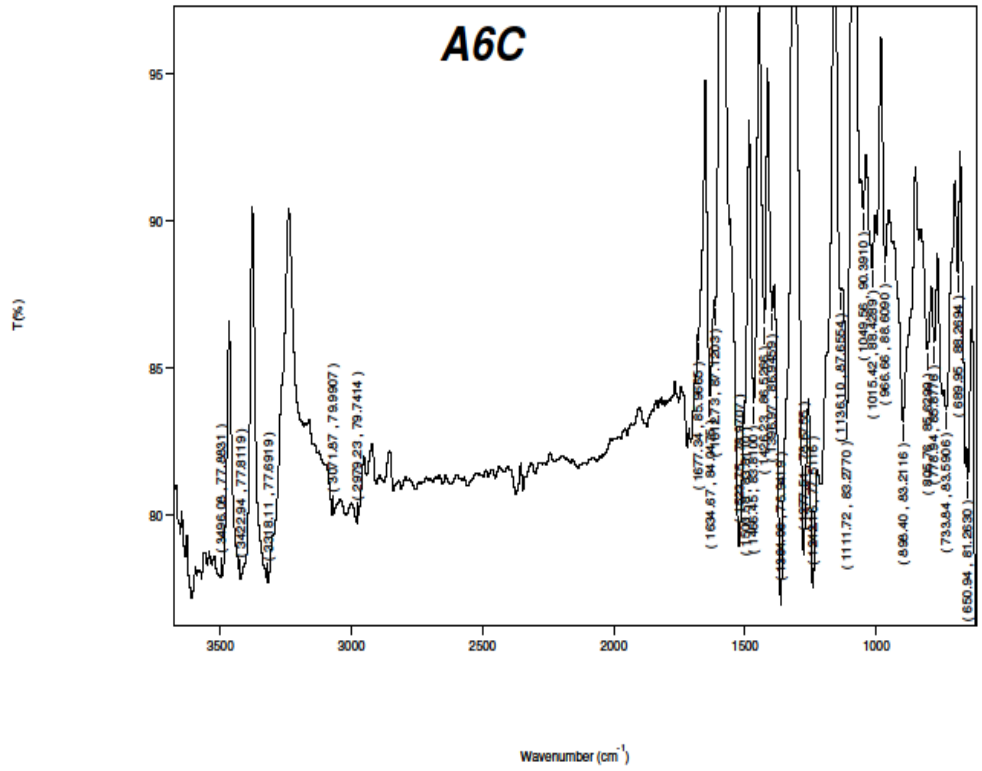

Appendix 25: ^{1}H NMR spectrum of A8C (Jatrorrhizine) in methanol-d at 400 MHz

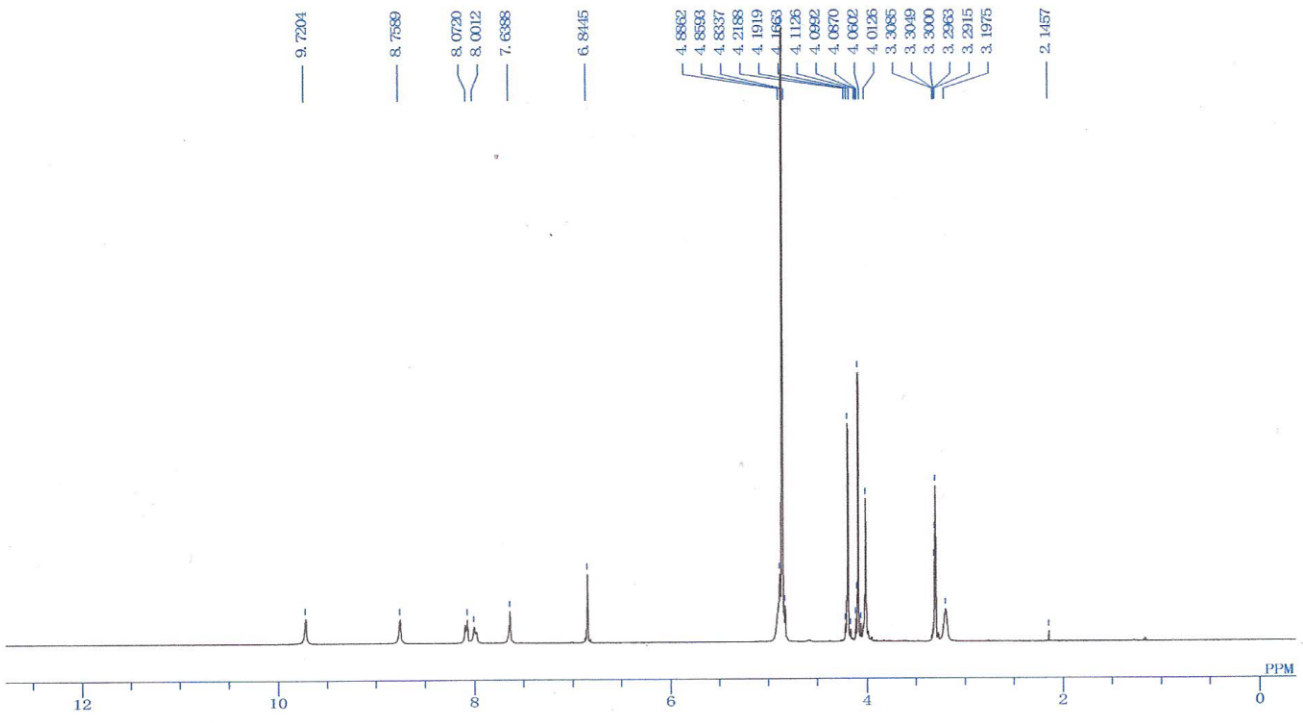

Appendix 26: ^{13}C NMR spectrum of A8C (Jatrorrhizine) in methanol-d at 100 MHz

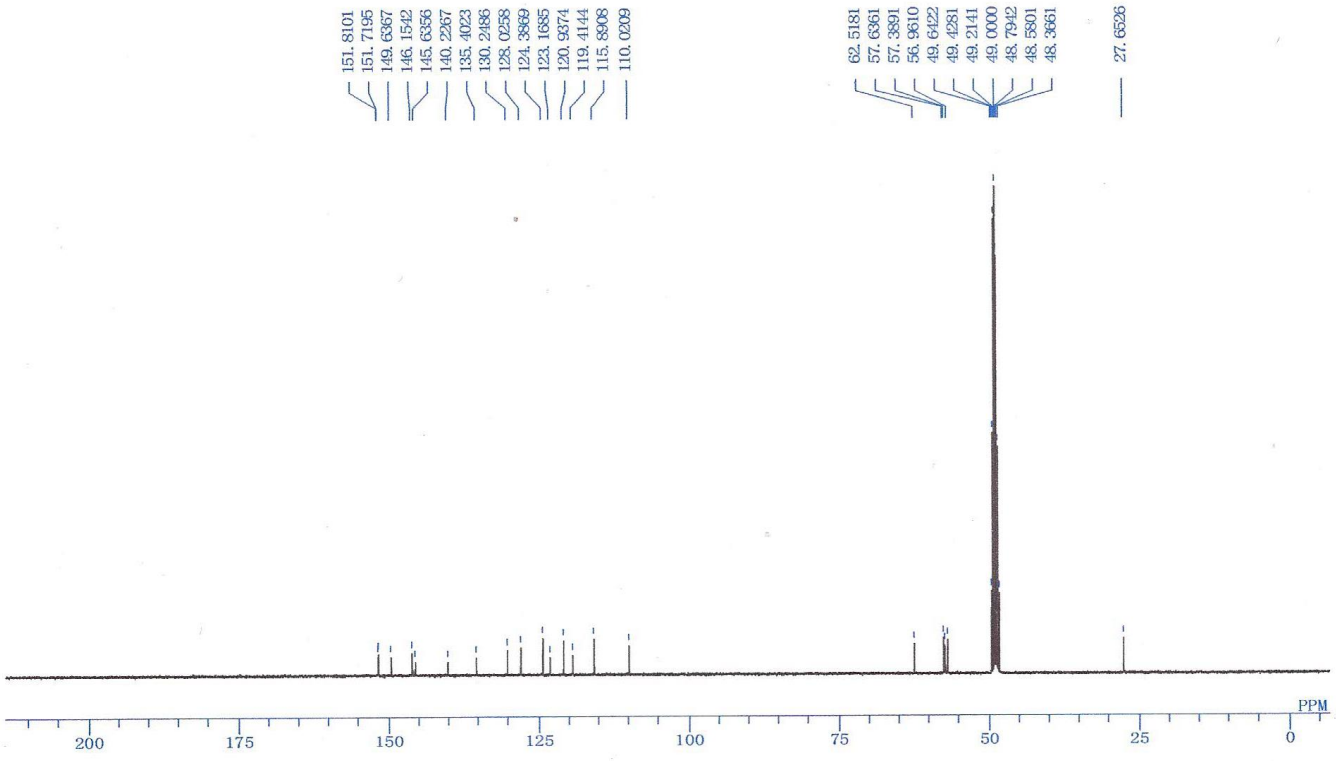

Appendix 27: GC-MS spectrum of A8C (Jatrorrhizine) in methanol

Spectrum 1A Plot - 6/6/2016 10:50 AM

1 A Scan 2239 from ... 1 (2016-06-01)\886-pes2-16 - a8 c 6-1-2016.sms

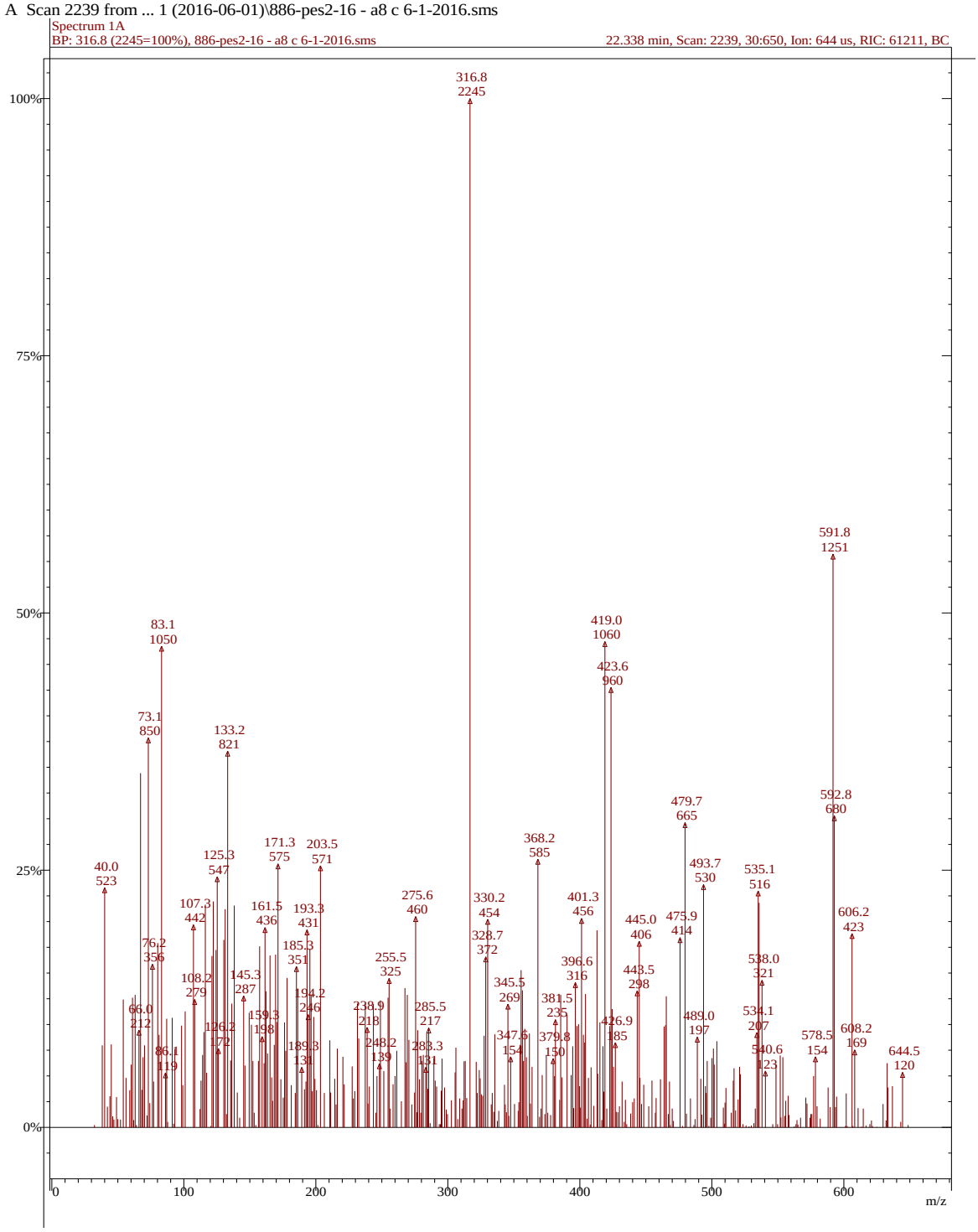

Appendix 28: I.R spectrum of A8C (Jatrorrhizine) in potassium bromide

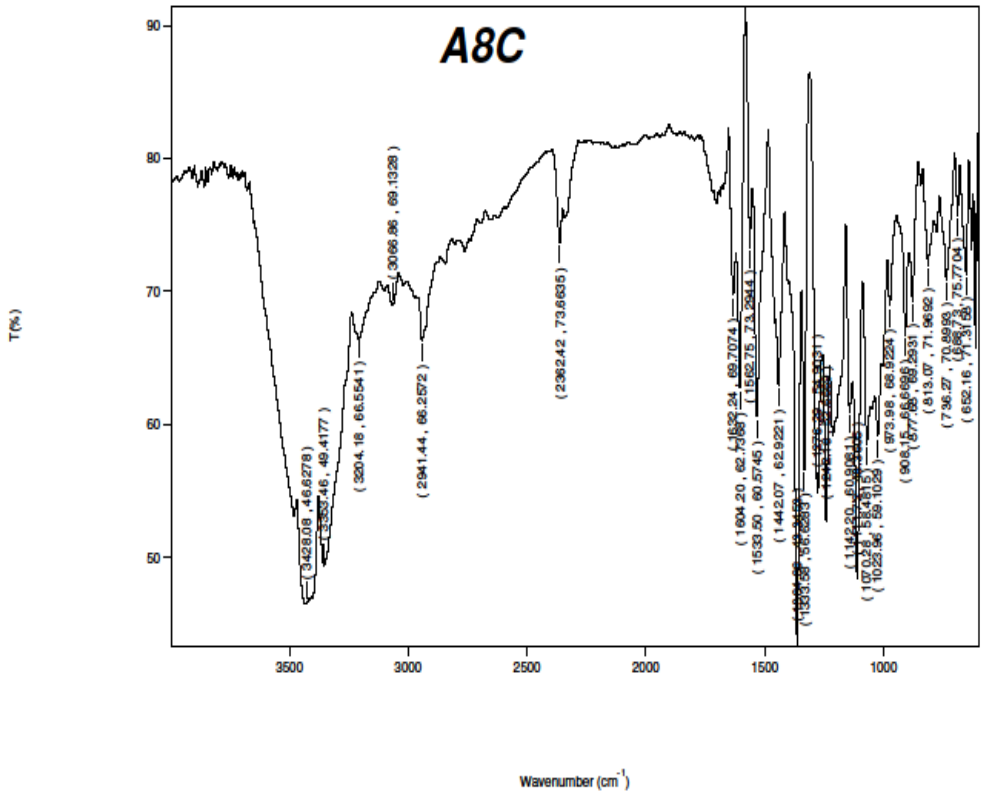

Appendix 29: ^{1}H NMR spectrum of A9C (Palmatine) in methanol-d at 400 MHz

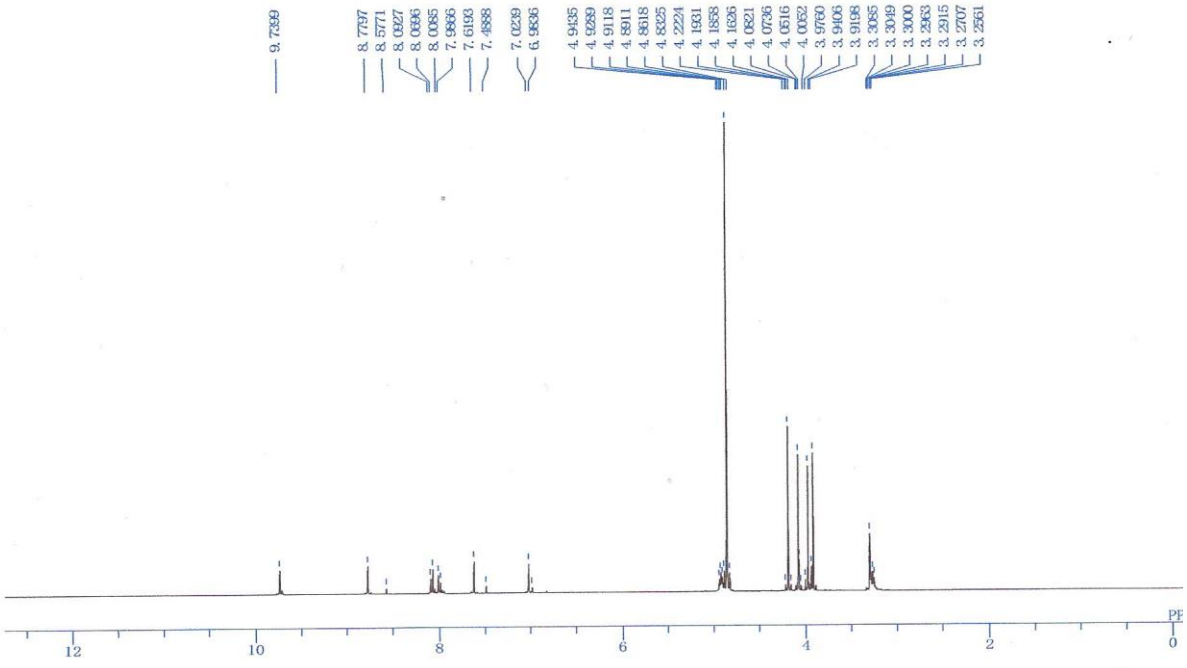

Appendice 30: ^{13}C NMR spectrum of A9C (Palmatine) in methanol-d at 400 MHz